Universitat de Girona

ASSESSMENT AND OPTIMISATION OF THE OPERATION OF INTEGRATED MEMBRANE SYSTEM FOR WASTEWATER RECLAMATION

Julian Mamo

Universitat de Girona

DOCTORAL THESIS

ASSESSMENT AND OPTIMIZATION OF THE OPERATION OF INTEGRATED MEMBRANE SYSTEMS FOR WASTEWATER RECLAMATION

JULIAN MAMO

2018

This thesis contains appendices

Universitat de Girona

DOCTORAL THESIS

ASSESSMENT AND OPTIMIZATION OF THE OPERATION OF INTEGRATED MEMBRANE SYSTEMS FOR WASTEWATER RECLAMATION

JULIAN MAMO

2018

Doctoral Programme in Water Science and Technology

Supervisors:
Dr. Joaquim Comas
Matas, Dr. Ignasi
Rodríguez-Roda, Dr.
Hèctor Monclús Sales

Thesis submitted in fulfilment of the requirements for the degree of Doctor from the University of Girona and meets the requirements for an International Doctorate
This thesis contains appendices

The research was supported by

The Spanish Ministry of Economy and Competitiveness (project WaterFate; CTM2012-38314-C02-01) and supported by the Generalitat de Catalunya (Consolidated Research Groups 2014SGR291 and 2014-SGR-1168)

And

The People Program (Marie Curie Actions) of the European Union's Seventh Framework Programme FP7/2007-2013, under REA agreement 289193.

This publication reflects only the author's views and the European Union is not liable for any use that may be made of the information contained therein.

Furthermore

The research was supported by the staff of the wastewater treatment plants of Castell-Platja d'Aro and Quart (Girona, Spain) who allowed the operation of the pilot plants at their facilities.

Certificate:

The thesis entitled **Assessment and Optimization of the operation of integrated membrane system for wastewater reclamation** presented by Julian Mamo has been supervised by Dr. Joaquim Comas Mata, Dr. Ignasi Rodríguez Roda Layret and Dr. Hèctor Monclús Sales from the University of Girona and it fulfil the requirements for the degree of Doctor (and meets the requirements to opt for an International Doctorate).

This certificate, original and signed by supervisors, proves the doctoral candidate has carried out the research work under the supervisor's guidance.

In Girona, on Monday, 22 October 2018

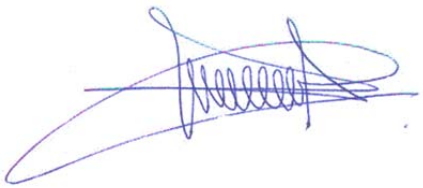

Dr. Joaquim Comas Matas Dr. Ignasi Rodríguez-Roda Layret Dr. Hèctor Monclús Sales

Acknowledgments

This thesis would not have been possible without the assistance of many people to whom I am grateful.

Firstly, I would like to thank my supervisors Quim, Ignasi and Hector without whom this thesis would not have been possible and thanks to their friendship, patience and guidance this work was carried out. Secondly, I would like to particularly thank the MBR team, Hector, Sara and Montse for teaching me so much, and for their friendship. I would also like to thank all my colleagues at LEQUIA who thought me so much and for their company and hospitality throughout my stay in Girona: Sara, Montse, Tiago, Elena, Serni, Antonia, Anna, Alba C, Alba A, Teresa, Sebas, Mael, Alexandra, Narcis, Tico, Pau, and Ramon.

I would also like to thank the researchers at LEQUIA and ICRA who each helped shaped different chapters within this work, María Jesús García-Galán (Chapter 4), Maria José Farré (Chapter 5) and Jose Porro (Chapter 8). I would like to thank a number of ICRA researchers and staff who helped in various ways; from advice, to helping with equipment and analysis and the development of the control software: Wolfgang Gernjak, Gianluigi Buttiglieri, Lluis Corominas, Lluis Bosch, Sara Rodriguez, Núria Cáceres and Sara Insa

I would also like to thank the students who did their traineeship or final year project with me who helped with the operation of the pilot plant: Marc Cespedes, Maria Caldero, Meritxell Masachs, Alexandra Marti, Marc Lucas and Renata Finocchiaro.

I would also like the thank the Sanitas fellows: Antonia, Lara, Elisa, Usman, Ramesh, Kim, Celia, Laura, Marina and Jose. I would also like to thank the Biomath team for their hospitality during my stay in Gent: Ingmar, Wouter, Elena, Usman and the rest of the research group.

I would also like to thank the personnel at the two wastewater treatment plants where the pilot plant was in operation: Jordi Munoz and staff at Castel d'Aro EDAR, Benjamin and Marta and staff at Quart EDAR.

I would also like to thank the Industrial partners who assisted in various means: Adiquimica (Barcelona) who provided membranes and carried out membrane analysis and Casasmasgrau, (Llagostera) who assisted in the maintenance of the pilot plant.

Last but not least, I would like to thank Therese, Peter and our families for their constant support and patience.

Table of Contents

List of Tables

List of Figures

Nomenclature

Acronyms

AOP	Advanced Oxidation Process
CEC	Compounds of Emerging Concern
DBP	Disinfection By-Product
DO	Dissolved Oxygen
DPR	Direct Potable Reuse
DWTP	Drinking Water Treatment Plant
EC	Electrical Conductivity
Elem.	Membrane element
IMS	Integrated Membrane System
IPR	Indirect Potable Reuse
LMH	Litres per square meter per hour
LRV	Log Removal Value
MF	Microfiltration
MLD	Million Litres per Day
NaCl	Sodium Chloride
NDMA	Nitrosodiemethylamine
NF	Nanofiltration
PV	Pressure vessel
RO	Reverse Osmosis
SI	Stability Index
TDS	Total Dissolved Solids
TMP	Trans-membrane Pressure
TOC	Total Organic Carbon
TSE	Treated Sewage Effluent
UF	Ultrafiltration
UV	Ultraviolet
UWWTD	Urban Wastewater Treatment Directive
VFD	Variable Frequency Drive
WFD	Water Framework Directive
WGWRP	Windhoek Goreangab Water Reclamation Plant
WWTP	Wastewater Treatment Plant

List of Symbols

A	Aperture area (m^2)
c_c	contraction coefficient
C_c	Solute concentration concentrate
c_d	discharge coefficient
C_f	Solute concentration, feed (system)
C_m	Solute concentration, feed (membrane)
C_p	Solute concentration permeate
c_v	velocity coefficient
d	Aperture diameter
EC	Electrical Conductivity
J_C	Contaminant mass flux
J_P	Permeate salt mass flux
P	Pressure
Q_c	Flowrate concentrate
Q_c	Contaminant flow
Q_d	Flowrate, to drain
Q_f	Flowrate, feed (system)
Q_f	Feed flow
Q_m	Flowrate, feed (membrane)
Q_p	Flowrate permeate
Q_P	Permeate flow
ρ	Density

Summary

The combination of two membrane technologies coupled together in series has become a standard technology when it comes to producing reclaimed water of high quality for potable reclamation or industrial applications. This combination of two membrane processes is referred to as integrated membrane systems (IMS). Despite the widespread experience gained utilizing such a process technology around the world, there are a number of aspects of the process technology which require further investigation including the fate of compounds of emerging concern (CEC), the control of *N*-Nitrosodimethylamine (NDMA) formation, the use of energy associated with the process and the total cost of producing the reclaimed water, and monitoring membrane integrity in RO treatment processes. The objective of this work was to further the knowledge in one aspect related to each of these four challenges and then bring each of these areas together in the discussion to understand whether proposing a decision support system for the online monitoring and operation of integrated systems would allow improvements to the current state-of-the-art.

The first results chapter deals with the fate of pharmaceuticals and their transformation products through the MBR-RO/NF process. The majority of published work focus on the removal of parent compounds of CEC through treatment processes. Often these parent compounds are excreted from the human body with a number of human metabolites which could be found at concentrations much greater than the corresponding parent chemical and can themselves be pharmacologically active (Petrie et al., 2015). For this reason, the focus of this work was to advance the knowledge in terms of understanding the fate of a number of pharmaceuticals and particularly their main human metabolites through the IMS process. The results showed that the two consecutive membrane processes, when seen as a whole, become a highly efficient process to remove all the studied compounds. When comparing the removal efficiencies of the RO and NF membranes, as expected, the RO membrane showed near complete removals (>99%) of all the compounds over various process conditions, whereas the NF membrane resulted also in high removal efficiencies (> 90%).

It has been shown that nitrifying WWTPs are better able to remove nitrosamines precursors when compared to non-nitrifying facilities (Sgroi et al., 2016a). Due to the poor removal of nitrosamines by RO and NF membranes and the high energy cost of removing them using UV processes as a last step in a treatment train, the focus of the second chapter of work was the removal of NDMA formation potential and individual precursors under nitrifying and non-nitrifying conditions (achieved by changing the aeration conditions of the bioreactor). The work also looked at the removal of NDMA formation potential and individual precursors by using an NF membrane to understand whether an

NF membrane would provide a high enough rejection of NDMA to achieve potable reclamation water quality targets. The results showed that during normal aerobic operation, implying a fully nitrifying system, the MBR pilot plant was able to reduce NDMA formation potential above 94%, however this removal percentage was reduced to values as low as 72% when changing the conditions to avoid nitrification. These results suggest that a fully nitrifying MBR system will support better removal of NDMA precursors during wastewater reclamation.

Unlike seawater RO systems, were systems operate with fairly constant process conditions due to the relatively constant feedwater salinity and temperature, wastewater shows diurnal variations which are catchment dependant. The objective of the next chapter was to explore whether these diurnal variations in wastewater quality, in terms of inorganic constituents and temperature, would justify the modification of RO process conditions (in terms of system recovery and pre-treatment dosing) to minimise the operational cost while considering the control of membrane fouling. The results showed that although there are limitations to the use of electrical conductivity (EC) as a main parameter to deduce the individual ionic constituents in a wastewater, given the right assumptions, the work has shown that it is possible to obtain a useful profile for a particular EC value which could be used in an online / real-time optimisation system. Through the presentation of a case considering the cost of energy and pre-treatment chemicals, the work showed that there is scope for online optimisation tool in terms of associating a cost to the current operating process conditions and then questioning whether there is a more cost-effective way to 'set' the system.

An EC sensor is a standard component on any RO/NF system. The way it is currently utilised in a system doesn't provide much information to the operator in terms of membrane integrity monitoring. The final results chapter explores the limits of detection of membrane integrity methods using EC sensors and provides a number of strategies to obtain a better characterisation of membrane integrity.

The results are brought together in the discussion of the work to provide a framework together with an initial rule-base for a knowledge-based decision support system for the real-time control of integrated membrane systems for wastewater reclamation.

Resum

La combinació de dos tecnologies de membrana acoblades en sèrie ha esdevingut un tecnologia consolidada degut a la capacitat de produir aigua d'elevada qualitat i potencialment reutilitzable per aplicacions industrials com fins i tot per ser potabilitzada. Tot i l'elevada experiència adquirida en aquests processos combinats, encara hi ha aspectes del procés que calen una investigació més profunda que inclogui el coneixement sobre l'eliminació dels compostos emergents, el control de la formació de N-Nitrosodimetilamines (NDMA), l'ús de l'energia associada amb el procés incloent el cost total de produir l'aigua reutilitzable, i el seguiment de la integritat de la membrana en el tractament amb osmosi inversa (OI). L'objectiu d'aquest treball recau en avançar en el coneixement dels aspectes relacionats amb cada un dels quatre reptes esmentats, per aconseguir discutir de forma conjunta la millor forma d'integrar aquest nou coneixement adquirit proposant un sistema d'ajuda a la decisió pel control i seguiment de l'operació de sistemes integrats de membrana (SIM).

El **primer capítol** de resultats encara l'avaluació dels fàrmacs i els seus productes de transformació a través del procés MBR-RO/NF. La majoria dels estudis publicats es centra en l'eliminació de compostos emergents i dels seus derivats a través del procés de membranes. La majoria dels compostos son excretats pels essers humans i es poden trobar a concentracions més elevades que els seus respectius compostos químics i poden ser farmacològicament actius. Per aquesta raó, el treball centra la recerca en avançar en el coneixement sobre entendre com aquests compostos es comporten i es transformen en esl SIM. Els resultats demostren com un procés combinat de membranes esdevé un procés altament eficient per l'eliminació dels compostos. Com era d'esperar el sistemes OI presenten rendiments molt elevats d'eliminació (>99%) tot i que els processos de NF assoleixen rendiments no menyspreables (>90%).

S'ha demostrat que les plantes de tractament d'aigües residuals (EDARs) amb processos de nitrificació son més eficients a l'hora d'eliminar precursors de les nitrosamines comparat amb aquelles que no tenen nitrificació. Degut al baix rendiment en eliminació de les nitrosamines en sistemes RO i NF i l'elevat cost en l'eliminació, utilitzant processos ultra-violeta com a darrera etapa d'un tractament, aquest **segon capítol** centra la recerca en l'eliminació dels precursors de NDMA i el seu potencial de formació sota condicions nitrificants i no nitrificants en un sistema combinat MBR-NF/RO. Els resultats han demostrat que en condicions nitrificants el procés MBR assoleix una reducció del potencial de formació de NDMA del 94% mentre que es redueix a un 72% quan la nitrificació es limita. Aquestes resultats suggereixen que un MBR amb completa nitrificació afavorirà

un completa eliminació dels precursors de NDMA durant el procés de tractament de l'aigua per reutilització.

L'aigua de mar tractada amb processos RO no presenta elevades oscil·lacions (temperatura i conductivitat) i per tant són sistemes que operen amb condicions bastant estables, en canvi l'aigua residual presenta variacions i elevats canvis en qualitat en un mateix dia. L'objectiu del **tercer capítol** de la tesi es explorar com aquesta variació diària de la qualitat de l'aigua d'entrada en termes de, constituents inorgànics i temperatura, justificaria la modificació de les condicions del procés de RO per minimitzar els costos operacionals mentre es controla l'embrutiment de les membranes. Els resultats han demostrat que encara que hi ha limitacions en l'ús de la conductivitat elèctrica com a paràmetre de seguiment per quantificar els compostos iònics en l'aigua residual, és possible utilitzar un perfil útil que pot ser usat de forma contínua i en línia per l'optimització del procés. El treball ha mostrat l'acoblament dels costos amb l'operació del procés, relacionant els costos energètics amb el pretractament amb compostos químics.

El sensor de conductivitat elèctrica (CE) és un paràmetre habitual en sistemes NF/RO. Aquest paràmetre, però, tot i que s'utilitza de forma habitual en aquests processos no proporciona molta informació al operaris sobre la integritat del sistema. El **darrer capítol** de resultats avalua els límits de detecció de la metodologia de la integritat de la membrana utilitzant sensors CE per proporcionar estratègies per caracteritzar millor la seva integritat.

Els resultats es combinen a la discussió de la tesi per proporciona un marc de treball junt amb una base de regles inicial per un sistema d'ajuda a la decisió basat en el coneixement pel control en temps real dels sistemes integrats de membrana per la recuperació d'aigües residuals.

Resumen

La combinación de dos tecnologías de membrana acopladas en serie se considera como una tecnología con un gran potencial para producir agua de levada calidad para ser potencialmente reutilizada en aplicaciones industriales y usada en procesos de potabilización. La elevada experiencia adquirida y demostrada en estos procesos combinados aún presenta un potencial recorrido en investigación para esclarecer el destino de compuestos emergentes, el control de la formación de N-nitrosaminas (NDMA), el uso de la energía asociada en el proceso incluyendo el coste total de producir el agua reutilizable y el seguimiento de la integridad de las membranas del proceso de osmosis inversa (OI o del inglés RO). El objetivo de este trabajo es profundizar en el conocimiento de los aspectos relacionados con cada uno de los cuatro retos anteriores, para conseguir discutir de forma conjunta la mejor estrategia para integrar el conocimiento nuevo adquirido proponiendo un sistema de ayuda a la decisión (SAD) para el control y seguimiento de la operación en sistema integrados de membrana (SIM).

El **primer capítulo** de resultados afronta la evaluación de los fármacos y sus derivados a través de un proceso MBR-NF/RO. La mayoría de los estudios publicados se han centrado en la eliminación de compuestos emergentes y sus derivados a través de la filtración. La mayoría de estos compuestos son excretados por el ser humano y se pueden encontrar en concentraciones más elevadas que sus respectivos compuestos químicos y pueden ser farmacológicamente activos. Por esta razón, el trabajo se centra en avanzar en el conocimiento para entender en mayor grado cómo estos compuestos se comportan en estos SIM. Los resultados han demostrado que dos procesos de membrana contiguos consiguen un elevado rendimiento de eliminación. Siendo la RO el proceso con rendimientos mayores (>99%) que la NF (>90%).

Se ha demostrado que las Estaciones de Tratamiento de Aguas Residuales (EDARs) con procesos de nitrificación son más eficientes a la hora de eliminar las nitrosaminas comparados con aquellas EDARs sin nitrificación. Debido al bajo rendimiento de eliminación de nitrosaminas en sistemas RO y NF y a su elevado coste operacional cuando se le acopla un proceso UV como última etapa, este **segundo capítulo** afronta la investigación de la eliminación de los precursores de los NDMA y su potencial de formación bajo condiciones nitrificantes y no-nitrificantes en un sistema combinado MBR-NF/RO. Los resultados han mostrado que en condiciones nitrificantes el proceso MBR alcanza unos rendimientos de reducción del potencial de formación de NDMA en un 94%, mientras que si se

limita la nitrificación el potencial se reduce al 72%. Estos resultados sugieren que un MBR con nitrificación completa favorecerá la eliminación de los precursores de NDMA durante el proceso de tratamiento de agua para reutilización.

Aunque el agua de mar tratada con procesos de RO presenta estabilidad de condiciones, en términos de temperatura y conductividad, el agua residual presenta mayores oscilaciones y perfiles diarios. El tercer capítulo de la tesis explora como esta variación diaria del agua de entrada, en base a temperatura y constituyentes inorgánicos, puede justificar la modificación de las condiciones de operación para minimizar costes y controlar el ensuciamiento de las membranas de RO. Los resultados han demostrado que todavía hay limitaciones en el uso de la conductividad eléctrica (CE) como parámetro de seguimiento para cuantificar los compuestos iónicos, por ello este **tercer capítulo** del trabajo ha demostrado que es posible utilizar un perfil único de forma continua y en línea para la optimización del proceso. También se ha demostrado que los costes de operación están relacionados con el coste energético y el uso de compuestos químicos en el pre-tratamiento del proceso.

El sensor de CE es un parámetro habitual en sistemas de NF/RO, aunque proporciona mucha información sobre el proceso todavía no ayuda a cuantificar la integridad de la membrana. Este **último capítulo** evalúa los límites de detección en la metodología de integridad de la membrana utilizando el sensor CE para proporcionar estrategias para mejorar su integridad.

Los resultados se han combinado en la discusión para proporcionar un marco de trabajo junto a una base de reglas iniciales para un sistema de ayuda a la decisión basado en el conocimiento para el control en tiempo real de sistema integrados de membrana para la recuperación de aguas residuales.

List of Publications/Conferences/Final projects supervised

The following is a list of publications that have been included as part of this doctoral thesis:

Mamo, J., García-Galán, M.J., Stefani, M., Rodríguez-Mozaz, S., Barceló, D., Monclús, H., Rodriguez-Roda, I., Comas, J., 2018. Fate of pharmaceuticals and their transformation products in integrated membrane systems for wastewater reclamation. Chem. Eng. J. 331, 450–461. https://doi.org/10.1016/j.cej.2017.08.050

Mamo, J., Insa, S., Monclús, H., Rodríguez-Roda, I., Comas, J., Barceló, D., Farré, M.J., 2016. Fate of NDMA precursors through an MBR-NF pilot plant for urban wastewater reclamation and the effect of changing aeration conditions. Water Res. 102, 383–393. https://doi.org/10.1016/j.watres.2016.06.057

The following is a list of publications that has resulted from this work:

Finocchiaro, R., Farré, M.J., Mamo, J., Roccaro, P., 2017. On-Line Monitoring of NDMA Precursors in MBR-NF Pilot Plant by Using Fluorescence EEM, in: Mannina, G. (Ed.), Frontiers in Wastewater Treatment and Modelling: FICWTM 2017. Springer International Publishing, Cham, pp. 172–177.

Farré, M.J., Insa, S., Mamo, J., Barceló, D., 2016. Determination of 15 N-nitrosodimethylamine precursors in different water matrices by automated on-line solid-phase extraction ultra-high-performance-liquid chromatography tandem mass spectrometry. J. Chromatogr. A. 1458, 99-111.

Chapter 1 - Introduction

This chapter provides a general introduction to the research topic. A more detailed introduction to each chapter is provided in each of the individual chapters.

1.1 Wastewater Reclamation

In large parts of the industrialised world, wastewater from domestic and industrial sources is treated before being discharged into the environment. The degree to which wastewater is treated is typically prescribed by discharge regulations which in Europe are outlined in the *Urban Wastewater Treatment Directive* (Directive 91/271/EEC). This would typically involve the removal of biodegradable organic matter and suspended solids before discharge in a process which is termed a secondary treatment of wastewater (after a primary treatment process referring to the removal of only a portion of organic matter and suspended solids). When there are large volumes of wastewater being discharged into the environment or the water is being discharged into an ecologically sensitive area, then nutrient removal, namely nitrogen and phosphorous, is also required.

As the availability of local natural water supplies in many arid and semi-arid regions of the world diminishes, increasing pressure from population growth and raising standards of living require the reliance on 'alternative' or 'non-conventional' water supplies such as the desalination of sea and brackish waters or the treatment of wastewater to a degree that enables reclamation. The required water quality and thus the degree of further treatment following the secondary treatment process depends on the planned reclamation application. According to Tchobanoglous et al. (2003) there are seven main areas of water reclamation namely

i. agricultural irrigation
ii. landscape irrigation, including the irrigation of parks, golf courses, residential and roadside landscaping etc.
iii. industrial reclamation and recycling including cooling water, boiler feed, process water, etc.
iv. groundwater recharge for groundwater replenishment and saltwater intrusion barriers
v. recreational/environmental uses including stream-flow augmentation, lakes and ponds, etc.
vi. non-potable urban uses such as fire protection, air conditioning and toilet flushing
vii. potable use including blending in water supply reservoirs, surface water or groundwater reserves which are utilised for potable purposes.

Potable water reclamation applications are those which produce potable water as its final product. In literature, we typically find potable water reclamation applications classified into three different types, de facto potable reclamation, indirect potable reclamation and direct potable reclamation. De Facto potable reclamation is common in the EU and around the world (Drewes et al., 2017). Figure 1-1 (a) gives a representation of de facto reclamation were reclaimed water from a wastewater treatment plant (WWTP) serving an upstream town or city is discharged into a river and then

abstracted again by the next town or city before being treated at a drinking water treatment plant (DWTP) for use by the city and finally being treated in a WWTP before being discharged back into the environment.

Indirect potable reclamation (IPR) is the augmentation of natural drinking water supplies (typically either surface water or groundwater) using reclaimed water via an environmental buffer as shown in Figure 1-1 (b). Such water reclamation schemes typically involve tertiary or advanced treatment processes such as membranes and/or advanced oxidation processes (AOP) which go a step further than typical WWTPs. IPR has been practiced in the U.S., Singapore, Australia and Belgium in the EU among other places around the world for more than 50 years, some of which have been producing large quantities of water for a number of years including the 380 000 m^3/day Orange Country Groundwater Replenishment Scheme (California, US) and the Changi indirect reuse plant in Singapore producing 450000 m^3/day. This long-term operational experience together with advancements in microbiology, toxicology and analytical chemistry have provided a high degree of confidence in the practice of drinking water augmentation.

Direct potable reuse (DPR) is the immediate addition of highly treated sewage effluent (TSE) either directly to a drinking water distribution system, or to the raw water supply directly upstream of a drinking water treatment facility as shown in Figure 1-1 (c). There are currently two plants doing DPR in the world, Windhoek Goreangab Water Reclamation plant (WGWRP) (Winhoek, Namibia) and Big Spring Water Treatment Plant in Texas (Texas, US). Wichita Falls (Texas, US) temporarily carried out DPR in 2014 for 11 months and is in the process of implementing a permanent IPR scheme. There are also a number of DPR schemes in the US which are in different phases of planning and approval including the Village of Cloudcroft and El Paso Advanced Water Purification facility which is under regulatory approval (USEPA, 2017)

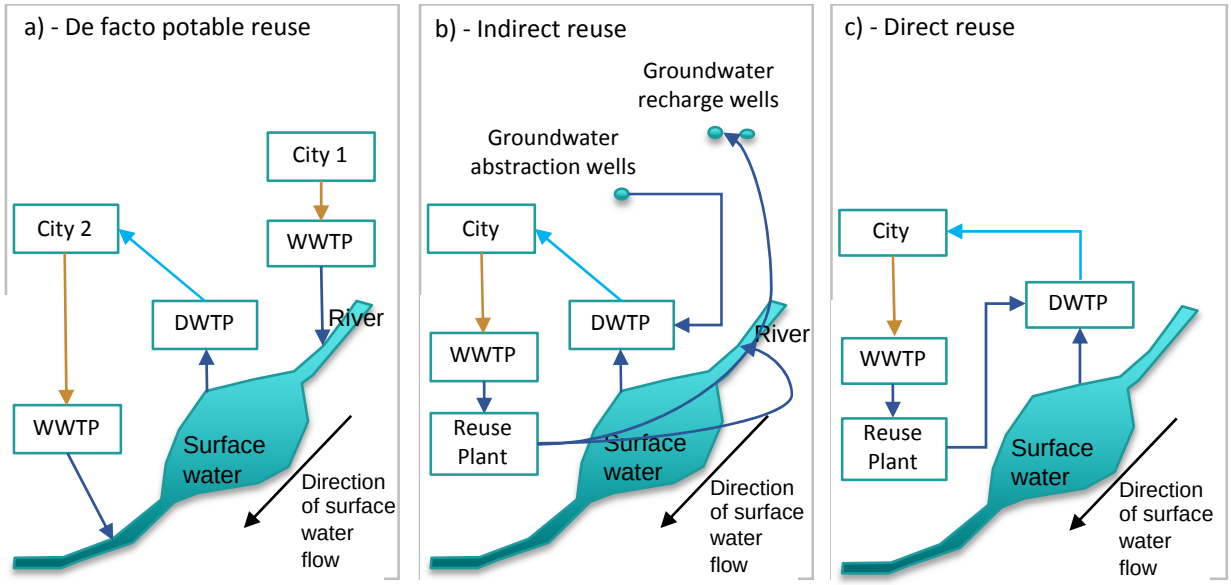

Figure 1-1: Schematic illustrating different types of potable reclamation schemes

As wastewater reclamation gains traction around the world there has been an increasing amount of data from operational reclamation trains to allow a broad consensus on the technologies that will comprise a typical water reclamation treatment train, and the ability for these processes to offer sufficient barriers to remove all pathogens and compounds of emerging concern (CEC) safe for potable use without the use of an environmental buffer. Reviewing potable water reclamation treatment trains shows that typically a number of technologies, as shown in Figure 1-2 (USEPA, 2017), combining conventional, membrane, AOP and biological filtration/adsorption in series to offer redundancy in system performance and ensure a robust treatment process reducing the health-based risk of reusing wastewater.

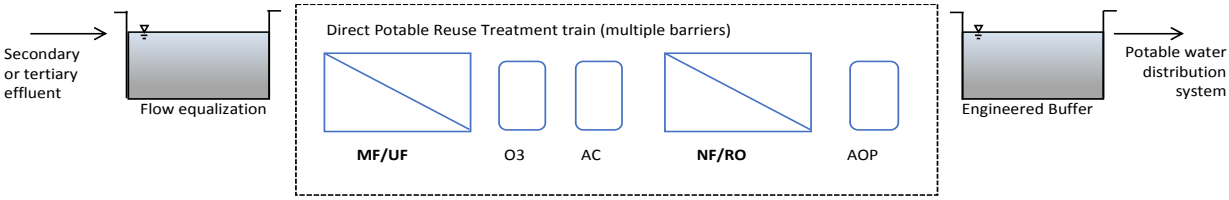

Figure 1-2: Typical water reclamation treatment train

1.2 Membrane Technology

Membrane technologies are becoming a standard form of advanced wastewater treatment processes when the reclamation application requires the removal of both suspended and dissolved organic constituents after the secondary treatment process. Membranes serve as a selective barrier which can allow the passage of certain constituents while retaining particulate, colloidal and dissolved matter typically between 0.0001µm and 1µm (Tchobanoglous et al., 2003). The operating range of membrane processes is typically broken down into four types as given in Table 1-1 below.

With regards to wastewater reclamation, microfiltration (MF) and ultrafiltration (UF) are typically utilised as a pre-treatment for disinfection where the objective is to remove residual suspended solids following a secondary treatment process before disinfection with chlorine or UV, or else as a pre-treatment step to remove residual colloid and suspended solids before a Nanofiltration (NF) or Reverse Osmosis (RO) treatment step. In wastewater reclamation, NF and RO are typically utilised either when the salinity of the treated wastewater restricts its application for agricultural, landscaping or industrial use or when certain dissolve constituents need to be removed usually prior to potable water reclamation applications.

Table 1-1: Characteristics of membrane processes (Tchobanoglous et al., 2003)

Membrane process	Typical operating range (μm)	Typical constituents removed
MF	0.08-2	TSS, turbidity, protozoan oocysts and cysts, some bacteria and viruses
UF	0.005-0.2	Macromolecules, colloids, most bacteria, some viruses, proteins
NF	0.001-0.01	Small molecules, some hardness, viruses
RO	0.0001-0.001	Very small molecules, color, hardness, sulphates, nitrate, sodium and other ions.

Although the majority of the operational wastewater reclamation facilities utilizing Integrated Membrane Systems (IMS) referred to in this chapter operate at a municipal level and have a high throughput, such processes have also been downscaled to produce tens of cubic meters per day particularly in hotels and resorts. Often there isn't much information available about smaller scale facilities other than pilot facilities for research purposes. For this reason, apart from considering the requirements of high capacity systems, one should also consider smaller decentralized water reclamation systems which have their own operational challenges including the lack of economies of scale for extensive water quality analysis and online monitoring systems and that such systems operate mostly unmanned.

1.3 Integrated Membrane Systems and colloidal fouling control

IMS are treatment processes (also known as treatment trains) which combine two membrane processes in series, typically MF or UF followed by NF or RO. Other than providing an additional barrier for the removal of constituents as given in Table 1-1, the first membrane process is essential as a pre-filtration step for the removal of particulate and colloidal solids which must be removed prior to the wastewater reaching the NF or RO membrane to keep the second membrane process operating in a sustainable manner. Colloidal fouling is one of the primary forms of fouling in wastewater treatment utilizing RO and NF membranes and may consist of both organic foulants as well as inorganic foulants such as aluminium silicates (Bartels et al., 2005). NF and RO membranes get fouled very quickly if the feedwater does not meet certain requirements in terms of colloidal

constituents, and therefore this 'pre-treatment' step is always necessary when employing dense membranes to treat wastewater.

Figure 1-3 shows various combinations of treatment trains which utilize both membrane technologies together with other non-membrane technologies mostly involving disinfection and/or AOP. Sometimes specific treatment steps such as electrodialysis is utilised depending on the feedwater quality and the reuse application. The first set of configurations (Figure 1-3 a, b, c), where IMS are utilized to further treat secondary treated wastewater with or without nitrification and biological nutrient removal, are referred to as 'polishing' systems, while those systems which treat primary treated wastewater (Figure 1-3 d, e) are referred to as 'Total' systems (Raffin et al., 2012) typically utilizing membrane bioreactor (MBR) technology.

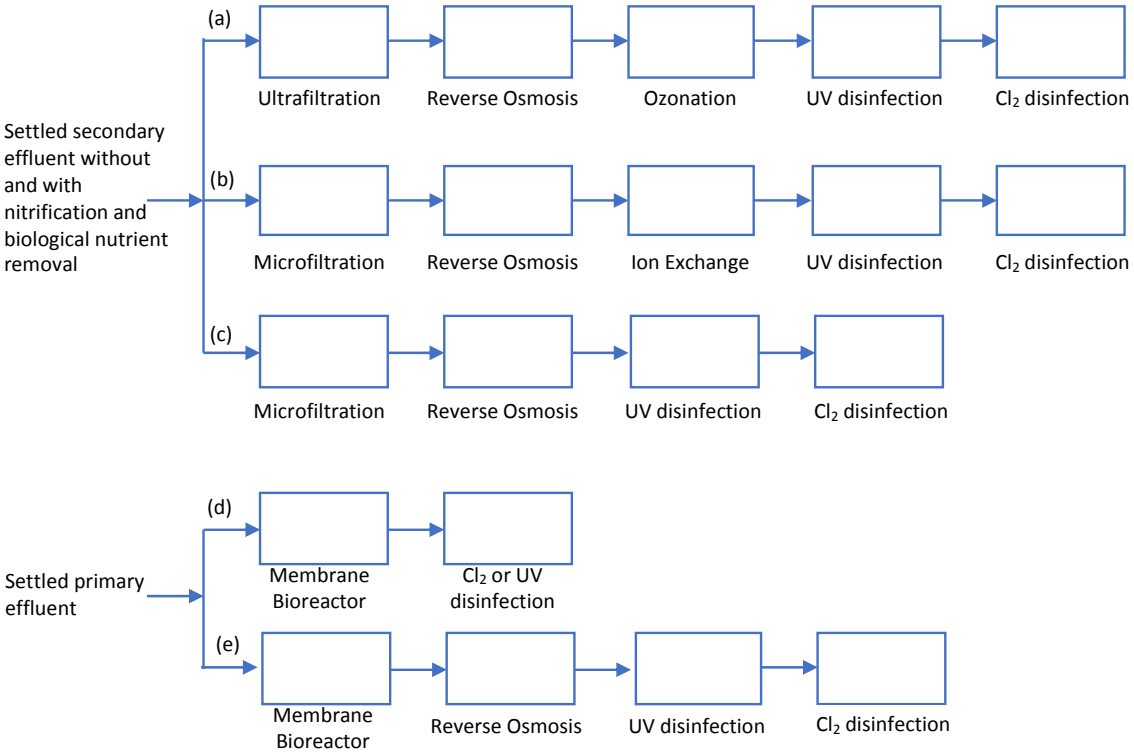

Figure 1-3: Membrane water reclamation process configurations (Tchobanoglous et al., 2003)

MBR technologies utilize a membrane to separate the treated wastewater from the active biomass in an activated sludge process. The membrane can either be immersed in the bioreactor or external to the bioreactor. In immersed systems, permeate is extracted from the biomass through the membrane (MF or UF) by the application of a vacuum (typically operated with a trans-membrane pressure of 300-400 mbar). Aeration is applied below the immersed membrane to apply a shearing action by rising air bubbles. Aeration can either be continuous aeration or intermittent. Various studies have shown that the quality of the MBR effluent is suitable for various use applications where high quality effluent is required (Bérubé, 2010; Côté et al., 2004; Daigger et al., 2015; Marti et

al., 2011) or as a pre-treatment process for RO or NF technologies (Alturki et al., 2010; Chon et al., 2011; Dialynas and Diamadopoulos, 2009; Garcia et al., 2013). Further information about the application and operation of MBRs can be found in Judd and Judd (2008) and previous PhD dissertations carried out within the LEQUIA research group (Dalmau Figueras, 2014; Gabarrón Fernández, 2014; Monclús Sales, 2011)

Typically, total systems employing MBR are suitable for newly conceived projects, while polishing plants are typically utilized when the need arises to upgrade the quality of the effluent from an existing conventional WWTP for industrial or potable reclamation. Table 1-2 gives a number of advantages for the two different approaches. The costs involved in operating various configurations of IMS are further discussed in section 1.9.3.

Table 1-2: Advantages of using MBR vs CAS+MF/UF as a pre-treatment step to RO membranes

Approach	Advantages of one approach over the other	Reference
MBR	Efficient use of space: The ability to couple the bioreactor with the secondary separation process whilst producing permeate which is suitable to feed dense membranes is an advantage if land availability is restricted or expensive.	(Judd and Judd, 2008)
	Reduced excess sludge production	(Wagner and Rosenwinkel, 2000)
	High biomass concentrations and long sludge retention time (SRT) positively affects the overall activity of slow growing microorganisms acting in nitrification.	(Côté et al., 2004)
	High biomass concentrations and long SRT has also been shown to positively affect slow growing microorganisms which are better able to degrade specific refractory pollutants	(Clara et al., 2005)
	Higher stability and ability to withstand shock loads	(Melin et al., 2006)
	Reduced operating cost: Because immersed systems typically operate using low suction pressures, the operating cost of immersed systems is typically lower than that of pressurized systems.	
CAS + MF/UF	Flexibility: An additional clarification step allows an intermediate product water quality to be produced at a lower cost to MBR permeate if an application is available or if there are periods of the year when there is no demand for the high-quality product.	
	Lower capital costs: Since the feedwater in polishing systems has already been clarified, the fluxes which can be achieved in pressurized MF/UF will be much higher than in MBR. This increased permeate flux will require a smaller effective membrane area and thus reduce the capital cost of the system	
	Suitable to retrofit conventional WWTP.	

A number of pilot studies have compared the quality of MBR permeate to permeate from an CAS+MF facility and showed that using MBR permeate it has been possible to operate the RO at elevated fluxes. Qin et al. (2006) showed that utilizing an MBR process, due to the improved nutrient removal efficiencies of the MBR over the CAS, it was possible to operate the RO at a sustainable flux

of 22 $Lm^{-2}h^{-1}$ without additional cleaning, while it was only possible to operate at a flux of 17 $Lm^{-2}h^{-1}$ when treating CAS treated effluent using MF membranes. As part of a WateReuse Foundation project titled 'Pilot-Scale Oxidative Technologies for Reducing Fouling Potential in Water Reuse and Drinking Water Treatment Membrane Systems', Hydranautics showed that it is possible to operate sustainably at an elevated flux of 23.7 $Lm^{-2}h^{-1}$ when utilizing MBR permeate as feed which is above the typical average permeate flux rates recommend when treating wastewater (Hydranautics, 2010). Following the results from Qin et al. (2006), the Public Utilities Board (PUB) in Singapore mention that it is exploring the implementation of the MBR-RO process for Changi Water Reclamation Plant which is currently operating with MF+RO. This is being carried out because the process is producing equal or better quality water than the current process and the MBR process requires a smaller footprint than the current activated-sludge/MF/RO process with the MBR replacing the aeration tanks, final sedimentation tanks and MF tanks (Lee and Tan, 2016).

Table 1-3 provides a list of the ten largest operational reclamation facilities which utilize membranes. The list shows that six out of the ten largest facilities in the world are based on MF/UF alone with the majority of these being installed to improve the quality of secondary treated effluent for irrigation. It is clear that the facilities which require the RO step did so to produce a product water suitable either for potable or industrial reclamation.

Table 1-3: List of the large membrane based water reclamation facilities (Gagne, 2005; Lee and Tan, 2016; M. Raffin et al., 2012)

Facility	Membrane Type	Application	Capacity m^3/day	Year Commissioned
Doha North, Qatar	MF/UF	Irrigation	440 000	2011
Sulaibiya, Kuwait	MF/UF + RO	Irrigation	375 000	2004
Orange County, USA	MF/UF + RO	Groundwater recharge	328 000	2008
Changi, Singapore	MF/UF + RO	Industry, IPR	232 000	2010
Ulu Pandan, Singapore	MF/UF + RO	Industry, IPR	191 000	2007
Bedok and Kranji	MF/UF + RO	Industry, IPR	159 000	2009, 2008
Gwinnet County, GA, USA	MF/UF	Irrigation	289 000	2005
Doha South, Qatar	MF/UF	Irrigation	187 000	2012
Qinghe Phase II, China	MF/UF	Industry, Irrigation, non-potable reuse	180 000	2010
Agra, India	MF/UF		144 000	2010
Doha west, Qatar	MF/UF	Irrigation	135 000	2009
Bundamba, Australia	MF + RO	Industry, IPR	100 000	2008
Gibson Island, Australia	MF + RO	Industry, IPR	100 000	2008
Luggage Point, Australia	MF + RO	Industry, IPR	100 000	2008

In the majority of cases, MF or UF processes have replaced coagulation/flocculation/clarification processes and/or multimedia filtration which were previously employed to condition the feedwater to be suitable for RO/NF processes. Figure 1-4 shows the difference in process flow before (a) and after (b) the introduction of MF membranes into the process train at the Orange County Groundwater Replenishment System (GWRS). Built in 1976 the initial Water Factory 21 (Figure 1.4 a) had a treatment capacity of 15 MGD and was utilised for groundwater recharge as a seawater intrusion barrier. In 2004 the facility was replaced by the GWRS and currently produces 100 MGD for IPR through groundwater recharge via direct injection and spreading basins (USEPA, 2017).

A widely used measurement to determine the suitability of a water to be treated by RO and NF membranes is the Silt Density Index (SDI). The test utilizes a 0.45 μm (47mm diameter filter) at a specified pressure of 2.1 bar to measure the difference between the initial time to collect a sample of 500 mL and the time it takes to collect a 500 mL sample after 15 minutes of water passing through the membrane. The SDI is define by the following equation (Tchobanoglous et al., 2003):

$$SDI = \frac{100\ (\ 1 - \frac{t_i}{t_f})}{t}$$

Where t_i: time to collect the initial sample of 500 mL

t_f: time to collect the final sample of 500 mL

t: total time of running the test (typically 15 minutes).

To take into account the rate of change of resistance other tests have been developed such as the modified fouling index (MFI) where the volume of water is recorded every 30 seconds over a 15-minute filtration period (Dow Water & Process Solutions, 1995).

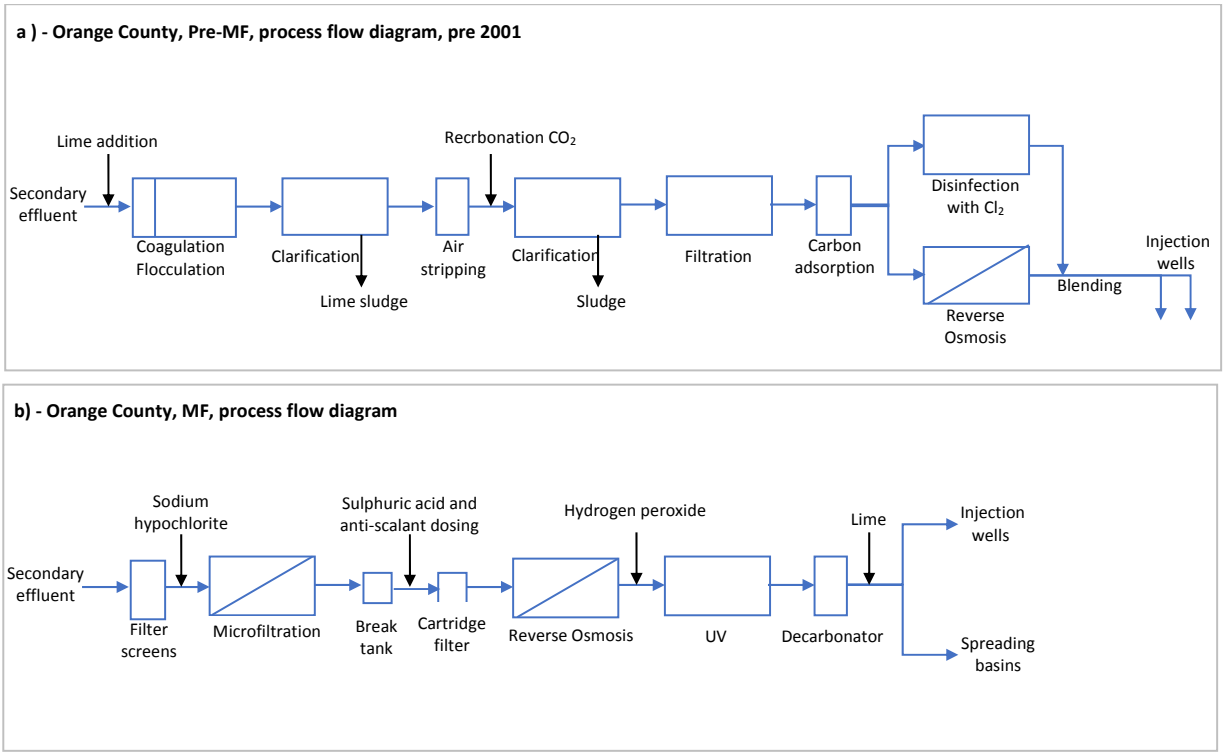

Figure 1-4: Comparison of Orange Country process flow, pre and post introduction of MF pre-treatment (Tchobanoglous et al., 2003)

RO and NF membranes typically require an SDI of less than 3 to operate sustainably over the long term (Dow Water & Process Solutions, 1995). To meet these feedwater quality requirements, MF and UF have become a standard pre-treatment for RO and NF treating wastewater. It has been shown that MF and UF is able to consistently produce an SDI between 0.5 and 2.5, whilst an SDI of 4.5 to 6 is typically achieved utilizing lime clarification and media filtration (Bartels et al. 2005).

1.4 RO/NF feedwater and pre-treatment

Other than colloidal fouling which is controlled using MF or UF membranes, other forms of fouling must also be controlled when considering RO and NF membrane technologies. Table 1-4 provides an overview of the various types of membrane fouling associated with the RO and NF treatment of wastewater. Membrane fouling will affect the pre-treatment and cleaning requirements, together with the operating conditions, capital and operating costs and membrane performance and is therefore a constant consideration when speaking about RO and NF membrane technologies.

Table 1-4: Different types of membrane fouling, their respective responsible constituents and control measures (adapted from Dow Water & Process Solutions, 1995; Tchobanoglous et al., 2003)

Type	Responsible Constituents	Mitigation measures
Fouling	Colloidal matter – both organic and inorganic	Pre-treatment of secondary effluent by chemical clarification, multimedia filtration, MF or UF for the removal of colloidal particles
	Bacteria and other microorganisms	Disinfection of feed water using chlorine or UV and the removal of any residual oxidants
	Dissolved organic matter	- Ensure secondary treatment process operates well - Dosing of a coagulant prior to MF or UF pre-treatment - Reduce flux rate.
Scaling	- Calcium carbonate - Calcium phosphate - Silica	Controlling the precipitation of such sparingly soluble salts by: - Controlling system recovery - Reducing the pH of the feedwater - Dosing of antiscalants
Irreversible damage	- Acids - pH extremes - Free chlorine or other oxidants	Typically controlled by limiting the frequency, duration and concentration of contact of membranes to such substances for necessary cleaning procedures The presence of free chlorine is typically monitored utilising redox probes and is removed utilising sodium bisulphite, sodium thiosulphate or activated carbon.

1.4.1 Biological fouling

Due to concentration polarization, dissolved nutrients entering with the feed water enrich the membrane surface with dissolved nutrients making ideal conditions for growth of microorganisms on the membrane surface. Concentration polarization is the increase in concentration of a solute in a thin boundary layer at the feed side of a membrane surface (Dow Water & Process Solutions, 1995). Once established it is difficult to remove due to the protection offered by the biofilm to sheer forces and biocides and will re-establish itself quickly if not completely removed during a chemical cleaning procedure. Biological fouling will reduce the permeability the membrane and lead to an increased pressure drop along the feed channel.

Biological fouling is effectively controlled by preventative mechanisms including the removal of bacteria in the feedwater by using MF or UF membranes together with the continuous or intermittent use of a chloramine residual (Bartels et al., 2005). Unlike free chlorine which has very limited uses with polyamide membranes before reducing the performance, RO membranes show a higher tolerance to chloramines. Typically a chloramine concentration of between 2-5 mg/L is dosed to MF or UF pre-treated feedwater for biofouling control. Van Houtte and Verbauwhede (2008) reported that the initial dose of 3.6 mg/L of sodium hypochlorite and 2.5 mg/L of ammonium chloride was reduced by moving from a continuous dosing to intermittent dosing according to the temperature of the water. This measure reduced the consumption of sodium hypochlorite by 20%

and that of ammonium chloride by 35%, reducing operational costs significantly whilst controlling biofouling. Bartels et al. (n.d.) states that as long as there is effective filtration of colloidal material from the in-coming feedwater, and there is chlorine dosing to maintain a few parts per million (ppm) of chloramines, the RO membranes can operate very stably. This is confirmed by the numerous operating facilities operating sustainably.

That said, while minimizing the dose of chloramines for biofouling control, it is important that the initial dose is sufficient to be effective even on the last membrane elements in the final stage of the RO system. Raffin et al. (2012) mentions that a chloramine dose of 1 mg/L did not control the microbial population in the feedwater. Since the rejection of chloramines by the RO membrane is low, the residual chloramines concentration decreases along the length of the membrane (Xu et al., 2010) which explains why no residual chloramines were measured in the concentrate of the three-stage system by Raffin et al. (2012), but measured in the permeate of the system.

Another important control measure is limiting the amount of nutrients, particularly phosphate, in the membrane process feedwater by ensuring good biological nutrient removal in the secondary treatment process (Dow Water & Process Solutions, 1995). Vrouwenvelder et al. (2010) showed that low phosphate concentrations (< 0.3 μg/L) in the feedwater controlled the formation of biofilms even when there were high organic carbon concentrations. The study also showed that dosing phosphonate based antiscalants had a significant effect on biofouling when compared to no biofouling when only acid or phosphonate-free antiscalants where dosed. This study states that "since no biofouling was observed at low phosphate concentrations, restricting biomass growth by phosphate limitation may be a feasible approach to control biofouling, even in the presence of high organic carbon levels'' (Vrouwenvelder et al., 2010).

1.4.2 Organic fouling

Secondary treated wastewaters can contain relatively high concentrations of dissolved organic material, with a Total Organic Carbon (TOC) concentration typically between 5 and 20 mg/L and a Biochemical Oxygen Demand of between < 2 – 10 mg/L (Bartels et al., 2005; Gagne, 2005; Tchobanoglous et al., 2003). RO membrane manufacturers recommend that suitable pre-treatment is included when the TOC of a feed water is above 3 mg/L to avoid the adsorption of organic substances on the membrane surface causing flux loss (Dow Water & Process Solutions, 1995).

Measures to control organic fouling include the selection of the right type of membrane, use of a coagulant prior to the MF or UF pre-filtration process or reducing the average permeate flux (Bartels et al., 2005).

As mentioned when speaking about biofouling, a key measure is to ensure that a robust biological nutrient removal process is well designed and well operated to control the amount of dissolved organic material in the effluent of the secondary treatment process.

1.4.3 Scaling

The main sparingly soluble salts which need to be controlled in RO/NF systems treating wastewater are calcium carbonate ($CaCO_3$), calcium phosphate ($Ca_3(PO_4)_2$) and silica (Bartels et al., 2005; Chesters et al., 2007; Dow Water & Process Solutions, 1995; Greenberg et al., 2005; Malki and Abbas, 2013; M. Raffin et al., 2012; Marie Raffin et al., 2012).

The solubility of $CaCO_3$ depends on the pH of the systems as shown in the following equation:

$$Ca^{2+} + HCO_3^- \leftrightarrow H^+ + CaCO_3$$

Typically, calcium carbonate scaling is controlled by adding acid to shift the equilibrium to keep it in a dissolved form. This is typically expressed by the Langelier Saturation Index (LSI) where at the pH of saturation (pH_s), the water is in equilibrium with $CaCO_3$. To control calcium carbonate scaling by acid addition alone, the LSI in the concentrate stream must be negative (ASTM, n.d.; Dow Water & Process Solutions, 1995). Typically, when other salts are close to saturation a scale inhibitor is also utilized. Alternatively, the system recovery can be reduced to reduce the concentration of the sparingly soluble salt in the feed/concentrate stream.

Calcium phosphate precipitation often occurs on the last membrane element of the last stage of the RO plant, where phosphate is concentrated.

Malki and Abbas (2013) showed that the best way to control the precipitation of silica on RO in reclamation applications is to inhibit the formation of phosphate salts. They also showed that silica polymerized within and around the phosphate salt precipitation is not removed when phosphate is cleaned using low pH cleaners or online using periodic drops in pH. Typically calcium phosphate fouling is controlled by acidifying the feedwater and utilising a proprietary antiscalant(Bartels et al., 2005).

Of the nine plants surveyed by Raffin et al. (2012), three facilities said they utilize only acid for pH control, while two facilities said they use both acid and an antiscalant, while one facility mentioned that it uses only antiscalant in its scaling control. Typically, it is $Ca_3(PO_4)_2$ precipitation that limits the recovery of a system. One example of this found in literature is the Sulaibiya Water Reclamation Plant (Kuwait City) operating at 85% recovery (3-stage, PO_4^{3-} concentration in feed < 15 mg/L) which “is limited by calcium phosphate precipitation” (Gagne, 2005). Although no information is given in Raffin’s survey about the type of chemicals added to control scaling, it is assumed that acid addition

(AlGhusain, 2013) and an antiscalant are also added. In the case of Singapore's NEWater facilities dosing of sulphuric acid was reported for Cranji (2-stage, 75% recovery) and Ulu Pandan (2-stage, 80% recovery) NEWater facilities following the experience at the Bedok facility which experienced calcium phosphate fouling and was later controlled using "acidification of the feed or optimization of the antiscalant" (Bartels et al., 2005). Orange County Groundwater Replenishment Scheme (3-stage, 85% recovery) on the other hand uses a combination of both sulphuric acid and antiscalant (AWC A-102 Plus) (M. Raffin et al., 2012)

There has been a push for a reduction in the use of acid in controlling precipitation for reasons of health and safety in the transporting, handling and storing of acid and to reduce the susceptibility of plant piping and equipment to corrosion (Chesters et al., 2007). Moreover significant quantities of acid are usually required when there is a high bicarbonate concentration in feedwater which is normally the case for secondary treated wastewater. Raffin et al. (2012b) showed that replacing acid dosing with antiscalants could amount to a cost reduction of 67–77% for zero acid dosing when compared to pH adjustment to 6.25.

Although in some cases antiscalant supplier's software shows that under certain conditions no pH adjustment is necessary while using antiscalant, in practice it is hard to operate such facilities without pH adjustment (Greenberg et al., 2005; Raffin et al., 2012). Again, the importance of nutrient removal, including P removal, as part of the secondary treatment process is highlighted to control fouling and thus the sustainable operation of such reclamation facilities utilising RO/NF membrane processes.

1.5 Membrane type - RO and NF membranes

Unlike RO, NF membranes are not a complete barrier to dissolved solids and in water treatment applications are typically utilized for the removal of multivalent metallic ions. The parameters which characterize the performance of a membrane are the water permeability and the solute permeability (Dow Water & Process Solutions, 1995). For NF membranes the solute permeability depends both on the type of solute but also on the type of membrane. The difference in performance between 'tight' NF membranes and 'low energy' RO membranes is sometimes minimal with 'tight' NF membranes with a low permeability showing osmotic pressure differences similar to RO membranes. The difference in rejection performance of NF over RO membranes is primarily in terms of monovalent ion separation (Bellona et al., 2012).

Membrane manufacturers typically have a range of both RO and NF membranes each having a particular permeability with membranes having a higher permeability marketed as low energy membranes while membranes with a lower permeability referred to as high rejection (HR)

membranes. Fouling Resistant (FR) membranes are also marketed and utilized by reclamation facilities and these are said to 'minimize or retard biofouling' when utilized with or without intermittent dosing of a biocide. Another development for RO/NF membranes used in wastewater reclamation is the use of thicker feed channel spacer which reduces pressure losses in the feed channel along the pressure vessel (PV) (Bartels et al., n.d.; Dow Water & Process Solutions, 1995).

Using bench experiments, Yangali-Quintanilla et al. (2010), concluded that NF may be preferable over RO membranes in terms of being an effective barrier for organic contaminants with reduced operation and maintenance costs (O&M). Bellona et al. (2012) showed that an NF membrane with a high permeability (Dow Filmtec NF270) operated at significantly higher specific fluxes with minimal flux decline when compared to the RO membrane tested (Industry standard Hydranautics ESPA2 membrane) which could translate into significant annual cost savings in terms of decreased energy use and cleaning requirements. In terms of water quality, the major limitation of the NF membrane was the poor rejection of nitrate and the inability to meet the California Department of Public Health's Groundwater Recharge draft regulations TOC limit of 0.5 mg/L with permeate concentrations averaging 0.62 mg/L, which was met using the ESPA2 membrane using the same feedwater.

1.6 RO/NF System Design

The RO/NF system design is particularly conditioned by the quality of the feedwater coming in contact with the membrane. In the case of RO/NF as part of an IMS for wastewater reclamation, the quality of the raw influent water entering the WWTP, the performance of the biological wastewater treatment process and the MF/UF pre-treatment. The concentration of fouling constituents on the membrane surface increases with (1) the permeate flux, the permeate flow rate per unit membrane area (L m^{-2} h^{-1}), and (2) the system recovery for a single element, which is the ratio of the permeate flow to the feed flow (%).

The average permeate flux of a system, which is the ratio of the total system permeate flow to the total active membrane area, is one of the principle values which characterizes a system and typically better-quality feedwater will allow the operation of higher fluxes. System designs operating on similar feedwater designed with a high flux value place emphasis on minimizing the capital cost while designs operating at a lower flux will be minimising the long term operational cost (Dow Water & Process Solutions, 1995). Operating reclamation facilities have an average permeate flux between 17 and 20 L m^{-2} h^{-1} (Bartels et al., n.d.; M. Raffin et al., 2012). It is assumed that the lower average system flux seen in the NEWater plants in Singapore (18 and 17 L m^{-2} h^{-1} for Ulu Pandan and Cranji respectively) come from the piloting work and early experience with reclamation facilities operating

on secondary treated wastewater and the organic fouling and calcium phosphate scaling experienced during the initial days of operation (Bartels et al., 2005). Many other facilities such as Orange County GWRS, Luggage Point Australia, operate with fluxes in the region of 20 L m^{-2} h^{-1} sustainably and this seems to be a relatively standard value. Although there are cases where it was possible to increase the flux values beyond this point (as mentioned earlier when describing the benefits of using MBR over CAS+MF/UF), increasing above this recommend limits begins to reduce the amount of crossflow which sweep solids from the surface of the membrane. It has been shown that there is an optimum ratio of crossflow to permeate flow to keep the surface clean and minimize the energy consumption (Bartels et al., n.d.). This is particularly important in the latter stages of a multistage system which is common in reclamation systems operating at high system recovery, as explain in the following paragraphs. There are a number of design options to increase the flux in the latter stages of a system where the rising osmotic pressure reduces the element flux significantly when compared to the initial elements. Such design options include

- the introduction of an inter-stage booster pump (or an energy recovery device),
- use elements with thicker spacers to lower the pressure loss through the PV (Bartels et al., n.d.) or
- utilizing membranes with a lower permeability in the first positions and membranes with higher water (and salt) permeability in the latter stages as is commonly done with seawater systems (Dow Water & Process Solutions, 1995).

Factors which typically determine the system recovery include (1) the need to minimize the concentrate flow rate, (2) the cost implications in terms of feedwater treatment and pumping and (3) the demand for product water in comparison to the available feedwater. The specified recovery rate determines the number of stages which are required. As the recovery rate increases the more elements are required in series. The standard recovery rate for wastewater reclamation facilities ranges between 75 and 85%. Systems operating with a recovery rate between 75% and 80% would typically operate with a 2-stage system (such as the NEWater plants in Singapore, or the Torreele plant in Belgium), and systems operating with a recovery rate of between 80 and 85% (or higher) would operate with a 3-stage system (such as Sulaibiya in Kuwait, Orange County, US and Luggage Point, Australia). Each stage would consist of a PV each containing between 6 and 7 membrane elements. To maintain a minimum flowrate in the second and third stages of a system, the number of PVs is reduced in the latter stages.

The feedwater constituents, feedwater temperature together with the process design would have a direct impact on the fouling potential of the system and as explained earlier, the fouling potential of

the feedwater typically dictates the process design. Table 11-2 in the annex provides an overview of the key process conditions for seven operating facilities.

1.7 Post -treatment

AOP are typically included in a potable reclamation treatment train for further disinfection and for the removal of CEC that pass through the RO or NF membrane process such as N-Nitrosodimethylamine (NDMA). AOPs are processes utilizing hydroxyl radicals to induce the conversation of the initial pollutant into several intermediates (Cheng et al., 2017). Many of the plants surveyed by Raffin (2012) included the photolysis process utilizing a combination of hydrogen peroxide and ultraviolet irradiation (UV) with a fluence anywhere between 300 – 1000 mJ/cm^2 depending on whether the objective is disinfection or the destruction of CEC like NDMA which require a high fluence to meet the objective.

A secondary disinfectant typically in the form of sodium hypochlorite is also dosed when the water requires a residual disinfectant particularly if the water will be stored or used in industrial applications. Permeate water may also require pH correction typically utilizing sodium hydroxide or using CO_2 stripping to raise the pH before distribution (Gagne, 2005) or to be similar to natural waters in groundwater recharge applications (Van Houtte and Verbauwhede, 2008). Other common post-treatment processes include remineralization through the addition of calcium carbonate or through blending with feedwater when allowable.

1.8 System control and online optimization

System control in RO/NF systems typically includes the online measurement of a variety of water quality parameters (such as EC, pH, redox, temperature, turbidity) as well as process parameters (flow rate and pressure). These measurements are typically utilised by a PLC for process control through the regulation of pumps and actuated valves while protecting the system if certain set-points are not maintained through alarms for operator intervention or the safe shut-down of equipment.

Process control is an integral part of any RO/NF process. For smaller plants process control may be as simple as an on/off valve that is triggered when a measured variable is deviated from a desired set point. The standard for small RO/NF systems is controllers using proportional/integral (PI) or combined proportional, integral and derivative (PID) controllers. Initial multi-loop controllers proposed by Alatiqi et al. (1989) employed a first cascade type controller using the feed water pH and the conductivity to control scale formation and to control the feed pressure using a second

cascade controller according the permeate flux by closing the concentrate valve to increase the feed pressure.

Various work has been undertaken with regards to the optimisation of RO process conditions mostly for seawater systems. Abbas (2005) utilized a data based linear model to predict permeate flow rate and permeate conductivity through changing the feed pressure and feed pH. This utilized data from a specific RO system to derive the initial linear model and is therefore system specific. Alahmad (2010) utilized a linear regression to develop empirical models for recovery ratio, feed quality, permeate quality (TDS) and power consumption utilizing feed flow, feed quality, feed pressure, feed pH and feed temperature as inputs. The outputs of the model closely match those obtained from DOW Filmtec's RO Simulation software ROSA.

Fuzzy logic, neural networks, genetic algorithms and probabilistic reasoning have all been applied for RO system control. Zilouchian and Jafar (2001) utilized a neural network and fuzzy logic control system in seawater RO pilot plant to take a number of inputs (temperature, feed TDS, feed pH, feed flow rate, feed pressure, concentrate pressure, permeate flow rate, permeate conductivity, salt rejection, recovery, scale index) and use these in a data-based neural network to control the actuated concentrate valve.

Ghobeity and Mitsos (2010) utilize a RO model for the purposes of RO system energy minimization. Various input parameters are considered, such as membrane permeability, concentration polarization, temperature effects, membrane fouling, and Variable Frequency Drive (VFD) efficiency, in order to use mixed-integer non-linear programming (MINLP) to predict plant energy usage. The authors use a mostly analytical model with several correlations, and also examine the effects of time-varying electricity cost on the overall system operation cost.

Bartman et al. (2010) integrated a Specific Energy Demand (SED) based energy optimization algorithm into feedback control. A RO system model was derived from mass and energy balances and then combined with energy analysis equations. The controller uses multiple system variables and a user defined permeate production rate to calculate the optimal operating set-points that minimise the specific energy consumption of the RO system and satisfy the process and control system constraints.

When it comes to optimisation specifically for wastewater applications, Raffin et al. (2011) utilized a Box-Behnken approach to optimize MF flux backwash frequency, chloramine dose and chloramine dosing point together with RO flux, recovery, pH and antiscalant dose using a simple experimental plan combined with statistical analysis to define the optimal operating conditions to minimize membrane fouling.

Environmental decision support systems (EDSS) are multi-level, knowledge-based computer systems that not only reduce decision-making time, but also improve the consistency and quality of the decisions by offering the most relevant criteria for the evaluation of various alternatives. EDSS have been used to deal with complex problems and assist in automated learning processes by integrating Artificial Intelligence (AI) techniques with statistical/numerical methods under a common architecture (Poch et al., 2004).

1.9 IMS Operational Challenges

Experience gained in the operation of IMS systems for the reclamation of wastewater has shown that the production of high-quality product water is technically and economically feasible. Although the potential of the technology has been demonstrated through the increasing capacity of such facilities, there are a number of challenges which need to be addressed through further research and development. The following section gives a brief overview of a number of these challenges.

1.9.1 Compounds of emerging concern

Through the development of analytical techniques, a number of chemical compounds, which until recently have not been detected and lesser so regulated, have been detected in potable water, wastewater and the aquatic environment, many at very low concentrations. According to the EU's Joint Research Centre, the concern raised by these compounds is due to "either a knowledge gap about the relationship of the substances' concentrations and possible (eco)toxicological effects – usually due to chronic exposure, or the lack of understanding how such substances interact as chemical mixture" (JRC, 2017). The document also refers to a study (Drewes et al., 2013) which states that "It is commonly accepted that today a frequent monitoring for every potential chemical substance is neither feasible nor plausible. Research is focusing on the development of a science-based framework to guide the identification of CEC that should be monitored or otherwise regulated, including the context of reclaimed water use, especially for potable use".

Both RO and NF have been shown to a high efficiency in the removal of both organic and inorganic CEC (Alturki et al., 2010; Bellona et al., 2004; Garcia et al., 2013; Radjenović et al., 2008).

Studies have shown that there are a number of processes which affect the removal efficiency of these solutes by membranes including membrane properties, solution chemistry and the physicochemical properties of the contaminants. Separation of trace contaminants by membrane processes is primarily based on size exclusion, although electrostatic interactions between charged solutes and negatively charged membranes also typically have an important role for charged solutes (Bellona et al., 2004).

Hydrophobic trace contaminants have been shown to absorb to membrane surfaces reducing the rejection of these contaminants through both RO and NF although this has been shown to be particularly important when considering NF processes. A number of other factors typically also affect the removal of the target PhACs by membrane processes which are not always properly considered when reporting removal efficiencies of the membrane processes involved, including the membrane condition (with regards to organic, inorganic and biological fouling), membrane process conditions (membrane recovery and average permeate flux) and feed water quality including temperature, pH and concentration particularly due to urban activity and weather related events (such as storms or rain periods).

Table 1-5 shows the rejection of a variety of CEC by RO and NF membrane processes operating with real wastewater. Most of the data is from pilot or full-scale facilities operating advanced treatment trains for wastewater reclamation. The data shows that although the range of rejections by both RO and NF membranes is quite large, the rejection can be as high 99% for high rejection RO membranes, although this is very dependent on the type of membrane which is utilized and the properties of the contaminant in question. It is important to note that membrane processes do not degrade pollutants but concentrate the pollutants into a smaller volume waste stream which requires appropriate biological and/or chemical treatment processes for safe disposal back into the environment.

Table 1-5: Rejection rates of various CEC by RO and NF processes operating with real wastewater

Compound	Concentration in the influent (µg/L)[1]	Membrane, type	Rejection rate (%)	Reference
Acetaminophen	0.05	RO, BW30LE	85.6	(Radjenović et al., 2008)
	0.04-0.23	RO, BW30	99.6-99.9	(Bellona and Drewes, 2007)
	0.04-0.23	NF, NF90	99.2-99.9	
Atenolol	1.82	RO, TR70-HF	> 99	(Cartagena et al., 2013)
Azithromycin	0.118	RO, TR70-HF	> 99	
Carbamazepine	0.05	RO, BW30LE	98.5	(Radjenović et al., 2008)
	0.3	NF, NF-4040	89	(Yoon et al., 2006)
	0.08-0.11	NF, NF90	81.0-92.4	(Radjenović et al., 2008)
	0.08-0.11	RO, BW30	84.8-93.1	
	0.083	RO, TR70-HF	> 99	(Cartagena et al., 2013)
Cashmeran	0.0059	RO, BW30	99.4	(Dolar et al., 2012)
	0.0059	RO, LE	99.5	
	0.0059	RO, XFR	99.7	
Clarithromycin	2.02	RO, TR70-HF	> 99	(Cartagena et al., 2013)
Codeine	0.152	RO, TR70-HF	> 99	
Diazepam	0.017	RO, TR70-HF	> 99	
Diclofenac	0.27-0.44	NF, NF90	87.5-98.1	(Bellona and Drewes, 2007)
	0.27-0.44	RO, BW30	88.3-95.9	
Erythromycin	0.049	RO, TR70-HF	> 99	(Cartagena et al., 2013)
Gemfibrozil	0.2	NF, NF-4040	87	(Yoon et al., 2006)
Ibuprofen	n.d. - 0.08	NF, NF90	99.4-99.8	(Bellona and Drewes, 2007)
	n.d. - 0.08	RO, BW30	99.4-99.8	
Ketoprofen	0.08	NF, NF-4040	75	(Yoon et al., 2006)
Metoprolol	0.049	RO, TR70-HF	> 99	(Cartagena et al., 2013)

Naproxen	0.2	NF-4040	87	(Yoon et al., 2006)
Ranitidine	0.485	RO, TR70-HF	> 99	(Cartagena et al., 2013)
Salicylic acid	0.18	NF, NF-4040	100	(Yoon et al., 2006)
	0.0036	RO, BW30	61.3	
Sildenafil	0.0036	RO, LE	6.7	(Dolar et al., 2012)
	0.0036	RO, XFR	92.4	
Sulfamethoxazole	0.102	RO, TR70-HF	> 99	(Cartagena et al., 2013)
	0.00046	RO, BW30	98.1	
Tadalafil	0.00046	RO, LE	98.1	(Dolar et al., 2012)
	0.00046	RO, XFR	98.1	
Triclosan	n.d. - 0.07	NF, NF90	79.2-82.1	(Bellona and Drewes, 2007)
	n.d. - 0.07	RO, BW30	79.2-84.4	
	0.0065	RO, BW30	85	
Vardenafil	0.0065	RO, LE	59.1	(Dolar et al., 2012)
	0.0065	RO, XFR	83.2	

[1] Influent to the membrane process (typically effluent from a conventional activated sludge process followed by a filtration or an MBR process.

1.9.2 NDMA

The addition of chlorine to waters containing organic matter has caused concern because of the formation of a variety of organic compounds containing chlorine which are known or suspected potential human carcinogens even at the low concentrations at which they are detected. Typical classes of such compounds, which are collectively known as disinfection by-products (DBPs), include trihalomethanes (THMs), haloacetic acids (HAAs) and aldehydes (Tchobanoglous et al., 2003).

N-Nitrosodimethylamine (NDMA) is a DBP that belongs to the nitrosamines group that have been found to be potent carcinogens in drinking water supplies (EPA, n.d.). NDMA formation is of concern to water treatment plants where chloramination is used, particularly where wastewater effluents form part of the source water, that is in potable reclamation applications (Sgroi et al., 2015). A number of regulatory agencies have established standards for NDMA in drinking water. California's Department of Public Health set a 10 ng/L notification level, the World Health Organisation (WHO) set a guideline value of 100 ng/L for NDMA in drinking water while the Australian Guidelines for Water Recycling set a guideline value of 10 ng/L (NRMMC-EPHC-AHMC, 2006).

It is generally accepted that the main mechanism of NDMA formation involves the nucleophilic substitution reaction between an organic nitrogen compound contain the N, N-dimethylamino group and dichloramine, which coexist with Monochloramine under typical chloramination conditions. It has been proposed that nearly all nitrosamine formation can be explained by the reaction between dichloramine and secondary amine precursors to form a chlorinated unsymmetrical dialkylhydrazine intermediate which is then oxidized by DO to the corresponding nitrosamine. Other studies have shown that tertiary and quaternary amines, which are important functional groups for pharmaceuticals also serve as nitrosamine precursors (Shen and Andrews, 2011a). Upon exposure to

chlorine or chloramines, quaternary and tertiary amines are degraded to secondary amines which result in nitrosamine formation (Kemper et al., 2010a).Most research on nitrosamine precursors has used formation potential (FP) tests, which maximizes the nitrosamine formation from water matrices using much higher Monochloramine doses than applied during water treatment (i.e. application of 140 mg/L Monochloramine for 10 days), as a surrogate to evaluate the presence of NDMA precursors in water (Mitch and Sedlak, 2004).

Nitrosamine precursors are readily removed by biological treatment (Mitch et al., 2003). Removal of NDMA precursors generally exceeding 70% during biological treatment of wastewater have been reported by several studies (Mitch and Sedlak, 2004; Sedlak et al., 2005). On the other hand, NDMA is not generally well removed by membrane processes (Fujioka et al., 2013a). MF and UF have been shown not to remove nitrosamines, while RO and NF rejection of nitrosamines ranges from negligible to greater than 90% depending on the membrane type, feed temperature, membrane permeate flux, feed pH, ionic strength, membrane fouling and to nitrosamines molecular size (Fujioka et al., 2012, 2013a). To measure the rejection of NDMA precursors by membrane process, the NDMA FP has been used as a surrogate. MF/UF were shown to remove up to 10 % NDMA FP, while NDMA FP rejection by most RO membranes is more than 97% (M. J. Farré et al., 2011; Krauss et al., 2010a; Mitch and Sedlak, 2004). Despite this, the RO permeate can still contain significant concentrations of NDMA precursors able to produce NDMA formation at levels higher than the 10 ng/L limit set for potable reclamation applications under chloramine doses typical for drinking water disinfection.

UV treatment is the most commonly employed nitrosamine mitigation strategy, especially for NDMA, and typical potable reclamation trains use a combination of RO and high-dose UV treatment to meet potable water reclamation requirements of 10 ng/L. Since a UV fluence of approximately 1000 mJ/cm^2 is required for a 1-log reduction in NDMA, UV treatment for nitrosamine destruction is much more energy intensive and expensive than UV applications strictly for disinfection.

1.9.3 Water cost and energy use

'Alternative' water supplies often imply higher capital and operational costs for the water supplier when compared to traditional supplies (ground or surface waters which require less treatment), which are not always directly recoverable through the water tariffs set by the regulator. In Europe, the Water Framework Directive (Directive 2000/60/EC) states that the water user must bear the full cost of the water production, transport and distribution. For 'total' solutions where an MBR is used to treat primary effluent, then the total cost would be divided between a sewerage tariff for the treatment to meet effluent quality standards meeting the Urban Wastewater Treatment Directive

(UWWTD) (Directive 91/271/EEC) and the reclaimed water tariff for the reclamation process. Table 1-6 provides some information about the cost and specific energy consumption (SEC) reported in literature for the operation of IMS for wastewater reclamation. The specific energy consumption (SEC) for the facilities included in this table range between 0.7 and 2.3 kWh/m^3 of product water produced. These values include only the cost of the MF/UF process and the RO process and not pre-treatment and post-treatment processes. Information given in Raffin (2012) showed that the pre-treatment process for the Orange County facility had a SEC of 0.0012 kWh/m^3 and a post-treatment treatment SEC of 0.084 kWh/m^3. Realistically, as shown in Table 1-6, the SEC from a polishing plant treating secondary treated wastewater would be in the range of 2.3 – 2.6 kWh/m^3, although lower consumption values could be achieved depending on the wastewater quality and temperature. On the other hand when considering 'Total' systems which utilise MBR, Daigger et al. (2015) reported that the Gippsland Water Factory (Australia), which treats 35000 m^3/day, averaged a SEC of 3.04 kWh/m^3 of which on average 0.73 kWh/m^3 of product water was utilised by the RO. It is important to note the lower SEC shown by the facilities utilising immersed UF systems of 0.26, 0.18 and 0.24 kWh/m^3 for the Orange County, Torreele and Rincon de Leon facilities respectively. The low energy consumption of 0.29 kWH/m^3 for the 2-stage RO unit of the Ulu Pandan plant could be due to the low TDS of the feedwater (500 - 1300 mg/L) and lower recovery of 80% (2-stage) requiring a maximum feedwater pressure of 9.8 bar. This can be compared to the higher value of 1.2 KWh/m^3 for the Sulaibiya plant which operates with an average TDS of 1300 mg/L (maximum 3000 mg/L) at a higher recovery of 83% (3-stage), with both facilities operating with a feedwater temperature of 25-35°C and low permeate TDS requirements of 250 µS/cm and 100 mg/L respectively (AlGhusain, 2013; Gagne, 2005; Yuen, 2008).

To put the values of SEC in context, the Ashkelon seawater desalination plant which desalinates Mediterranean seawater (Feed TDS 40700 mg/L, Feed T 15-30°C), which is considered to include various innovative features to minimise the energy use for a large-scale facility has a maximum nominal SEC of < 3.9 kWh/m^3. According to the Orange County Water District (www.ocwd.com), the energy use to obtain final product water from the Orange County Groundwater Replenishment System is a third of that to desalinated Pacific Ocean seawater and half that of pumping water from Northern California to Southern California.

With regards to the approximate costs of water, it was reported that in 2005 the approximate costs of water from the Torreele facility in Belgium was 0.46 €/m^3. This cost was broken down into 33% operation cost, 33% investment cost, 22% maintenance cost and 13% as the cost for discharge of the concentrate (Van Houtte and Verbauwhede, 2008).

Table 1-6: Specific energy consumption (SEC) and water cost for a number of wastewater reclamation facilities

Facility		Luggage Point	Ulu Pandan	Sulaibiya	Orange Country GWRS	Torreele	Rincon de Leon WWTP-WRP
Country		Australia	Singapore	Kuwait	USA	Belgium	Spain
Feed		Secondary + N removal	Secondary	Secondary + N&P removal	Secondary	Secondary + N&P removal	Secondary
MF/UF Type		Pressurized (0.2 µm)	Pressurized (0.1 µm)	Pressurized (0.03 µm)	Immersed (0.04 µm)	Immersed (0.02 µm)	Immersed
Average flux	LMH	20	18		20	20	15
Recovery		0.85	0.8	0.83	0.85	0.75	0.73
MF SEC	kWh/m^3	1.4	0.4	1.1	0.26	0.18	0.24
RO SEC	kWh/m^3	0.9	0.29	1.2	0.52	0.63	0.9
Total SEC	kWh/m^3	2.3	0.69	2.3	0.78	0.81	1.14
Cost				0.180 KD/m^3		0.46 €/m^3	0.25 €/m^3
Reference		Raffin et al. (2012)	Raffin et al. (2012)	AlGhusain (2013), Gagne (2005), Raffin (2012)	Raffin et al. (2012)	Van Houtte & Verdauwhede (2008)	Melgarejo et al. (2016), Garcia Lillo (2014)

1.9.4 Concentrate disposal

The disposal of concentrate generated by RO/NF systems is a barrier to uptake of such systems for inland locations (Herman et al., 2017), while being a key design requirement for facilities discharging their concentrate stream in environmentally sensitive areas. Contaminants accumulated in the concentrate streams during membrane processes could be 6-7 times more concentrated than in the feed water (CAS+MF/UF or MBR effluent) (Solley, 2010).

Minimizing the volume of the concentrate stream to be treated or disposed of implies the increasing of the system recovery of the RO/NF system. A number of studies have demonstrated the operation of RO membranes in wastewater reclamation working at recoveries as high as 90% (Joss et al., 2011). Different options for the treatment of RO/NF concentrate stream from wastewater treatment plants have also been investigated in order to lower its impact before discharge into the natural environment (Pérez-González et al., 2012). A number of studies have investigated the introduction of partial recirculation of the RO/NF concentrate stream back to the MBR feed mainly focusing on the TOC removal efficiency and the effect on aerobic respiration (Lew et al., 2005) and precipitation of inorganic salts in the MBR (Joss et al., 2011).

Table 1-7 provides wastewater discharge limits according to the EU´s UWWTD together with typical constituents in RO concentrate from literature. Assuming a complete rejection of solutes, the concentration of solutes in the concentrate will be the concentration in the feed multiplied by the concentration factor (CF = 1/(1-Recovery)) which will be between 4 and 6.7 for a recovery 75% and 85% respectively. Meeting the regulated concentration of organic matter and solids is typically not difficult. Meeting the limits imposed on total nitrogen and total phosphorous is very much

dependent on the influent concentrations in the catchment and the design and operation of the nutrient removal processes. To meet the nutrient discharge limits, the Bundamba Advanced Water Treatment Plant (Australia) included a concentrate treatment process which consists of a nitrifying moving bed biofilm reactor (MBBR), a solids contact clarification process treating water from the MBBR and the downstream filter backwash for chemical phosphorous removal and solids separation and a denitrifying sand filter with methanol dosing (Solley, 2010). As shown in Table 1-7, the effluent from this treatment process meets the nutrient discharge limits set by the UWWTD. Other than limits on nutrients and suspended solids when discharging concentrate into environmentally sensitive areas or municipal sewage systems, many water reclamation facilities, particularly those in industry face restrictions on the electrical conductivity (or total dissolved solids), or specific ions such as chloride, sulphate or boron. Blending with lower salinity waters or utilising zero-liquid-discharge technologies (which are often costly to operate) are ways of abiding with such discharge restrictions but are often limiting considerations when considering RO/NF in reclaiming wastewater.

Table 1-7: Wastewater discharge concentration requirements and reported nutrient concentrations in 4 operating reclamation facilities (Solley, 2010; Van Houtte and Verbauwhede, 2008)

Parameters	Concentration Limit (91/271/EEC)	Reported concentrations in IMS concentrate (mg/L)			
		Torrelle	Luggage Point	Gibson Island	Bundamba
Biochemical oxygen demand (BOD5 at 20 °C)	25 mg/L O_2	7			
Chemical oxygen demand (COD)	125 mg/L O_2	86			
Total suspended solids	35 mg/L (> 10 000 p. e.) 60 mg/L (2 000-10 000 p. e.)	12.7			
Total phosphorus	2 mg/L P (10 000 - 100 000 p. e.) 1 mg/L P (> 100 000 p. e.)	5.9	3.0 ± 0.3	3.2 ± 1.4	1.1 ± 0.5
Total nitrogen	15 mg/L N (10 000 - 100 000 p. e.) 10 mg/L N (> 100 000 p. e.)	21.7	28 ± 5	12.1 ± 0.8	13.3 ± 1.6

Toreelle – pre-treatment, UF, RO and UV
Luggage Point, Gibson, Bundamba - pre- treatment, MF, RO, UV/peroxide AOP and chlorination processes. Bundamba includes a concentrate treatment step to meet local discharge standards

As the fate of CEC through the wastewater treatment process and in the aquatic environment is included on the monitoring list of regulators (WFD, Annex X), further processes, such as AOPs, might be required for reduction prior to environmental discharge (Justo et al., 2013; Umar et al., 2014; Zhou et al., 2011).

1.9.5 Process integrity

A crucial aspect to operating any reclamation treatment technology involves demonstrating that the process is actually removing pollutants and pathogens as designed according to intended

application. For many pollutants that pose a chronic risk it is often acceptable to demonstrate their removal periodically. On the other hand, for pathogens that present an acute risk, periodic sampling does not suffice. This means that in order to operate potable reclamation treatment with a high level of confidence regarding treatment scheme reliability, real-time detection of product quality and treatment process deviations coupled with timely decision making is of critical importance. Crook (2010) proposed a rigid protocol, which includes multiple treatment barriers and adequate instrumentation to rapidly detect changes in water treatment performance, and surrogate monitoring, for preventing improperly treated recycled water from entering a potable water distribution system, which could significantly reduce the time to identify and react to a treatment process failure. Surrogate parameters are operational parameters which are utilised instead of directly measuring hazards. A good example of this is turbidity which is typically utilised as an indicator of filtration plant performance and can be a surrogate for the removal of Cryptospodium, Giardia and viruses (NRMMC-EPHC-AHMC, 2006).

Each treatment process making up an individual barrier within the DPR treatment train requires a specific method of ensuring the integrity of the process. For example, typically MF or UF membranes in drinking water treatment are tested daily using a pressure decay test that would detect the presence of breaches smaller than Cryptosporidium oocysts and Giardia cysts that MF membranes are designed to remove. UV treatment systems have a photodiode installed to ensure that designed irradiation dose is actually being supplied to inactivate pathogens. Chlorine disinfection is typically monitored using continuous measurement of residual free chlorine after a determined contact time.

Since very large volumes of produced water would be required to measure pathogens directly the concept of log removal values (LRVs) of surrogate parameters was introduced, where one log unit removal by a treatment process represents a 90% removal (LRV = $\log[C_f/C_p]$, where C_f are C_p are the solute concentration in the feed and permeate respectively). The efficacy of treatment processes in removing pathogens are assigned LRVs through the use of challenge tests at high concentrations of pathogens and through the use of online surrogate sensors and/or offline parameters which demonstrates that the process is working correctly to achieve the designed level of treatment.

The California Department of Public Health set a pathogen log reduction target of 12-log virus removal, 10-log Giardia and 10-log Cryptosporidium from the point of entry of raw wastewater to the point of water consumption. Treatment processes making up the multiple treatment barriers typically include conventional primary and secondary treatment, tertiary treatment including MF or UF followed by RO and an AOP typically involving UV disinfection. The use of MF/UF, RO, and an AOP processes followed by storage in a groundwater basin for two or more months is typically sufficient to meet these LRV requirements. As part of the DEMOWARE project (EU FP7 project

Innovation Demonstration for a Competitive and Innovative European Water Reuse Sector) results from the full scale Toreele (Belgium) and pilot scale Shafdan (Israel) demonstrated LRV values greater than 10 for Bacteria (E. Coli), Viruses (som. Coliphage) and Parasites (C. Perfringens) (Kraus et al., 2016).

1.9.6 Public Perception

The acceptance of reclaimed water by a community is a key aspect in the development of a water reclamation scheme. Poor public perception could potentially delay or prevent the implementation of a project, or worse, potential users of reclaimed water could refuse to utilise the provided reclaimed water for a target application once a scheme is operating. In an article reviewing Singapore's experience with reclaimed water (referred to as NEWater in Singapore), Lee and Tan (2016) describe that it was strong government support and public acceptance which enable the successful uptake of the technology. The paper describes how Singaporeans had to be convinced that the NEWater was safe to use. This was carried out through the development of an extensive public communications plan, ongoing public education in schools, community events, opening a NEWater Visitor Centre, together with the engagement of media which were taken on a study trip to overseas reclamation projects and a dialogue with other water users such as the wafer fabrication industry. Other successful large-scale reclamation projects all describe strong public outreaches as a key factor to the users building trust in the quality of the reclaimed water.

The DEMOWARE project reviewed international experiences of stakeholder participation in water reclamation projects and argues that "public support and opposition to recycled water is fundamentally influenced by trust, including trust in the technical process and regulation, trust in the water reuse organisation itself, and ultimately, trust in the quality and safety of the final product: reused water". It also highlights the importance of the timing of public involvement opportunities, ideally before planning of concrete projects (Brouwer et al., 2015).

Chapter 2 - Objectives

The following chapter provides specific objectives for each of the 4 results chapters together with an overall objective of proposing a framework which can form the basis for a knowledge-based decision support system for integrated membranes systems.

2.1 Structure

Figure 2-1 gives an overview of the thesis structure and is followed by specific objectives for each of the four research areas which were investigated separately. The discussion brings together the four results chapters to propose a framework and concepts which can form the basis for a knowledge-based decision support system for integrated membrane systems.

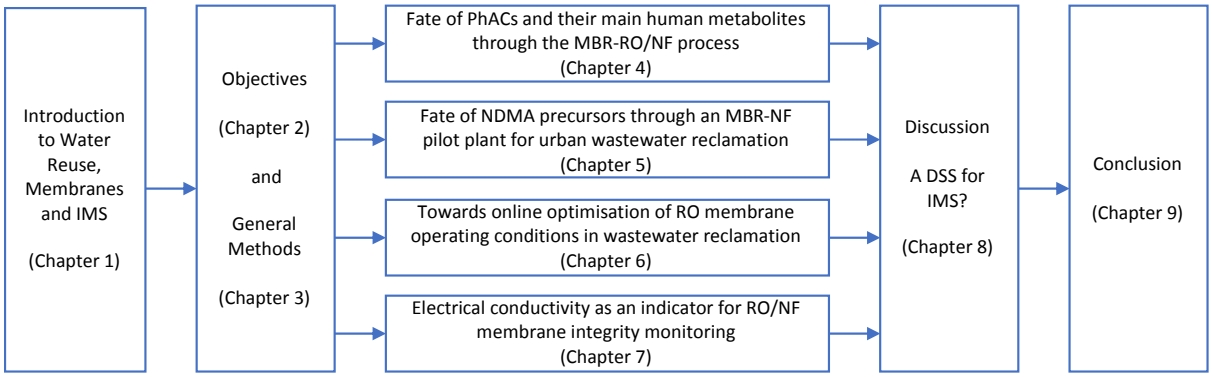

Figure 2-1: Overview of the thesis structure

2.2 Specific Objectives

The specific objectives of each of the four main chapters are the following:

- **Chapter 4** - To investigate the occurrence and fate of 13 pharmaceutically active compounds together with their main human metabolites and transformation products through an MBR process followed by either a RO membrane or an NF membrane treating urban wastewater.
- **Chapter 5** - To investigate the occurrence and fate of NDMA formation potential (FP) as well as individual NDMA precursors by an MBR pilot plant again treating urban wastewater. The removal of NDMA FP as well as individual NDMA precursors were investigated when affecting changes to the nitrification performance of the MBR, modified by changing the DO concentration in the aerobic compartment. The individual precursors investigated include antibiotics and other CEC that contain the dimethylamine-moiety responsible for NDMA formation. Additionally, the investigated MBR effluent is also treated by a NF system for water reclamation. Hence, the study also presents the rejection of these individual NDMA precursors by a NF membrane and compares them with up-to-date published literature.
- **Chapter 6** – To understand whether the diurnal variation in feed water constituents and temperature of the RO/NF feed water (MBR effluent) would justify the modification of system operation conditions, and if so provide a protocol for the automatic regulation of IMS recovery to obtain the lowest water cost possible through savings in terms of specific energy requirements, the optimized use of scale inhibitors and acid.

- **Chapter 7** - To investigate a number of strategies to utilise the available EC sensor to enhance its potential in the verification of integrity of RO membranes in real time. This will be shown by first determining the smallest contaminant flow of water that can be detected as a change in EC of 0.01 µS/cm between 'breach circumstances' and 'non-breach circumstances', then understanding how the ratio of EC probes to the number of PVs affects the sensitivity of an EC probe to detect a breach in a membrane and finally understanding whether introducing a 'slug' of higher salinity will affect the sensitivity of the EC method.

The following is the hypothesis of the thesis:

Integrated membrane systems for wastewater reclamation can be operated with a high level of confidence with regards to membrane integrity, process reliability and performance optimization by utilizing real time detection of water quality fluctuations and treatment process condition deviations which can be processed to make real-time critical process decisions to ensure the safety of reclaimed water delivered to customers while optimizing process performance.

Chapter 3 - Methodology

The following chapter outlines the general experimental program of the work carried out. Due to the diverse nature of the work, detailed methods utilised in each chapter are explained in the individual chapters. The work can be divided into two distinct but interconnected parts: an experimental component where a pilot plant was operated over two experimental periods; and a more theoretical component of the work which included utilising the knowledge and data gained over the experimental period and using models to develop and further test ideas.

3.1 MBR-RO/NF Pilot Plant

During the first experimental period the MBR-RO/NF pilot plant (referred to as the pilot plant) was located at the wastewater treatment plant of Castell-Platja d'Aro (Girona) shown in Figure 3-1. During the second experimental period the pilot plant was moved to the wastewater treatment plant of Quart (Girona). This WWTP treats urban wastewater with a capacity of 3.4 m^3 day^{-1}.

Figure 3-1: The containerised MBR-RO pilot plant, (a) external view, (b) internal view.

Water from the intake of both WWTPs was obtained directly following a coarse screen of the influent to the WWTP. A large peristaltic pump (Watson Marlow, Bredal) was used to pump the water from the influent tank to a manually cleaned pre-screening mesh and a primary settling tank to prevent large material reaching the bioreactor. A submersible pump within the primary settling tank was used to transfer the water to a mixed 500 L equalisation tank via a 1mm mesh filter which continuously feeds the bioreactor using a positive advance pump (Seepex pump).

The MBR has a total volume of 2260 L and is divided into four compartments according to the University of Cape Town (UCT) configuration for nutrient removal (Monclús et al., 2010). The first tank (320 L) has anaerobic conditions suitable for biological phosphate removal which is carried out by poly-phosphate accumulating organisms. The second tank has anoxic conditions suitable for nitrate removal which is carried out by denitrifying organisms. The third tank (520 L) is the aerobic

tank which provides the conditions required for the removal of organic matter and the nitrification process. Porous diffusers were used to oxygenate the water utilising a DO sensor in the tank together with a PID controller and an actuated valve to control the DO level in the tank. The final tank (1100 L) contains submerged micro-filtration flat sheet membrane from Kubota having a total surface area of 8 m^2 and a pore size of 0.4 µm which was also aerated for membrane scour. The aeration in the membrane tank was controlled using air flowrate together with a PID controller and a second actuated valve. Three recirculation pumps were utilised to transfer mixed liquor suspended solids between the membrane tank and the aerobic tank, between the aerobic tank and the anoxic tank and between the anoxic tank and the anaerobic tank as shown in Figure 3-2 below.

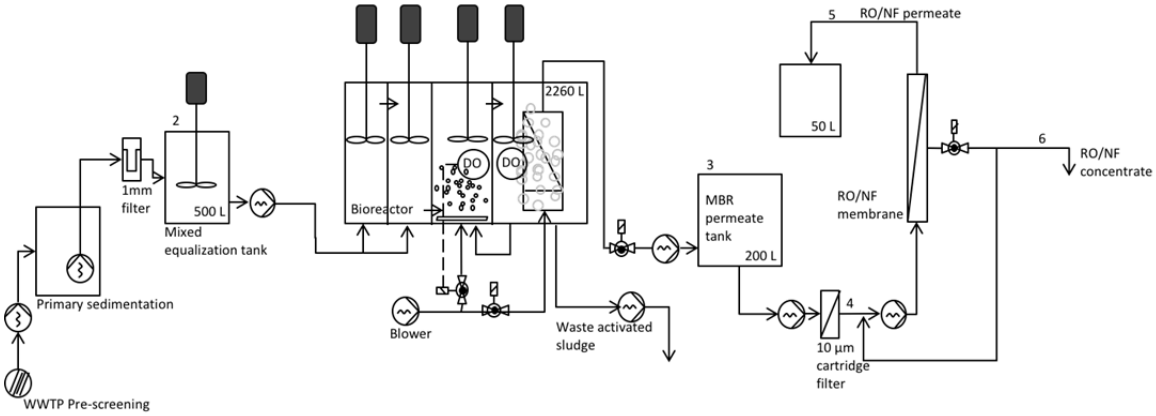

Figure 3-2: Scheme of the MBR-RO/NF pilot plant showing the typical sampling points: (1) sewage, (2) influent tank, (3) MBR permeate tank, (4) RO/NF feed, (5) RO/NF permeate and (6) RO/NF concentrate

Permeate was obtained by applying a vacuum pressure drop over the membranes using a positive advance pump (Seepex Pump) at a flux of between 20 and 25 LMH (160 - 200 L/h) with filtration cycles typically of 9 minutes followed by 1 minute of relaxation. Pressure transducers were utilized to measure the transmembrane pressure (TMP) to continuously monitor membrane fouling.

A permeate tank collected MBR permeate, which is then fed to a RO/NF system consisting of VFD controlled high-pressure pump and a single 4" x 40" membrane element. The two membranes utilised during this study were a DOW Filmtec NF90 (NF) membrane and a Hydranautics ESPA2 (RO) membrane. One RO membrane and one NF membrane was chosen to be able to carry out a comparison of the two different types of membranes. The criteria for choosing the membranes was their popularity for use in full scale facilities (particularly for the RO membrane) and the availability of comparable data in literature particularly with regards to the removal of PhACs by the membrane.

Internal concentrate recirculation to the feed of the membrane was employed to increase the system recovery while remaining within membrane supplier's specifications (see Figure 3-3). The VFD and the actuated concentrate valve allowed the system to be operated at a constant average

permeate flux based on a fixed permeate flow set point of 135 L h^{-1}. Both membranes were operated at a system recovery rate (Q_p/Q_f) of 75% and a flux (Q_p/Membrane surface area) of 18 L m^{-2} h^{-1}; this last value remains within the average system flux of different operating installations, which usually ranges between 16.8 and 21 L m^{-2} h^{-1} (Raffin et al., 2012). The recovery of the membrane element (Q_p/Q_m), which includes the concentrate recirculation, was set at 12.5% within the manufacturer's guidelines and similar to those used in the operating plants surveyed by Raffin et al., (2012), which ranged between 8.6 and 12.7 %.

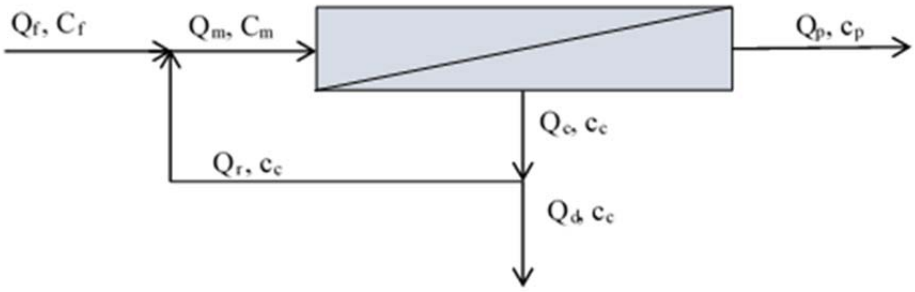

Figure 3-3: Detailed scheme of the membrane system showing the inlet flow (Q) and concentration (C) of the system feed (f), membrane feed (m), permeate (p), concentrate (c), recirculation (r) and drain (d).

Figure 3-4: Pilot RO system utilised in study

Due to the concentrate recirculation aforementioned, the composition of the feed water to the membrane was a blend of fresh feed water from the MBR and recirculated concentrate (Figure 3-3). This meant that the feed concentrations of the solutes were higher than those normally found in

ordinary feed water. The removal efficiencies of the RO and NF membranes were thus calculated using a mass balance through the membrane, as shown in Equation 1:

$$C_m = \frac{Q_p \times C_p + Q_c \times C_c}{Q_m} = \frac{Q_f \times C_f + Q_r \times C_c}{Q_m} \quad [1]$$

Where C_m is PhACs concentration in the membrane system feed water, Q_p is the permeate flow, C_p is the PhACs concentration in the permeate, Q_c is the concentrate flow, C_c is the PhACs concentration in the concentrate, Q_m is membrane system feed flow, Q_f is the system feed flow without recirculation, C_f is the concentration in the feed water without recirculation and Q_r is the recirculated flow. Equation 2 was used to ensure that the results obtained for the system feed, permeate and concentrate make sense:

$$Q_f \times C_f - Q_p \times C_p = Q_d \times C_c \quad [2]$$

where Q_d is the drain flow from the membrane system. Finally, equation 3 calculated the membrane rejection as follows:

$$\text{Membrane Rejection} = \left(1 - \frac{C_p}{C_m}\right) \times 100 \quad [3]$$

The higher concentration of the membrane feed can simulate the last element within the multi stage plug-flow membrane configuration typically employed in a full-scale system. On the other hand, the higher fluxes tested for the NF membrane give an indication of the high fluxes expected in the first membranes of a PV.

The data acquisition system allowed for the continuous monitoring and control of online flow rates, conductivities, temperature, pH, redox potential (ORP), trans-membrane pressure, air scouring frequency and DO.

3.2 Experimental periods

The experimental work was carried out over two experimental periods of six months, each of which had different objectives.

The objective of the first experimental period was an investigation into the fate of pharmaceutically active compounds and their transformation products through membrane bioreactors and RO (and NF) membranes. The remainder of this first experimental period was utilized to develop and test a control strategy for the optimization of integrated membrane processes (MBR +RO/NF) with regards to system recovery, average permeate flux and pre-treatment dosing, according to the variations in quality of the feed water to minimize the water cost.

The second experimentation period was primarily designed that following the initial start-up period a four month, twice weekly sampling campaign will be carried out to understand the fate of NDMA precursors through the MBR-NF pilot plant under changing aeration conditions.

During the second experimental procedure work was also carried out on the treatment of NF concentrate from the MBR-NF system using AOP namely UV/H2O2. Laboratory tests as well as pilot experiments were carried out to investigate the effect of different AOP process conditions on the treatment objectives which include the reduction in organic content of the concentrate, the mineralization of specific PhACs and the increase of biodegradability of recalcitrant organics. Although a significant amount of work was carried out, this part of the work was dropped for the purposes of finishing the PhD thesis.

3.3 Common Experimental Methods

Samples were also analysed for total suspended solids and volatile suspended solids (TSS & VSS; APHA standard method 2540D), total and soluble chemical oxygen demand (COD; APHA standard method 5220B), biochemical oxygen demand (BOD; WTW, Oxi Top), dissolved organic carbon (DOC; Shimadzu TOC-V_{CSH} analyser), ammonium (BUCHI B-324 distiller, Titrino 719S Methrohm) and total Kjeldahl nitrogen (BUCHI B-324 distiller, Titrino 719S Methrohm). Nitrites (NO_2^--N), nitrates (NO_3^--N), and phosphates (PO_4^{3-}-P), together with other major ions (Na^+, K^+, Mg^{2+}, Ca^{2+}, Cl^-) were analysed using ion chromatography (Metrohm 761-Compact; APHA standard method 4110B).

Chapter 4 - The fate of PhACs and their transformation products through the MBR-RO/NF process

This chapter was redrafted from:

Mamo J., García-Galán M.J., Stefani M., Rodríguez-Mozaz S., Barceló D., Monclús H., Rodriguez-Roda I., Comas J. (2018). Fate of pharmaceuticals and their transformation products in integrated membrane systems for wastewater reclamation. Chemical Engineering Journal 331, 450-461.

4.1 Introduction

As human health is increasingly depending on pharmaceutical products, the scientific community together with environmental and public health authorities have made a significant effort in understanding the fate of pharmaceutically active compounds (PhACs) both through engineered urban wastewater treatment processes as well as in the natural environment. This has been reflected in the high number of scientific publications devoted to this subject in the last two decades. On the contrary, modification of legal regulations up to now is basically inexistent. However, water scarcity and water reclamation have become essential issues in water resource management worldwide, always considering the conservation of aquatic ecosystems as a final goal and main driver of the involvement of the scientific community.

So far, most of the research carried out regarding the fate of PhACs through MBR processes has mainly focused on the study of parent compounds, neglecting their metabolites. Only recently, the environmental presence of human metabolites and different transformation products (TPs) of these PhACs has been included within the scope of removal efficiency studies of different wastewater treatments technologies (Fatta-Kassinos et al., 2011; García-Galán et al., 2012; García-Galán et al. 2016). It should be considered that, once released onto the environment, these metabolites and TPs can be innocuous (Garcia-Galan et al., 2016), but also equally and even more toxic than the original substance against different aquatic organisms. Furthermore, the coexistence of the original drugs with these metabolites and TPs could lead to additive, antagonistic and/or synergetic effects which are hard to predict and that should be investigated. For instance, the assessment of the ecotoxicity of the photoproducts of the anti-inflammatory diclofenac (DCF) or naproxen has provided the evidence that acute and chronic toxicity can be greater for these photoproducts than for the parent compounds (Fatta-Kassinos et al., 2011). Effective concentration values (EC_{50}) obtained after 15 min assays for the antibiotic sulfapyridine (SPY) and its acetylated metabolite, N^4-acetylsulfapyridine (acSPY), demonstrated that the marine bacteria *Vibrio fischerii* was more sensitive to the presence of the metabolite than to the original drug, and according the EU legislation (Directive 93/67/EEC), the former could be categorized as toxic (García Galán et al., 2012).

On the other hand, it has been demonstrated that conventional activated sludge (CAS) treatment processes in waste water treatment plants (WWTPs) do not adequately remove many of the most commonly used PhACs such as DCF, the anticonvulsant carbamazepine (CBZ) or the antibiotic sulfamethoxazole (SMX) (Gros et al., 2010; García-Galán et al., 2011). Different studies have demonstrated that membrane bioreactors (MBRs) are capable of removing moderately biodegradable and hydrophobic trace organic pollutants more efficiently than CAS treatments

processes (Alturki et al., 2010). During the last years, MBR technology has become an accepted alternative to CAS processes for municipal wastewater treatment, not only regarding PhACs removal but also the overall water quality (Judd and Judd, 2008). Furthermore, the combination of MBR technology followed by the RO process or NF is typically used when high quality product water is required for planned potable reclamation or when a reduction in salinity is required for irrigation reclamation applications (M. Raffin et al., 2012). Different works have demonstrated that both membrane processes alone yield high rejection rates for PhACs, usually >80% (Bellona and Drewes, 2007; Radjenović et al., 2008). Various studies have shown that the combination of the MBR process with RO or NF results in higher removal rates for a wide range of PhACs, present in the wastewater (feed stream) to be treated; these are concentrated into a stream of water known as the concentrate stream (also known as the reject or brine stream) (Taheran et al., 2016), leaving a permeate stream (also known as the product stream) with very low concentrations of the contaminants of interest. A recent work by Dolar et al. (Dolar et al., 2012), which was carried in the same WWTP as this work, showed that removal rates for 22 PhACs by a Ropur TR70-4021-HF-RO membrane were above 99%.

A number of factors affect the removal of PhACs by the MBR-RO/NF process (Bellona and Drewes, 2007) which are not always properly considered when reporting removal efficiencies of the membrane processes involved. These include the membrane type (affecting molecular weight cut-off, surface morphology, hydrophobicity and charge), membrane fouling, membrane process parameters (membrane recovery and average permeate flux) and feed water quality including temperature, pH and concentration, particularly due to urban activity and weather-related events (such as rain periods). Furthermore, a number of studies have also shown that NF and ultralow pressure RO membranes are not perfect barriers for various CEC including endocrine disruptors and some PhACs such as SMX or CBZ. (Fujioka et al., 2010; Kimura et al., 2004).

It should also be considered that significant savings could be made in terms of energy reduction and chemicals and concentrate disposal costs when using NF in the place of RO membranes (Yangali-Quintanilla et al., 2010). NF membranes are found in similar spiral wound configurations to RO membranes, making the switch during routine membrane replacement a feasible option to make.

Taking all this information into consideration, the objective of the present study is to evaluate and compare MBR-RO and MBR-NF in terms of pollutant removal efficiencies. With this aim, the fate of 13 PhACs together with their main human metabolites and TPs (20) was investigated in both configurations.

4.2 Methodology

4.2.1 MBR-RO/NF pilot plant

For this experiment the MBR-RO/NF pilot plant was installed within the facilities of the full-scale WWTP of Castell-Platja d'Aro. The wastewater was primarily composed of domestic wastewater. The operating conditions and membrane properties of the MBR and RO and NF membrane systems are given in Table 4-1 and Table 4-2 respectively.

Table 4-1: MBR membrane processes conditions

	Units	**Value**
Membrane Area	m^2	8
System flow (Q)	Lh^{-1}	140
Permeate flow	Lh^{-1}	150
System flux	$Lm^{-2}h^{-1}$	18.8
HRT	Hours	16
Solids concentration (MBR tank)	$g\ L^{-1}$	7
SRT	Days	30
Filtration - relaxation cycles	Min	9:1
Air scour flow rate	$m^3 \cdot h^{-1}$	10
DO aerobic set point	$mg\ O_2 \cdot L^{-1}$	0.5

Table 4-2: RO and NF membrane processes conditions and membrane properties

Membrane		**ESPA2 LD-4040**	**NF90 - 4040**
Membrane surface area	m^2	7.43	7.62
Permeate flux (average)	$Lm^{-2}h^{-1}$	18	18 (26, 32)
Permeate flow	Lh^{-1}	135	135 (196, 240)
Feed pressure	bar	6.5	3.3 (4.5, 5.7)
System recovery	%	75	75
Membrane Properties			
Material		Polyamide	Polyamide
NaCl Rejection	%	99.6	85 – 95
Surface charge		Negative	Negative
MWCO estimate	Da	≈100	≈200
Surface roughness	nm	30.0	63.9

No antiscalants or biocides where used in the pre-treatment of the MBR effluent before being fed to the RO or NF membranes, which led to membrane fouling over the experimental period (7000 L m^{-2} of permeate produced).

4.2.2 Sampling and sample preservation

Samples were taken during two consecutive years (2013 and 2014). Sampling was carried out during four weeks in each campaign during the dry weather flow to avoid the dilution of influent due to a combined sewage system in the town (between April-May 2013 and in May 2014, respectively). Grab samples of MBR influent, MBR effluent/RO/NF feed, RO/NF permeate and RO/NF concentrate were taken twice per week during both experimental periods (four weeks each), always considering a temporal shift between sampling the influent and effluent of the MBR equal to the hydraulic retention time (HRT) of the reactor. Additionally, during the second year, integrated samples were taken from the WWTP influent sewage (after a coarse screen) every two hours to obtain the range and variation of concentrations of the target compounds during a 24-hour period.

Water samples were collected in 1 L amber PET bottles (pre-rinsed with Milli-Q water) and filtered on-site through a 1.2 µm microfiber filter followed by a 0.45µm nylon membrane filter. They were stored at 4ºC during transportation and frozen upon arrival to the laboratory.

4.2.3 Chemicals and reagents

HPLC-grade solvents (water, methanol (MeOH), acetone and acetonitrile (ACN)) and formic acid (HCOOH) (98–100%) were supplied by Merck (Darmstadt, Germany) and Thermo Fisher Scientific (Thermo Scientific, Franklin, MA, US). High purity standards (>99%) of the PhACs acetaminophen (ACM), sulfamethoxazole (SMX), sulfapyridine (SPY), sulfamethazine (SMZ), sulfadiazine (SDZ), venlafaxine (VFX), diazepam (DZP), carbamazepine (CBZ), diclofenac (sodium salt) (DCF), fluoxetine (FXT), metoprolol (MTP), ranitidine (RTD) and the metabolites norverapamil (desVPM), norfluoxetine (norFXT) and 2-OH-carbamazepine (2-OH-CBZ) were purchased from Sigma-Aldrich (St. Louis, MO, USA). High purity standards for the metabolites 4-nitro-sulfamethoxazole (n-SMX), 4'-OH-diclofenac (4-OH-DCF), diclofenac amide (adDCF), acridone (ACRO), D,L-N-desmethylvenlafaxine (N-desVFX), D,L-O-desmethylvenlafaxine (O-desVFX), N^4-acetylsulfapyridine (acSPY), N^4-acetylsulfamethazine (acSMZ), N^4-acetylsulfamethoxazole (acSMX), nordiazepam (norDZP), 3-OH-acetaminophen (3-OH-ACM), 10,11-epoxy carbamazepine (epo-CBZ), metoprolol acid (MTPA), α-OH-metoprolol (α-OH-HMTP) and O-desmethylmetoprolol (O-DMTP) were purchased from Toronto Research Chemicals (TRC Inc., Ontario, Canada). Verapamil (VPM) was obtained from the European Pharmacopoeia (EP). Isotopically labelled compounds, used as internal standards were purchased from Sigma-Aldrich (fluoxetine-d_5), TRC (verapamil-d_6, diclofenac-d_4, 4'-OH-diclofenac-d_4, sulfamethoxazole-d_4, N^4-acetylsulfapyridine-d_4, N,L-O-desmethylvenlafaxine-d_4 and acetaminophen-d_4), Cerilliant (Texas, U.S.A.) (diazepam-d_5) and from CDN isotopes (Quebec, Canada) (carbamazepine-d_{10} and venlafaxine-d_6). Stock standard solutions for each of the analytes were prepared in MeOH at 1 mg mL^{-1} and

stored in the dark at −2 ◦C. Standard solutions of the mixtures of all compounds were made at appropriate concentrations and used to prepare the aqueous calibration curve and also to perform the recovery studies. Stock standard solutions for the internal standards were prepared similarly. Aqueous standard solutions always contained <0.1% of MeOH.

4.2.4 UHPLC-MS2 analysis

Analysis of the PhACs was performed adapting the methodology by García-Galán *et al*. (2016). Briefly, fully automated on-line pre-concentration of samples, aqueous standards and operational blanks was performed using a Thermo Scientific EQuan^{TM} system (Thermo Scientific, Franklin, MA, US), by means of two LC columns, the first for pre-concentration of the sample and the second for chromatographic separation. The flow rate for the chromatographic separation was set to 500 µL min^{-1}, being eluent A ACN, and B UPLC grade water slightly acidified with 0.01% HCOOH. MS/MS analysis were carried out on a TSQ Vantage triple quadrupole mass spectrometer (Thermo Scientific, Franklin, MA, US), equipped with an electrospray (ESI) turbo spray ionization source. The target compounds were analysed in both positive and negative ionization mode simultaneously (polarity switch mode). For increased sensitivity, two selected reaction monitoring (SRM) transitions per compound were monitored, one for quantitation and the other for positive confirmation. To improve the performance of the triple quadrupole, time-specific SRM windows were adjusted to the retention times of each target compound. A complete list of the target PhACs and their main human metabolites and TPs are given in Table 4-3. Their physico-chemical properties are given in Table 11-3 in the Annexes.

Table 4-3: Pharmaceuticals (PhACs), metabolites and transformation products (TPs) investigated in this study (metabolites and TPs in italics).

Therapeutic class	Compound		CAS number	Formula	MW (g/mol)
Antibiotics	Sulfapyridine	SPY	144-83-2	$C_{11}H_{11}N_3O_2S$	249.3
	N^4–acetylsulfapyridine	acSPY	19077-98-6	$C_{13}H_{13}N_3O_3S$	291.3
	Sulfamethoxazole	SMX	723-46-6	$C_{10}H_{11}N_3O_3S$	253.3
	N^4–acetylsulfamethoxazole	acSMX	21312-10-7	$C_{12}H_{13}N_3O_4S$	295.3
	Nitrosulfamethoxazole	n-SMX	29699-89-6	$C_{10}H_9N_3O_5S$	283.3
	Desaminosulfamethoxazole	des-SMX			238.1
	Sulfamethazine	SMZ	57-68-1	$C_{12}H_{14}N_4O_2S$	278.3
	N^4-Acetylsulfamethazine	acSMZ	100-90-3	$C_{14}H_{16}N_4O_3S$	320.4
	Sulfadiazine	SDZ	68-35-9	$C_{10}H_{10}N_4O_2S$	250.3
	N^4-Acetylsulfadiazine	acSDZ	127-74-2	$C_{12}H_{12}N_4O_3S$	292.3
Anti-depressants	Venlafaxine	VFX	93413-69-5	$C_{17}H_{27}NO_2$	277.4
	N–Desmethylvenlafaxine	N-desVFX	149289-30-5	$C_{16}H_{25}NO_2$	263.4
	O–Desmethylvenlafaxine	O-desVFX	93413-62-8	$C_{16}H_{25}NO_2$	263.4
	Fluoxetine	FXT	54910-89-3	$C_{17}H_{18}F_3NO$	309.3
	Norfluoxetine	norFXT	83891-03-6	$C_{16}H_{16}F_3NO$	295.3
	Diazepam	DZP	439-14-5	$C_{16}H_{13}ClN_2O$	284.7
	Desmethyldiazepam	norDZP	1088-11-5	$C_{15}H_{11}ClN_2O$	270.7
Psychiatric drugs	Carbamazepine	CBZ	298-46-4	$C_{15}H_{12}N_2O$	236.3
	10,11-Epoxy–Carbamazepine	epo-CBZ	36507-30-9	$C_{15}H_{12}N_2O_2$	252.3
	2–Hydroxycarbamazepine	2-OH-CBZ	68011-66-5	$C_{15}H_{12}N_2O_2$	252.3
	Acridine	ACRI	260-94-6	$C_{13}H_9N$	179.1
	Acridone	ACRO	578-95-0	$C_{13}H_9NO$	195.2
Analgesics/ anti-inflammatories	Diclofenac	DCF	15307-86-5	$C_{14}H_{11}Cl_2NO_2$	296.2
	4-OH-diclofenac	4-OH-DCF	64118-84-9	$C_{14}H_{11}Cl_2NO_3$	312.2
	Diclofenac–amide	adDCF	15362-40-0	$C_{14}H_9Cl_2NO$	278.1
	Acetaminophen	ACM	103-90-2	$C_8H_9NO_2$	151.2
	3-OH-acetaminophen	3-OH-ACM	37519-14-5	$C_8H_9NO_3$	167.2
B-Blockers	Metoprolol	MTP	37350-58-6	$C_{15}H_{25}NO_3$	267.4
	Metoprolol–acid	MTPA	56392-14-4	$C_{14}H_{21}NO_4$	267.3
	Alfa–Metoprolol–OH	α-OH-MTP	56392-16-6	$C_{15}H_{25}NO_4$	283.4
	Ranitidine	RTD	66357-35-5	$C_{13}H_{22}N_4O_3S$	314.4
Calcium channel blocker	Verapamil	VPM	52-53-9	$C_{27}H_{38}N_2O_4$	454.6
	Norverapamil	norVPM	67018-85-3	$C_{26}H_{36}N_2O_4$	440.6

4.2.5 Other analyses

All samples were analysed according to standard methods (Eaton et al., 2005) for conventional physical and chemical parameters: total suspended solids and volatile suspended solids (TSS & VSS; APHA standard method 2540D), total and soluble chemical oxygen demand (COD; APHA standard method 5220B), dissolved organic carbon (TOC; Shimadzu TOC-V_{CSH} analyzer), ammonium (BÚCHI B-324 distiller, Titrino 719S Methrohm) and total Kjeldahl nitrogen (BÚCHI B-324 distiller, Titrino 719S Methrohm). Nitrites (NO_2^--N), nitrates (NO_3^--N) and phosphates (PO_3^{4-}-P), together with other

major ions (Na^+, K^+, Mg^{2+}, Ca^{2+}, Cl^-) were analysed using ion chromatography (Metrohm 761-Compact; APHA standard method 4110B).

4.3 Results

4.3.1 MBR performance

The pilot plant was operating in a similar configuration over both experimental periods, maintaining an SRT of 30 days and a flux of 19 L m^{-2} h^{-1} (see Table 4-1). Dalmau et al., (2014) previously investigated the effect of aeration on biological and filtration performance of the same MBR pilot plant. These authors focused in the modification of the DO set-point in the aerobic compartment followed by modifications of the air-scour flow rate in the membrane tank. They found that the optimal value was a DO set-point of 0.5 mg O_2 L^{-1} in the aerobic tank and that the activity of nitrifiers was significantly reduced when the DO set-point decreased to lower values. For this reason, the DO set-point in the aerobic tank was maintained at 0.5 mg O_2 L^{-1}, whereas the air scour flow rate was kept at 10 m^3 h^{-1} to ensure that fouling was not an issue (TMP < 30 mbar). The results given in Table 4-4 show that during both years, the pilot plant was working under nitrifying conditions, consistently reducing NH_4^+ to values < 1 mg L^{-1}. On the contrary, denitrification was very low, particularly during the 2014 campaign. The anaerobic conditions in the first tank of UCT configuration enhanced the development of phosphate accumulating organisms (PAOs), responsible of enhanced biological phosphorous removal (EBPR). The increment of phosphorous removal efficiencies from 42% to 70% is attributed to the increment of the influent COD, one of the limiting factors in EBPR (Monclús et al., 2010; Puig et al., 2008) and that was three times higher in 2014 than in 2013.

Table 4-4: Average conventional water quality parameters showing MBR, RO and NF performance over the experimental periods. A RO membrane was tested during the 2013 experimental period while a NF membrane was tested during the 2014 experimental period.

		2013			2014		
MBR Water Quality							
Parameter	Units	Influent	Effluent	Removal	Influent	Effluent	Removal
COD total	(mg/L)	188	16.6	91%	412	45	89%
COD soluble	(mg/L)	65	-		163	-	
TKN total	(mg/L)	29	1.8	94%	55	1.5	97%
NH_4^+	(mg N/L)	18	0.4	98%	34	1.0	97%
NO_3^-	(mg N/L)	0.9	4.7		0	12	
NO_2^-	(mg N/L)	0.4	0.1		0	0	
Total-N	(mg N/L)	30.3	6.6	78%	55	13.5	75%
PO_4^{3-}	(mg/L)	1.4	0.8	42%	3.6	1.1	70%
pH		7.6	-		7.5	-	
T	°C		20			22	
Turbidity	NTU		< 0.3			< 0.3	
RO and NF Water Quality							
Parameter	Units	RO feed	RO permeate	Removal efficiency	NF Feed	NF Permeate	Removal efficiency
EC	(µS/cm)	909	27	97%	1016	81	92%
Temperature	°C	20.2	-		24	-	
pH		7.1	6.4		7.4	6.5	
Cl^-	(mg/L)	129	2.8	98%	156	14.1	91%
NO_3^-	(mg/L)	3.6	0.3	91%	13.4	4.4	67%
PO_4^{3-}	(mg/L)	0.2	< LOD		0.3	< LOD	
SO_4^{2-}	(mg/L)	31.8	0.06	99.8%	28.1	0.2	99.2%
Na^+	(mg/L)	112	5.1	95%	113	17.1	85%
K^+	(mg/L)	15.9	0.6	96%	20.5	2.7	87%
Mg^{2+}	(mg/L)	13.7	0.03	99.7%	17.6	0.1	99.4%
Ca^{2+}	(mg/L)	113.3	0.9	99.2%	83.8	1.5	98%

4.3.2 Occurrence of PhACs in raw urban wastewater and influent

4.3.2.1 Sewage wastewater and primary treatment

Sewage samples were taken only during the campaign of 2014 (during 24 h, at 2h intervals). During this campaign, 2 of the studied compounds were detected at average concentrations > 1 μg L^{-1} in these samples: one metabolite, MTPA (1.4 μg L^{-1}) and the anti-inflammatory ACM (30.3 μg L^{-1}). Similar concentrations were found in influent samples in the same campaign (see Figure 4-1). The yearly consumption of ACM is estimated to be 700-1400 tons per year in Spain (Ortiz de García et al., 2013). ACM is usually amongst the PhACs detected at highest levels, together with other anti-inflammatories such as ibuprofen (Gros et al., 2012; Pedrouzo et al., 2011). Variations in the levels of the PhACs studied before and after primary sedimentation (comparison between sewage samples and influent samples, see Figure 4-1) ranged from barely no change for the metabolites norDZP (0.19%) and O-desVFX (2.5%), to a reduction of more than 50% of the initial concentration for acSMX (50.36%) (the reduction for the parent compound, SMX, was 47%), DZP (51.2%) and FXT (56.2%). On the contrary, norFXT increased slightly (10.5%) from the sewage to the influent of the WWTP. However, a mass balance with FXT would not be accurate as its concentration was much lower than the metabolite's. DCF concentration remained quite the same during this primary treatment (increase of 6.6%), whereas its hydroxylated metabolite doubled its concentration during this primary treatment, going from an average value of 452 ng L^{-1} to 904 ng L^{-1}. It is known that human metabolism of DCF yields a 50% of the total dose as 4-OH-DCF and its glucuronide conjugate (Stierlin et al., 1979), which could have deconjugated during this first phase of the treatment and reverted to 4-OH-DCF, contributing to the observed increase. This phenomenon was observed for SPY and its acetylated metabolite, acSPY. In this case, acSPY concentration decreased a 12.5% during primary treatment whereas that of SPY increased approximately in the same proportion (10%). A deconjugation of acSPY during this primary treatment could justify these results, as demonstrated in a previous publication by García-Galán et al. (2012), who observed the back-transformation of at least a 50% of the initial concentration of the acetylated metabolite in the parent compound in a simulated fixed-bed bioreactor during several days.

Figure 4-2 shows a 24-hour profile of DCF, CBZ, VFX and MTP together with their human metabolites and TPs in the sewage. For all of them, a similar evolution through time is observed for parents and products. Table 11-4 in the Annex shows the concentrations measured in the sewage samples during 2014.

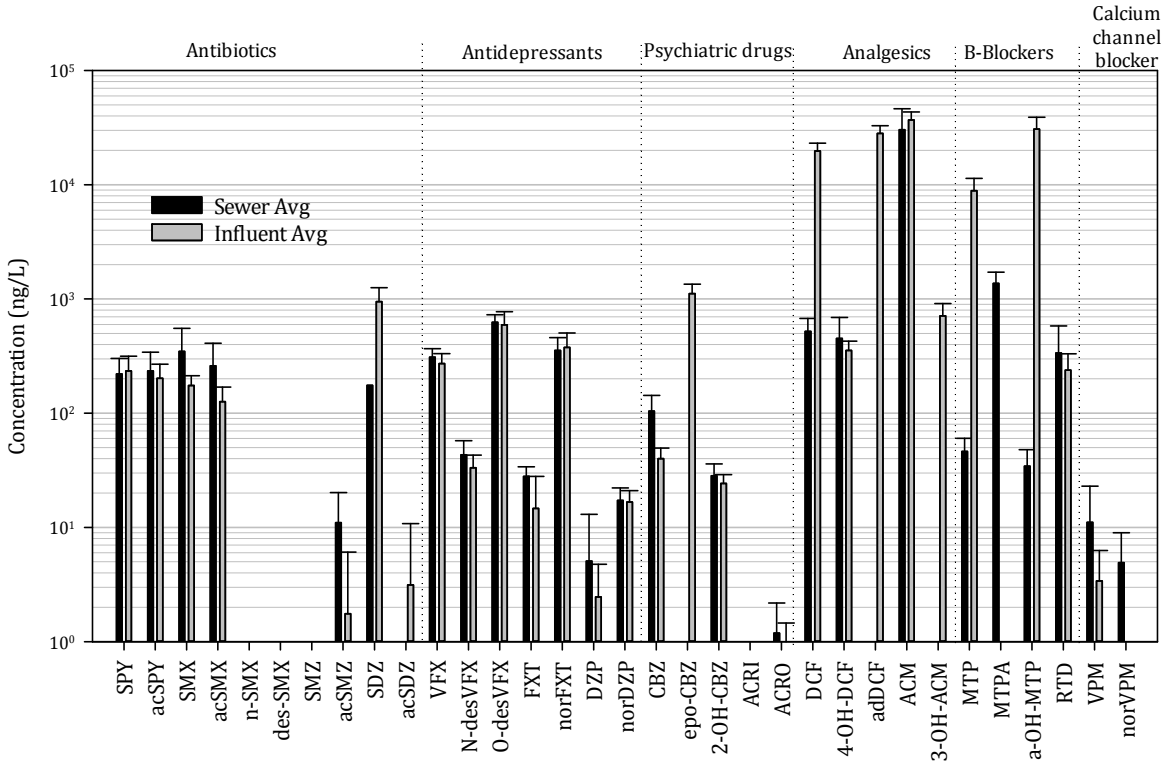

Figure 4-1: Measured concentrations (ng L-1) of the studied compounds in WWTP inlet (sewage) and following primary treatment (influent) of the sampling campaign in 2014. Gaps in the figure show that the analyte was not detected.

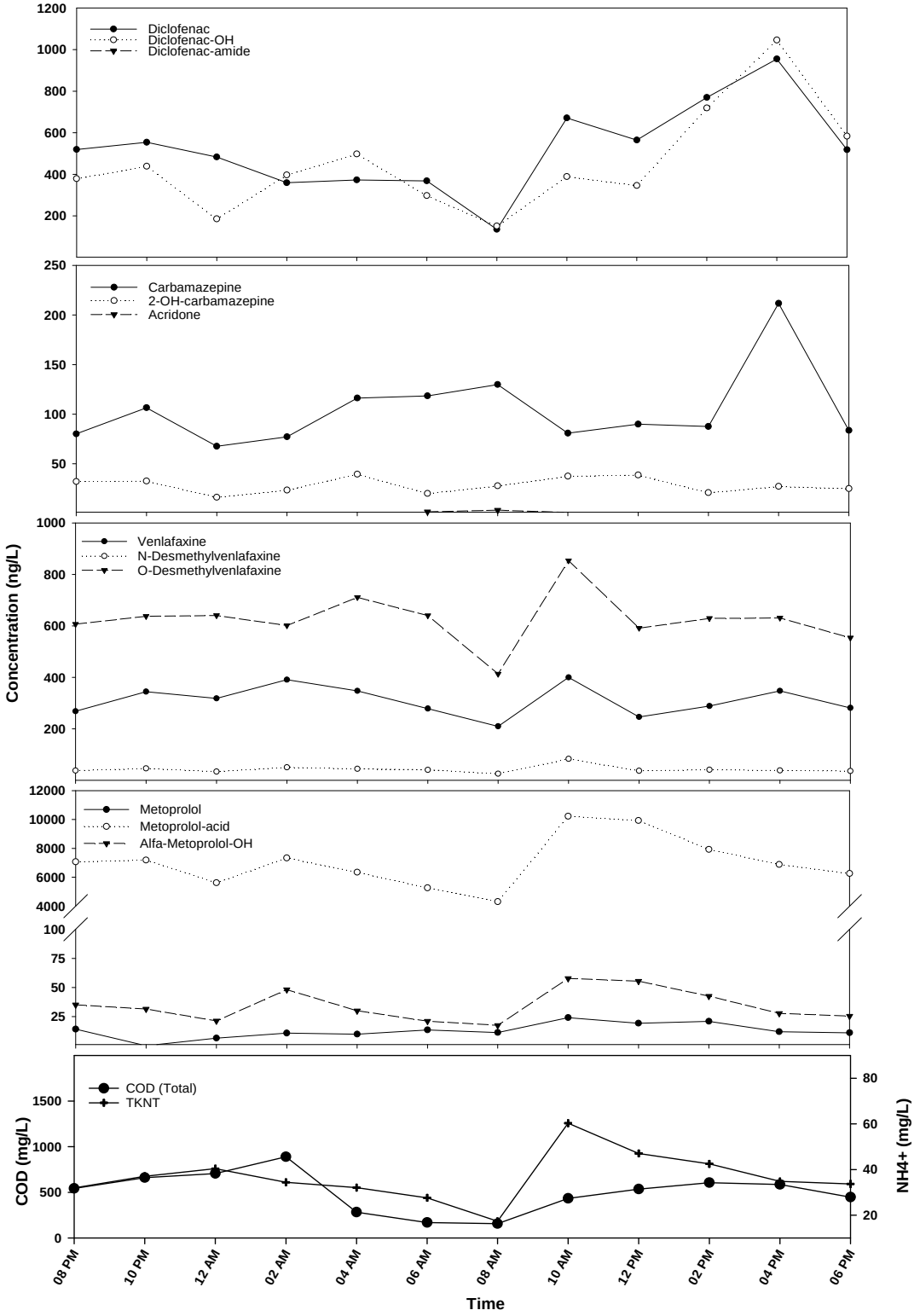

Figure 4-2: Concentration profile of diclofenac, carbamazepine, venlafaxine and metroprolol and their corresponding metabolites in the sewage samples over a 24-hour period, and evolution of the chemical oxygen demand (COD) and total Kjeldahl Nitrogen (TKN_T) over the same period.

4.3.2.2 Influent wastewater

In 2013, the highest concentrations detected in the influent samples corresponded to the same compounds as in 2014 but at lower concentrations. This could be due, amongst other reasons, to heavy rain events registered during April 2013 on the same week that sampling began, and also to a higher precipitation average during the sampling period in that year. As mentioned in the previous section, ACM was detected at the highest concentrations in both campaigns (see Table 11-5 in the Annex).

Regarding MTP and its metabolites, concentrations found for MTPA were slightly higher than those published by Rubirola et al., who detected levels ranging between 119 ng L^{-1} and 298 ng L^{-1} in influent wastewaters of two WWTPs in Catalonia (Spain) (Rubirola et al., 2014). Another publication made an estimation of the presence of this metabolite in WWTP influents at concentrations around 2 µg L^{-1} (Kern et al., 2010). The MTPA/MTP ratios in the influent ranged between 60-80, and are in accordance with the metabolic excretion rates of these compounds, as MTP is excreted in a 60-65% as MTPA, and only a 3-10% is excreted in its original form (Kern et al., 2010). Table 4-5 shows the concentration ratios between the parent drugs and their metabolites along the different treatment steps. As observed, the ratios are generally maintained between the sewage samples and the influent samples for all the target compounds.

4.3.3 Removal of PhACs by MBR

Out of the 13 parent compounds and 20 metabolites and TPs analysed, 10 parent compounds and 8 of their metabolites were observed at concentrations ten-times greater than their corresponding limit of detection (LOD) in the MBR effluent samples (LODs are given in Table 11-6). Due to the high number of studied compounds, concentrations below this threshold are not discussed in detail in this section.

Despite being the compound detected at the highest level in the influent samples, ACM was completely eliminated during the MBR treatment in both campaigns (see Figure 4-3). As they are hydrophilic compounds, adsorption to biomass is usually negligible and biodegradation should be considered the main removal mechanism (Guerra et al., 2014). On the contrary, concentrations of MTPA in the MBR effluents were higher than those detected in the influent in most cases, with average negative elimination rates of -52% and -42% in 2013 and 2014, respectively. These results could indicate the formation of this compound as biodegradation product of the parent compound MTP; however, as shown in Table 4-5, MTPA/MTP ratios are maintained in influent and effluent samples (being only slightly higher in the effluent for the samples of 2013), indicating that MTP is also not eliminated during MBR treatment and, similarly to MTPA, concentrations were usually

higher in the effluent samples, with average negative elimination rates of -38% and -45% (2013 and 2014 respectively, see Figure 4-3). Rubirola et al. reported a similar behaviour for MTPA and observed a concentration for MTPA 10 times higher in effluent than in the influent wastewater in a conventional WWTP. The authors attributed these high concentrations to the generation of MTPA from atenolol, the major β-blocker present in influent wastewaters (up to 2 orders of magnitude higher than MTP) (Rubirola et al., 2014). Indeed, Radjenovic et al. demonstrated in a previous study that MTPA was also a primary degradation product for atenolol in MBR-sludge batch experiments, in which MTPA was detected simultaneously to the immediate degradation of atenolol and reached a 40% of the initial spiked concentration of atenolol after only 1 day (Radjenovic et al., 2008). Despite it was out of the scope of this work, atenolol is frequently detected in MBR influent wastewaters (Gros et al., 2012; Kostich et al., 2014). Therefore, the higher concentrations of MTPA in the MBR effluent could be attributed to atenolol degradation during treatment.

Table 4-5: Concentration ratios between the investigated pharmaceuticals and their main metabolites and transformation products along the wastewater treatment

		Sewage	MBR influent	MBR effluent	RO/NF FEED	RO/NF PERMEATE	RO/NF CONCENTRATE
acSPY/SPY	*2013*	*no data*	1.5	1.2	1.3	0	1.5
	2014	1.06	0.9	1.2	0	0	0
acSMX/SMX	*2013*	*no data*	0.5	0.3	0	0	0
	2014	0.8	0.7	0	0	0	0
norVFX/VFX	*2013*	*no data*	0.2	0.2	0.2	-	0.3
	2014	0.14	0.1	0.1	0.1	0.3	0.1
O-desVFX/VFX	*2013*	*no data*	2.9	3	3.1	1.1	3.6
	2014	2.04	2.2	2.6	2.5	4.2	2.6
N-desVFX/VFX	*2013*	*no data*	0.2	0.2	0.2	-	0.2
	2014	*0.14*	0.1	0.1	0.1	0.3	0.1
norFXT/FXT	*2013*	*no data*	72.4	-	-	-	46.4
	2014	*4.7*	106.4	51.9	49.7	12.5	12.5
norDZP/DZP	*2013*	*no data*	1.7	3.5	56.5	-	3.6
	2014	*7.82*	9.8	12.5	14.2	-	5
4-OH-DCF/DCF	*2013*	*no data*	0.7	1.2	1.4	0	0.9
	2014	0.84	1.7	1.3	3.4	0	1.6
MTPA/MTP	*2013*	*no data*	30.8	35.7	39.3	0	25.4
	2014	30.4	28	27	33.7	0	17.7
α-OH-MTP/MTP	*2013*	*no data*	0.8	0.5	0.2	0	0.4
	2014	0.7	0.6	-	0.4	0	0.2

VFX and their two metabolites also showed negative removals in both campaigns, with higher concentrations after MBR treatment. These results are in accordance with previous studies in which negative elimination rates were obtained after CAS treatment (Gasser et al., 2012; Schlüsener et al., 2015). The limited sorption to the biomass of these compounds (low solid-water distribution coefficient (K_d)) and their resilience to biodegradation could explain partly this poor removal. This could also explain the results obtained for DZP and norDZP, with very low or negative elimination rates for both analytes in both campaigns. The same applies for the very low removals observed for CBZ or DCF; in this case, as mentioned in section 4.3.2., it is usually attributed not only to low biodegradability and low K_d values, but also to deconjugation of human phase II metabolites (that may not have been included in the monitoring), parent compound formation by enzymatic reactions from phase I metabolites or desorption from particulate matter (Verlicchi et al., 2012). For instance, removal efficiencies of DCF varied from negative values to an elimination of 76%. As mentioned in section 4.3.2, the SRT during both campaigns was 30 days. According to Clara et al., SRTs > 10 days enhance the biodegradation of PhACs such as DCF, whereas for CBZ there would not be any significant improvement (Clara et al., 2005). Indeed, for CBZ only negative removal values were obtained in both campaigns. In the present study, metabolites of CBZ also presented negative elimination rates (data from 2013) and therefore no correspondence could be established. Low removals of CBZ have been frequently reported by many researchers, and it is usually considered as a non-degradable, recalcitrant compound (Radjenovic et al., 2007).

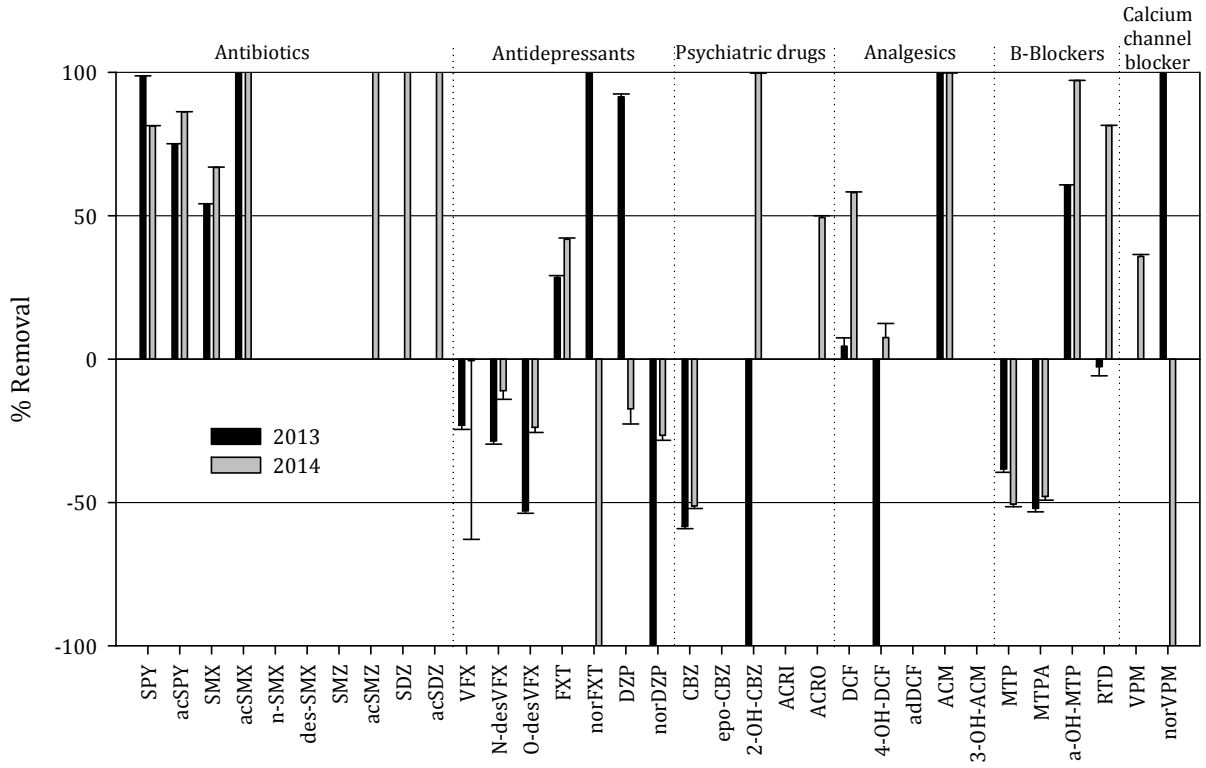

Figure 4-3: Removal (%) of the studied PhACs, metabolites and TPs during treatment in the MBR.

The acetylated metabolite of SMX was fully eliminated after MBR treatment in both campaigns. On the contrary, the concentration of SMX was only partially reduced, with removal rates ranging from 57-70% in 2013 and 60-84% in 2014. Xia et al. published similar removal values for SMX in an MBR but demonstrated that longer SRTs resulted in a better efficiency (Xia et al., 2012). Trinh et al. estimated a removal of 62% for SMX during MBR treatment (SRT of 15 d) and attributed a 59% of it to biotransformation, neglecting the possibility of adsorption to biomass. Other publications also highlighted biotransformation as the main removal mechanism for SMX (Göbel et al., 2007; Xia et al., 2012). Considering these previous results, despite the biodegradation of SMX during MBR, acSMX does not seems to be a potential biodegradation by-product of SMX, as it is not detected in the MBR effluent. A rapid hydrolysis and degradation of the metabolite itself could account for the incomplete removal of SMX in case it reverted back into the parent compound, as demonstrated for SPY (García Galán et al., 2012). The high removal efficiencies obtained in this work can be attributed to the high SRT and the mixed liquor suspended solids (MLSS) concentrations in MBRs (Fernandez-Fontaina et al., 2012).

4.3.4 Removal of PhACs by RO and NF

Water from the MBR system provided feed water with a Silt Density Index (SDI) consistently less than 5, (15 minutes), and often below an SDI of 3, making the water suitable for treatment by spiral wound RO and NF membrane processes in terms of particulate and colloidal matter. During the first 7 days of operation, in which PhACs monitoring took place, the RO membrane required a feed pressure of 6.5 bar, whereas the NF membrane required nearly half the operating feed pressure at 3.3 bar to produce a similar average permeate flux of 18 L m^{-2} h^{-1} at 75% recovery. Table 4-4 shows the performance of the RO and NF membranes in terms of conventional water quality parameters showing that on average, while the RO membrane had a rejection of 97% of the total dissolved solids (TDS) (measured as EC), whereas the NF membrane yielded a rejection of 92%.

As mentioned earlier, the main removal pathways of the target compounds during MBR treatment are biodegradation and their adsorption into the sludge, whereas their rejection through the submerged membranes can be considered negligible (Yu et al., 2006). The fate of those compounds that were not fully removed by the MBR process was then investigated as they passed through RO and NF membranes separately. The rejection results for the RO and NF membranes are given in Figure 4-4. The RO process resulted in a removal > 99%, for all the compounds evaluated. The few compounds which were still detected in the RO permeate at concentrations ten-times greater than their LOD (see Table 11-6 in the Annex) were O-desVFX (1.59±0.96 ng L^{-1}) which was detected in five out of the seven samples, α-OH-MTP (3.10 ± 3.12 ng L^{-1}) which was detected in four out of the seven samples, MTPA detected in two samples (5.39 ± 8.85 ng L^{-1}), epo-CBZ (0.93 ng L^{-1}), acSPY (1.5 ng L^{-1}) and SMX (5.47 ng L^{-1}) which were each detected in one sample. ACRI (1.35 ng L^{-1}) and RTD (0.02 ng L^{-1}) were also detected but below ten-times their LOD.

The NF membrane showed high removal efficiencies (>90%) for most of the studied compounds, although as expected, these removals were lower than those obtained with the RO membrane. At a similar flux, O-desVFX was found at 52 ng L^{-1} in the permeate of the NF membrane, a concentration 50 times greater than that of the RO permeate. A number of compounds and their metabolites were also detected in the permeate of the NF membrane while being completely removed by the RO membrane, including 4-OH-DCF (18 ng L^{-1}), VFX (10.72 ng L^{-1}) and N-desVFX (2.4 ng L^{-1}), FXT (1.24 ng L^{-1}), norFXT (15.52 ng L^{-1}), CBZ (15.52 ng L^{-1}), epo-CBZ (10.73 ng L^{-1}), 2-OH-CBZ (10.73 ng L^{-1}), MTP (10.55 ng L^{-1}) and RTD (3.33 ng L^{-1}). On the contrary, α-OH-MTP, which was also detected at low concentrations in the RO permeate was consistently well below LOD in the NF permeate samples.

As mentioned earlier in the paper, the MWCO for the ESPA2 RO is less than 100 Daltons (Bellona et al., 2012), whereas that of the NF membrane is approximately 200 Daltons (Alturki et al., 2010). The

compounds with the lowest MW amongst those compounds included in this study were ACM and its metabolite 3-OH-ACM (151 g mol^{-1} and 167 g mol^{-1} respectively) as well as ACRI (179.1 g mol^{-1}) and ACRO (195.2 g mol^{-1}). However, the benefit of integrating MBR with a RO process can´t be demonstrated in our study for these particular compounds, as all these PhACs had been completely removed during MBR treatment. Radjenović et al., (2008) investigated the rejection of ACM in a full-scale DWTP comparing RO (BW30LE-440) and the same NF membrane used in this study (NF90). The results showed that the RO membrane had a rejection of 85.6% for ACM, whereas the NF90 membrane had a lower rejection for ACM (44.6%).

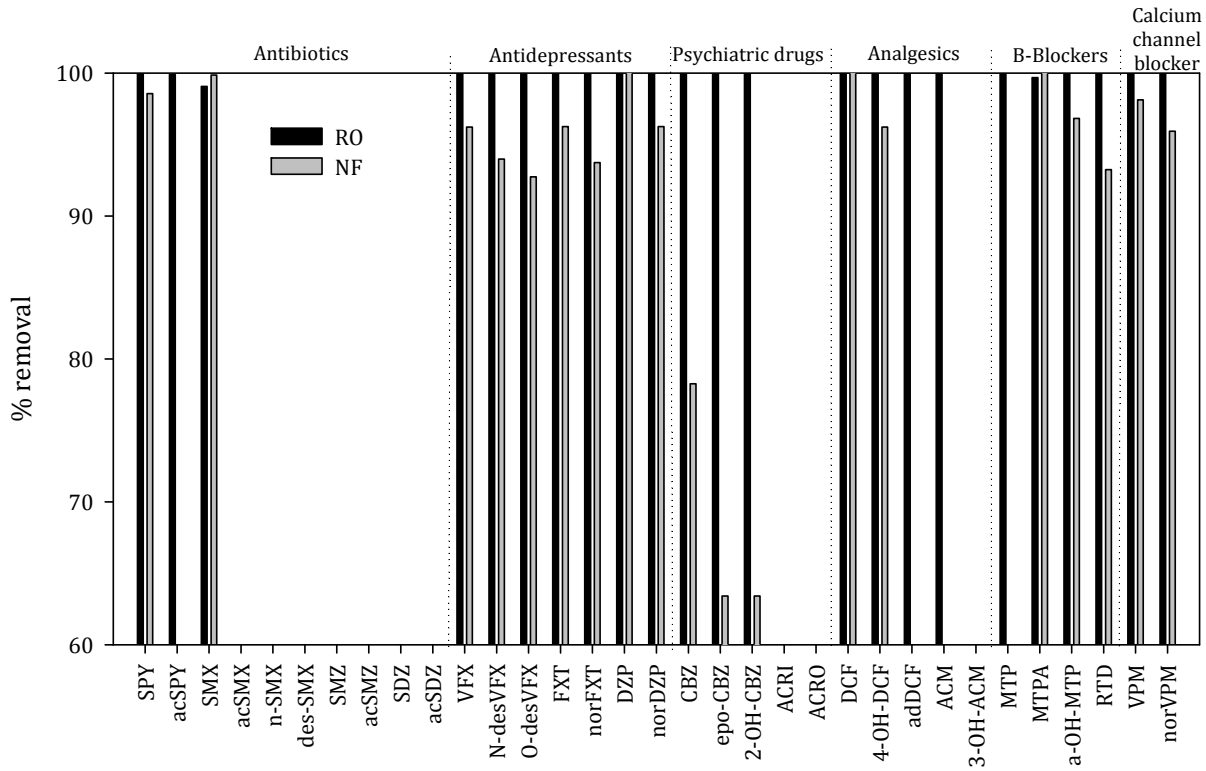

Figure 4-4: Removal (%) of the studied PhACs, metabolites and TPs by RO and NF membranes. Gaps in the figure show that the analyte was not detected.

Various studies have shown that there are a number of processes which affect the removal of solutes by membranes including membrane properties, the chemistry of the solution and the physicochemical properties of the contaminants (Bellona et al., 2004; Taheran et al., 2016). Although separation of trace contaminants by membrane processes is primarily based on size exclusion, net sorption at the membrane-solute interface plays an important role. Various studies have shown that size exclusion is responsible for rejection of uncharged and hydrophilic substances while electrostatic interactions between charged solutes and negatively charged membranes have an important role for charged solutes (Alturki et al., 2010; Taheran et al., 2016).

It is quite clear that the negatively charged RO and NF membranes used in this work had a significant effect on the lower rejection of positively charged compounds, since the few compounds detected above the LOQ in the permeate stream for both membranes were positively charged, including VFX, FXT, MTP and RTD.

When comparing the results to those of Radjenović et al., (2008), we observe that they obtained similar results for SMX and DCF (rejection >99%) working with the NF90 membrane, but also a higher rejection for CBZ (99.7%, at a flux of 22.9 L $m^{-2}h^{-1}$), compared to the results obtained in this study, of only 78% at a flux of 18 L $m^{-2}h^{-1}$ and 89% at a flux of 26 L $m^{-2}h^{-1}$.

4.3.5 Effect of average permeate flux on PhAC removal

As the flux of the NF90 membrane was increased from a relatively conservative flux of 18 L $m^{-2}h^{-1}$ to an average permeate flux of 26 and 30 L $m^{-2}h^{-1}$, the rejection of the studied PhACs, metabolites and TPs also increased. Higher rejection at higher fluxes occurs due to the increased dilution of the constituents of interest within the permeate channel, as more water passed through the membrane. This increase in the rejection as the flux increases is typically observed in RO systems when measuring the concentrations of ionic constituents (Cl^-, NO_3^-, PO_4^{3-}, SO_4^{2-}, Na^+, K^+, Mg^{2+}, Ca^{2+}) and EC. Figure 4-5 shows the effect on the rejection of the studied compounds when the average permeate flux for the NF membrane was increased from 18 L $m^{-2}h^{-1}$ to 26 L $m^{-2}h^{-1}$ and 30 L $m^{-2}h^{-1}$. The compounds which had rejections lower than 90% at an average permeate flux of 18 L $m^{-2}h^{-1}$, such as CBZ and MTP, increased these rates from 78% to 89% (at 26 L $m^{-2}h^{-1}$) and 97% (at 30 L $m^{-2}h^{-1}$) in the case of CBZ, and from 57% to 63% and 73 % for MTP. Compounds which had moderate rejection rates above 90%, such as VFX, N-desVFX or O-desVFX, increased to high rejection rates (>97%); as expected, those compounds which had high rejection rates (>97%) at the lower flux of 18 L $m^{-2}h^{-1}$ increased to near complete rejection; these include SPY (99% to 100%), FXT (96 to 100%), 4-OH-DCF (96% to 99 and 100%), α-OH-MTP (97% to 100%) and VPM (98% to 100%).

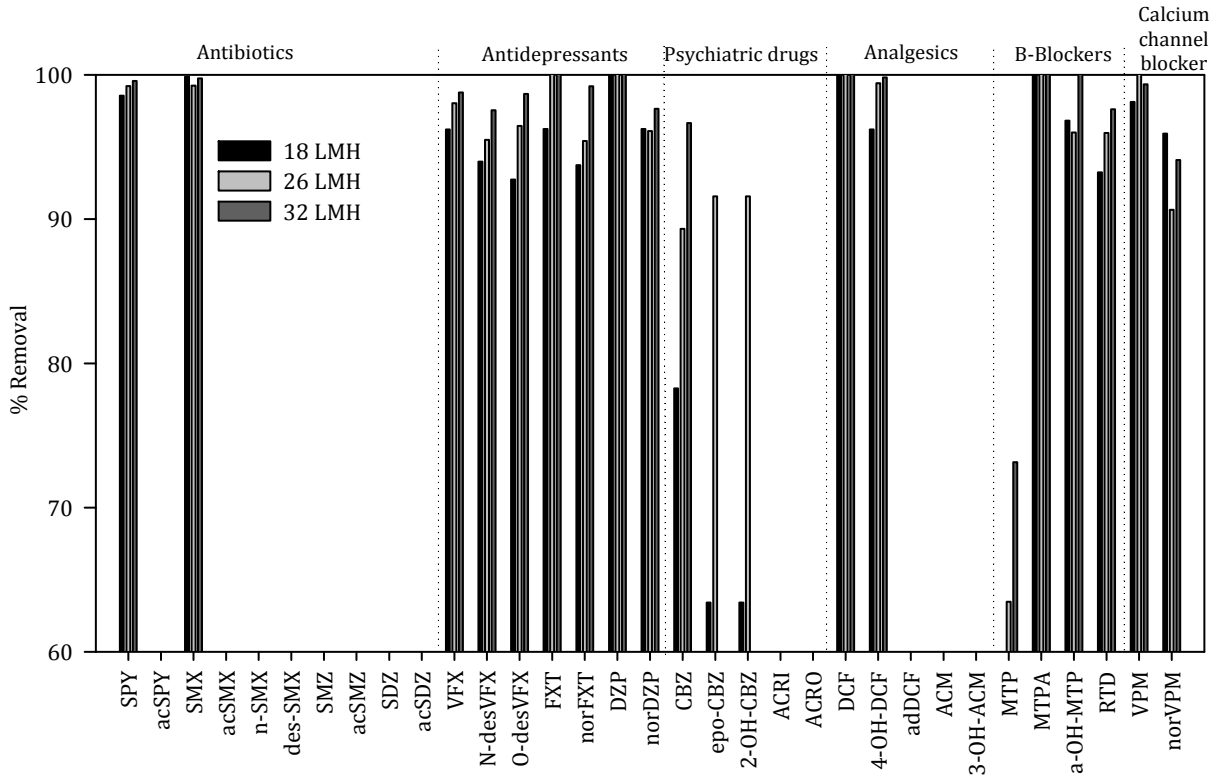

Figure 4-5: Removal (%) of the studied PhACs, metabolites and TPs by a NF membrane at different average permeate fluxes. Gaps in the figure show that the analyte was not detected.

4.3.6 Concentration of PhACs in the concentrate stream

The concentrations of the PhACs, metabolites and TPs in the concentrate stream are interesting from two different points of view. The first is the recognition that, although the concentrate stream may meet discharge limits for conventional regulated parameters such as nutrients (if a biological nutrient removal process is included and it is functioning correctly), the concentrate stream has high concentrations of the target compounds compared to those of the final effluents and even influent of the MBR process. As also noted in the work by Rodriguez-Mozaz et al., (2014), the concentrate stream poses a serious threat to aquatic ecosystems if discharged to water bodies. A number of options are discussed in the review by Pérez-González et al., (2012) to reduce the organic pollutant load in this concentrate stream prior to the release into the environment, by AOPs such as ozonation, fenton processes, photocatalysis and photo-oxidation, sonolysis and electrochemical oxidation. The second aspect is that, since this is a concentrate stream, we can identify compounds which had been removed by the MBR treatment to levels below the method LODs for the MBR effluent stream, but which had not actually been fully removed.

The compounds with concentrations > 500 ng L^{-1} in the concentrate stream during the RO and NF sampling campaigns included VFX and its metabolite O-desVFX, norFXT, DCF and 4-OH-DCF and MTPA (see Figure 11-1 and Table 11-7).

As expected, for those compounds which had similar concentrations in the RO/NF feed, the concentration of the RO concentrate was higher than that measured in the NF concentrate, due to the higher rejections by the RO membranes. This could be demonstrated by the concentration factor (CF), which is the ratio of the concentration in the membrane concentrate to that in the feed water. In theory, assuming perfect removal of solutes by a membrane, a system recovery of 75% should yield a CF of 4 (1/ (1-0.75)). In our case, the CF depended on the rejection of the particular compound by each of the membranes. For instance, the CF for the RO membrane (the membrane having a rejection closer to 100%) was usually higher than the theoretical value of 4 because concentrate recirculation was employed to comply with the membrane manufacturer operating specifications, as explained in section 3.1. The CFs for the compounds found to have the highest concentrations in the RO & NF concentrate were: VFX: 3.7 to 2.5, O-desVFX: 4.3 to 2.6, DCF: 4.5 to 4.4, 4-OH-DCF: 1 to 2.3, MTPA: 1.6 to 0.5. The CF for norFXT for the RO membrane could not be calculated since the concentration of the MBR effluent was < LOD, but a concentration of 3046 ng L^{-1} was measured in the concentrate.

4.4 Conclusion

This work allowed us to compare the removal of selected PhACs, metabolites and their TPs through MBR-RO and MBR-NF processes treating real wastewater to understand the extent of the difference in the rejection of such compounds when using low pressure NF membranes in the place of RO membranes. An automated analytical methodology based on LC-LC-MS/MS was used to quantify the concentration of 14 parent compounds and 22 of their metabolites from the sewage, to primary treatment, through to the MBR and finally through the RO or NF membranes. The results showed that the two consecutive membrane processes, when seen as a whole, become a highly efficient process to remove all the studied compounds, generating a highly concentrate stream which would require further treatment processes before being discharged into the natural environment. When comparing the removal efficiencies of the RO and NF membranes, as expected, the RO membrane showed near complete removals (>99%) of all the compounds over various process conditions, whereas the NF membrane resulted also in high removal efficiencies (> 90%). The results also showed that the rejection of the NF membrane increased significantly when the average permeate flux of the NF membrane was increased to 30 L m^{-2} h^{-1}, but still operating at feed pressures lower than that of the RO membrane operating at an average flux. The choice between using a RO versus a

tight NF membrane very much depends on the reclamation application and the discharge limits set. In terms of PhACs and their metabolites and TPs, for instance, if concentrations below 20 ng L^{-1} are acceptable in the permeate water, then using tight NF membranes similar to those utilized in this study would reduce the pumping power required to obtain the same amount of water by nearly half. If lower concentrations are required (i.e. below 5 ng L^{-1}), then a RO membrane will be required. Increasing the flux of the NF membrane will reduce the concentrations close to those obtained by the RO membrane, but would then require a similar pumping power as the RO membrane and probably suffer in terms of increased membrane fouling and would therefore make sense to keep using a RO membrane at a conservative flux.

Chapter 5 - Fate of NDMA precursors through an MBR-NF pilot plant for urban wastewater reclamation

This chapter was redrafted from:

Mamo J., Insa S., Monclús H., Rodriguez-Roda I., Comas J., Barceló D., Farré M.J. (2016). Fate of NDMA precursors through an MBR-NF pilot plant for urban wastewater reclamation and the effect of changing aeration conditions. Water Research 102, 383,393.

5.1 Introduction

N-nitrosodimethylamine (NDMA) is a DBP classified as "B2 carcinogen - reasonably anticipated to be a human carcinogen" by the United States Environmental Protection Agency (EPA, 2017). It is believed that precursors of NDMA are largely anthropogenic in origin, in contrast to other conventional DBPs such as trihalomethanes (THMs) and haloacetic acids (HAAs), where natural organic matter is the main precursor pool (Bond et al., 2011). Therefore, the formation of NDMA is highly relevant to water reclamation or drinking water supplies impacted by wastewater (Schreiber and Mitch, 2006; Zeng et al., 2016).

While THM and HAA precursors are difficult to characterize as different fractions of natural organic matter may generate these DBPs upon disinfection, some particular NDMA precursors might be easier to monitor because, according to the published literature, nitrosamine precursors have a functional group that can release a secondary amine (Choi and Valentine, 2002; Dotson et al., 2009; Krauss et al., 2010b; Mitch and Sedlak, 2002). The majority of studies of NDMA formation have concentrated on dimethylamine as a precursor, a compound present in human urine and faeces, as well as being a common product of the chemical industry (Krauss et al., 2010b; Zeng and Mitch, 2015). However, the conversion of dimethylamine (DMA) to NDMA by monochloramination is rather inefficient, with yields of 0.5% (Sacher et al., 2008). Recent studies focused on the yield of NDMA formed from other individual compounds, including pharmaceuticals (Shen and Andrews, 2011b), pesticides (Chen and Young, 2008), cationic polymers and ion exchange resins employed during water treatment (Kohut and Andrews, 2003) as well as other quaternary amines that are used in toiletries (Kemper et al., 2010b). Although some precursors may have up to a ~90% molar yield (e.g., tertiary amines containing a β-aromatic ring such as ranitidine) most of them have low molar yields (e.g., ~2%) (Shen and Andrews, 2011a). Unfortunately, specific watershed-associated precursors responsible for significant NDMA formation have not yet been identified (Krasner et al., 2013a; Shah et al., 2012a).

Population increase, particularly in cities, and scarce water resources have raised the demand for use of highly treated municipal wastewater as a supplemental source of potable water. Studying the fate of DBP precursors during secondary effluent treatment is of importance as an increasing number of municipal wastewater treatment plants (WWTPs) are engaged in the practice of potable reclamation of treated wastewaters worldwide. NDMA formation in wastewater effluents can vary greatly. As an example, high variability in NDMA concentration and its precursors were reported in the secondary effluent of 7 different WWTPs in U.S.A by Sedlak et al., (2005) with values of up to 29,000 ng/L. On the other hand, (M. J. Farré et al., 2011) found concentrations of NDMA precursors

between 350 and 1,000 ng/L in secondary effluents of 6 WWTPs in South East Queensland (Australia).

Generally, removal of precursors can be achieved easier than the removal of NDMA itself. Previous work has investigated the fate of NDMA precursors through different barriers used for water reclamation such as MF followed by RO (M. J. Farré et al., 2011; Fujioka et al., 2013b; Sato et al., 2014; Sgroi et al., 2015) and ozone followed by biological carbon filtration (Maria José Farré et al., 2011; Gerrity et al., 2014). Membrane bioreactors (MBR), which combine biological-activated sludge process and membrane filtration, have become more popular in recent years for the treatment of wastewaters, particularly when the conventional activated sludge (CAS) process cannot cope with either composition of wastewater or fluctuations of wastewater flow rate. MBR technology is also used in cases where demand on the quality of effluent exceeds the capability of CAS. Many reports have focused on the removal of pharmaceuticals by MBR (Kimura et al., 2005; Radjenović et al., 2009; Reif et al., 2008). Also, several studies reported that nitrifying conditions in the activated sludge system were responsible for the elimination of pharmaceuticals in wastewater (Batt et al., 2006; Tran et al., 2009), hence it could be hypothesized that this same microbial population would be more effective in removing NDMA formation potential too. In fact, recently, Sgroi and co-authors (2016) observed that NDMA formation upon ozonation during water reclamation was lower in effluents treated for nitrogen removal and by extended biological oxidation. Therefore, they conclude that a complete biological nitrification was a strategic and essential treatment to reduce NDMA formation. Also, several studies (Dytczak et al., 2008; Phan et al., 2014) have investigated the impact of DO concentration and/or oxidation reduction potential (ORP) conditions on trace organic contaminants. However, a clear consensus has not been reached to date and a focused study that investigates specifically the removal of NDMA formation potential through MBR is still missing in the literature.

This work investigates the removal of NDMA formation potential (FP) as well as individual NDMA precursors by an MBR pilot plant that treats urban wastewater. Specifically, this paper explores how changes of the nitrification performance of the MBR, modified by changing the DO concentration in the aerobic compartment, affect the removal of NDMA formation potential and individual NDMA precursors. The individual precursors investigated include antibiotics and other CEC that contain the dimethylamine-moiety responsible for NDMA formation. In particular, we have measured the occurrence and fate of the following compounds: azithromycin, citalopram, clarithromycin, erythromycin, ranitidine, chlorotetracycline, doxycycline, oxytetracycline, roxithromycin, spiramycin, tetracycline, tylosin, and finally venlafaxine and its metabolite o-desmethylvenlafaxine.

Additionally, the investigated MBR effluent is also treated by a NF system for water reclamation. Hence, the study also presents the rejection of these individual NDMA precursors by a NF membrane and compares them with up-to-date published literature.

Finally, the effluent from the full scale WWTP, where the MBR pilot plant was located, was also evaluated for NDMA FP and individual precursors and compared to the MBR pilot plant effluent.

5.2 Methodology

5.2.1 Chemicals

All chemicals used for the analysis were of analytical grade and commercially available. NDMA (5000 µg/mL in methanol) had a purity of >99.9% and was obtained from Supelco. Deuterated d_6-NDMA was used as internal standard, (Sigma-Aldrich). For the NDMA formation potential test, ammonium chloride (>99.5%, Sigma-Aldrich), sodium hydroxide (ACS, ISO, Reag, Sharlau) and sodium hypochlorite solution (reagent grade, available chlorine ≥4%, Sigma-Aldrich) were used. Potassium dihydrogenphosphate (KH_2PO_4, >99%, Sigma) and disodiumhydrogenphosphate ($Na_2HPO_4 \cdot 2H_2O$, >99%, Sigma) were used to prepare pH buffer solutions. To quench the chloramines, sodium sulphite (>98%, Sigma) was employed. Commercial DPD (N,N-diethyl-p-phenylenediamine) test kits (LCK310, Hach Lange) were used for the analysis of free and total chlorine using a Hach DR2800 spectrophotometer. For solid phase microextraction (SPME), sodium chloride (ACS, ISO, Reag, Sharlau) was used. SPME fibres from Supelco (85µm CAR/PDMS, Stableflex, 24Ga) were employed.

All individual NDMA precursor standards were of high purity grade (>90%). Venlafaxine, azithromycin, clarithromycin, roxithromycin, spiramycin, ranitidine, tetracycline, oxytetracycline, erythromycin and chlorotetracycline were purchased from Sigma-Aldrich as hydrochloride salts. Doxycycline and tylosin were acquired as hyclate and tartar salt, respectively. Citalopram was obtained as hydrobromide salt. O-desmethylvenlafaxine was purchased from Toronto Research Chemicals. Isotopically labelled compounds, used as internal standards, were venlafaxine-d_6, erythromycin-N,N-dimethyl-^{13}C, purchased from Sigma–Aldrich. Azithromycin-d_3 and tetracycline-d_6 were purchased from Toronto Research Chemicals. Cimetidine-d_3 and citalopram-d_4 (as hydrobromide) were purchased from CDN isotopes. These internal standards were chosen according to previously published methodologies (Gros et al., 2013a, 2012). Both individual stock standard and isotopically labelled internal standard solutions were prepared in methanol at a concentration of 1000 mg/L. After preparation, standards were stored at −20 °C. Special precautions have to be taken for tetracycline and tetracycline-d_6, which have to be stored in the dark, since it has been demonstrated that tetracycline antibiotics are photolabile (Eichhorn and Aga, 2004). Fresh stock antibiotic solutions were prepared monthly due to their limited stability. Stock solutions for the rest

of substances were renewed every six months. Working standard solutions, containing all pharmaceuticals, were also prepared in water and were renewed before each analytical run by mixing appropriate amounts of the intermediate solutions. Separate mixtures of isotopically labelled internal standards were prepared in methanol and further dilutions in water for on-line analysis.

5.2.2 MBR-NF pilot plant

For this part of the experiment the pilot plant was installed at the WWTP of Quart (Girona) to treat domestic wastewater. WWTP primary effluent was taken after the coarse screen of the WWTP and pumped to the pilot plant, which had a capacity of 3.4 m^3/day. Aeration within the aerated tank was controlled based on the DO set-point while the air scour flow rate was maintained at 10 m^3/h within the membrane tank to control membrane fouling. Biomass was wasted from the membrane tank hourly to maintain a solid retention time (SRT) of 30 days initially until June 30th and then reduced to 19±1 days such that SRT never became the limitation factor for nitrification. Permeate was obtained by applying a vacuum pressure drop over the membranes using a positive advance pump (Seepex) at a flux of 25 L/m^2·h (200 L/h) with filtration cycles of 9 minutes followed by 1 minute of relaxation (See Appendix 3 Table 11-10 for operational parameters of the MBR). The membrane tested was a NF90- 4040 membrane (DOW Filmtec).

The operating conditions of the NF system are given in Table 5-1. Internal concentrate recirculation was employed to increase the system recovery while remaining within membrane supplier's specifications. The VFD and the actuated concentrate valve allowed the system to be operated at a constant average permeate flux based on a fixed permeate flow set point of 135 L/h. For most of the test period a system recovery (Qp/Qf) of 75% and a net flux (Qp/Membrane surface area) of 18 L/m^2·h was utilized. During the last week of the experiment, the system recovery was set to 50%. The recovery of the membrane element (Qp/Qs) which includes concentrate recirculation was set at 12.5% within the manufacturer's guidelines.

5.2.3 Experimental Methodology

To change the nitrification conditions, different DO set-points were applied in the aerobic compartment of the pilot plant in order to understand the effect of nitrification on the removal of NDMA precursors. Two different operational conditions for the aerobic compartment were studied: experimental period 1 with DO in aerobic compartment equal or higher than 0.5 mg O_2/L (until August 5th) and experimental period 2 with DO lower than 0.5 mg O_2/L.

Sampling was carried out generally twice per week from 15 of May 2015 to 27 of August 2015 during dry weather flow to avoid the dilution of influent due to a combined sewage system. Figure 3-2 in the methodology shows the sampling points in a scheme of the pilot plant. 24-hour composite samples were taken for the MBR influent (1), MBR effluent (2), while grab samples were taken for the NF system feed (3), NF permeate (4) and NF concentrate (5). Samples were collected in pre-rinsed PET bottles. Samples were filtered through a 1.2 µm microfiber filter (Merck Millipore) followed by a 0.45 µm nylon membrane filter (Merck Millipore) before analysis. Composite samples were taken using an auto sampler which drew a sample every hour over a 24-hour period. Prior to this sampling, a 24-hour profile experiment was also carried out on the 12 of May 2015 to screen the concentration of NDMA precursors following the primary screen of the WWTP (Figure 11-2 in the annexes).

Table 5-1: Parameters describing the NF system and NDMA FP concentrations in the feed, permeate and concentrate. LOQ=50 ng/L

Flow rates-->	**NF system Feed**	**Internal recycle**	**Permeate**	**System conc**	**Membrane feed**	**Membrane Conc**	**System recovery**	**Membrane recovery**	**NDMA FP concentrations**			
Date	Q_f	Q_r	Q_p	Q_i	Q_s	Q_c (=Q_r+Q_i)	= Qp / Qf	=Qp / Qs	**System Feed**	**Permeate**	**System Concentrate**	**% membrane rejection**
	L/h	L/h	L/h	L/h	L/h	L/h			(ng/L)	(ng/L)	(ng/L)	%
15/05/2015	170	1040	135	35	1210	1075	79.4%	11.2%	1132	81	1415	**93.6%**
20/05/2015	183	895	136	47	1078	942	74.3%	12.6%	417	<LOQ	569	**>90.0%**
27/05/2015	179	893	136	43	1072	936	76.0%	12.7%	276	<LOQ	870	**>93.5%**
19/06/2015	188	896	135	53	1084	949	71.8%	12.5%	282	<LOQ	911	**>93.8%**
26/06/2015	178	903	135	43	1081	946	75.8%	12.5%	337	<LOQ	1018	**>94.4%**
1/07/2015	178	900	135	43	1078	943	75.8%	12.5%	358	206	555	**60.0%**
9/07/2015	182	891	135	47	1073	938	74.2%	12.6%	325	<LOQ	908	**>93.7%**
15/07/2015	178	902	135	43	1080	945	75.8%	12.5%	138	<LOQ	595	**>90.5%**
22/07/2015	178	902	135	43	1080	945	75.8%	12.5%	238	91	775	**86.8%**
29/07/2015	178	902	135	43	1080	945	75.8%	12.5%	202	<LOQ	413	**>86.4%**
12/08/2015	182	898	135	47	1080	945	74.2%	12.5%	2153	113	6462	**98.0%**
13/08/2015	182	898	135	47	1080	945	74.2%	12.5%	720	121	2606	**94.7%**
21/08/2015	178	902	135	43	1080	945	75.8%	12.5%	2406	100	6484	**98.2%**
25/08/2015	265	815	135	130	1080	945	50.9%	12.5%	1510	58	2881	**97.7%**
26/08/2015	265	815	135	130	1080	945	50.9%	12.5%	1862	79	2182	**95.9%**
27/08/2015	265	815	135	130	1080	945	50.9%	12.5%	1437	63	2164	**96.7%**

5.2.4 Analysis of NDMA formation potential and individual NDMA precursors

NDMA precursors were quantified by first carrying out an NDMA formation potential (FP) test on the water samples and then analyzing the generated NDMA by SPME followed by gas chromatography coupled to a triple quadrupole mass spectrometer (GC-QqQ). For the NDMA FP test, the protocol published by Mitch et al. (2003) was followed. Briefly, 140 mg/L monochloramine prepared at pH 8 was added to a 10 mM phosphate buffered filtered sample. During the FP test samples were stored in the dark and at ambient conditions (T=21±1^{o}C) for 7 days. After this contact time chloramines were quenched with 2.5 g of sodium sulfite (Sacher et al., 2008). NDMA FP of the pharmaceuticals investigated was performed by adding 140 mg/L chloramine to a 10 mM phosphate buffered solution of 2 mg/L of the specific compound. Such a high concentration was used to ensure we could measure NDMA formation even in those precursors with very low NDMA yield.

The procedure for NDMA analysis was modified from the headspace method proposed by Grebel et al., (2006).

Specific CEC acting as NDMA precursors were analysed by fully automated on-line pre-concentration using EQuan MAX^{TM} technology coupled to a TSQ Vantage triple quadrupole mass spectrometer (Thermo Fisher Scientific) (on-line SPE-UHPLC-MS-MS) equipped with an electrospray ionization source (ESI) following the method described by Farré et al., (2016) and the details can be found in Table 11-9 in the Annexes.

5.2.5 Other analyses

Samples were also analysed for total suspended solids and volatile suspended solids (TSS & VSS; APHA standard method 2540D), total and soluble chemical oxygen demand (COD; APHA standard method 5220B), biochemical oxygen demand (BOD; WTW, Oxi Top), dissolved organic carbon (DOC; Shimadzu TOC-V_{CSH} analyzer), ammonium (BUCHI B-324 distiller, Titrino 719S Methrohm) and total Kjeldahl nitrogen (BUCHI B-324 distiller, Titrino 719S Methrohm). Nitrites (NO_2^--N), nitrates (NO_3^--N), and phosphates (PO_4^{3-}-P), together with other major ions (Na^+, K^+, Mg^{2+}, Ca^{2+}, Cl^-) were analysed using ion chromatography (Metrohm 761-Compact; APHA standard method 4110B).

5.3 Results

5.3.1.1 Fate of NDMA precursors through the MBR

Analytical results of a 24 h sampling campaign of the primary effluent were used to characterize the wastewater composition, in particular the concentration of NDMA precursors (i.e, through NDMA FP). Concentrations of NDMA precursors in the primary effluent ranged from 4,000 to 7,700 ng/L, rather presenting arbitrary variation than a characteristic daily profile. Results of this sampling profile can be found in the Figure 11-2 in the Annexes. The concentration of NDMA precursors found in this study is similar to previously published data where the range of NDMA FP measured was 2,400 to 9,400 ng/L (Sedlak et al., 2005). As shown later, during the entire study the concentration of the NDMA FP measured in the influent of the WWTP ranged from 3,120 to 11,120 ng/L.

The main aim of this study was to investigate how the MBR pilot plant performance could affect the removal of NDMA precursors; hence, the aeration conditions of the MBR aerobic compartment were changed according to the details described in Table 5-2 (i.e. DO in aerobic compartment equal or higher than 0.5 mg O_2/L until August 5th and then DO lower than 0.5 mg O_2/L). This table also shows MBR influent and effluent ammonia and nitrate concentrations during this experimental period to confirm that the changing nitrification conditions were fully accomplished. Other analytical parameters are summarized in Table 11-11 in the Annexes. Dalmau and co-authors (2014), previously investigated the effect of aeration on biological and filtration performance of the same MBR pilot plant. To this aim, they planned two sets of experiments: Experiment A used a modification of the DO set-point in the aerobic compartment and Experiment B involved a modification of the air-scour flow rate in the membrane tank. They found that the optimal value was a DO set-point of 0.5 mg O_2/L in the aerobic tank and that the activity of nitrifiers was significantly reduced when the DO set-point was decreased to lower values. Besides, in these conditions, the air scouring used in the membrane tank was not enough to support nitrification, as in our current study.

Figure 5-1 shows the NDMA formation potential of both influent and effluent at the MBR during the sampling period as well as the percentage of NH_4^+ removal. No background NDMA could be measured above the limit of quantification in any of the influent samples. As no disinfectants were used through the plant, NDMA background measurements were not further investigated. As seen in Figure 5-1 as well as in Table 5-2, it is quite evident that during normal nitrification conditions the MBR was able to reduce NDMA precursors (i.e., NDMA FP) above 94% (values measured from 27/5/2015 until 12/8/2015). However, this removal percentage was reduced to values as low as 72% when changing the conditions

to inhibit nitrification (values measured until 28/8/2015). Values obtained for 15/5/2015 and 20/5/2015 also show a lower percentage of NDMA FP removal (i.e., 91 and 93%) in accordance with the aeration conditions that minimized nitrification conditions used during these dates. These results corroborate the findings of Sgroi et al., (2016) who observed that NDMA formation upon ozonation was lower in effluents treated for nitrogen removal and by extended biological oxidation. Hence, we also conclude that a complete biological nitrification was a strategic and essential treatment to reduce NDMA formation. In agreement, we also observed a lower total Kjeldahl nitrogen removal when nitrification conditions were minimized (see Table 11-11 in the Annexes).

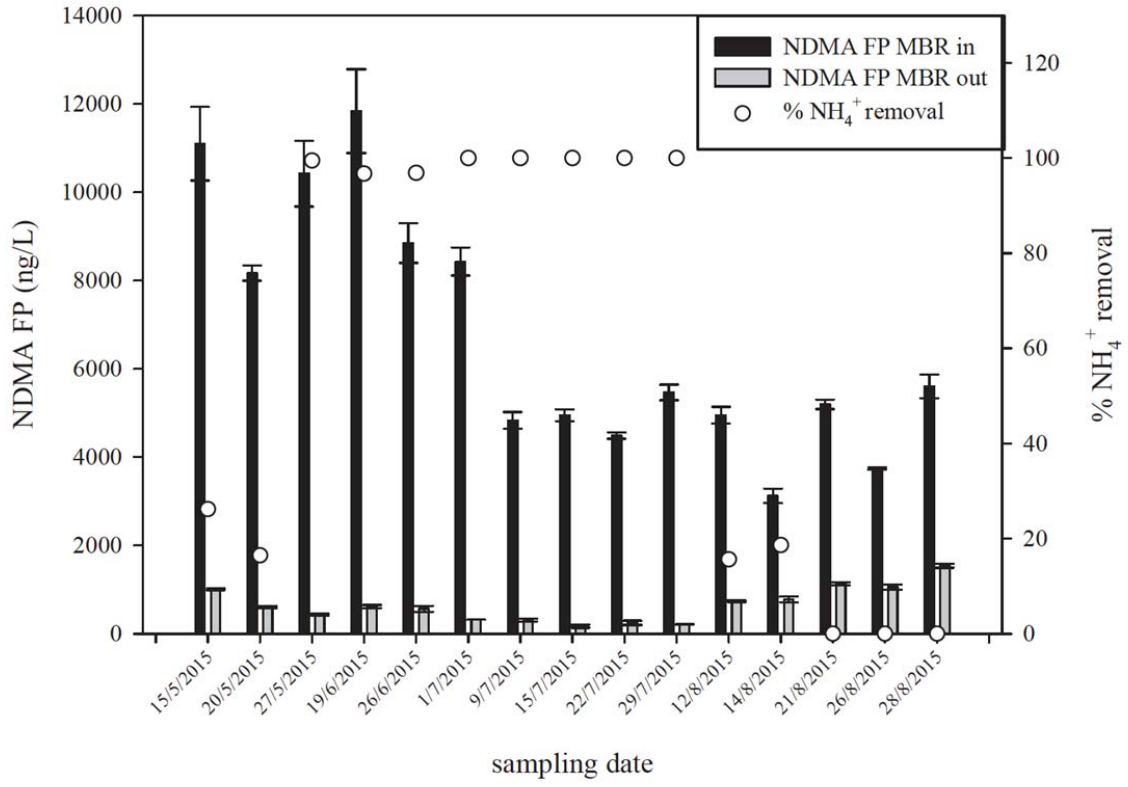

Figure 5-1: NDMA FP (ng/L) and percentage NH_4^+ removal at the MBR pilot plant. Error bars correspond to the standard deviation (n≥3) or to the range (n=2) of the replicates measured.

Our results showed that changes of the SRT, which decreased from 30 to 17 days, did not affect the removal of NDMA FP by the MBR (Table 5-2). The DOC in the MBR permeate was higher than expected as observed in other similar MBR systems operated at Bedok Water Reclamation Plant (Singapore), where DOC was generally below 5 mg/L compared to an average of 12 mg/L measured during our

experiments (Judd and Judd, 2008). This may be due to the age of the membranes being utilized, but also simply due to the different characteristics of DOC in different studies.

Table 5-2: Effect of solid retention time (SRT) and dissolved oxygen (DO) on the percentage of NDMA precursor removal by the MBR. n.m= not measured. LOQ =0.001 mg/L.

Date	SRT (days)	DO in Aerated tank (mg/L)	NH_4^+ (in)	NH_4^+ (out)	NO_3^- (in)	NO_3^- (out)	% NDMA removal MBR
28-Apr	30	1.0	63.1	46.6	0.11	0.4	n.m
4-May	30	1.0	68.1	0.1	0.14	6.7	n.m
7-May	37	1.0	47.0	0.7	0.17	2.5	n.m
15-May	30	0.0	63.1	46.6	0.11	0.4	91
20-May	30	0.0	37.6	31.4	0.14	0.2	93
27-May	30	1.0	116.6	0.6	0.03	0.0	96
19-Jun	30	1.2	64.17	2.09	0.07	4.7	95
26-Jun	30	0.8	66	2.05	0.10	n.m	94
1-Jul	19	0.6	49,93	< LOQ	0.05	16.9	96
9-Jul	18	0.6	48,3	< LOQ	n.m	n.m	94
15-Jul	18	0.6	52,44	< LOQ	0.00	18,39	97
22-Jul	17	0.6	44,1	< LOQ	0.00	21.4	95
29-Jul	19	0.6	53.6	< LOQ	0.06	28.3	96
5-Aug	20	0.5	47.85	< LOQ	0.09	30.4	n.m
12-Aug	19	0.0	47.75	40.3	0.09	0.4	85
13-Aug	20	0.0	49.47	40.25	0.07	0.1	75
21-Aug	20	0.0	56.61	57.53	0.02	0.1	78
26-Aug	20	0.0	56.18	56.84	0.09	0.1	72
28-Aug	20	0.0	48.42	55.15	0.03	0.0	73

Similar to previous published data (Sedlak et al., 2005) no clear correlation was observed between NDMA precursor concentrations and variables such as COD or BOD_5 (Figure 11-3 and Figure 11-4 in the

Annexes for correlations at the influent and effluent of the MBR, respectively). However, a correlation could be observed for DOC and NDMA FP in the MBR permeate. This correlation was particularly strong (R^2>0.7) when only using the values where nitrification was minimized (Figure 5-2). That probably means that NDMA precursors are compounds that are well removed under nitrifying conditions. Hence, this observation supports the hypothesis that nitrification is a good strategy to minimize NDMA formation potential of wastewater effluents.

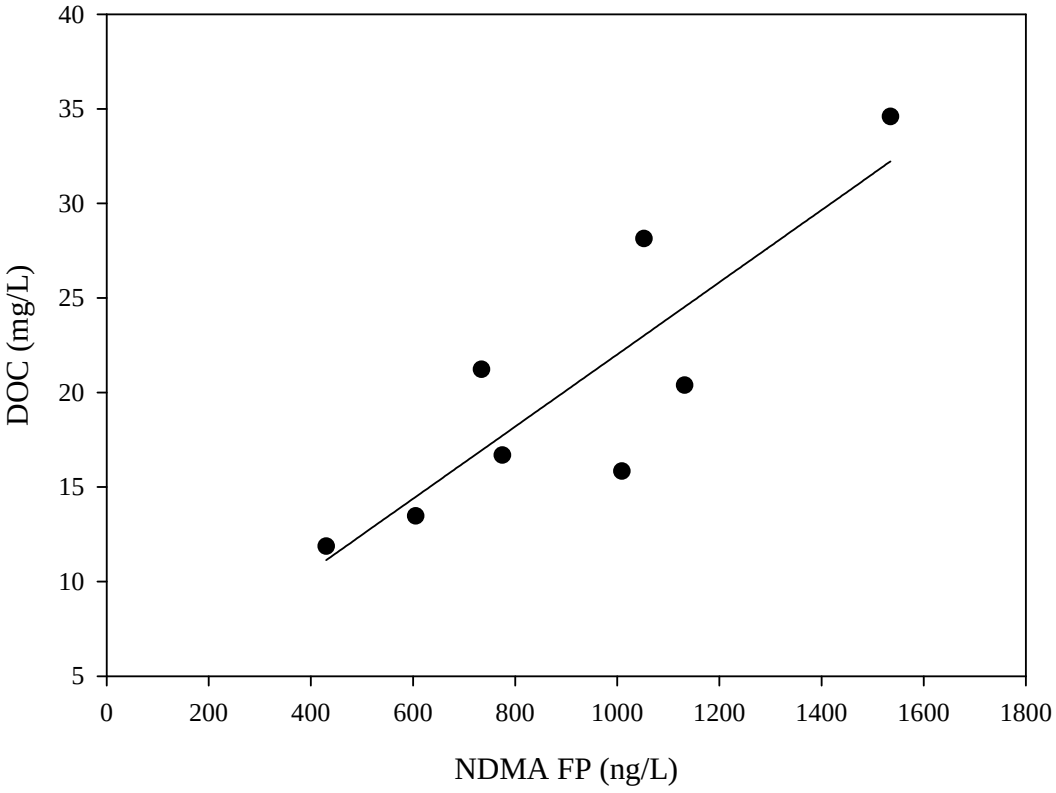

Figure 5-2: Correlation between NDMA FP (ng/L) and DOC (mg/L) at the MBR pilot plant effluent during anoxic operation.

The TMP averaged -32 mbar until the 5th of August when the DO set-point was changed to 0 mg/L to stop nitrification. As expected, when the DO set point was reduced, the TMP increased to -195 mbar due to the effect of the low DO concentration on the quality of the activated sludge.

5.3.2 Fate of individual NDMA precursors through the MBR

Mitch and Sedlak, (2004) found that biological treatment effectively removed the known NDMA precursor dimethylamine, lowering its concentration to levels that could not produce significant

quantities of NDMA upon disinfection. However, biological treatment was less effective at removing other dissolved NDMA precursors, even after extended biological treatment. Dimethylamine was not measured in this study but the NDMA FP after the biological treatment was just above 100 ng/L under nitrifying conditions, and around 1,000 ng/L when nitrification was avoided. Therefore, in order to investigate whether or not nitrification affects individual NDMA precursors the same way than NDMA formation potential, specific dimethylamino-moiety-containing compounds were measured. The list of specific NDMA precursors investigated in the study given in section 5.1 was created based on occurrence data (Gros et al., 2013b, 2012), and on the potential to generate NDMA (Roback, 2015; Schmidt et al., 2006; Shen and Andrews, 2011a). Figure 5-3 shows experimental NDMA FP for these specific precursors experimentally measured (Farré et al., 2016).

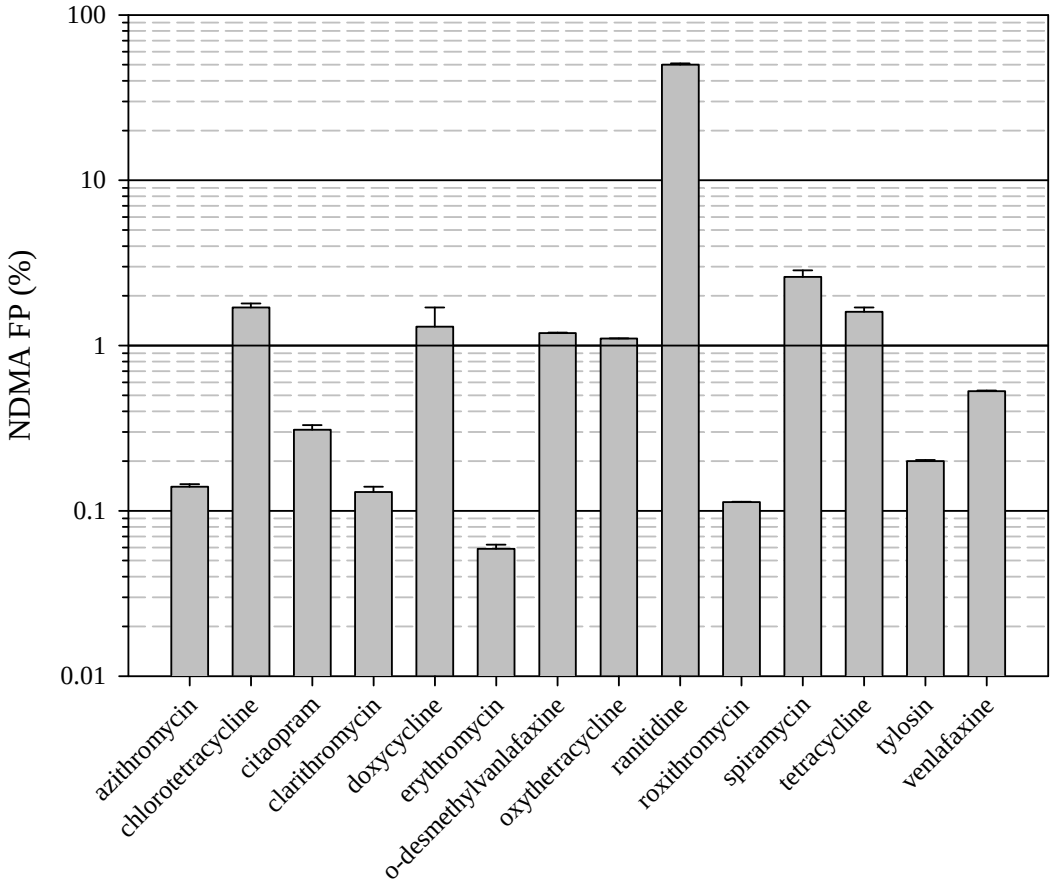

Figure 5-3: NDMA FP of the individual compounds investigated. NDMA FP test are performed in HPLC water during 7 days at ambient temperature. Error bar corresponds to the range of two measurements.

Among the fourteen investigated compounds, only 7 were detected. Chlorotetracycline, doxycycline, oxytetracycline, roxithromycin, spiramycin, tetracycline and tylosin were the non-detected compounds, in agreement with previous research conducted in the same geographic region (Gros et al., 2013b, 2012).

Table 5-3 shows the concentration of the analysed compounds that were detected across the pilot plant including the subsequent NF step that will be discussed later. Again, this data mostly agrees with occurrence data from the same region previously published. For example, citalopram was found at 303±46 ng/L (error for this and subsequent values corresponds to the standard deviation of 17 measures corresponding to 17 sampling days) at the influent of the MBR and this value decreased to 220±36 ng/L after the MBR treatment. Gros et al., (2012) measured 319 ng/L and 163 ng/L at the influent of two urban WWTPs that were able to reduce the values to 288 and 49 ng/L, respectively, after conventional biological treatment. Erythromycin was detected at 90±115 ng/L and 37±32 ng/L at the influent and effluent of the MBR while Gros et al., (2012) measured 63 ng/L and 35 ng/L at the influent and 17 ng/L and 14 ng/L at the effluent of the two investigated conventional WWTPs. Values observed for venlafaxine, ranitidine and clarithromycin were even closer to previously published data. On the other hand, azithromycin was detected at an average concentration of 1,510±729 ng/L and 499±279 ng/L at the influent and effluent of the MBR, respectively. This value is higher than the ones published by Gros et al., (2013), who reported values between 184 ng/L and 403 ng/L at the influent of different WWTPs. Also, very high concentrations were found for the venlafaxine metabolite o-desmethylvenlafaxine, as the influent concentration in our study was 4,196±929 ng/L. However, similar high concentrations of this metabolite were previously found in the influent of various WWTPs in Canada (Lajeunesse et al., 2012).

Data showing the removal of both, NDMA FP and individual NDMA precursors by the MBR is plotted in Figure 5-4. As mentioned earlier, NDMA FP removal decreased from more than 94% to 72% when nitrification was inhibited. This decrease was also reflected in the removal efficiencies of azithromycin (68 to 59%), citalopram (31 to 17%), venlafaxine (35 to 15%), and erythromycin (61 to 16%), where the values correspond to the average during nitrifying and non-nitrifying conditions, respectively. The removal of clarithromycin, o-desmethylvenlafaxine, and ranitidine could not be correlated that clearly with the nitrification inhibition as it varied strongly during the experiment time. However, lower removal rates were observed during the last three sampling events for clarithromycin and ranitidine in agreement with the hypothesis that nitrification increases the removal of NDMA precursors. In particular the percentage of removal decrease from 86 to 24% and from 77 to 57% for clarithromycin

and ranitidine, respectively, when considering the last three samples for the non-nitrifying system. Removal results for ranitidine and erythromycin are in accordance with data published by Radjenovic et al., (2007), who reported an average removal by an MBR of 95 and 67.3% for ranitidine and erythromycin, respectively. (Suarez et al., 2010) also found that erythromycin was only significantly transformed in the aerobic conventional biological reactor (>80%), although we still observed also a low (16%) removal under non-nitrifying conditions. In that same study the anti-depressant citalopram was moderately biotransformed under both, aerobic and anoxic conditions (>60% and >40%, respectively), which is slightly higher than our results. Also, azithromycin and clarithromycin were removed up to 55% and 20%, respectively in a conventional water treatment plant as reported by Göbel et al., (2007). Gros et al., (2012) found a removal up to 37% for venlafaxine in a conventional urban WWTP, which also agrees with the results presented in this study. No previous published information has been found for the removal of the venlafaxine metabolite o-desmethylvenlafaxine by biological treatment.

According to the data presented in Table 5-3 (i.e., concentration of NDMA precursor measured in each sample), Figure 5-3 (i.e., percentage of NDMA FP of individual precursors) and using Equation 5.1, 2-6% of the NDMA FP experimentally measured could be explained by the presence of the individual precursors measured.

$$\%\,\boldsymbol{NDMAFP\ explained} = \frac{\sum_{n=i}^{\frac{C_i \times NDMAFP_i \times MW_{NDMA}}{MW_i \times 100}}}{NDMAFP_s} \times \mathbf{100} \qquad \text{Equation 5.1}$$

The equation corresponds to the sum of individual theoretical NDMA FP obtained for all measured compounds divided by the NDMA FP measured in the samples by means of the NDMA FP test. Where C_i is the concentration (ng/L) of the individual NDMA precursor *i* detected (for example ranitidine), $NMDAFP_i$ is the NDMA formation potential of the individual precursor *i*, MW_{NDMA} is the molecular weight of NDMA, MW_i is the molecular weight of the individual precursor *i*, and NDMA FP_s is the NDMA formation potential of the sample measured (ng/L).

Table 5-3: Maximum, minimum and average concentration expressed in ng/L of the detected compounds across the MBR pilot plant.

Compound		Conc.MBR influent (ng/L)	Conc. MBR effluent (ng/L)	Conc. NF feed (ng/L)	Conc. NF perm (ng/L)	conc. NF concentrate (ng/L)
azithromycin	max	2492.7	1103.2	1439.9	26.6	3313.0
	min	378.3	168.9	125.6	2.5	515.6
	average	**1510.4**	**499.7**	**594.9**	**7.4**	**1507.1**
	st. dev (n=17)	729.1	279.1	373.5	5.5	908.3
citalopram	max	360.6	298.2	275.0	65.8	880.4
	min	205.6	162.4	180.0	2.6	268.5
	average	**303.8**	**220.5**	**218.7**	**27.0**	**583.9**
	st. dev (n=17)	46.4	36.1	24.7	19.0	171.7
erythromycin	max	549.0	143.2	141.2	0.8	460.0
	min	16.3	8.3	8.0	<LOQ	20.9
	average	**90.0**	**37.8**	**33.0**	**0.3**	**113.2**
	st. dev (n=17)	115.3	32.1	30.0	0.3	114.6
venlafaxine	max	741.2	515.7	477.1	111.6	1524.3
	min	433.8	313.4	276.6	9.6	539.7
	average	**568.0**	**399.1**	**360.4**	**50.4**	**1139.3**
	st. dev (n=17)	79.9	53.3	49.7	34.2	347.4
clarithromycin	max	367.0	302.0	286.8	2.3	567.1
	min	202.4	<LOQ	< LOQ	< LOQ	4.1
	average	**306.1**	**75.6**	**66.9**	**1.3**	**163.4**
	st. dev (n=17)	50.2	94.3	89.9	0.8	180.5
o-desmethylvenlafaxine	max	5988.9	2002.5	1831.9	187.0	5743.2
	min	2070.3	870.5	646.5	39.7	1927.9
	average	**4196.5**	**1467.6**	**1392.3**	**107.2**	**3825.6**
	st. dev (n=17)	929.7	345.6	348.9	41.7	1174.3
ranitidine	max	1091.4	165.8	164.9	7.7	378.0
	min	83.0	28.2	13.0	2.2	60.5
	average	**365.1**	**71.8**	**72.4**	**4.7**	**189.8**
	st. dev (n=17)	271.7	37.3	40.0	1.6	100.0

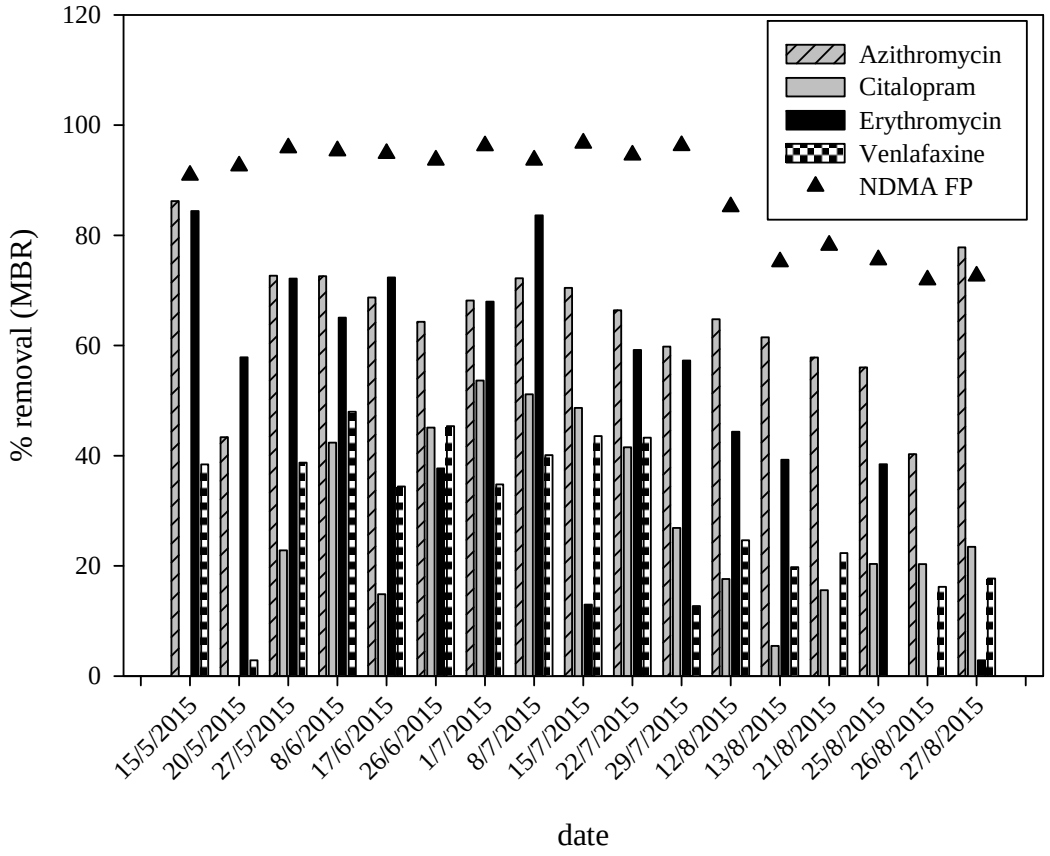

Figure 5-4: Percentage of NDMA FP and individual NDMA precursor removal by the MBR.

According to these results and in agreement with previous studies (Krasner et al., 2013b; Shah et al., 2012b), the specific watershed-associated precursors responsible for significant NDMA formation have not been identified in this study either. However, although previous reports have shown the removal of these compounds, it is the first time that NDMA FP is monitored through an MBR and related to the fate of specific NDMA precursors.

5.3.3 Fate of NDMA formation potential and individual precursors through the nanofiltration system

As shown in Figure 3-2, the effluent of the MBR was used as feed solution for the NF membrane system aiming to achieve higher quality suitable for water reclamation. Therefore, the concentration of NDMA FP and individual precursors was also measured at the feed, permeate and concentrate streams of this system. Table 5-1 shows the concentration of NDMA FP as well as other operational parameters.

Removal percentages were obtained according to equation 2 and 3, establishing a mass balance using the flows and concentrations of the permeate and concentrate streams.

$$C_m = \frac{Q_p \times C_p + Q_c \times C_c}{Q_m} \quad \text{equation 2}$$

$$\text{Membrane Rejection} = \left(1 - \frac{C_p}{C_m}\right) \times 100 \quad \text{equation 3}$$

Where C_m is the concentration in the membrane feed concentration, Q_m is the membrane feed flow, Q_p is the permeate flow, C_p is the permeate concentration, Q_c is the concentrate flow and C_c is the concentrate concentration.

As shown in Table 5-1, the percentage of NDMA FP removal for the NF process was above 90% (average 95.9±3.2%), except for a couple of samples not included in this calculation (i.e., 1/7/2015 and 22/7/2015). It is worth mentioning that the removal of NDMA FP by the NF system was not affected by the operational changing conditions of the MBR pilot plant. Therefore, in such a coupled system, a high NDMA FP removal would be achieved even if the MBR cannot operate under fully nitrifying conditions. Maximum NDMA FP concentrations measured in the permeate were 120 ng/L, which is close to the 100 ng/L limit set by the World Health Organization for drinking water (2011). Farré et al. (2011a) reported a rejection over 98.5% in a full-scale reclamation plant using RO membranes, which are 'tighter' than NF membranes. The NDMA FP concentration obtained in the NF permeate indicates that further treatment such as UV/H_2O_2 may be necessary if this effluent would be used for water reclamation for potable purposes in countries where the regulation is around 10 ng/L such as California (OEHHA, 2006) or Australia (QPC, 2005).

The average results for the NF removal of the targeted individual NDMA precursors were: 99.2±0.6 %, 94.5±3.1%, 93.0±11.9%, 99.3±1.2%, 96.6±1.9, 95.0±3.5% and 96.6±1.9% for azithromycin, citalopram, clarithromycin, erythromycin, ranitidine, venlafaxine and o-desmethylvenlafaxine, respectively, where the error corresponds to the standard deviation of 17 measurements corresponding to 17 different sampling days. The highest rejection shown for azithromycin (MW=748.98 g/mol) and erythromycin (MW=733.93 g/mol) above 99% can be explained in terms of steric hindrance assuming the molecular weight (MW) of the two compounds is an adequate parameter to reflect the molecular size and their exclusion by the NF membrane having a molecular weight cut off (MWCO) of approximately 200 Da according to the manufacturer. The results for azithromycin corroborate what Liu et al. (2014) showed in lab scale experiments using synthetic wastewater and a different commercial NF membrane (NFX, Synder Filtration) where > 98% rejection was obtained at 0.2 MPa and a higher rejection of > 99% at 0.4

MPa probably due to dilution effects at the higher flux. The rejection of citalopram of more than 92% (average 94.5±3.1%) is slightly higher than that obtained by Flyborg et al. (2010) who reported rejections above 90% at a recovery of 50% and a lower rejection of 85% at a recovery of 90 % using real wastewater and another tight NF membrane (ESNA1-LF-4040, Hydranautics) with a MWCO of approximately 150 Da according to the manufacturer. In our study, the change in system recovery from 75% to 50 % (maintaining a constant membrane recovery of 12.5%) during the last three samples did neither affect the membrane rejection statistically significantly for total nor for individual NDMA precursors. In membrane cell filtration experiments with synthetic feed solutions, ranitidine was removed more than 95% by both, a NF90 and an N270 according to López-Muñoz et al. (2012), which is similar to 96.6±1.9% observed in this study. Miyashita et al. (2009) investigated the rejection of other individual NDMA precursors (i.e., secondary amines such as dimethylamine, methylethylamine, diethylamine, and dipropylamine) through three different NF membranes and found a nitrosamine precursors rejection over 98%.

The relatively high permeate water temperature of 32.2±2.8ºC was due to the high temperatures being experienced over the experimental period and the fact that the pilot system was housed in an exposed shipping container. As expected, on the two days where the permeate temperature was recorded to be particularly high (9/7/2015 – 37.3 ºC and 5/8/2015 – 37.5 ºC) we saw a significant drop in rejection of all major ionic salts, with chloride rejection dropping to 92% and 91% respectively from an average of 96% (Table 5-4). This could also be observed for the rejection of target NDMA precursors below the average (ranitidine dropping from 96.6±1.9% to 93.9% and 92.1% respectively).

Table 5-4: Rejection of parameters measured by the NF membrane. O-desven stands for o-desmethylvenlafaxine

Date	Electrical cond.	DOC	TKN	NH_4^+	ALC	Na^+	K^+	Mg^{2+}	Ca^{2+}	Cl^-	$N\text{-}NO_3^-$	SO_4^{2-}	$P\text{-}PO_4^{3-}$	azithromycin	citalopram	erythromycin	venlafaxine	clarithromycin	o-desven	ranitidine
	%	%	%	%	%	%	%	%	%	%	%	%	%	%	%	%	%	%	%	%
20/5/2015	97.7	**92.1**	100.0	100.0	96.1	94.6	95.8	99.3	90.4	96.4	85.1	NR	NR	99.9	99.6	99.7	99.2	100.0	98.9	96.0
27/5/2015	97.0	**95.2**	100.0	99.7	89.4	95.0	96.1	99.6	98.2	97.2	85.9	97.8	NR	99.9	98.7	100.0	97.8	100.0	98.4	98.9
19/6/2015	96.3	**91.1**	100.0	100.0	93.6	93.7	95.0	99.8	98.5	95.9	81.8	99.9	99.6	99.3	90.7	100.0	95.8	62.1	98.3	98.1
26/6/2015	95.6	**93.7**	100.0	-	92.5	92.4	93.9	99.5	98.8	96.3	86.8	99.7	97.1	99.5	97.5	99.9	98.3	98.9	98.3	98.5
1/7/2015	94.4	97.7	100.0	-	86.6	91.4	92.5	99.1	97.4	95.4	81.2	99.2	98.1	99.8	97.0	100.0	98.1	99.6	98.0	98.5
9/7/2015	92.6	97.5	60.1	-	91.8	**88.6**	**90.4**	99.1	97.7	**92.1**	93.5	99.5	97.9	99.6	95.3	100.0	95.0	100.0	94.4	93.9
15/7/2015	95.5	98.0	87.2	-	90.1	NR	93.9	99.5	98.7	96.2	83.2	99.9	NR	NR	NR	NR	NR	NR	NR	NR
22/7/2015	94.4	97.0	87.2	-	79.6	90.9	NR	98.4	NR	95.0	NR	NR	89.6	99.5	93.2	99.2	91.7	79.3	96.2	97.5
29/7/2015	92.2	NR	NR	-	78.6	88.1	NR	97.9	96.4	94.2	80.0	99.3	98.8	99.5	92.0	96.8	87.6	99.3	94.0	96.0
5/8/2015	**86.0**	**87.9**	NR	-	**61.5**	**81.0**	**73.8**	**93.4**	**90.9**	**90.5**	NR	99.2	96.7	97.8	88.7	96.2	89.6	89.6	92.5	92.1
12/8/2015	96.2	98.7	90.1	95.0	87.5	94.5	94.8	99.1	98.2	97.0	NR	99.7	97.3	98.9	92.5	99.6	93.3	100.0	94.5	95.1
12/8/2015	95.1	98.2	93.6	94.7	68.4	93.0	93.3	98.9	98.0	97.0	80.0	99.7	99.3	98.9	92.0	99.6	92.0	93.9	96.7	96.1
21/8/2015	96.5	98.8	95.3	-	93.7	95.3	94.5	99.5	96.2	97.0	NR	99.9	98.9	99.0	96.9	99.8	97.8	73.5	98.3	97.7
25/8/2015	95.8	97.7	93.9	96.6	91.2	94.4	94.6	98.4	97.1	97.0	NR	NR	99.0	99.0	94.7	100.0	96.7	99.7	96.4	96.6
26/8/2015	96.0	97.7	94.7	96.9	93.8	95.2	95.8	98.5	94.9	96.5	NR	98.1	96.8	98.9	95.2	100.0	96.6	99.5	97.6	97.6
27/8/2015	95.9	98.8	93.7	98.6	91.5	95.1	95.9	98.2	95.1	97.2	NR	**88.6**	99.2	98.8	94.1	98.9	95.9	99.4	96.3	96.7
Average	94.8	96.0	92.6	89.7	86.6	92.2	92.9	98.6	96.4	95.7	84.2	98.5	97.6	99.2	94.5	99.3	95.0	93.0	96.6	96.6
Stand Dev	2.8	3.3	10.4	24.0	9.8	3.9	5.7	1.5	2.6	1.9	4.3	3.1	2.6	0.6	3.1	1.2	3.5	11.9	1.9	1.9

5.3.4 Comparing the removal of NDMA precursors by MBR pilot plant versus full scale conventional biological treatment

Samples from the full-scale conventional treatment were also taken during the last month of sampling (22nd of July to 27th of August). These results allowed us to draw conclusions on the comparison of conventional treatment and MBR during both, nitrifying and non-nitrifying conditions.

Table 5-5 shows the percentage of removal at the MBR pilot plant versus the full scale conventional WWTP for the 7 detected compounds as well as for the total NDMA formation potential. During aerobic conditions the MBR was clearly able to remove a higher percentage of azithromycin, citalopram and erythromycin than the full scale conventional WWTP, whereas higher average removals lacking statistical significance were observed for venlafaxine, ranitidine, clarithromycin and o-desmethylvenlafaxine. When comparing the results obtained under non-nitrifying conditions, we could observe still a higher percentage of removal for azithromycin, citalopram and erythromycin at the MBR, while similar results were obtained for the remaining compounds when comparing both the MBR and the full scale conventional WWTP. Interestingly, during MBR aerobic operation, the removal of NDMA FP measured at MBR was similar to the removal of NDMA FP measured at the WWTP. Nevertheless, during MBR non-nitrifying conditions, the performance of the WWTP in terms of NDMA FP removal was better than of the MBR, which again supports the idea that a fully nitrifying MBR system is required for an optimal removal of NDMA precursors during wastewater treatment (see Figure 5-5).

Table 5-5: Comparison of the removal of pharmaceuticals by the MBR vs the conventional WTP. n.m=not measured. Bold numbers correspond to the MBR aerobic operational conditions. O-desven stands for o-desmethylvenlafaxine.

sampling date	azithromycin MBR	azithromycin WWTP	citalopram MBR	citalopram WWTP	erythromycin MBR	erythromycin WWTP	venlafaxine MBR	venlafaxine WWTP
22/07/2015	**66%**	**48%**	**42%**	**28%**	**59%**	**20%**	**43%**	**36%**
29/07/2015	**60%**	**45%**	**27%**	**2%**	**57%**	**45%**	**13%**	**16%**
12/08/2015	65%	17%	18%	10%	44%	30%	25%	33%
13/08/2015	61%	18%	5%	5%	39%	38%	20%	22%
21/08/2015	58%	23%	16%	14%	0%	0%	22%	28%
25/08/2015	56%	37%	20%	7%	38%	25%	0%	27%
26/08/2015	40%	11%	20%	5%	0%	0%	16%	25%
28/08/2015	78%	67%	23%	10%	3%	0%	18%	33%

sampling date	ranitidine MBR	ranitidine WWTP	clarithromycin MBR	clarithromycinWWTP	o-desven MBR	o-desven WWTP	NDMA FP MBR	NDMA FP WWTP
22/07/2015	**73%**	**84%**	**43%**	**61%**	**60%**	**70%**	**95%**	**95%**
29/07/2015	**84%**	**60%**	**90%**	**97%**	**51%**	**68%**	**96%**	**95%**
12/08/2015	84%	44%	97%	97%	64%	63%	85%	93%
13/08/2015	n.m	n.m	98%	98%	76%	77%	75%	83%
21/08/2015	92%	81%	100%	99%	85%	84%	78%	95%
25/08/2015	53%	57%	23%	55%	65%	73%	76%	94%
26/08/2015	62%	54%	6%	43%	74%	73%	72%	90%
28/08/2015	56%	84%	44%	42%	74%	74%	73%	93%

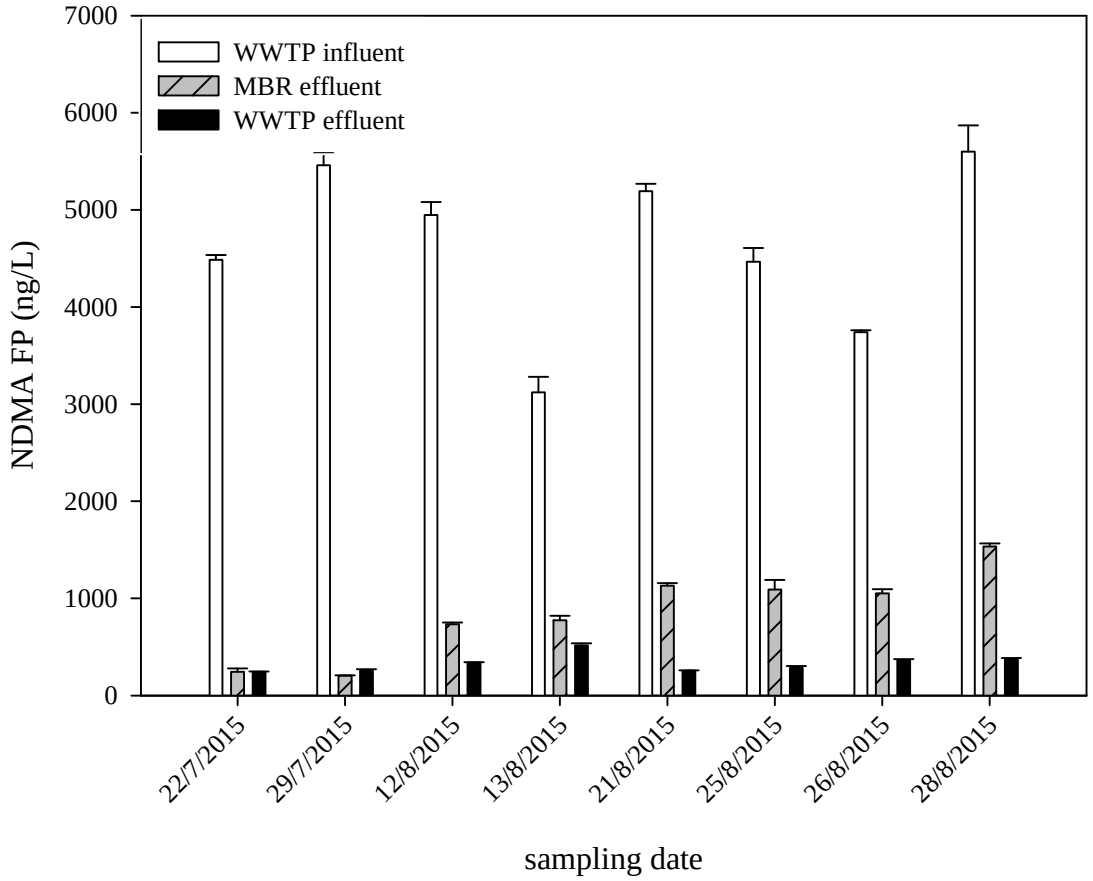

Figure 5-5: Concentration of NDMA FP at the effluent of the MBR vs the WWTP.

5.4 Conclusions

The removal of NDMA FP and individual NDMA precursors by an MBR pilot plant that treats urban wastewater has been investigated. In particular, changes in the percentage of removal due to the variation of nitrifying and non-nitrifying conditions of the MBR were studied. The individual NDMA precursors investigated were: azithromycin, citalopram, erythromycin, clarithromycin, ranitidine, venlafaxine, and its metabolite o-desmethylvenlafaxine. Other compounds such as chlorotetracycline, oxytetracycline, roxithromycin, spiramycin, tetracycline, and tylosin were also measured but neither detected in the pilot plant nor the full scale WWTP.

During normal aerobic operation, implying a fully nitrifying system, the MBR pilot plant was able to reduce NDMA formation potential above 94%, however this removal percentage was reduced to values as low as 72% when changing the conditions to avoid nitrification. This decrease was also observed for azithromycin (68 to 59%), citalopram (31 to 17%), venlafaxine (35 to 15%), and erythromycin (61 to 16%), where the values correspond to the average measured during the nitrifying *versus* no-nitrifying periods. These results suggest that a fully nitrifying MBR system will support better removal of NDMA precursors during wastewater reclamation.

The effluent of the MBR was used as feed of a NF system. High removal for both NDMA FP (>90%) and individual NDMA precursors (>94%) was observed. Within the frame of the experiment duration (four months) this high removal was independent of the nitrifying conditions of the MBR and operating settings of NF system, showing that NF can be regarded as a reasonably independent barrier for NDMA precursors even when the nitrification in MBR could not be fully accomplished. However, the NDMA FP measured in the NF permeate was in many cases above 100 ng/L, which is above the regulation set for NDMA itself for potable water reclamation in countries such as U.S.A. and Australia.

Finally, the concentration of NDMA precursors at the MBR effluent was compared to the concentration at the effluent of the full scale conventional biological WWTP treating the same influent. A similar performance was observed for both systems during nitrifying conditions in the MBR. However, the WWTP performed better than the MBR operated with non-nitrifying conditions, which again supports the hypothesis that a fully nitrifying MBR system is more suitable to achieve high removal of NDMA precursors during wastewater treatment.

Chapter 6 - Towards online optimisation of RO systems in IMS

This chapter seeks to understand whether there is scope in optimising RO process conditions in real-time to minimise energy use according to the diurnal fluctuations in EC and temperature and then proposes a protocol for such a process. The introduction builds on sections 1.4.1 and 1.4.3 in the overall introduction. The methodology and results show how influent wastewater quality data was utilised to understand the variation in wastewater quality for one particular WWTP and then utilises an offline model to understand whether cost savings can be made by varying the RO system recovery and pre-treatment dosing according to the feedwater EC and temperature.

6.1 Introduction

Unlike the feed water of a seawater RO plant, where the temperature and the concentration of the main ionic contributors are seasonal but relatively constant on a day-to-day basis (dependant on the type of intake utilized), wastewater feed to an RO plant is subject to variations in flow and load due mainly to predictable changes in urban activity (normal diurnal cycle, week-ends and holidays), accidental releases of industrial effluents and weather related events such as storms or long rain periods (Bonté et al., 2008).

The cost of electrical energy required to operate a wastewater reclamation plant utilising RO is significantly affected by rapidly changing energy prices and by the specific energy demand of the plant which is in turn affected by the operational conditions and influent characteristics of the plant, including the system recovery, the feedwater temperature, and EC (which is utilized as a surrogate for salinity).

On the other hand, tertiary effluent to be fed to a RO system for water reclamation typically has a high fouling potential which leads to operational problems if not well controlled in the design and operation of the plant. Fouling can be due to microbiological growth (biofouling), precipitation of sparingly soluble inorganic salts, particulate and colloidal matter and organic molecules. Biofouling can be inhibited by intermittent or continuous injection of chlorine-based disinfectants, such as chloramine, while organic colloidal and particulate fouling is controlled by MF or UF pre-treatment. Strategies for avoidance of scaling due to inorganic salts involve lowering the pH by dosing hydrochloric or sulfuric acid, dosage of scale inhibitors, namely antiscalants, and limiting the recovery of the system (Dow Water & Process Solutions, 1995).

The assessment of the dosage of antiscalant and acid is based on the feed water composition and the calculation of saturation indices for inorganic salts at the design recovery rate (Bartels et al., 2005; Dow Water & Process Solutions, 1995). Raffin et al. (2012) showed that utilising an effective antiscalant to control inorganic scaling at neutral pH would reduce the operating cost significantly. That said, although antiscalant suppliers software show that this is possible under certain conditions, in practice lowering the pH to some degree is essential to control the precipitation of inorganic salts (Greenberg et al., 2005; Marie Raffin et al., 2012).

Reviewing feedwater electrical conductivities of various operational plants shows that, as expected when treating wastewater, the plants received a feedwater having a range of salinities. In 2005, the Torreele plant (Belgium) operated at an average EC of 1161 µS/cm (approx. conversion to TDS 581 mg/L), but had a range between 442 – 1442 µS/cm (approx. conversion to TDS 216-723mg/L) and an average temperature of 15.3°C (range between 9.8 and 22.3°C) (Van Houtte and Verbauwhede,

2008). The Sulaibiya facility in Kuwait, the largest IMS facility in the world operated with a feedwater having an average EC of 2550 µS/cm (converted from a TDS of 1280 mg/L) and a maximum EC of 5700 µS/cm (converted from a TDS of 3014 mg/L)(Gagne, 2005),while the Ulu Pandan facility in Singapore operated with a feedwater EC ranging between 800 and 2000 µS/cm (TDS between 500 and 1200 mg/L)(Yuen, 2008). The reclamation facility in Leon (Spain) has a feedwater EC which varies between 2065 and 2542 µS/cm (Average 2338 µS/cm) (Melgarejo et al., 2015). Of the reviewed reclamation facilities in Table 11-1, all the facilities had fixed system recoveries, except the Torreele facility (Van Houtte and Verbauwhede, 2008) which operated with a system recovery between 75 and 80% recovery.

Van Houtte and Verbauwhede (2008) report that an online optimisation strategy made it possible for the Torreele facility (Belgium) to make significant operational cost savings. The strategy was made up of two components, (i) the control of recovery by setting a relationship between the feedwater conductivity and recovery, as well as (ii) the discontinuous use of chloramination according to the temperature of the feedwater. The recovery control strategy allows the recovery of the system to be increased without any additional chemical injection and without raising the risk of fouling, thus allowing a net decrease of energy consumption per cubic meter of produced water (Van Houtte and Verbauwhede, 2008). Although details of the recovery control strategy are not given in the paper, it is assumed that an empirical relationship between conductivity and EC was utilised to minimise the energy use, but how this was done was not published. This work seeks to expand on the idea presented by Van Houtte and Verbauwhede (2008) and explore ways in which this optimisation strategy specific to a wastewater quality and IMS design can be extended to other operating systems to utilise the EC and Temperature sensor information to operate at set-points which will ultimately produce water at the lowest cost.

The other study which sought to optimise the operational conditions specifically for IMS used in wastewater reclamation was that by Raffin et al. (2011) which utilized a Box-Behnken approach to optimize MF flux backwash frequency, chloramine dose and chloramine dosing point together with RO flux, recovery, pH and antiscalant dose using an experimental plan combined with statistical analysis to define the optimal operating conditions to minimize membrane fouling. While the study was comprehensive in how it looked at the effect of combinations of parameters on membrane fouling, the work did not look at how these process conditions are affected by changing influent water quality and how the data can be utilised in real time.

The objective of this work is to understand whether the diurnal variation in feed water constituents and temperature of the feed would justify the modification of system operation conditions, and if so provide a protocol for the automatic regulation of IMS recovery to obtain the lowest water cost

possible through savings in terms of specific energy requirements, the optimized use of scale inhibitors and acid and a reduced volume of brine for disposal (if a cost is associated to this).

6.2 Methodology

The methods section of this chapter is broken down into four subsections. The first describes the different datasets used to understand the variation in feedwater quality and the relationship between the individual constituents and EC. The second section describes how the feedwater quality profiles defined in the first section are input to an offline model varying the feedwater EC, temperature and system recovery. The third section describes the concept of fouling potential for a particular feedwater profile at a particular temperature and system recovery. The last section describes how the simulations and fouling potential calculations were utilised to determine the considered water cost.

6.2.1 Wastewater quality data

This work utilizes three datasets of wastewater quality reaching the RO/NF membranes. The first dataset was a 24-hour profile where composite samples were taken every hour utilizing an auto sampler from the primary effluent of the Quart WWTP (24 samples, Dataset 1, Table 11-12). The second dataset (Dataset 2, Table 11-13) was obtained from a three-month operational period, again at the Quart WWTP, where sampling was carried out twice per week using 24-hour composite samples from the MBR effluent (17 samples), with a sample every hour over a 24-hour period. The third dataset (Dataset 3, Table 11-14) was obtained from another three-month operational period where sampling was carried out twice per week using grab samples from the RO feed (17 samples) this time when the pilot plant was operating at Castell-Platja d'Aro. All sampling was carried out during dry weather flow to avoid the dilution of influent due to a combined sewage system, to only account for the diurnal variation without dilution. Samples were filtered through a 1.2µm microfiber filter followed by a 0.45µm nylon membrane filter before analysis. The three datasets are provided in section 11.4.3.

Samples were also analysed for dissolved organic carbon (TOC; Shimadzu TOC-V_{CSH} analyzer), ammonium (BÚCHI B-324 distiller, Titrino 719S Methrohm) and total kjeldahl nitrogen (BÚCHI B-324 distiller, Titrino 719S Methrohm). Nitrites (NO_2^--N), nitrates (NO_3^--N) and phosphates (PO_3^{4-}-P), together with other major ions (Na^+, K^+, Mg^{2+}, Ca^{2+}, Cl^-) were analysed using ion chromatography (Metrohm 761-Compact; APHA standard method 4110B).

The data was used to generate feedwater quality profiles utilized in the RO simulations explained in the next section. The simulations were run using feedwater quality profiles from the 24-hour profile

(24 samples), which were actually WWTP primary effluent samples rather than MBR permeate which is the stream which actually reaches the RO membrane. The ionic constituents which are typically affected by the secondary treatment process, namely NH_4^+, HCO_3^- and PO_4^{3-}, were obtained from samples following the MBR treatment process. For the simulation, this 24-hour profile (Dataset 1) was chosen over the other two datasets, to get an indication of the variability of the ionic constituents in a single day rather than an average concentration over a 24-hour period.

The EC of water is based on the presence of ions and is commonly used as a surrogate parameter for the concentration of dissolved mineral substances in a water which is commonly termed TDS. RO processes have EC sensors installed on the feed and permeate streams as standard. For the purposes of this work, the range of feedwater EC measured in dataset one was divided into three, low EC, average EC and high EC. The average feedwater EC was defined as the arithmetic mean of the values over the 24-hour period, while the low and high feed water EC profiles were defined as the average EC minus the standard deviation over the 24-hour period and the average EC plus the standard deviation over the 24-hour period respectively.

For this reason, the first thing that was done was to see whether there was a direct relationship between the EC values and the major ions making up the ionic content of the wastewater, namely the cations; calcium (Ca^{2+}), magnesium (Mg^{2+}), sodium (Na^+), potassium (K^+) and anions; chloride (Cl^-), sulphate (SO_4^{2}), phosphate ($P\text{-}PO_4^{3-}$) and bicarbonate (HCO_3^-) measured as Alkalinity. Since our wastewater always had a pH below 8.3, the acid consumption (alkalinity) at a pH of 4.3 (m value) was assumed to correspond to the bicarbonate ion content. In this work, borrowing terminology from oceanography, the individual ions which were found to be correlated to the total ionic content are termed conservative ions. Those ions whose concentration was dependent on the biological process which preceded the RO process and thus did not correlate to the EC were termed non-conservative ions.

The principle of electro neutrality which is commonly used to check the accuracy of the chemical analysis, where the sum of the positive ions (cations) must equal the sum of negative ions (anions) in solution, was utilised to ensure that the feedwater quality profile entered into the simulation software is acceptable. Table 6-1 provides the concentrations of the individual constituents making up the low, average and high EC feedwater quality profiles utilised in the RO simulations. The concentrations given in the table are measured values, except those given in brackets which are the values used in the simulations. Sodium (Low EC) or bicarbonate (Average EC and High EC) was used to balance the composition, whilst keeping the same osmotic pressure as far as possible. For the purposes of demonstrating how an online optimisation strategy can be useful, for the calcium

phosphate stability index a feed concentration of 15 mg/L was considered, which double the amount which was typically found in the influent wastewater.

Table 6-1: Feedwater quality profiles utilised in simulations, EC and individual ionic constituents are measured experimentally except the values were a measure value measured value in. TDS was calculated as the sum of the ions.

Profile Name			Low EC	Average EC	High EC
Cations	Ca^{2+}	mg/L	59	69.5	86
	Mg^{2+}	mg/L	7.8	16.5	16.3
	Na^{+}	mg/L	115.8 (134)	159	169
	K^{+}	mg/L	13.5	20	33.3
Anions	HCO_3^{-}	mg/L	240	182 (277)	583 (427)
	Cl^{-}	mg/L	192.4	253.6	228.2
	SO_4^{2-}	mg/L	18	18	18
	PO_4^{3-}	mg/L	1.0 (15)	7.4 (15)	9.5 (15)
TDS	(Sum of major ions)	mg/L	666	808	978
EC		µS/cm	1198	1364	1664

6.2.2 RO simulations

RO Simulation Software is commonly made available by RO membrane manufacturers and typically utilized by process engineers both in the design of RO and NF systems and during the operation of RO membrane systems to be able to predict RO performance under changing conditions (including in the normalization of performance data to changing feedwater salinity and temperature). One such software was utilized in this study (Reverse Osmosis System Analysis, ROSA, DOW Water and Process Solutions) to simulate changes in feed water temperature and ionic content to understand how changes in process conditions could impact energy use and pre-treatment chemical use to operate sustainably at the lowest water cost.

To demonstrate the development of a control system, a typical wastewater reclamation design configuration was assumed. From a review of existing water reclamation facilities presented in Chapter 1, it can be seen that existing facilities can be divided into two, those operating with a two-stage design operate with a recovery of 75- 80% while those using a three-stage design typically operate at recoveries between 80 and 86% recovery. The higher recoveries are typically limited by calcium phosphate precipitation.

For this study a virtual plant with a two-stage design was assumed operating with a recovery between 75 and 80%, with a train producing 5000 m^3/day. A capacity between 5000 and 15000 m^3/day is a typical capacity for a single train in large facilities which would have a number of treatment trains each operating independently with a separate high-pressure pump to allow flexibility in the production capacity. The configuration consisted of 28 PVs in the first stage followed by 12 PVs in the second-stage each having seven (7) membrane elements (staging ratio between 2

and 2.2, with the staging ratio being defined as (1/ (1-[System Recovery])) $^{(1/[\text{Number of stages}])}$). The membrane element assumed in the model was a Filmtec BW 30-400 which is a commonly specified element for brackish water applications. The system was designed to run at an average permeate flux of 20 LMH which is typical for such facilities.

Although the measured feedwater pH varied between 7 and 7.8, a constant value of 7.3 was utilized for each simulation. For each simulation the feedwater pH to control the precipitation of calcium carbonate scale was calculated to obtain and Langlier Saturation Index (LSI) below a value of 1. The Feed EC given in the simulation matrix refers to the three feedwater profiles detailed in Table 6 1. The feedwater pressure together with the permeate conductivity as well as any design warnings at the simulated feedwater conditions were recorded in a spreadsheet (Microsoft Excel). This data, together with the feedwater quality data was then used to calculate the fouling potential and the water cost described in the following sections.

Table 6-2 below shows the simulation matrix with each of the different cases simulated covering different feedwater (feed) EC, for a low temperature case (13, 15 and 17°C) and a high temperature case (23, 25 and 27°C) at three different recoveries (75, 77.5 and 80%). Three different recoveries were simulated as the increase in cost varies reasonably linearly when considering only the cost of electricity and the cost of chemicals, although this will be very much dependent on a case by case basis.

Since feedwater temperature has a high impact on energy use and precipitation of sparingly soluble salts in RO membrane systems, two temperature ranges were simulated to understand whether different ranges of diurnal temperature variations affect the energy saving potential.

The Feed EC given in the simulation matrix refers to the three feedwater profiles detailed in Table 6-1. The feedwater pressure together with the permeate conductivity as well as any design warnings at the simulated feedwater conditions were recorded in a spreadsheet (Microsoft Excel). This data, together with the feedwater quality data was then used to calculate the fouling potential and the water cost described in the following sections.

Table 6-2: RO simulation matrix showing the simulation reference number divided into two, (a) low temperature case and (b) high temperature case, were for each feedwater temperature and feedwater EC the recovery is modified between 75% and 80%.

(a)	Low Temperature Simulation Reference Number									
	Temp.	**13°C**			**15°C**			**17°C**		
	Recovery	**75.0%**	**77.5%**	**80.0%**	**75.0%**	**77.5%**	**80.0%**	**75.0%**	**77.5%**	**80.0%**
Feed EC	**Low EC**	1	2	3	4	5	6	7	8	9
	Avg EC	10	11	12	13	14	15	16	17	18
	High EC	19	20	21	22	23	24	25	26	27

(b)	High Temperature Simulation Reference Number									
	Temp.	**23°C**			**25°C**			**17°C**		
	Recovery	**75.0%**	**77.5%**	**80.0%**	**75.0%**	**77.5%**	**80.0%**	**75.0%**	**77.5%**	**80.0%**
Feed EC	**Low EC**	28	29	30	31	32	33	34	35	36
	Avg EC	37	38	39	40	41	42	43	44	45
	High EC	46	47	48	49	50	51	52	53	54

6.2.3 Inorganic Fouling potential

Other than energy use, changes in the RO operating conditions and influent characteristics have a significant impact on the inorganic fouling potential. The inorganic fouling potential is defined in this work as the susceptibility of membrane fouling to begin under certain process conditions (system recovery, temperature) given a certain feedwater make-up (pH, individual ionic constituents). RO simulation software typically provides saturation indices for the predominant sparingly soluble salts individually. From literature (Bartels et al., 2005; Marie Raffin et al., 2012) as well as from membrane autopsies carried out on the tested membranes as part of this work (results given in 11.4.1) it was shown that the predominant sparingly soluble salts which could potentially foul the membranes in wastewater reclamation applications are: calcium carbonate, calcium sulphate, silica and calcium phosphate. In this work calcium carbonate and calcium phosphate are considered, as these were shown to be the sparing soluble salts whose precipitation on the membrane surface needed to be controlled given the feedwater constituent concentrations considered.

The following are the equations utilised to calculate the inorganic scaling potential considering only calcium carbonate and calcium phosphate. For any particular case (system and feedwater), it is important to understand which soluble salts can potentially foul a membrane and include them into the calculation of inorganic fouling potential. The equations reproduced below are standard calculations given in the ASTM procedures (ASTM, n.d.) and described in detail in membrane

manufacturers technical manuals (Dow Water & Process Solutions, 1995). These were included in the spreadsheet to automatically calculate the inorganic fouling potential of the feedwater.

The inorganic fouling potential of calcium carbonate is typically characterised using the Langelier Saturation Index (LSI). The data required to calculate this value is given in Table 6-3, while the calculations and figures used in these calculations are given in

Table 6-4, Figure 6-1, Figure 6-2 and Figure 6-3 respectively. The equations of the lines given in the graphs below were utilised in the excel sheet to approximate the constants.

Table 6-3: Information required to calculate the LSI

Ca_f	Calcium concentration in feed as $CaCO_3$	mg/L
TDS_f	Concentration of TDS in the feed	mg/L
Alk_f	Alkalinity in the feed as $CaCO_3$	mg/L
pH_f	pH of the feed solution	
T	Temperature of the feed solution	°C
Y	Recovery of the RO system,	expressed as a decimal

Table 6-4: Equations utilised to calculate the LSI (Dow Water & Process Solutions, 1995)

Calcium concentration in concentrate stream, Ca_c, as $CaCO_3$ in mg/L	$Ca_c = Ca_f\left(\frac{1}{1-Y}\right)$
TDS in concentrate stream, TDS_c, mg/L	$TDS_c = TDS_f\left(\frac{1}{1-Y}\right)$
Alkalinity in concentrate stream, Alk_c, as $CaCO_3$ in mg/L	$Alk_c = Alk_f\left(\frac{1}{1-Y}\right)$
Calculate free carbon dioxide content C in the concentrate stream by assuming that the CO_2 concentration in the feed $C_c = C_f$.	The concentration of free carbon dioxide in the feed solution is obtained from Figure 6-1
Calculate the pH of the concentrate stream, pH_c, using the ratio of alkalinity in the concentrate stream, Alk_c, to the free CO_2 in the concentrate	The pH of the concentrate stream is also obtained from Figure 6-1
Obtain pCa as a function of Ca_c pAlk as a function of Alk_c	pCa and pAlk are obtained from Figure 6-2
C as function of TDS_c and temperature (assuming temperature of concentrate is equal to temperature of feed)	C is obtained from Figure 6-3
Calculate pH at which the concentrate stream is saturated with $CaCO_3$, pH_s	pH_s = pCa + pAlk + C
Calculate the LSI of the concentrate, LSI_c	$LSI_c = pH_c - pH_s$

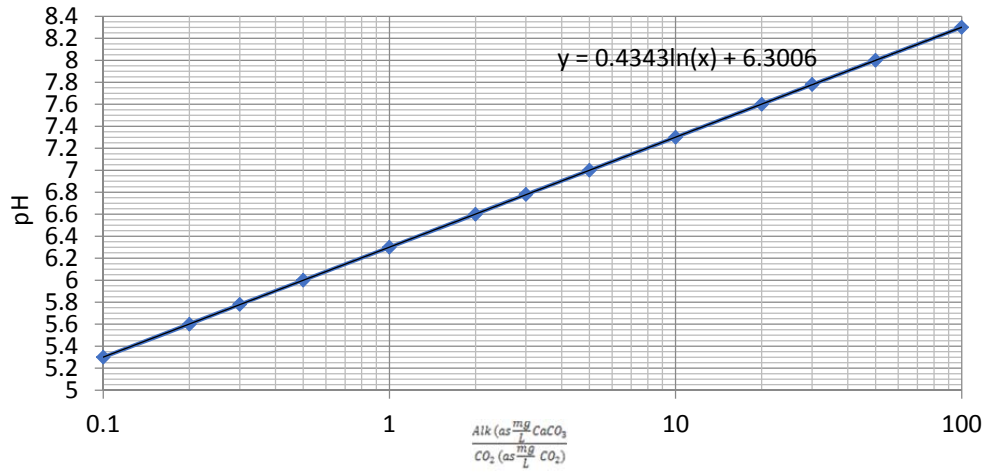

Figure 6-1: pH versus methyl orange alkalinity/free CO2

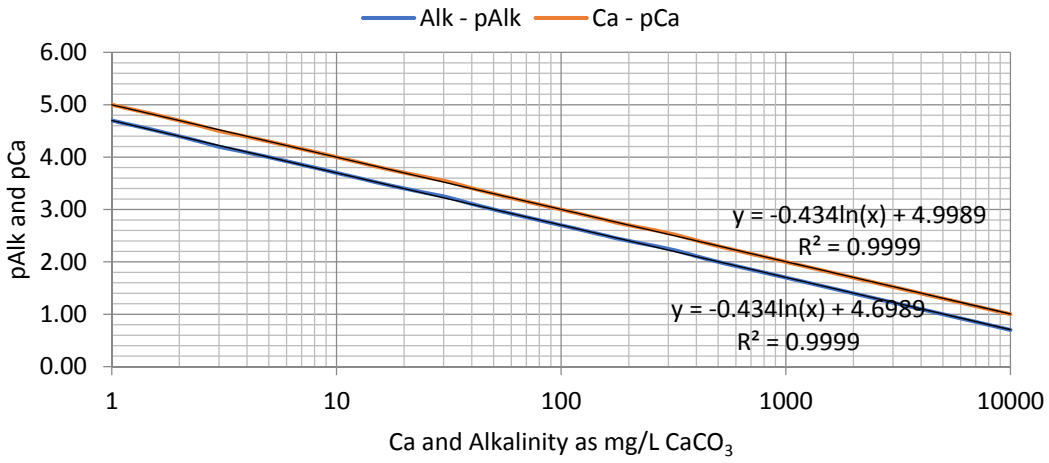

Figure 6-2: Conversion of calcium alkalinity to pCa and pAlk

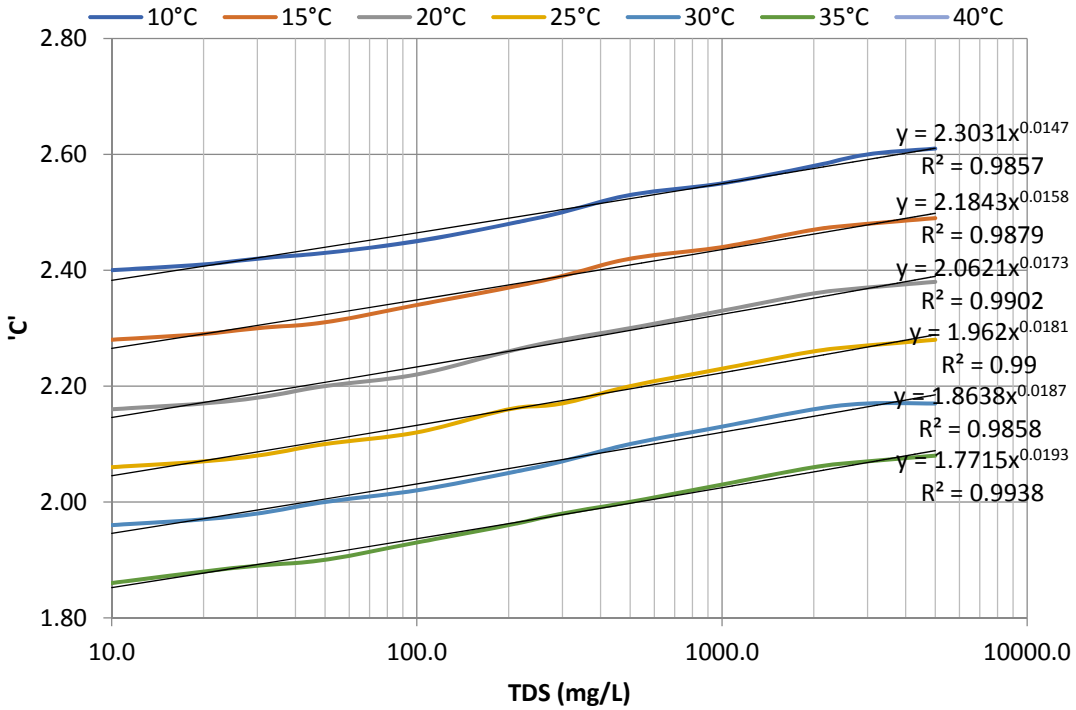

Figure 6-3: 'C' versus TDS and temperature. C is a constant which is a function of TDS and water temperature.

The calcium phosphate stability index proposed by Kubo et al. (1979) gives an indication of the potential for scaling considering the concentrations of calcium and phosphate present together with feedwater pH and temperature. The information needed in the calculation together with the equations to calculate this stability index are shown in Table 6-5 and Table 6-6 respectively. A negative stability index (SI) signifies a low potential for calcium phosphate scaling while a positive value indicates the potential for calcium phosphate scaling (Dow Water & Process Solutions, 1995).

Table 6-5: Information required to calculate the calcium phosphate stability index

Ca_f	Calcium concentration in feed as $CaCO_3$	mg/L
PO_{4f}	Concentration of phosphate in the feed	mg/L
pH_f	pH of the feed solution	
T	Temperature of the feed solution	°C
Y	Recovery of the RO system,	expressed as a decimal

Table 6-6: Equations utilised to calculate the calcium phosphate stability index (Dow Water & Process Solutions, 1995)

Calcium concentration in concentrate stream, Ca_c, as $CaCO_3$ in mg/L	$Ca_c = Ca_f\left(\frac{1}{1-Y}\right)$
Phosphate concentration in concentrate stream, PO_{4c}, mg/L	$PO_{4c} = PO_{4f}\left(\frac{1}{1-Y}\right)$
Critical pH, pH_c, calculated by the following experimental equation	$pH_c = \frac{11.755 - \log(Ca_c) - \log(PO_{4c}) - 2\log t}{0.65}$
Stability Index, SI	$SI = pH_f - pH_c$

Although initially it was thought that a single value can be deduced by combining the various stability indices to show how a combined inorganic fouling potential varies as the system recovery, feedwater EC and feedwater temperature varies, it was decided to keep these values separate. This was done not to lose the information being provided with respect to each individual sparingly soluble salt. For the example described in this paper sulphuric acid was continuously dosed at a concentration to keep the concentrate LSI below a value of 1. The LSI is not plotted with changing system recovery and feedwater EC and temperature because it is maintained constant and a cost attributed to the acid consumed as described in the next section. An antiscalant was also dosed at a fixed dose of 2 mg/L.

6.2.4 Water cost

Although electrical energy utilised in the treatment process makes up a significant portion of the total cost of water produced; as shown in section 1.9.3 the cost of chemicals, maintenance and personnel all contribute to the specific cost of water. In this work, the costs considered were the cost of electrical energy for the feed pump and that of the high-pressure pump together with the cost of chemicals in the pre-treatment of the RO to control inorganic fouling. The cost of biofouling control which is typically carried out using chloramines was not included in this work. Typically, the biofouling potential is linked to the quality of the secondary effluent from the proceeding process, both in terms of organic matter as well as nutrients as well as the feedwater temperature. This is touched on briefly later in the paper. Table 6-7 below provides the cost assumptions utilised in this work, while Table 6-8 provides the equations utilised in calculating the considered water cost.

Table 6-7: Cost assumptions utilized in the model to obtain a water cost.

High pressure pump efficiency (pump* motor), Eff_{HP}		80%
Feed water pressure	bar	2.1
Feed pump efficiency (pump * motor), Eff_f		80%
Cost of Energy (Assumed energy cost, which is bound to change by country and possibly even time of day).	€ / kWh	0.2
Cost of Acid	€/L	0.00019
Cost of Antiscalant	€/g	0.00388
Cost of Concentrate disposal	€/m^3	0
Pre-stage Δ Pressure (bar)		0.345
Flow Factor (coefficient utilized to consider membrane condition)		0.85

Table 6-8: Information and equations used to calculate the considered water cost

Q_p	Permeate flow (m^3/h)	
Y	Recovery of the RO system,	Expressed as a decimal
Q_f	Feed flow	$Q_f = \frac{Q_p}{Y}$
Pumping Cost		
P_f	Feed pressure (bar)	Pressure fed to high pressure pump, assumed 2.1 bar
P_{HP}	Membrane Feed Pressure (bar)	Determined from ROSA
SEC_f	Feed pump specific energy consumption	$SEC_f = \frac{Q_f \times 1000 \times 9.81 \times P_f \times 10.197}{3600000 \times Eff_f \times Q_p}$
SEC_{HP}	High pressure pump specific energy consumption	$SEC_{HP} = \frac{Q_f \times 1000 \times 9.81 \times (P_{HP} - P_f) \times 10.197}{3600000 \times Eff_{HP} \times Q_p}$
SEC_{pump}	Specific Energy Consumption for pumping	$SEC_{pump} = SEC_f + SEC_{HP}$
$Cost_{energy}$	Cost of energy, €/m^3 produced	$\text{Cost of Pumping Energy} = SEC_{pump} \times \text{cost of energy}$
Pre-Treatment Cost		
$Dose_{acid}$	Acid Dose, mg/L	In this case determined from ROSA
$Dose_{as}$	Antiscalant Dose, mg/L	Typically obtained from software provided by the antiscalant supplier
$Cost_{acid}$	Cost of acid, €/m^3 produced	$Cost_{acid} = \frac{1000}{Y} \times \frac{Dose_{acid}}{1000} \times \text{Cost of acid}$
$Cost_{as}$	Cost of antiscalant, €/m^3 produced	$Cost_{as} = \frac{1000}{Y} \times \frac{Dose_{as}}{1000} \times \text{Cost of antiscalant}$
$Cost_{pt}$	Cost of pre-treatment, €/m^3 produced	$Cost_{pt} = Cost_{acid} + Cost_{as}$

Concentrate Disposal		
Q_c	Concentrate flow	$Q_c = Q_f - Q_p$
$Cost_{conc}$	Cost of concentrate disposal, €/m^3 produced	$Cost_{conc} = Q_c \times$ Cost of concentrate disposal
Considered Cost		
$Cost_{tot}$	Cost of pumping + pre-treatment + concentrate disposal	$Cost_{tot} = Cost_{energ} + Cost_{pt} + Cost_{conc}$

In this work an approximation for the cost of chemicals to control inorganic fouling was represented by the cost of sulfuric acid (H_2SO_4, 98% concentration) to obtain a Langelier Saturation Index of just below 1 (0.85 – 1) to control calcium carbonate precipitation. An antiscalant was then dosed with at a concentration of 2 mg/L, dosed continuously. In practice the use of antiscalant and acid together with limiting membrane operating conditions is typically determined in collaboration with antiscalant suppliers which was not carried out as part of this work. The representation of pre-treatment chemicals in the considered cost was based on acidification since the use of proprietary antiscalants is very specific to the chemical manufacturer. Basing the scaling fouling control on acidification allows the generalisation of the contributing cost of pre-treatment under different operating conditions. No cost was also attributed to routing clean-in-place (CIP) operations or membrane replacement as these are very specific to a facility in terms of feedwater quality and process conditions.

No cost was also attributed to brine disposal as it was considered that changes in process conditions (namely recovery) will not change the mass of contaminants discharged into the natural environment. On the contrary, if concentrations of contaminants are regulated rather than mass loading (as is currently done in the UWWTD for nutrients), then further treatment processes may be prescribed prior to discharge depending on system recovery. The volumetric flow of the concentrate stream would need to be considered in calculating the water cost as given in Table 6-8.

6.3 Results

6.3.1 Variation in wastewater quality

Figure 6-4 shows the variability of EC and the major constituents over a 24-hour period. Since the catchment for this WWTP is predominantly domestic households and the length of sewage network is not substantial, as expected the results show two peaks in activity one after 8 am and one towards

the end of the day close to 8 pm. EC (Figure 6-4 a) and organic matter (given as total COD, Figure 6-4d), each register these loading peaks.

The Pearson Product-Moment correlation coefficients and P-values for each of the considered cations and anions with respect to EC from datasets 1,2 and 3 are given in

. These results show that the ionic constituents can be divided into two, those which correlate with EC (referred to as conservative ions in this work), namely Cl^-, Na^+, K^+ and to a lesser extent Mg^{2+}, and those which don't correlate well with EC (referred to as non-conservative ions in this work), namely Ca^{2+}, HCO_3, SO_4^{3-} and PO_4^{3-}. The 24-profile of the conservative and non-conservative ions are shown Figure 6-4 (b) and Figure 6-4 (c) respectively.

From the three datasets available (worksheets given in section 11.4.3) we can see that the conservative ionic content makes up on average between 36% and 51% of the TDS, while the non-conservative ions make up the remainder. Given this distinction between the conservative and non-conservative ions, it is also important to note that the non-conservative ions are those which (1) are affected by preceding biological secondary treatment processes and (2) are the predominant ions which have an effect on inorganic fouling: Ca^{2+}, PO_4^{3-}, HCO_3^- and SO_4^{2-}.

In terms of concentration, the highest non-conservative ion is bicarbonate. As part of the two-step process of biological nitrification, 7.14 g of alkalinity as $CaCO_3$ is required per gram of ammonia nitrogen converted to nitrate (Tchobanoglous et al., 2003). For this reason, apart from the concentration of HCO_3 in the feedwater reaching the WWTP, the concentration of NH_4^+ in the influent water together with the activity of the nitrifying bioreactor will all impact the concentration of HCO_3^- reaching the RO membrane. The concentration of PO_4^{3-} is particularly affected by whether biological or chemical treatment processes are included as part of the secondary/tertiary treatment process for the removal of this nutrient. In a previous experimental period, the pilot plant was operated using a University of Cape Town configuration (Anaerobic-Anoxic-Aerobic with recycles) for biological removal of both nitrogen and phosphorous and was achieving P-PO_4^{3-} concentrations in the effluent consistently less than 1 mg/L. Other than the requirement of including P removal techniques as part of the secondary treatment process for regulatory requirements, when the water is going to be further treated using RO membranes, a cost-benefit analysis needs to be undertaken to decide whether it is cheaper to include P-removal or control calcium phosphate ($Ca_3(PO_4)_2$) scaling in the pre-treatment of the RO.

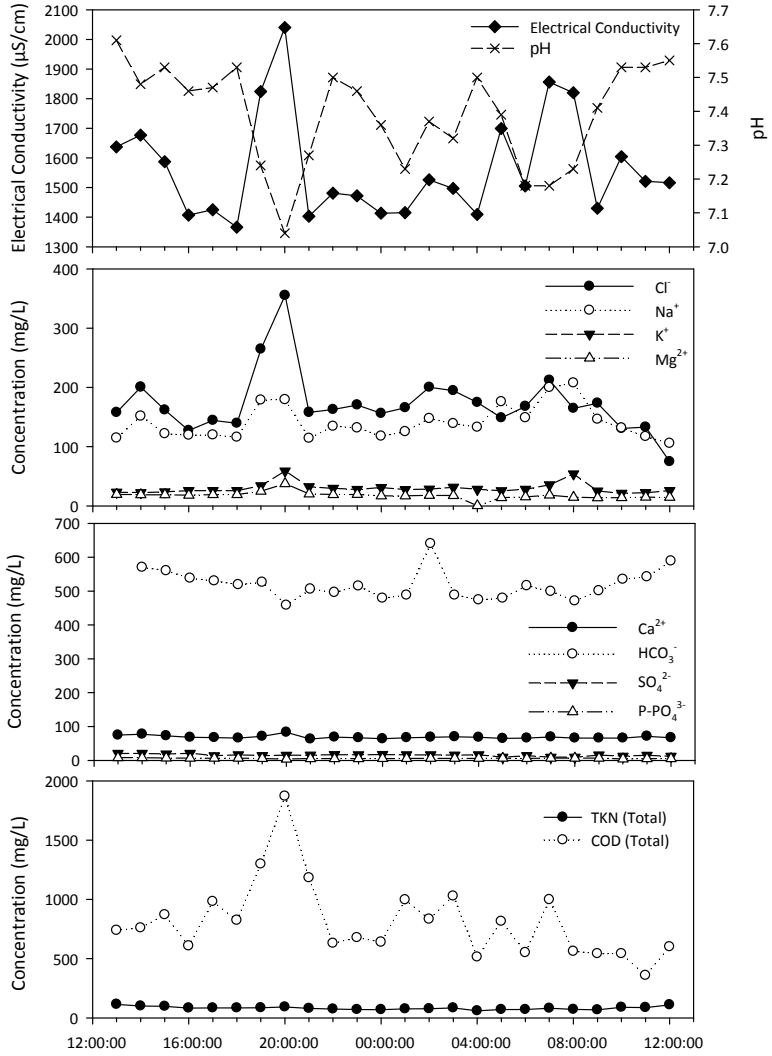

Figure 6-4: Variation of composition of influent wastewater over a 24-hour period, from top (a) showing EC and pH, (b) showing the concentration of chloride (Cl^-), sodium (Na^+), potassium (K^+) and magnesium (Mg^{2+}), (c) showing the concentration of calcium (Ca^{2+}), bicarbonate (HCO_3^-), sulphate (SO_4^{3-}) and phosphate (PO_4^{3-}), and (d) showing the concentration of Total Kjeldahl nitrogen (TKN) and total chemical oxygen demand (COD).

Table 6-9: Correlations between EC and individual ions

		Ca^{2+}	Mg^{2+}	Na^+	K^+	HCO_3^-	Cl^-	SO_4^{2-}	$P\text{-}PO_4^{3-}$
Dataset 1	Correlation coeff.	-0.041	0.463	0.767	0.651	-0.181	0.831	-0.386	-0.075
n=23	P Value	0.851	22.7E-3	12.4E-6	5.7E-4	0.409	9.0E-7	0.063	0.728
		No corr.				No corr.		No corr.	No corr.
Dataset 2	Correlation coeff.	0.133	0.46	0.609	0.565	0.671	0.708	-0.524	0.539
n=17	P Value	0.610	0.0635	9.5E-3	0.0283	3.2E-3	1.5E-3	0.037	0.0313
		No corr.	No corr.						
Dataset 3	Correlation coeff.	0.718	0.761	0.793	0.636	0.22	0.606	0.228	0.256
N=17	P Value	1.16E-3	3.84E-4	1.44E-4	6.07E-3	0.391	16.7E-3	0.378	0.377
						No corr.		No corr.	No corr.

6.3.2 RO simulations and considered water cost

Figure 6-5 shows the relationship between acid dose and temperature as the recovery increases from 75% to 80% for the three cases of EC which could be used as a way to control the acid dose according to the feedwater temperature and feedwater EC to ensure the dosing of the right amount of acid for the specific process conditions. Figure 6-6 and Figure 6-7 give an overview of the results for the low and high temperature cases modelled respectively. The results show the contribution of the cost of energy and the cost of chemicals to the considered water cost as the recovery increases from 75% to 80%, both individually and as the sum of the two values. The word 'considered' was included with the term 'water cost' because in this example only energy from the feed pump and high-pressure pump together with the chemical cost to control inorganic fouling is considered in the water cost as explained in the methods section. Figure 6-6 and Figure 6-7 are made up of 9 sub-figures corresponding to the experimental matrix given in Table 6-2 (a) and (b) respectively. Each set of three sub-figures in the horizontal direction have the same feedwater EC, while each set of three sub-figures in the vertical direction having the same feedwater temperature. The idea of presenting the results of the experimental matrix in this way is to provide a representation that can be used in developing a decision tree to control the recovery of the system according to the feedwater EC and feedwater temperature. Since the range of recoveries modelled is relatively small, with a difference of 5%, the relationship between the water cost and the recovery for was shown to be linear. This may change depending on the case, particularly if additional costs are included in the water cost calculation such as the changing efficiency of the pumps and motors for the given feed pressure and flow rate or if a larger system recovery range is considered.

It is clear that for the low temperature case (Figure 6-6); the considered water cost consistently decreases as the recovery increases. In this case it makes sense to consistently maximise the recovery of the system while keeping within the manufacturers membrane system design guidelines (maximum system average permeate flux, maximum element recovery, maximum permeate flow rate, minimum concentrate flow rate and maximum feed flow rate) as well as considering the precipitation of sparingly soluble salts.

In the simulated case, since calcium carbonate scaling is controlled mainly through the addition of acid and the pH of the feedwater is kept between 6.22 and 7.0 depending on the feedwater temperature, feedwater salinity and system recovery, the calcium phosphate ($Ca_3(PO_4)_2$) stability index is consistently below a value of 0. For this reason the risk of calcium phosphate fouling remains low for all the cases modelled in the low temperature case. If a lower degree of acidification was

utilised due to an increased dose of antiscalant in controlling $CaCO_3$ scaling, then the $Ca_3(PO_4)_2$ stability index could then be required to limit the recovery.

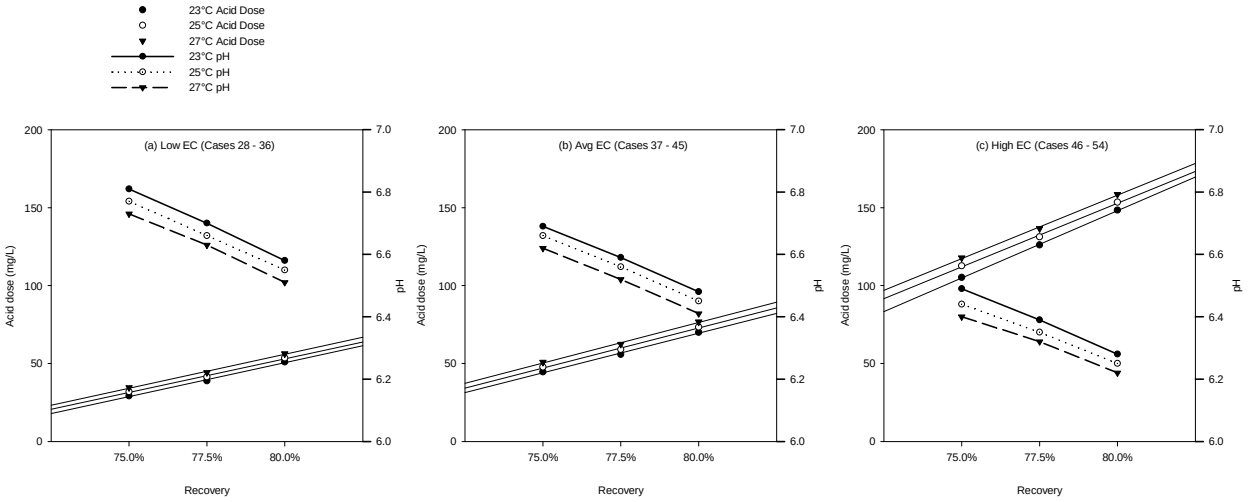

Figure 6-5: Relationship between temperature, pH and acid dose for different feedwater electrical conductivities (a) low EC, (b) average EC and (c) high EC cases.

For the low temperature case simply implementing such a strategy of maximising the system recovery while controlling the chemical dosing rate could lead to savings of between 0.001 and 0.005 €/m^3 of permeate produced depending on the feedwater EC and temperature. This cost saving was calculated as the difference between the cost of fixing the recovery at 75% when compared to operating at a recovery of 80% and translates to a cost saving between 0.5% and 4%.

The results of the simulations (not shown in this thesis) also show that as the temperature increases, the permeability of the membrane elements increase resulting in a risk to increased fouling particularly on the last elements of the first stage (elements 6 and 7) where the ratio of the permeate flow to the feed flow (membrane element recovery) increases beyond the manufacturers design guidelines.

Another idea which was explored when running the simulations was the ability to increase the system recovery during wet weather flow when the feedwater is diluted. The simulations showed that the ability for the system recovery to be pushed significantly during wet weather flow depends on the flexibility designed into the system to allow the recovery to be increased whilst respecting the manufacturer's membrane system design guidelines and scaling limits. Design features such as the use of interstage pumps, membrane configurations utilising an interstage design or membranes with reduced feed channel pressure loses due to wide feed spacers could all be incorporated to contribute to such flexibility.

For the high temperature case (Figure 6-7), the results are different to the low temperature case in the sense that for the low EC and average EC scenarios, whilst the considered water cost again decreases with increasing system recovery, the $Ca_3(PO_4)_2$ stability index now sets the limit for system recovery to reduce the potential of $Ca_3(PO_4)_2$ fouling. For the high EC scenario, unlike the low and average EC scenarios, we have a case where the considered water cost now increases as the system recovery increases due to the cost of acid to control $CaCO_3$ fouling. This fact together with the limit to system recovery set by the $Ca_3(PO_4)_2$ stability index, points to operating at a lower system recovery when the RO system is receiving high salinity water. At the high EC level, although the cost savings to operate at a lower recovery are minimal, due to the high fouling potential, it makes sense to operate with a lower system recovery closer to 75%. Without considering other cost factors previously described, this simplified case shows that such a system which would typically operate at a constant recovery of 75% could potentially make savings during the part of the day when the system recovery can operate at 80%, and then reduce the recovery during the two periods during the day when the EC typically increases to the high level.

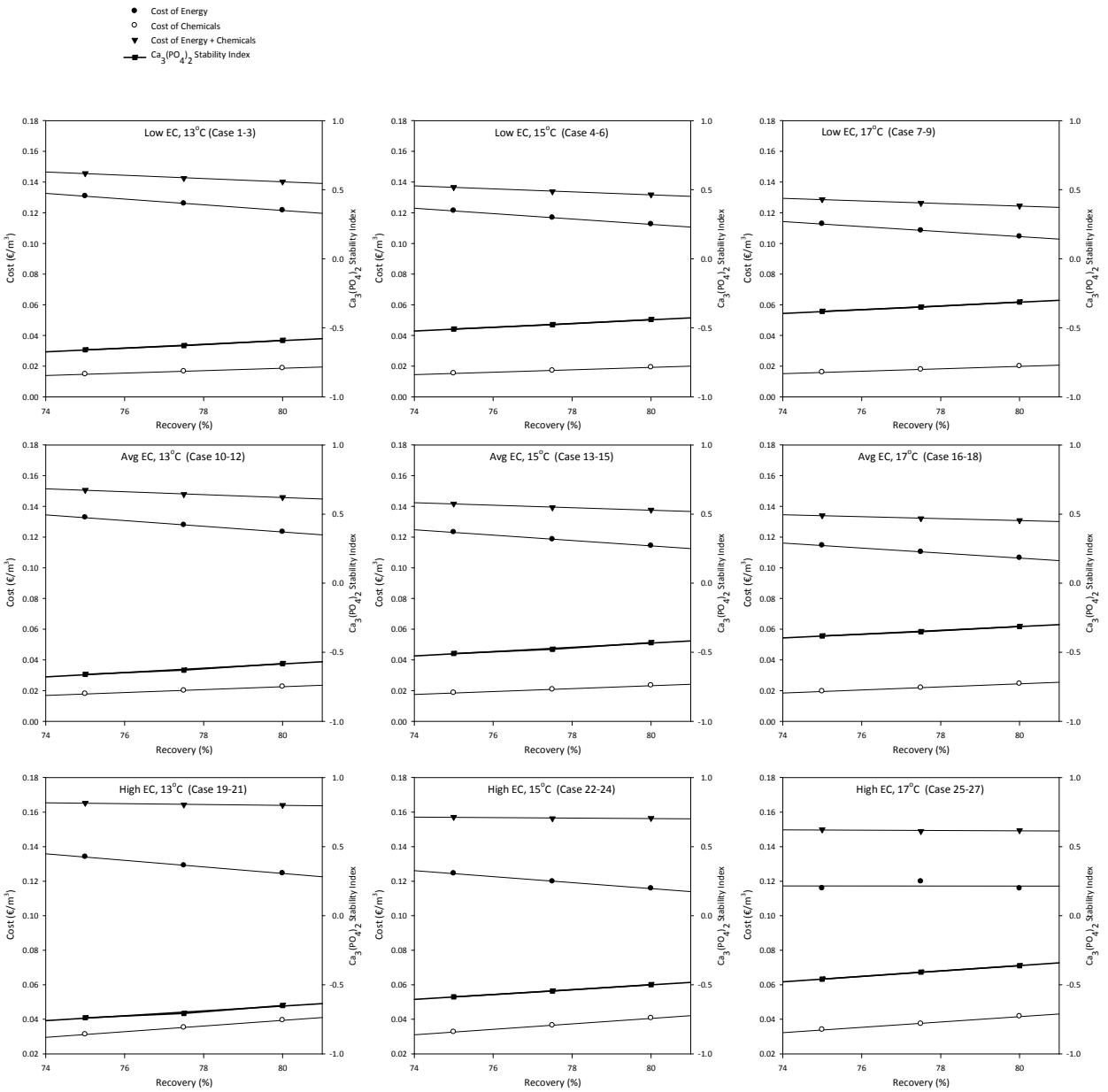

Figure 6-6: RO simulation results for the low temperature case, showing the $Ca_3(PO_4)_2$ stability index.

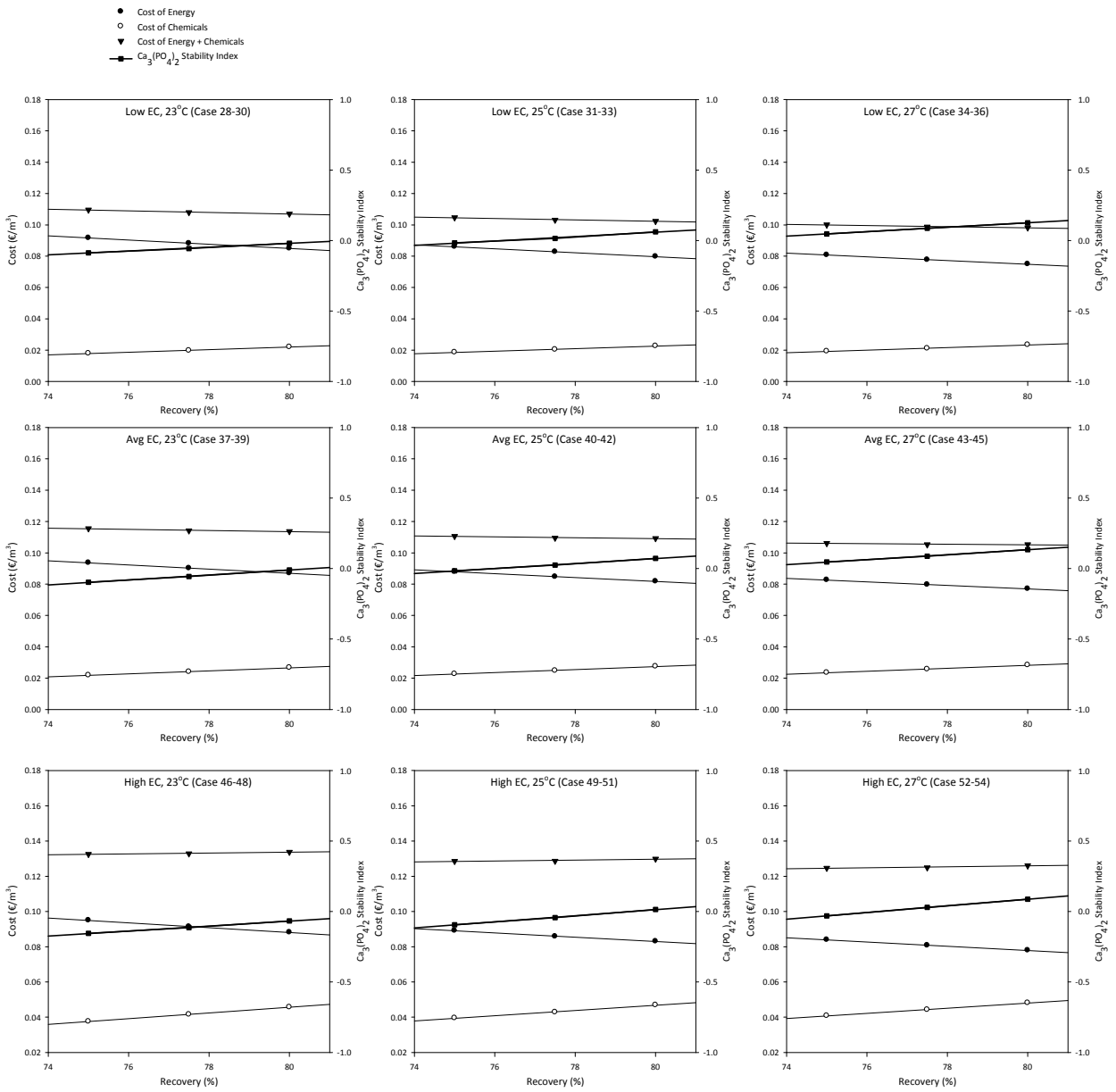

Figure 6-7: RO simulation results for the high temperature case, showing the $Ca_3(PO_4)_2$ stability index, $CaCO_3$fouling control by maintaining LSI < 1, $Ca_3(PO_4)_2$ controlled by limiting recovery so $Ca_3(PO_4)_2$ stability index <= 0.

Table 6-10 below provides the pH values to maintain an LSI of approximately 1 (also plotted in Figure 6-5 as a function of recovery) and the critical pH above which $Ca_3(PO_4)_2$ fouling will start to form for the given feedwater constituents and system configuration. The third value provided is the $Ca_3(PO_4)_2$ stability index calculated by subtracting the second from the first as described in the methods section and plotted in Figure 6-7. The lower of the two pH values could be used as the pH set point in the feedwater to control both the calcium carbonate and calcium phosphate scaling using pH adjustment.

Table 6-10: pH adjustment for calcium carbonate and calcium phosphate fouling control for the high temperature case

	Feedwater EC		**Low EC**			**Avg EC**			**High EC**		
	Feed water temperature		**23°C**	**25°C**	**27°C**	**23°C**	**25°C**	**27°C**	**23°C**	**25°C**	**27°C**
System Recovery	75.0%	pH for LSI = 1	6.810	6.770	6.730	6.690	6.660	**6.620**	6.490	6.440	6.400
		Critical pH $Ca_3(PO_4)_2$	6.897	6.786	6.683	6.788	6.676	**6.574**	6.646	6.534	6.431
		$Ca_3(PO_4)_2$ stability index	*-0.087*	*-0.016*	*0.047*	*-0.098*	*-0.016*	*0.046*	*-0.156*	*-0.094*	*-0.031*
	77.5%	pH for LSI = 1	6.700	6.660	6.630	6.590	6.560	6.520	6.390	6.350	6.320
		Critical pH $Ca_3(PO_4)_2$	6.757	6.645	6.542	6.647	6.536	6.433	6.505	6.393	6.290
		$Ca_3(PO_4)_2$ stability index	*-0.057*	*0.015*	*0.088*	*-0.057*	*0.024*	*0.087*	*-0.115*	*-0.043*	*0.030*
	80.0%	pH for LSI = 1	6.580	6.550	6.510	6.480	6.450	6.410	6.280	6.250	6.220
		Critical pH $Ca_3(PO_4)_2$	6.599	6.488	6.385	6.490	6.378	6.275	6.347	6.236	6.133
		$Ca_3(PO_4)_2$ stability index	*-0.019*	*0.062*	*0.125*	*-0.010*	*0.072*	*0.135*	*-0.067*	*0.014*	*0.087*

When required, we have two options for the control of calcium phosphate, either limiting the system recovery to ensure the calcium phosphate stability index remains less than 0 for a given feedwater EC and temperature or acidify the feedwater further to keep the stability index at or below 0. The importance of this increase in the dose of acid to control $Ca_3(PO_4)_2$ fouling beyond that to maintain an LSI of < 1 for calcium carbonate scaling control is highlighted in the Low EC and AVG EC at 25°C and Low EC and Avg EC at 27°C where the maximum recovery will be limited to 76% at 25°C and 72% at 27°C by the $Ca_3(PO_4)_2$ stability index. From Table 6-10, to maintain a recovery of 75% at 27°C (Avg EC case) the pH will need to be reduced slightly from 6.62 to 6.57 to maintain a $Ca_3(PO_4)_2$ stability index of 0 incurring an additional acid cost of 0.002 €/m^3 from 0.013 to 0.015 €/m^3 of permeate produced. Table 6-11 shows how the cost of acid increases if the recovery were to be increased.

Table 6-11: Difference in acid cost for Avg EC at 27°C to maintain an LSI <=1 and *$Ca_3(PO_4)_2$ stability index <= 0*

Recovery	**75%**	**77.5%**	**80%**
Cost of acid to maintain LSI <= 1 (€/m^3)	0.013	0.016	0.019
Cost of acid to maintain LSI <= 1 and *$Ca_3(PO_4)_2$ stability index <= 0* (€/m^3)	0.015	0.019	0.023
Difference (€/m^3)	0.002	0.003	0.004

6.4 Discussion

6.4.1 Information from EC with regards to ionic constituents

The inorganic constituents within a wastewater at any given time are influenced by a variety of interactions including the initial constituents making up the source municipal drinking water, be it ground, surface or desalinated water, together with inorganic constituents added to the water during its use and later as part of the wastewater treatment process. The results showed that using a single surrogate parameter, like EC, to determine or at best approximate, the concentration for each of the major ions making up wastewater is difficult due to the many factors contributing to the total ionic content which actually comes into contact with the membrane surface. The method proposed in this work to generate water profiles of different electrical conductivities by keeping the conservative water constituents as measured and then utilising maximum concentrations for the non-conservative ions which contribute to membrane fouling is one approach which could be adapted to operating reclamation facilities. No two systems will be operating with the same wastewater feed, and also biological system upsets, changes in sewage connections and concentrated loading of wastewater into a WWTP could all quickly change the constituents of the feedwater and therefore offline laboratory information must be continuously added into the system to build a database of feedwater quality data. Such a repository of feedwater quality data together with the experience of the process engineer could then be utilised in defining feedwater profiles linked to a specific feedwater EC to be used in the offline modelling process to generate a rule-base for online optimisation as shown in the next section.

6.4.2 Using the data generated to develop a decision tree

Table 6-12 below provides an example of a rule-base generated from the offline simulations to be used in the online optimisation of a RO system treating wastewater. The concept behind the rule-base is that for a particular range of feedwater EC and temperature, a specific system recovery and feedwater pH set-point is defined from the simulations. The specific range for each rule for both the feedwater EC and the temperature can be defined by the process engineer, and although three different profiles where defined in this work to minimise the number of set-point changes, such a decision should be made after testing the step-wise savings. That said, on a practical level, typically RO membrane systems prefer to operate at relatively constant conditions and therefore the number of EC and temperature profiles defined must consider the expected number of set-point changes per day.

Table 6-12: Example rule-base for high temperature case. CPSI: $Ca_3(PO_4)_2$ stability index, ME: Membrane element number.

(a)	(b)	(c)	(d)	(e)	(f)	(g)	(h)
Rule #	**EC Set-points**	**Temperature Set-points**	**Recovery for Min Cost**	**Fouling Potential**	**Recovery set-point**	**pH set-point**	**Acid Dose (mg/L)**
1	EC < LOW EC *EC < 1198 μS/cm*	T < LOW T *T < 23°C*	80%	$CaCO_3$ controlled, LSI < 1 + antiscalant 2 mg/L Low $Ca_3(PO_4)_2$ potential with acid dose based on LSI	80%	6.58 Based on LSI	51
2		LOW T < T < AVG T *23°C < T < 25°C*	80%	$CaCO_3$ controlled, LSI < 1 + antiscalant 2 mg/L High $Ca_3(PO_4)_2$ fouling potential at recovery > 76%	80%	6.49 Based on CPSI	59
3		AVG T < T < HIGH T *25°C < T < 27°C*	80%	$CaCO_3$ controlled, LSI < 1 + antiscalant 2 mg/L High $Ca_3(PO_4)_2$ fouling potential at recovery > 72% System recovery limited by max element recovery	77.5%	6.54 Based on CPSI	54
4		T > HIGH T T > *27°C*		High $Ca_3(PO_4)_2$ fouling potential – operate in safe mode Recovery reduced to minimise element recovery whilst acid dose increased to maintain production	70%*	6.38	68
5	LOW EC < EC < AVG EC *1198 μS/cm < EC < 1344 μS/cm*	T < LOW T *T < 23°C*	80%	$CaCO_3$ controlled, LSI < 1 + antiscalant 2 mg/L Low $Ca_3(PO_4)_2$ potential with acid dose based on LSI	80%	6.48 Based on LSI	69
6		LOW T < T < AVG T *23°C < T < 25°C*	77.5%	$CaCO_3$ controlled, LSI < 1 + antiscalant 2 mg/L High $Ca_3(PO_4)_2$ fouling potential at recovery > 76%	77.5%	6.54 Based on CPSI	62
7		AVG T < T < HIGH T *25°C < T < 27°C*	75%	$CaCO_3$ controlled, LSI < 1 + antiscalant 2 mg/L High $Ca_3(PO_4)_2$ fouling potential at recovery > 72%	75%	6.57 Based on CPSI	58
8		T > HIGH T T > *27°C*		High $Ca_3(PO_4)_2$ fouling potential – operate in safe mode Recovery reduced to minimise element recovery whilst acid dose increased to maintain production	70%*	6.28	93
9	AVG EC < EC < HIGH EC *1344 μS/cm < EC < 1664 μS/cm*	T < LOW T *T < 23°C*	75%	$CaCO_3$ controlled, LSI < 1 + antiscalant 2 mg/L Low $Ca_3(PO_4)_2$ potential with acid dose based on LSI	75%	6.49 Based on LSI	105
10		LOW T < T < AVG T *23°C < T < 25°C*	75%	$CaCO_3$ controlled, LSI < 1 + antiscalant 2 mg/L Low $Ca_3(PO_4)_2$ potential with acid dose based on LSI	75%	6.44 Based on LSI	113
11		AVG T < T < HIGH T *25°C < T < 27°C*	75%	$CaCO_3$ controlled, LSI < 1 + antiscalant 2 mg/L Low $Ca_3(PO_4)_2$ potential with acid dose based on LSI	75%	6.4 Based on LSI	118
12		T > HIGH T T > *27°C*	70%	High $Ca_3(PO_4)_2$ fouling potential – operate in safe mode Recovery reduced to minimise element recovery whilst acid dose increased to maintain production	70%	6.22	158
13	EC > HIGH EC *EC > 1664 μS/cm*	T < 27°C		$CaCO_3$ controlled, LSI < 1 + antiscalant 2 mg/L Low $Ca_3(PO_4)_2$ potential with acid dose based on LSI	75%	6.13	176
14		T > 27°C		Operate in safe mode	70%	6.13	176

6.4.3 A framework for the proposed online optimisation tool

Figure 6-8 provides a graphical representation of the proposed online optimisation tool. This framework is structured in three hierarchical levels: the real data level, the simulated data and online calculations level and the control actions level. The real data level involves the automatic or manual input of data into the online optimisation tool, this first level will also involve the trending of data. The simulated data level includes the rule base were the results from the offline modelling exercise are organised in such a way that the results can be useful. The final layer is the control action level, where set-points determined in the simulated data level will be translated into control actions. The next sub-sections will provide further details about the information and data utilised and generated in each of the layers.

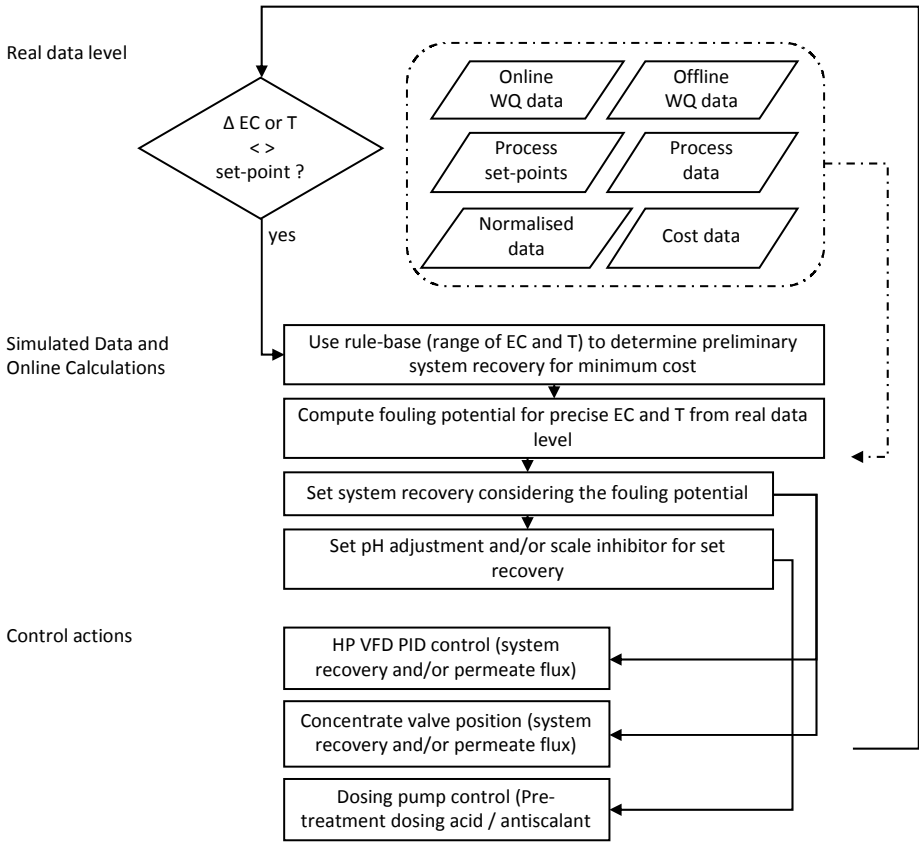

Figure 6-8: Preliminary IMS system control strategy, WQ: Water quality

6.4.3.1 Real Data Level

The real data level involves data and knowledge typically available to process engineers when taking decisions to manually modify process set points considering changes in feedwater quality and operational conditions to avoid membrane fouling while optimizing energy use. This data includes online water quality data, offline water quality data, process set-points, process data, normalised data and cost assumptions.

Online water quality data is the basis on which to take decisions in the proposed online optimisation tool. As a minimum this would include the EC, temperature and pH of the feed stream as presented in this work. Another sensor typically found on all RO plants is an EC sensor on the permeate stream to be used to calculate the normalised salt rejection and permeability to continuously have an indication of the condition of the membrane. Increasingly wastewater treatment plants are utilising online analysers or ion-selective sensors to measure the concentration of nutrients in the effluent. Including an online sensor for phosphate in the RO feed stream would reduce the uncertainty associated with the static value associated with the concentration of phosphate when calculating the calcium phosphate stability index as given in this paper. When working with online water quality data it is important to consider the buffering capacity of reactors and tanks in reducing the peaks and troughs of concentrations of constituents measured prior to such a tank. In practice the various treatment steps such as the primary sedimentation tank (if available) and the conventional activated sludge process would have quite an effect on the concentrations. Ideally measurements are made in the intermediate storage prior to the RO membrane storage, but this is not always possible or available.

Offline water quality analysis data is an important part of the knowledge base and will be required routinely as in any operating plant utilizing membranes. Water quality analysis results for the main ionic contributors together with indicators for bulk organic parameters should be input into the knowledge base for association and where possible correlation to online water quality data and fouling trends. It is important that the feedwater profiles utilised in the modelling step are continuously reviewed and updated with new water quality data to take into consideration changes in the wastewater quality over the lifetime of the system.

Operational set points are user defined set points that are essential in meeting the requirements of the water treatment plant such as product water demand and product water quality. Product water demand may be constant at full capacity if required, but the use of a storage buffer or fluctuating demand may give rise to energy saving control possibilities. Product water quality may be constant but may also be variable in the case of irrigated agriculture under wet and dry conditions, or the blending of the product water with other waters (such as surface or groundwater) of variable quality to obtain product water of a desired quality typically in terms of salinity, sodium, chloride, boron and sodium adsorption ratio for irrigation waters. Including important operational set-points into the rule-base may offer significant cost savings particularly when coupled to fluctuations in energy tariffs throughout the day.

Online process data typically includes pressure and flow data that is utilized by a Programmable logic controller (PLC) in the control of the system to operate at either constant feed pressure or constant

permeate flux mode. This information is important to be able to know the current operational set-points as well as to be utilised in the normalisation of salt rejection and permeate flux.

A data trending module is another important component of the real data level. In this level online and offline data available a number of monitoring parameters will be calculated periodically for operator reporting and for use in the membrane system optimization strategy. As is common to all membrane plants this will also include the normalization of feedwater EC and temperature to obtain normalized values for permeate flux and salt rejection according to the Standard Practice for Standardizing Reverse Osmosis Performance Data (ASTM Standard D4516-85). It is important that this normalized data is continuously recorded and made available to feedback to the rule-base to understand how optimization strategies are affecting membrane fouling.

Finally cost assumptions will also be entered by the user to ensure that optimization conditions utilize current costs including those for energy (€/kWh), acid and antiscalant (€/L), but also those of labour in the case of maintenance including the cost of clean-in-place (CIP) operations and the cost of brine disposal if costs can be associated with changing feedwater conditions.

6.4.3.2 Simulated Data and Online Calculations

Information from the real data level is then used to determine which rule applies for the current feed water analysis. In the example rule base given in Table 6-12 the applicable rule number (rule-base column a) is determined by fitting data from the real data level, into the provided EC range (rule-base column b) and temperature range (rule-base column c). The rule-base developed from the offline model provides a system recovery (rule-base column d) which already integrates the cost of energy for the feed pump and high-pressure pump together with the cost of acid and antiscalants, together with a pre-determined fouling potential (rule-base column e). The fouling potential considerations given in the rule base give a short comment whether the precipitation of the sparingly soluble salt is controlled or not. The fouling potential in this case considers the scaling indices for calcium carbonate and calcium phosphate, but others could be added as required by the particular feedwater and system configuration, together with an indication of whether the membrane manufacturer's system design guidelines are respected.

Although guide set-points are provided in the rule-base for system recovery (rule-base column d), pH set-point (rule-base column e) and acid dose (rule-base column f), the fouling potential calculations described in section 6.2.3 should also be calculated in real-time using the particular EC and temperature (and not the maximum value in the range as utilised when developing the rule-base) to determine a set-point for recovery, feedwater pH and antiscalant dose. The acid and antiscalant

doses are then determined utilising empirical equations from the offline model for the assumed feedwater alkalinity and measured feedwater pH.

It is important that new data from the real data level is included into the rule base as shown by the discontinuous line in Figure 6-8. The operator should be prompted to review the rule-base if the new information in the real data level is seen to not be fitting into the current rule-base or if the normalised salt rejection or normalised permeate flux shows that the fouling control strategies are not effective.

6.4.3.3 Control actions

Figure 6-9 shows a schematic of the control system to be implemented linking sensors and actuators to the control system. The determined set-points from the simulated data and online calculations step will then be translated into manipulate variables which are communicated to systems equipment. The system recovery is typically controlled through the use of a PID controller to control the feed flow rate using VFD on the high-pressure pump while the concentrate valve position is utilized to control the feed pressure. While the determined dose for acids and antiscalants is communicated to metering pumps to administer the correct amount of chemicals according to the feedwater flow (Q) and pH.

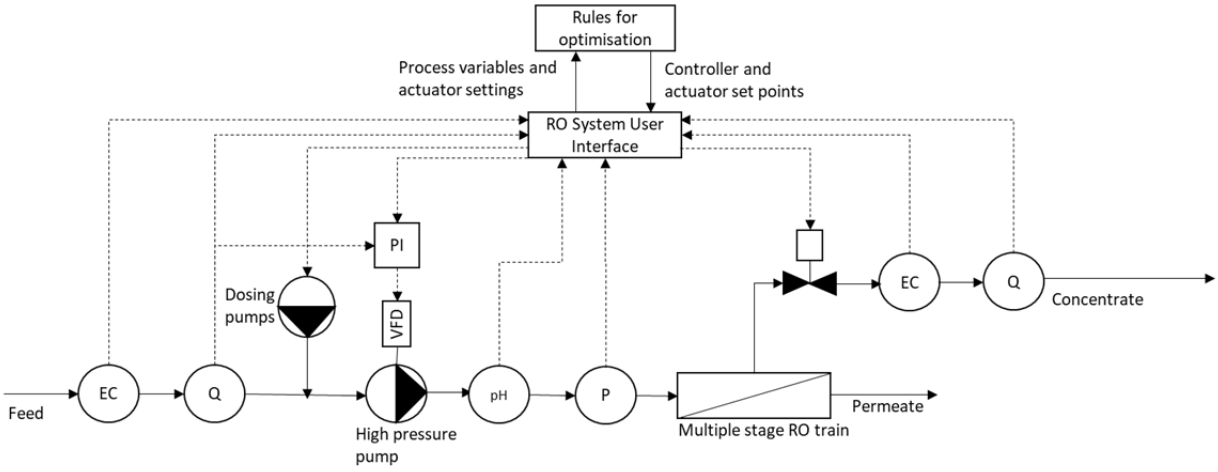

Figure 6-9: Sensors, actuators and controllers as part of the proposed optimization system (adapted from Bartman et al., (2010)), EC: EC sensor, Q: flow sensor, pH: pH sensor, P: pressure sensor, VFD, PI: proportional/integral controller.

6.5 Conclusion

This work provides a start to the reasoning process involved in optimizing RO process conditions in a wastewater reclamation facility which is constantly subject to variations in feed water quality due to predictable changes in urban activity (flow and load). Optimization will be carried out with regards to system recovery together with corresponding pre-treatment dosing (acid and antiscalant) to minimize the total water cost which includes the membrane fouling potential. This routine reasoning

process would be typically carried out by process engineers managing the plant but are often limited by the time that can be devoted to plant optimization. The following are the main conclusions from the work presented:

- Although there are limitations to the use of EC as a main parameter to deduce the individual ionic constituents in a wastewater, given the right assumptions, the work has shown that it is possible to obtain a useful profile for a particular EC value which could be used in an online / real-time optimization system. The discussion also provides some ideas on how other online and offline water quality data could be incorporated to obtain a more accurate instantaneous water quality profile if required and if it is financially feasible for a particular system.
- Through the presentation of a simple case study considering the cost of energy and pre-treatment chemicals, the work showed that there is scope for online optimization tool in terms of associating a cost to the current operating process conditions and then questioning whether there is a more cost-effective way to 'set' the system.
- Industry standard RO simulation software which is available from all membrane manufacturers was proposed as an offline method of developing a series of simulations whose results are used in creating rules for the online optimization system. The offline RO simulation software was chosen as method which can be understood, and the results conceptualized by plant operators.
- A preliminary decision tree for online system optimization was presented.

Further work, which needs to be undertaken to develop the concept further, is the following:

- Although the equations utilised in this work to predict the scaling at different process conditions are practical for control and automation purposes, the results should be corroborated with more complex chemical speciation models such as those included in Phreeqc (U.S. Geological Survey).
- Introducing concepts from Artificial Intelligence (AI) into the system architecture.
- Including feedback from antiscalant manufacturers to see whether concepts presented in this work could be built upon and how their product offering can be included into such an online system.
- Understand whether the usable lifetime of RO membrane elements is compromised over the long term working under varying process conditions.
- On a practical level, it has to be seen whether introducing an AI tool for the real-time control of a RO system actually provides a financial return over the operating life of the wastewater reclamation system.

The novelty of the work lies in bringing together online process and water quality data, offline water quality data together with historical process and water quality data and fouling trends to optimize

system operating conditions under constantly changing feedwater quality whose variability is inherent to municipal wastewater.

Such a product could enhance the market penetration of integrated membrane processes for wastewater reclamation for high value applications through the minimization of the total cost of water.

Chapter 7 - Electrical conductivity as an indicator for RO/NF membrane integrity monitoring

This chapter seeks to understand whether the commonly available electrical conductivity sensor can be better utilised to monitor RO membrane integrity and proposes strategies to enhance the potential of using such a method to monitor membrane integrity in real time.

7.1 Introduction

The RO process utilizes semipermeable membranes as a physical barrier to remove dissolved constituents primarily based on size exclusion. This process is typically responsible for the removal of the bulk dissolved constituents, typically bring down the TOC below 1 mg/L. RO membranes are also responsible for the removal of the majority of regulated and unregulated emerging organic substances to non-detectable levels.

Challenge tests have shown that viruses, which are the smallest pathogen when compared to bacteria or protozoa, can be removed beyond 6-log units and, since this is the smallest pathogen, RO membranes could, in theory, be attributed to 6-log removal credit for all pathogens.

However, similar to other treatment processes, RO process performance for virus removal is not determined by the ability of the membrane to remove the pathogen but rather by the ability to monitor integrity (Wintgens et al., 2005). The US EPA Membrane Filtration guidance manual (EPA, 2005) states that “spiral would RO membranes are not intended to be sterilizing filters and some passage of pores may occur despite the absence of pores in membranes, which may be attributable to slight manufacturing imperfections”. Further to this the manual states that NF/RO membranes are eligible to claim microbial removal credit, but it has to be based on demonstrated ability.

Various methods have been proposed for monitoring RO/NF membrane integrity in real time, with the most accessible being electrical conductivity, sulphate and TOC removal (Kumar et al., 2007). While these surrogate parameters have been accepted as appropriate parameters, they have been assigned very conservative log removal credits, as they are limited by the membrane’s rejection of salt in the case of EC or by the instrument sensitivity in the case of TOC. Typically, the LRV demonstrated for regulators for these surrogate parameters is not above 2-log removal. This means that there is a difference of up to 4-log removal credits in terms of demonstrated removal of pathogens and what can be confirmed continuously using EC or TOC sensors. Furthermore, quantifying the accuracy of EC and TOC measurements depends on their concentration in the feedwater. Variations in RO feedwater quality including changes in salinity, temperature and pH may appear as variability in membrane integrity indicators but may not be necessarily related to a breach in the membrane.

Membrane integrity breaches may occur due to various factors including membrane defects, insufficient or improper pre-treatment, chemical attack (such as oxidation due to pre-treatment chemicals or clean-in-place processes), faulty installation, failure of membrane assembly components (such as O-rings) and stresses associated with operating conditions such as water hammer or passage of sharp debris. An ideal monitoring system for RO/NF would be able to

continuously detect greater than 4-log and periodically up to 6-log removal for surrogate trace particles.

EC sensors are standard components of any RO system whether it is used for desalination or for wastewater reclamation. EC sensors are utilised to measure the salinity of the feedwater and the permeate water as these are key components in controlling system process conditions (membrane feed pressure to obtain a required permeate flow), controlling membrane fouling (through the regulation of system recovery to avoid the precipitation of inorganic constituents on the membrane surface) and characterising membrane condition. Since these sensors are so essential to process control, are relatively cheap to purchase and maintain and are easy to operate and calibrate they will be found both in large-scale municipal water reclamation facilities reclaiming tens of thousands of cubic meters of water per day or small-scale decentralised reclamation facility within a resort or hotel providing tens of cubic meters per day of water.

Over the years a number of other technologies have been developed and tested for membrane integrity verification including the 3D Trasar Technology from Nalco, Mem Shield from MINT and sulphate sensors. Trasar is an inert molecular tracer that can be detected down to concentrations of parts per trillion (ng/L) by fluorescence. It is currently used as part of a continuous online monitoring method for antiscalant dosed in RO facilities. The Trasar molecule is approximately 610 Da, which is comparable to the size of many viruses (which range in size from approximately 200 to 3000 Da). This is well above the molecular weight cut-offs of RO and NF membranes (which are in the range of 100 Da and 200–400 Da, respectively). MEM-SHIELD consists of both direct and indirect integrity testing. MEM-SHIELD claims to be able to reliably differentiate between 3-log removal and 4-log removal with further work being done to differentiate between 4-log and 5- log removal. The product is currently being tested at the Bedok Newater Factory in Singapore. Another potential method for RO integrity verification is sulphate, which has been reported to be reduced by >2-log (MWH, 2007). Sulphate rejection varied between 2- to 3-log depending on the RO manufacturer for a single stage system. A separate test using the best performing membrane was done to compare a single stage with a two-stage system. The results indicated that the rejection was approximately 3-log vs. 2.5-log, respectively.

Although these methods have been proven to be effective, they involve significant capital and operational investments and although these could be feasible for large scale water reclamation facilities, it is often very hard to justify such a capital and operational investment on smaller decentralised water reclamation facilities. The objective of this work is to investigate a number of strategies to utilise the commonly available EC sensor to enhance its potential in the verification of integrity of RO membranes in real time.

7.2 Methodology

The methodology utilised in this work was theoretical, utilising a combination of RO Simulation Software (Reverse Osmosis System Analysis, ROSA, DOW Water and Process Solutions) and a series of mass balances implemented in a spreadsheet (Microsoft Excel). The mass balances were carried out to utilise the results from the simulation (permeate flow and TDS) obtained for each membrane element within a PV and then manually introduce various contaminant mass flows in each membrane element to firstly understand the sensitivity of the method and to secondly understand how this could be enhanced for integrity monitoring. Table 7-1 provides a breakdown of the different components of the work.

Table 7-1: Methodology

	Component	Method
1	Estimation of water passage (mL/hr) through a breach of diameter (mm) at a particular feed pressure (bar)	Theoretical
2	Estimation of smallest detectable flow (mL/hour) for a breach through different membrane elements within a PV at 2.1) - different feed water salinities 2.2) - different ratios of EC probes to the number of pressure vessels (1:1, 1:6, 1:12, 1:24, 1:48)	Simulation 1 + Mass Balance
3	Application of a high salinity 'slug' (increasing the feedwater salinity for short period) to enhance the difference between breach and non-breach conditions	Simulation 2 + Mass Balance
4	Proposed strategies for integrity monitoring using EC sensors: 4.1) - Individual tree EC monitoring and comparison 4.2) - Simultaneous profiling 4.3) - Pulsed integrity monitoring	Theoretical

A consideration when trying to understand the resolution of using EC as an indirect method for monitoring membrane integrity is to understand the link between the size of pathogens that may pose an acute risk to public health and the flow rate of water through a breach in the membrane (Study component 1). To obtain an approximate relationship between the size of the breach (represented as a circle with diameter, d) and the volumetric flow (Q, m^3/s) of water from the feed/concentrate stream into the permeate stream through different sized breaches in the membrane (A, Aperture area of the circle, m^2) at different feed pressures (P, Pa), and density

(kg/m^3), Equations 7-1 and 7-2 were used with a contraction coefficient (c_c) of 0.62 and a velocity coefficient (c_v) of 0.97 to calculate the discharge coefficient (c_d).

$$\boldsymbol{c_d = c_c \times c_v} \quad \textbf{Equation 7-1}$$

$$\boldsymbol{Q = c_d \times A \times \sqrt{2 \times \frac{P}{\rho}}} \quad \textbf{Equation 7-2}$$

RO simulation software was used to simulate a two stage RO system which allowed the estimation of the smallest detectable flow of water (mL/hour) through a breach in a membrane (Study component 2). The modelled system configuration utilized DOW Filmtec BW30 440i membranes to produce a permeate flow of 185 m^3/hour at a recovery of 75%. The configuration consisted of 21 PVs in the first stage and 11 PVs in the second stage, both stages had 6 membrane elements within a single PV to operate at an average permeate flux of 23.6 LMH (litres per meter squared per hour). The system was modelled to be operating at a constant temperature of 15 °C, a pH of 7.6 and a flow factor of 0.85. The model was run using this same configuration for increasing feed water salinities of 500 mg/L, 1000 mg/L, 2081 mg/L, 5439 mg/L, and 11,476 mg/L modelled as Sodium Chloride (NaCl) in the place of TDS).

To convert permeate TDS (mg/L) to EC (µS/cm) three different equations were utilized depending on the range. Equation 7-3 is utilized for a TDS between 0 and 100 mg/L, Equation 7-4 was utilized for a TDS between 100 and 200 mg/L and Equation 7-5 was utilized for a TDS between 200 and 300 mg/L.

$$\boldsymbol{[TDS, 0-100 mg/L] = 2.108 \times [EC] + 0.5361} \quad \textbf{Equation 7-3}$$

$$\boldsymbol{[TDS, 100-200 mg/L] = 1.9749 \times [EC] + 13.114} \quad \textbf{Equation 7-4}$$

$$\boldsymbol{[TDS, 200-300 mg/L] = 1.9726 \times [EC] + 13.783} \quad \textbf{Equation 7-5}$$

The permeate flow (Q_P, m^3/hr), permeate TDS (C_P, mg/L), feed flow (Q_F, m^3/hr), feed TDS (C_f, mg/L) and feed pressure (P, bar) for each of the 12 membrane elements were recorded for each model run and input into a spreadsheet as given in Table 11-16. The modelled permeate flow rate and permeate TDS were then utilized to determine the permeate salt mass flux (J_P, g/h) using Equation 7.6 which influenced the permeate EC. The combined permeate TDS from a PV was calculated by dividing the sum of the salt mass flux of each membrane element by the sum of the permeate flows from each membrane element.

$$\boldsymbol{J_P = Q_P \times C_P} \quad \textbf{Equation 7-6}$$

The modelled feed TDS (C_F, mg/L) at each membrane element was then utilised to determine the contaminant mass flux (J_C, g/h) using Equation 7.7 as the contaminant flow of water (Q_C, mL/h) was increased from 1 mL/hr to 2600 mL/hr for each of the 12 membrane elements (2 stages each with 6 membrane elements).

$$J_C = Q_C \times C_F$$ **Equation 7-7**

The permeate concentration obtained under membrane breach circumstances and no membrane breach circumstances was then determined by dividing the sum of the salt mass flux and permeate flow for each of the 12 membrane elements. Under 'non-breach circumstances', the salt mass flux consisted only of the modelled permeate TDS for each of the membrane elements. While under 'breach circumstances', the salt mass flux consisted of the modelled permeate salt mass flux (J_P) for each of the membrane elements together with the contaminant mass flux (J_C). The salt mass flux was then divided by the permeate flow (Q_p) to obtain the permeate concentration.

Firstly, this process was utilized to determine the smallest contaminant flow of water (Q_c, mL/hr) that can be detected as a change in EC of 0.01 µS/cm (which is typically the minimum resolution of EC probes) between 'breach circumstances' and 'non-breach circumstances' (Study component 2.1).

Secondly the results were utilised to understand how the ratio of EC probes to the number of PVs affects the sensitivity of an EC probe to detect a breach in a membrane (Study component 2.2). These results consider the dilution effects of the permeate flow on a single EC probe from more than one PV (Banks of 6, 12, 24 and 48 PVs per EC probe). For example, if a bank of 6 PVs are connected to a single EC probe, then the contaminant flow passing through a single membrane element is diluted by permeate from six PVs (total of 36 membrane elements), making it harder to detect breaches in a membrane.

The final part of the work looked into how introducing a 'slug' of higher salinity will affect the sensitivity of the EC method (Study component 3). For this the same model was applied but this time changing the feedwater TDS (C_F) while maintaining a constant operational feed pressure (P) of 16 bar (15.7 bar at the membrane) for an operational feed TDS of 1000 mg/L. The slug of high salinity water utilised in the simulations ranged from 1000 mg/L to 12,000 mg/L with intervals of 1000 mg/L.

The slug concentration should be limited to ensure there is permeate flow from the last membrane element in a PV. This can be assured by having a positive net driving pressure (feed pressure minus the osmotic pressure) in the last membrane element. In this case the max feed TDS was 12,000 mg/L.

The work is concluded by applying the different components of the work to come up with improved monitoring strategies.

7.3 Results

7.3.1 Estimation of water passage through a membrane breach

The relationship between the rate of flow of water (mL/hour) expected to pass from the feed channel into the permeate channel through a breach of different diameters (0.01 – 40 µm) at different operating pressures (4 – 40 bar) is shown in Figure 7-1. Other than the size of the breach and the feed pressure, these values do not consider the affected of the physical characteristics of the breach and are therefore rough approximations. The figure shows that a breach having a diameter of 0.024 µm, the size of the MS2 Bacteriophages which are commonly used as microbiological indicators in wastewater reclamation, at a feed pressure of 4 bar would result in a flow of 0.03 µL/hr through the breach into the permeate steam. This flowrate would double if the membrane was operating at a feed pressure of 16 bar which is a more realistic value for RO systems operating at relatively high system recoveries > 70 %. Taking a breach with a diameter of 0.09 µm, the size of Adenovirus, another indicator organism, at a feed pressure of 16 bar we could expect a flowrate in the region of 0.8 µL/hr. When considering breaches in membranes in the range of the size of bacteria, which typically have a size between 0.2 and 10 µm, the flowrates increase significantly. For a breach with a diameter of 1 µm (Escherichia coli typically have a size of 3 x 1 µm) we would expect a flowrate of 0.1 mL/hr at a pressure of 16 bar.

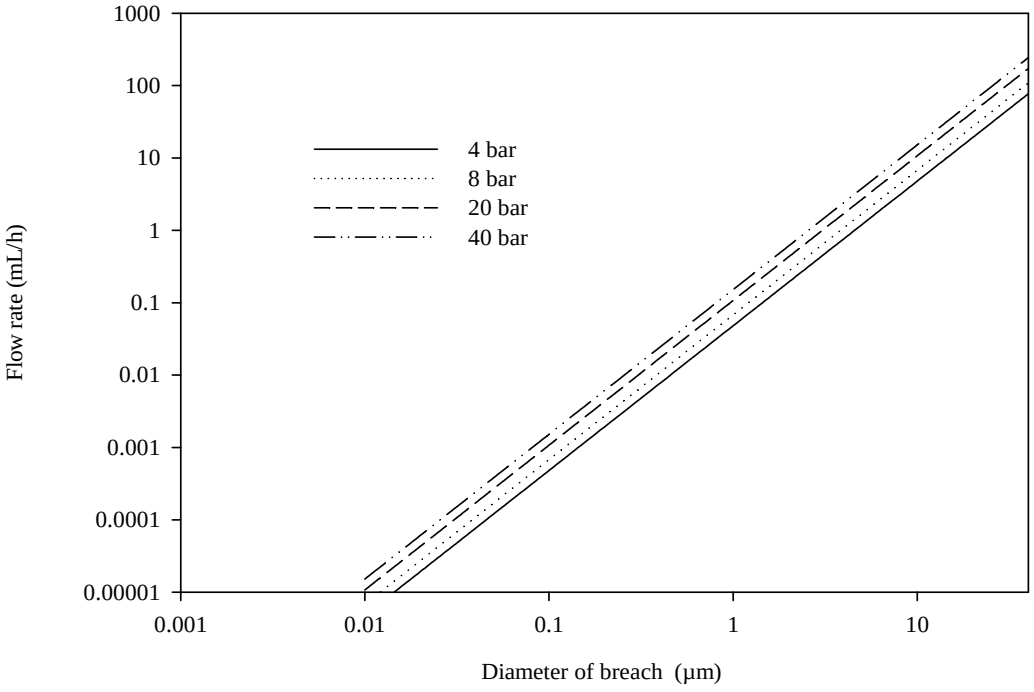

Figure 7-1: Approximate flow rate expected from breaches in a membrane of different diameters

7.3.2 Smallest detectable flow through a membrane breach

As feedwater passes through a single PV and permeate water is drawn through each membrane element sequentially, the feedwater increases in concentration as shown in Figure 7-2 below. This impacts the detection of breaches in a membrane since elements closer towards the concentrate end of the PV would have a greater chance of being detected due to the higher salinity of the volume of water passing from the feed channel through a breach into the permeate channel making the difference in conductivity between breech and non-breach conditions greater.

In addition to the location of the breach with a PV, the initial feedwater salinity also heavily impacts the ability to detect breaches when utilizing EC sensors. Figure 7-3 shows the smallest detectable flow of water of feed water salinities for a two-stage system assuming six membrane elements within each PV. The figure shows that when operating with a feed water having an EC of 1000 µS/cm a much higher flow of water is required to register a 0.01 µS/cm change in EC reading when compared to higher feedwater salinities. in the Annex 5 show the assumptions and results from these calculations. The values given in Figure 7-3 assume that an EC sensor is installed on the permeate port of each PV. This point of using higher salinity feed water to detect possible breach conditions leads to the possibility of introducing a ‘slug’ of high salinity water at periodic intervals while the system is running to be able to better detect issues with membrane integrity.

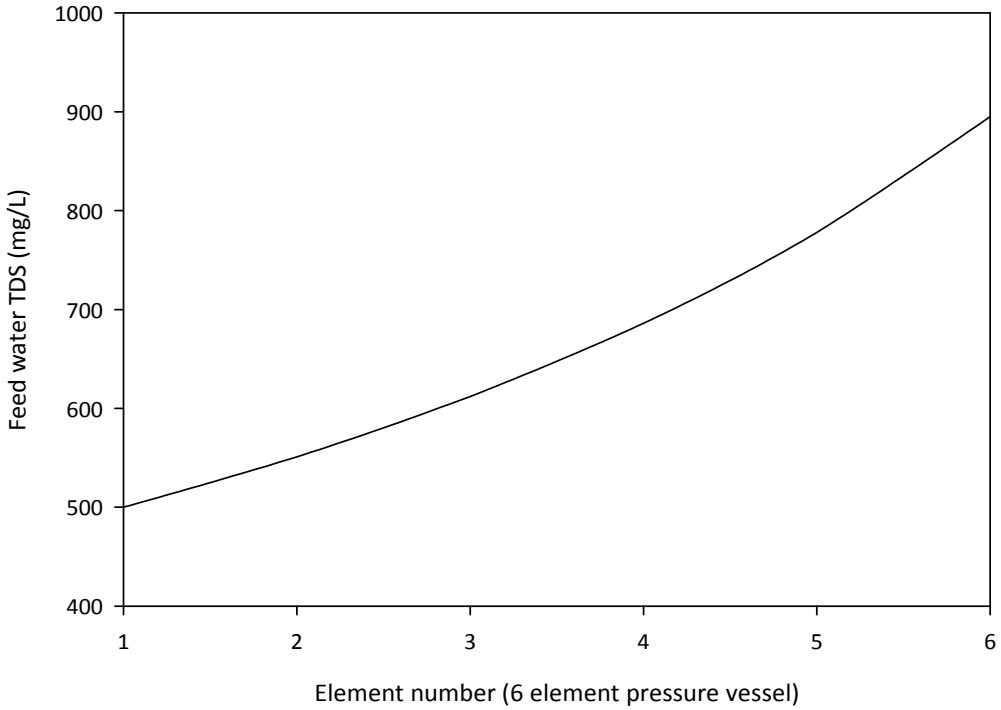

Figure 7-2: Increase in feedwater salinity entering each membrane element along a PV (Feed TDS of 500 mg/L)

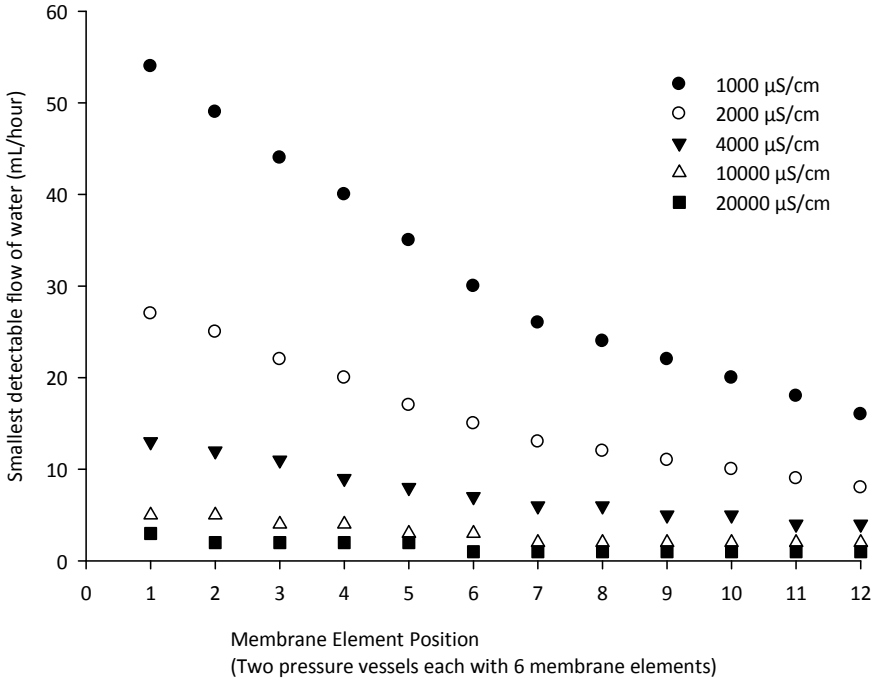

Figure 7-3: Smallest detectable flow of water at each membrane position for different feedwater salinities

Another central factor affecting the ability of an EC probe to detect breaches in a membrane is the number of PVs per EC probe. The larger the number of PVs per EC sensor, the higher the dilution factor applied. The integrity monitoring system would be most sensitive if an EC sensor would be

located on each permeate tube receiving permeate from the membrane elements within a single PV. In reality, this would be impractical and expensive. Figure 7-4 shows how the smallest detectable flow for a feedwater salinity of 1000 µS/cm changes according to the ratio of EC sensors to the number of PVs. For example, at this low feedwater salinity, the smallest detectable flow in the first membrane element with an EC sensor per PV is 54 mL/hr, as this increases to 12 PVs per EC sensor this value increases to 645 mL/hr (54*12). As the feed water EC increases to 2000 µS/cm, the smallest detectable flow in the first membrane element reduces by half that at a feedwater EC of 1000 µS/cm to 27 mL/hr. Table 11-17 in the Annex gives the full set of values for different conductivities.

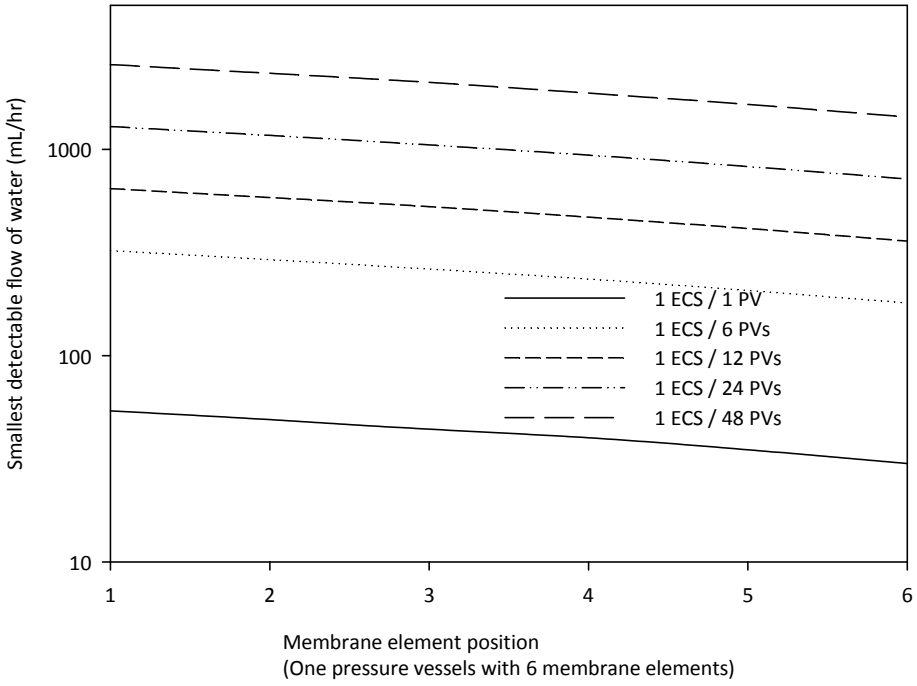

Figure 7-4: Smallest detectable flow for a feedwater salinity of 1000 µS/cm

7.3.3 Application of a high salinity slug

Figure 7-5 below shows how an increase in feed water salinity from 1000 mg/L to 12,000 mg/L can make a difference in detecting three different flowrates of feed/concentrate passing through a breach in the first membrane element (1,2 and 10 mL/hr). The values shown below again utilise an EC sensor per PV. If the ratio of EC sensors to pressure sensors becomes a more realistic 1 in 6, then the minimum flow through a breach which could be detected is just under 3 mL/hr if a slug of 12,000 mg/L is utilised. The figure is being shown to introduce the concept of how dosing a high salinity slug through the pressure vessel can increase the sensitivity of an EC sensor to detect even small flows of

water through a breach. The red line shows the smallest change that can be detected by a standard conductivity sensor, which is typically 0.01 µS/cm.

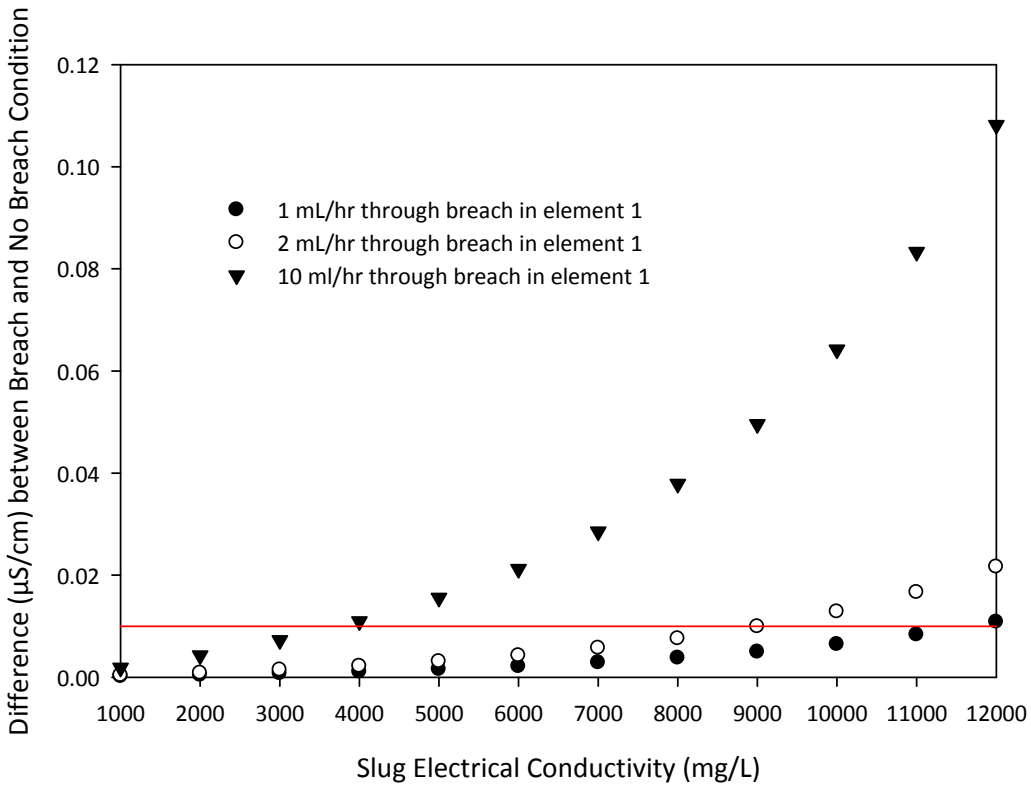

Figure 7-5: Difference in EC (µS/cm) between breach and non-breach conditions for different slug EC (µS/cm)

7.3.4 Proposed strategies for integrity monitoring using EC sensors

7.3.4.1 Individual tree EC monitoring and comparison

The sensitivity of utilizing EC for membrane integrity monitoring is severely compromised since EC sensors typically monitor a bank containing a large number of PVs and therefore any breach in a membrane is not detected because of the dilution effects of the permeate from each PV.

Therefore, first important outcome from this work is the importance of water reclamation facilities utilising RO/NF technology to have an EC sensor installed on the smallest practical number of PVs in the configuration. On retrofits this will typically be dictated by the piping configuration, but ideally this is kept to a maximum of 6 to 8 PVs per EC sensor. The Santa Cruz WD Seawater Reverse Osmosis Desalination Program Watershed Sanitary Survey and Pilot Testing Project (CDM, 2010) examined the industry standard of one EC sensor per bank and concluded it was not sensitive enough to detect breaches in O-rings or membrane ruptures. The study recommended one sensor per 'tree' of PVs, with a 'tree' comprising 10 PVs resulting in a higher sensitivity of the monitoring system. The report

concludes that analysing every single PV is impractical, but monitoring 'trees' is not overly complex or prohibitively expensive.

Following the work which was carried out for Chapter 6, the authors of this study attempted to implement an online normalisation software which continuous gathers signals from online instruments and normalizes the data according to the standard methods described by commercial membrane manufacturers (Dow Water & Process Solutions, 1995). The issue with EC is that it is influenced by the feedwater composition, feed pressure, temperature and recovery of the system. Normalisation of the permeate flow and salt passage is a standard procedure typically as an offline method (Excel spreadsheet) recommended by membrane manufacturers to distinguish between the mentioned changes and performance changes due to fouling. In this study the salt passage, both normalized and non-normalized, was calculated at intervals of between 1 and 10 seconds following which data points from a user defined moving window (typically taking 10s readings over 1, 5, 10 or 60 minutes depending on the parameter) calculates the mean and standard deviation of the data within the moving window. This considered operational events such as start-up or shut-down, permeate flushing and cleaning events in the NF system. Alerts were given to the user when the parameter exceeds the mean ± standard deviation (the operator can define the number of standard deviations limit). The signal to noise ratio (ratio of the mean to the standard deviation) for each of the calculated parameters was also calculated for each value to decide whether the upper and lower limits set were acceptable. The idea was to utilise a continuous printer similar to that typically installed with a foetal heart monitor to obtain a hardcopy of the results as a practical way of ensuring that integrity-monitoring results are continuously monitored and kept for audit purposes.

This process of normalisation compares the actual performance to a given reference considering the influent quality and operating parameters. The given reference may be either the design system performance or else the initial system performance. The problem faced was that there are a number of issues when it comes to the reliability of online normalized data which need to be taken into consideration including the sensor drift, the variability in wastewater quality, normalisation factors (including the assumptions made to convert EC to Total Dissolved Solids and those to calculate the osmotic pressure and membrane condition. These issues made it very difficult to utilise the normalised salt rejection to detect breaches in membrane integrity.

A simpler solution without having to normalise the data, comes about from having a number of 'trees' (each 'tree' made up of 6 – 8 PVs collecting permeate in a single pipe which is monitored by an EC sensor) fed from the same high-pressure pump. This makes it possible to compare EC measurements under near identical process conditions within the same bank removing the effect of changes in feedwater composition, feed pressure, temperature and recovery of the system and thus

removing the need for data normalization. Any discrepancy between permeate EC sensor measurements between the different trees should flagged and conductivity probing carried out on each of the PVs within the 'tree'.

Figure 7-6 shows the concept of monitoring separate trees within a treatment train, where for example the EC of the permeate from 'Tree 1A' is compared to the EC of the permeate of 'Tree1B' as both of these trees are fed by a single high-pressure pump. The same is done for the other treatment trains within the first and second stages of the RO/NF system. Apart from comparing measurements from different trees fed by the same high-pressure pump, the monitoring system must also be able to record and compare measurements from a single tree over a number of days.

Due to small pressure differences between different trees fed by the same high-pressure pump due to frictional losses and due to different configurations in piping, a compensation factor could be included to 'normalise' the effect of feed pressure throughout a single system.

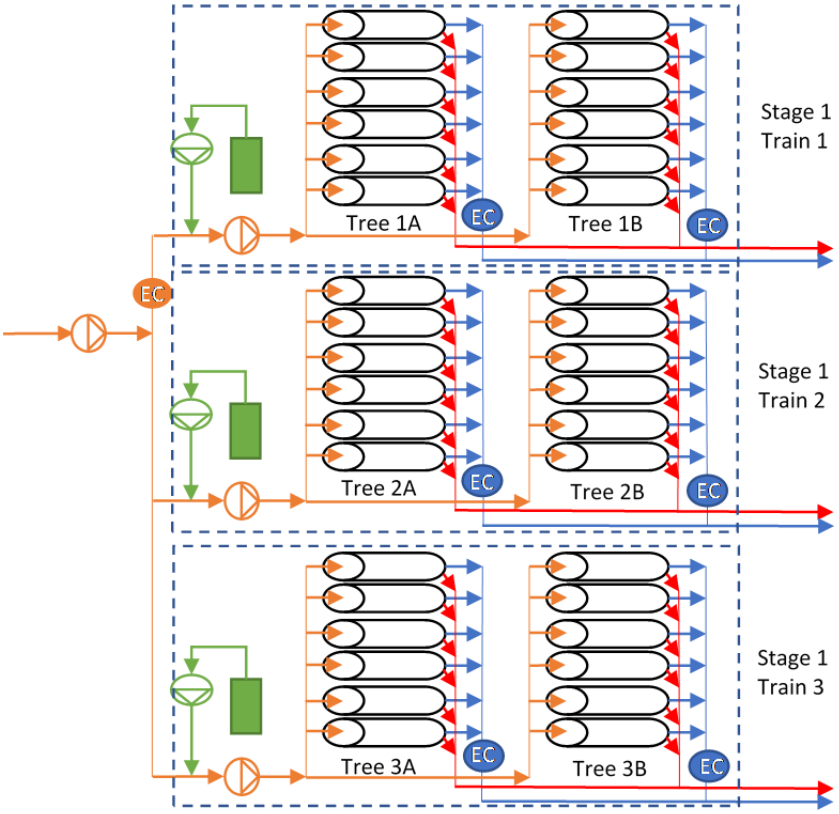

Figure 7-6: Concept of monitoring EC for different trees and comparing data within a single train.

7.3.4.2 Pulsed integrity monitoring

As shown in Figure 7-3 and Figure 7-5, as the conductivity of the feedwater increases from 1000 mg/L to 12,000 mg/L the sensitivity of the method increases significantly. This is shown as a

decrease in the smallest detectable flow of water passing from the feed channel through a breach into the permeate channel.

Depending on the operating pressure of the system, a slug of high conductivity solution (NaCl or other dissolved salt which will not precipitate on the membrane surface) could be introduced for a short period of time into the feedwater (10 to 60 s depending on the piping design, feed conductivity, and operating pressure). This slug of high conductivity solution would be introduced just upstream of the high-pressure pump as shown by the green dosing pump in Figure 7-6. The profile of salt rejection and permeability can then be compared when the slug is introduced with single PVs (if Supplementary EC PV monitoring is utilized for the optimum sensitivity) or comparing different 'trees' (if utilizing Individual PV tree EC monitoring and comparison). When choosing the concentration of the slug solution one must ensure that the osmotic pressure of the water is well below the operating pressure of the system. For example, for this simulated system 12,000 mg/L was the limit. Utilising pulsed integrity monitoring will increase the sensitivity of the method by a factor of the ratio of the slug EC to the operating EC. The increase in the permeate TDS during this short period of increased salinity is negligible. For example, if the system is typically operating at Feed TDS of 1000 mg/L and a slug of 12,000 mg/L is introduced, the permeate TDS will increase from 10 mg/L to 300 mg/L. Although this seems like a large amount this will be blended with permeate from the other treatment trains.

Pulsed integrity monitoring can be carried out once a day automatically during periods of low demand or as often as required, possibly even once an hour, but this shouldn't be needed. Generally, this would be required after any changes to a system are carried out, and on a daily basis for regulatory purposes. The sensors will be running continuously so any large breaches can be detected in real-time.

Although Figure 7-1 shows how depending on the size of the breach, by increasing the feed pressure by a few bars the flow rate through the breach may increase by an order of magnitude and thus increase the chances of being detected using EC sensors, this option of 'Pressure Induced Integrity monitoring' has limited applications in operating systems. This option is very much limited by the capacity of the high-pressure pump and the limiting maximum average permeate flux to avoid excessive membrane fouling and has to be carefully considered to ensure that the limiting process conditions (pressures and flows) are respected together with the membrane manufacturer design guidelines, to ensure that fouling is not exacerbated.

7.3.4.3 Discontinuous simultaneous individual PV monitoring and PV profiling

Another option could be to have a set of 6 EC sensors (or the number of PVs per tree) for simultaneous EC profiling. This set of sensors can be installed on the permeate tubes of the PVs making up one tree for a short period of time and different trees can be profiled on different days or when a breach is suspected giving a better sensitivity to breaches particularly when combined with pulsed integrity monitoring. An isolated sensor holder will be required on each permeate tube to make this feasible.

Conductivity probing is a commonly used method to determine the location of a breach within a PV. The probing process involves sampling permeate from along the permeate tube using a pipe inserted into the said tube. Any abrupt change in EC would indicate an integrity breach. By calculating where within the PV the sample is being taken from, an operator can determine whether the leak is from a connector or from the membrane element. It is recommended that such a process is carried out periodically or as required on a PV where a breach is suspected.

7.4 Discussion

The Membrane Filtration Guidance Manual (US EPA, 2005) states that continuous monitoring of RO integrity is required. As mentioned in the introduction, although RO and NF membranes typically achieve a significantly higher level of performance, measuring removal above 2-log units remains difficult using EC. And although adding a slug of high conductivity water increases the sensitivity of the EC sensor to detect a breach, it actually reduces the log units from 1.64 at a feed conductivity of 1000 µS/cm to 1.28 at a feed conductivity of 12,000 µS/cm. Therefore, if log removal remains the principal objective in measuring membrane integrity, other online methods or strategies such 3D Trasar Technology or Mem Shield should be applied. Although the capital and operation cost of operating such monitoring methods can be justified for large water reclamation schemes, it may be more difficult for smaller schemes where it is already hard to recover the O&M cost of operating a membrane system. The challenge is that smaller water reclamation schemes still require an online method for monitoring membrane integrity. The three-step strategy being proposed can be employed separately or else combined in a step wise manner.

Table 7-2 below gives an overview of the practicalities involved in the method together with an approximation of the improved sensitivity when employing the described strategies for the simulated two stage RO system described in section 7.2. The table shows that a flow of between 0.9 – 1.4 mL/hour could be detected when combining the methods which would approximate to an aperture diameter of between 2 and 4 µm for a system operating at a feed pressure of 16 bar.

In reality, this smallest detectable flow is likely to be 4-5 times higher than this because of the error in the reading, sensor drift and the fact that it would be very difficult to distinguish between changes of 0.01 μS/cm which is the detectable change in EC reading utilising in this work to obtain the smallest detectable flow.

Table 7-2: Three step strategy for improved integrity monitoring using EC sensors

Strategy	Hardware	Monitoring and Control	Improvement in integrity monitoring*
Individual tree EC monitoring and comparison	Additional EC sensors for individual PV trees, ideally one EC sensor per tree of 6-8 PVs Hardware to connect additional EC sensors to PLC	Logging permeate EC reading every 30 – 60 seconds, or average reading over a minute for every EC sensor Comparison of data between trees fed with the same high-pressure pump, and logging of values and time when difference exceeds an operator defined threshold Alarm when difference exceeds user defined/set limits	Smallest detectable flow of water (with EC sensor / 33 PVs) First element/Last element in two stage system (element 12): 891 / 264 mL/hr Smallest detectable flow of water (with EC sensor / 6 PVs) First element/Last element in two stage system (element 12): 161 / 45 mL/hr
Pulsed integrity monitoring	High pressure, high flow peristaltic dosing pump dosing just prior to high pressure pump The preparation of predetermine concentration of high salinity solution having an osmotic pressure below the operating feed pressure	Logging permeate EC reading every second over a period of 60 seconds for every EC sensor located within the train (i.e. fed by the same feed pump) Comparison of data over the 60 second period between trees fed with the same high-pressure pump, and logging of values and time when difference exceeds an operator defined threshold Alarm when difference exceeds user defined/set limits	Smallest detectable flow of water (with EC sensor / 33 PVs) First element/Last element in two stage system (element 12) with pulsed integrity monitoring: 44 / 30 mL/hr Smallest detectable flow of water (with EC sensor / 6 PVs): First element/Last element in two stage system (element 12) with pulsed integrity monitoring: 8 / 6 mL/hr
Simultaneous individual PV monitoring	Sensor holder on each PV permeate tube with ball valve to isolate sensor Set of 6 EC sensors (or number equal to PVs in a tree). Hardware to connect additional EC sensors to PLC Manual installation of set of EC sensors moved and installed from one tree to another	Identical to above, either logging EC readings every 30-60 seconds if under normal conditions, or logging EC readings every second for one minute if utilised in connection with pulsed in integrity monitoring.	Smallest detectable flow of water (with EC sensor / PV) First element/Last element in two stage system (element 12) **without** pulsed integrity monitoring: 27 / 8 mL/hr Smallest detectable flow of water (with EC sensor / PV) First element/Last element in two stage system (element 12) **with** pulsed integrity monitoring: 1.4 / 0.9 mL/hr

*Assumptions for improvements in integrity measurements: Initial number of PVs per EC sensor = 33, Number of PVs per EC sensor after retrofit = 6, Feed water salinity of 1000 mg/L, Operating pressure of 16 bar, High salinity slug of 8000 mg/L, smallest detectable flow assumed to be change in EC of 0.01 µS/cm.

7.5 Conclusion

The objective of this work was to show that more can be done in terms of integrity monitoring utilising a sensor which operators of RO/NF facilities are already familiar with, which if developed further would allow the creation of an 'open-source' standard method for improved integrity monitoring in smaller water reclamation facilities using RO/NF membranes. Which of the mentioned strategies would be best suited for implementation will very much depend on the system configuration, feedwater quality, membrane type, operating conditions and whether the integrity monitoring system is being retrofitted or is a being designed for a new installation.

As explained in the introduction, the multiple barrier concept is based on the principle of establishing a series of barriers to preclude the passage of microbial pathogens and harmful chemical constituents into the product water. For this reason, the EC integrity monitoring method proposed will be one of a number of online monitoring techniques within the IMS system, which as a minimum will also include the online monitoring of turbidity of the MBR (or MF/UF) permeate together with free chlorine residual in the disinfected permeate and/or transmissivity monitoring if UV disinfection is employed. These online methods must also be complemented with regular sampling and analysis for both microbial and chemical constituents of concern on a regular basis both as part of the initial system validation procedure, but also throughout operation.

Using a combination of these methods together with processing of the data in real time will allow continuous characterisation of process integrity to ensure the safety of the produced reclaimed water.

Chapter 8 - Discussion

This chapter seeks to bring together the knowledge presented in the four results chapters and obtained while operating the pilot facilities to propose a conceptual framework for the integration of expert knowledge into a knowledge-based decision support system.

8.1 Introduction

The objective of this final chapter is to show how the knowledge obtained while operating the pilot facilities and documented in the four preceding results chapters (removal of PhAC and their human metabolites, the control of NDMA precursors, RO process optimisation and EC integrity monitoring), together with other knowledge available in the literature or other expert knowledge can be integrated into a knowledge-based decision support system (KB-DSS). The system would integrate signals from a variety of typically available process and water quality sensors throughout the IMS together with offline data (namely results from laboratory analysis) which after processing, provides different levels of alerts and control actions. The KB-DSS is proposed to have two distinct components:

- IMS integrity module - Process integrity component utilising the work carried out in Chapter 4, 5, 7 together with the critical control points/operational monitoring as prescribed in water reclamation guidelines.
- IMS performance module –RO/NF performance utilising the work carried out in Chapter 6 together with work carried out by other authors

Currently the majority of IMS facilities operate using an 'open-loop' configuration using pre-defined or fixed process conditions which are modified by process engineers periodically as the need arises. A knowledge-based system is a computer program that emulates human expert reasoning processes when making decisions to confront problems (Comas et al., 2010).

The aim of this system will be the ability to automatically provide an online continuous record of system reliability to system operators and public health regulators integrating historical water quality data, instrument performance, maintenance data and system performance data to immediately detect quality and treatment variances as they occur, withholding product water from being discharged into the receiving network whilst providing decision aids to system operators in real time. The development of this knowledge-based system that integrates various sensors for timely feedback of high priority alerts, signalling deviations from defined water quality and operational parameters within the treatment process, is complex because of the intrinsic potential instability of sensor and process data, the uncertainty associated with information/knowledge, and the heterogeneity and quantity and quality of data. The objective of this chapter is to show how a KB-DSS can be developed as a tool for:

- reclaimed water providers to instil confidence in the continuous reliability and robustness of the multi-barrier process of which the membranes are essential components both to public health

regulators as well as the public in general, particularly where potable reclamation schemes are planned; and

- plant operators to optimize energy use and thus reduce the total cost of reclaimed water while ensuring the reliability of the membrane (and non-membrane) barriers within the process.

8.2 Architecture of knowledge-based DSS

The architecture of the DSS is based on three levels: data acquisition and validation (bottom level), reasoning and diagnosis/control (mid-level) and decision support (top-level). The overall framework of the DSS for IMS is shown in Figure 8-1 below.

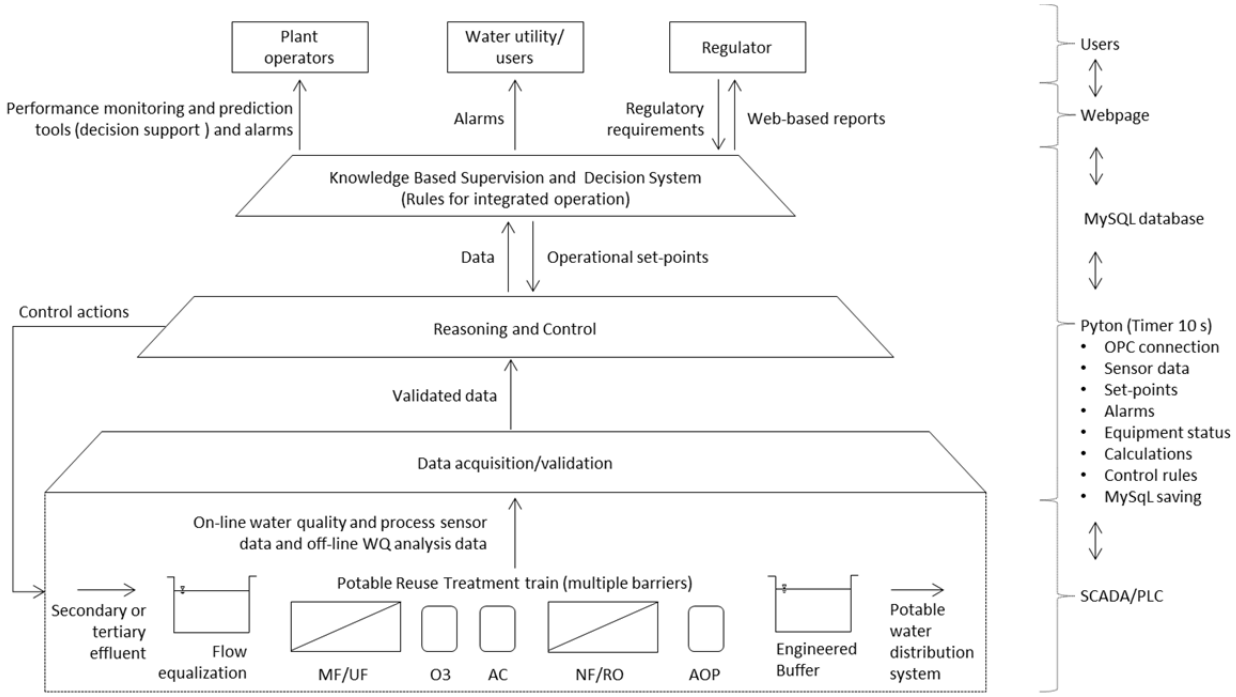

Figure 8-1: Architecture of the proposed knowledge-based control system, together with the applied components making up the knowledge-based system on the right side of the figure.

8.2.1 Data acquisition and validation level

The layer which interfaces directly with the hardware is the data acquisition and validation layer. Data acquisition is typically carried out using the SCADA/PLC system which continuously monitors and logs the data from the water quality sensors, process sensors as well as signals from the equipment such as VFDs (found on pumps and blowers) or actuated valves. This level will include three other important components: data validation, integration of offline data and instantaneous computation of monitoring parameters used to characterise a process. Table 8-1 provides an indicative list of the parameters which the data acquisition system will process. These include parameters for the MBR and RO/NF processes described in this work, as well as other critical control points as part of the multi-barrier treatment train (briefly in Chapter 1), which should be included in such a KB-DSS to comply with the monitoring requirements of critical control points as stated in numerous international guidelines for wastewater reclamation for various applications (JRC, 2017; NRMMC-EPHC-AHMC, 2006; USEPA, 2012; WHO, 2006).

Table 8-1: Indicative list of operational data for treatment processes making up a typical wastewater reclamation process to be included in the data acquisition and validation level (adapted from JRC, 2017; NRMMC-EPHC-AHMC, 2006; USEPA, 2012; WHO, 2006)

Treatment process	Operational data[1]	Frequency[3]	Monitoring	
			Process Integrity	Process Performance
Secondary Treatment process (Including MBR)	Flow rate (water, sludge wasting, internal recycles)	Online	CEC	Yes
	Dissolved oxygen (P)	Online	NDMA	Yes
	pH (P)	Online		Yes
	Temperature (P)	Online		Yes
	MLSS (P), MLSS characteristics	Online or offline (daily)	CEC, NDMA	Yes
	Total Nitrogen, Nitrate, Nitrite, (E)	Online or offline (daily/weekly)	NDMA	Yes
	Phosphorous (E)	Online or offline (daily/weekly)		Yes
	COD / BOD_5 (E)	Online or offline (daily/weekly)		Yes
MF/UF (Including MBR)	Permeate flow rate	Online		Yes
	TMP	Online	Membrane integrity	Yes
	Membrane aeration flow rate	Online	NDMA	Yes
	Turbidity (E)	Online	Membrane integrity	Yes
RO/NF (Each train requiring separate set of sensors)	Flow rate (I), (E)	Online		Yes
	Pressure (I)	Online		Yes
	Temperature (I)	Online		Yes
	EC (I), (E)	Online	Yes	Yes
	pH (I), (E)	Online		Yes
	Individual ionic constituents[2] (I), (E)	Offline (daily/weekly)	Yes	Yes
	TOC (E)	Online	Yes	Yes
UV disinfection / AOP	Flow rate (I)	Online	Yes	
	Turbidity (I)	Online	Yes	Yes
	UV intensity (P)	Online	Yes	

	UV transmissivity (I/P)	Online	Yes	Yes
Chlorination	Free chlorine residual (E)	Online	Yes	Yes
	pH (I)	Online	Yes	Yes
	Temperature (I)	Online	Yes	Yes
	Flow rate (I)	Online	Yes	Yes

[1] Sampling point / sensor location: Process influent/feed (I), Process effluent/permeate (E), Within process tank (P)
[2] Individual ionic constituents including; calcium (Ca2+), magnesium (Mg2+), sodium (Na+), potassium (K+) and anions; chloride (Cl-), sulphate (SO42), phosphate (P-PO43-) and bicarbonate (HCO3-).
[3] Frequency depends on the capacity of the reclamation facility

Another important component of the data acquisition system is the integration of offline analysis including laboratory data as well as other analysis results including tests typically carried out to characterise the MLSS such as settling volume or filterability for MBR or SDI for the RO/NF process. These will be input through a web interface by laboratory or plant personnel directly into a database repository (MqSQL) as part of the KB-DSS through a web-based portal. Sensor data may be used by more than one monitoring process. For example, EC in the feed and permeate streams of the RO/NF process will firstly be used for the monitoring of membrane performance through the trending of normalised salt rejection together and fouling potential of the feedwater at a given feedwater temperature and system recovery, but also be used in the integrity monitoring procedures as described in Chapter 7 and further discussed below.

Data validation will include noise reduction and the removal of outliers before being passed on to the next level where decisions will be taken, and control actions actuated. Various instantaneous sensor data will be used to derive monitoring parameters which will be logged every 10 seconds in the dynamic database (MySQL) and then filtered and hourly and daily averages calculated and registered. The data filtering process will involve the removal of values during downtime cycles such as during back-flushing, chemical cleanings or start-up periods. This will be done by excluding values within a significant range around the median (for example values > or < 50 % of the median) and finally a new average of the filtered values is recalculated and logged.

Monitoring parameters are those which will be utilised to detect changes in trends to provide real time information about process integrity and process performance.

Table 8-2 below provides a list of such monitoring parameters together with the information required from Table 8-1 to calculate these values.

Table 8-2: List of monitoring parameters by treatment process

Treatment process	Monitoring parameter	Data Required
Secondary treatment (incl. MBR)	COD & BOD removal, N removal, P removal, SS removal (Regulated parameters)	Influent and effluent: NH_4^+, TKN, NO_2^-, NO_3^-, PO_4^{3-}, COD & BOD, Suspended solids
	HRT, SRT	Water, Sludge, Recycles: Flow rate
MF/UF (incl. MBR)	Permeability	MBR Permeate: flow rate, MBR TMP
	TMP	MBR TMP
	Specific Aeration Demand	MBR Membrane: air flow rate
	Specific cost of secondary/tertiary treated water	Transfer pumps: power consumption, or flow rate and pressure Blowers: power consumption or flow rate and pressure
NF/RO	System Recovery	RO/NF Feedwater: Flowrate, RO Permeate: Flowrate
	Flux	RO/ NF Permeate: Flowrate
	Average and Standard deviation of Permeate EC (integrity)	RO/NF Permeate: EC (each tree)
	Normalised salt rejection	RO/NF Feedwater: EC, T, pH, pressure and flowrate
	Normalised permeate flow	RO/NF Permeate: EC, flowrate
	Fouling potential ($Ca_3(PO_4)_2$ stability index)	Secondary Effluent: PO_4^{3-} RO/NF Feedwater: EC, T, pH, offline ionic composition System recovery
	Fouling potential ($CaCO_3$ LSI)	RO/NF Feedwater: EC, T, pH, offline ionic composition System recovery
	Specific cost of water	Pumps: power consumption, or flow rate and pressure Permeate: Flow rate
UV /AOP	UV dose	Influent: Transmissivity, Flowrate, UV lamp: intensity
Chlorination	C*t	Influent/Effluent: Flowrate Effluent: Residual free chlorine

8.2.2 Reasoning and control level

The reasoning and control system utilises operational monitoring data (listed in Table 8-1) and monitoring parameters (listed in Table 8.2) as well as combinations of the two to obtain control actions from the rule-base. The rule-base is composed of a number of modules including the system integrity (critical control point) monitoring module, together with the MBR performance module and the RO performance module. Figure 8-4 provides three components as part of the system integrity monitoring module which are dealt with in this thesis and described further below. The rule-base included in the reasoning and control level in terms of system integrity will depend on the water reclamation application, with threshold limits defined by regulatory authorities.

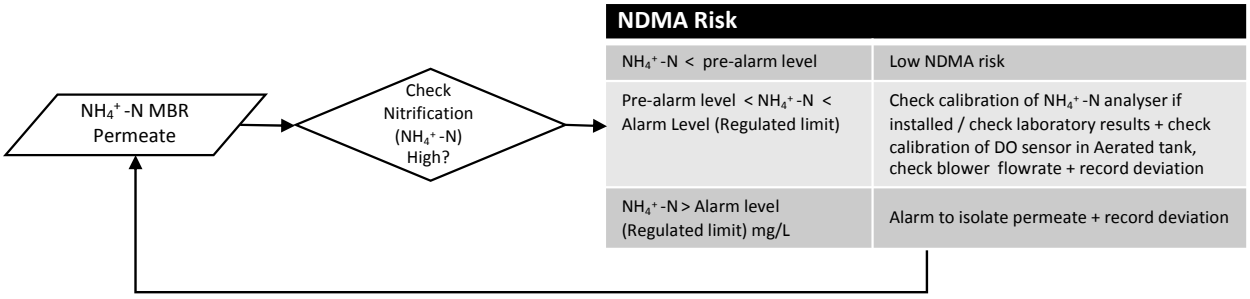

Figure 8-2: System Integrity Monitoring Module - NDMA risk

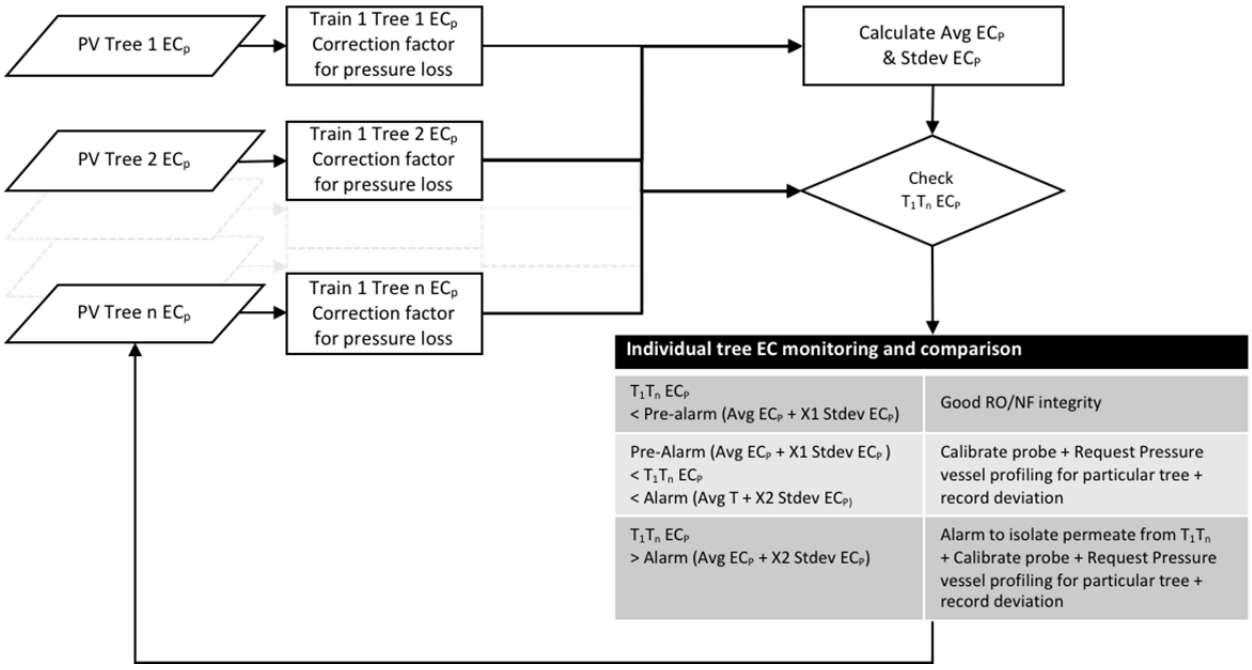

Figure 8-3: System Integrity Monitoring Module (b) Individual tree EC monitoring and comparison for single train supplied by a single high-pressure pump made up of a number of individual PV trees (n). Avg: Average, Stdev: Standard deviation, X1, X2: user defined constants.

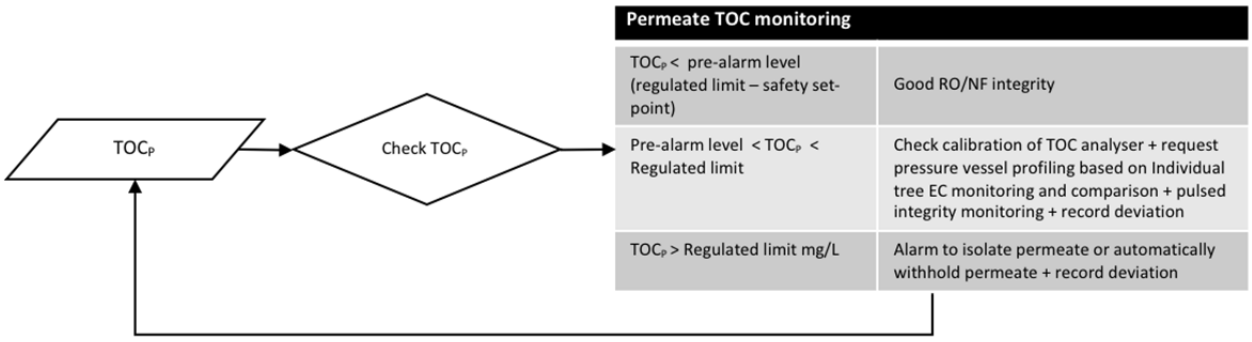

Figure 8-4: Permeate TOC monitoring on combined permeate stream.

The first component showed in Figure 8-4 deals with the removal of NDMA precursors by the MBR process. As concluded in Chapter 5, complete nitrification is an essential treatment step in ensuring a certain removal of NDMA precursors by the MBR treatment. For this reason, the concentration of NH_4^+ in the MBR permeate, whether measured by an online analyser or measured daily (or weekly) in the laboratory and then entered into the knowledge based-DSS, is included as an indicator to monitor the risk of NDMA exceeding regulated limits. The rule base described in Figure 8-4 provides three options: if the measured value is below a pre-alarm value of NH_4^+-N below a value of 0.4 mg/L

or as defined during process validation studies where NDMA formation potential is measured for a particular plant, then a time-stamped record of correct operation with regards to NDMA risk is logged. In the case that the NH_4^+-N concentration exceeds this pre-alarm values (with a safety factor applied to the threshold value), then an alarm is raised prompting the operator to firstly carry out repeat analysis in the laboratory to verify the initial results as well check the DO concentration in the aerated tank and the flow rate of the air from the blowers into the aerated tank. Exceeding the threshold value will divert product water away from recharge wells or distribution networks or shutting down the tertiary treatment processes completely until a solution to the deviation is implemented. For regulatory purposes any deviations need to be record with a time-stamp together with a prompt for the operator to input the control actions implemented to rectify the deviation.

Figure 8-3 provides a rule-base described in Chapter 7 where the EC of the permeate stream from a number of trees (groups of 6-8 PVs) fed by the same high-pressure pump is monitored continuously to generate a value for the average and standard deviation for all the permeate EC values. The permeate EC value from each tree is then compared to this pre-alarm value which would be calculated as the average value plus the standard deviation (a constant multiplied by the standard deviation) and if it exceeds this value a notification for probe calibration or value verification with a hand-held probe is requested, followed by manual PV probing to determine the location of the breach if it results that the sensor is operating correctly. If the value is higher than the alarm level (average plus a pre-set constant multiplied by the standard deviation) the water from the whole train is diverted away from the application until an operator can manually isolate the permeate from the PV tree producing questionable permeate quality.

Figure 8-4 shows a third rule monitoring the TOC concentration from an online TOC analyser taking permeate from a single train or multiple trains (the relationship between trees and trains is described in Figure 7-6). Again, the first level would be a pre-alarm level which prompts the operator to check the calibration of the TOC analyser followed by a request for PV profiling of a particular tree if the individual tree EC monitoring flags a particular tree which may have a breach. If no tree has been flagged by the individual tree EC monitoring, then the pulsed integrity monitoring procedure can be initiated (if available) to be able to detect smaller breaches and pinpoint PVs within a tree which should be further investigated with PV profiling. Finally, if the alarm concentration is exceeded then the product water is diverted away from the application until an operator can manually isolate the permeate from the PV tree producing a permeate of questionable quality.

The work presented in Chapter 4 shows how pharmaceuticals and their transformation products are removed through the membrane treatment process to produce a product with very low concentrations of these compounds. Although these compounds cannot be directly measured using

online sensors, surrogate parameters can be continuously monitored to characterise the operation of the processes making up the treatment train to be able to detect any changes to the process configuration which will be validated for the removal of CEC. Apart from the use of individual tree EC monitoring and comparison and the measurement of TOC in the permeate of the RO process as previously described, other parameters such as the flowrate of water and sludge through the secondary treatment process would be continuously monitored and logged (as listed in Table 8.1 and Table 8.2) to ensure that the HRT and SRT remain unchanged from those utilised in the process validation processes, and revalidation of the process will have to be carried out if any of the parameters are changed significantly. Other parameters to characterise the process such as the DO concentration in aerobic and anaerobic tanks together with online and offline sludge characteristics should all be included in such an integrity monitoring log to be able to show that the process is running with similar conditions to those when system integrity validation was carried out.

Although Figure 8-4 provides an example rule-base considering only NDMA risk, individual tree EC monitoring and comparison and permeate TOC monitoring, Table 8.1 and Table 8.2 provide a list of other critical control points which have been included in various water reclamation guidelines which could be converted into a comprehensive rule-base covering all processes making up the treatment train as is already done for individual processes to be able to redirect product water or shut down the process completely should the risk of delivering non-conforming water increase. For example, typically MF or UF membranes in drinking water treatment are tested daily using a pressure decay test that would detect the presence of breaches smaller than Cryptosporidium oocysts and Giardia cysts that MF membranes are designed to remove. UV treatment systems have a photodiode installed to ensure that designed irradiation dose is actually being supplied to inactivate pathogens. Chlorine disinfection is typically monitored using continuous measurement of residual free chlorine after a determined contact time. As previously mentioned a key component of such a system is a continuous record of deviations from validated process procedures.

The reasoning and control system may also have a separate module containing a rule-base for the optimisation of the RO process in terms of energy use and pre-treatment dosing to achieve the lowest water cost while controlling membrane fouling as described in section 6.4.2. As described in Chapter 6, the reasoning and control level will utilise operational data and monitoring data (Table 8.1 and Table 8.2) to adjust process parameters according to the quality of the influent water.

The reasoning and control system should also include a number of modules related to the performance of the MBR process based on previously published work including:

- Online monitoring of membrane fouling in submerged MBR (Monclús et al., 2011)

- Development of a control algorithm for air-scour reduction in membrane bioreactors for wastewater treatment (Ferrero et al., 2011; Monclús et al., 2015)
- Development of a decision tree for the integrated operation of nutrient removal MBRs based on simulation studies and expert knowledge (Dalmau et al., 2013)
- Development and validation of knowledge-based module for start-up operation using flat-sheet membrane bioreactor (Monclús et al., 2012)
- Knowledge-based system for automatic MBR control (Comas et al., 2010).

8.2.3 Knowledge based supervision and decision support Level

The knowledge-based (KB) supervision and decision support level is located at the top of the KB-DSS architecture presented in Figure 8-1. The function of this level is to supervise the control actions being proposed by the various modules making up the reasoning and control level. As suggested in Figure 8-1, this rule-base will supervise the integrated operation of the different processes making up the complete treatment train. Based on the data received from the data acquisition and validation level, the KB-supervision layer will provide specific alerts to the various users (as described in more detail in the following section). Alerts can either be either routine alerts, such as performance monitoring and prediction tools and alarms to operators or process integrity reports to regulators, or deviation/emergency alerts when either the performance or integrity of the system is non-compliant.

This supervision layer may also warn the user, deactivate the knowledge based control system by putting the system in a 'safe-mode' or withhold distribution of product water when encountering operational abnormalities such as system start-up periods, mechanical malfunctions, influent temperature, EC or pH out of range, poor biological nutrient removal, micro-biology related problems or bad sludge filterability (Comas et al., 2010).

The identification of these operational abnormalities may require the modification of set-point changes within one or more rule-bases. Ultimately the objective of the KB-supervision system is to oversee the integrated control of all the treatment processes and therefore any change in one of the treatment processes making up the treatment train resulting in the change in the quality of the water output and how this will affect subsequent processes needs to be considered at this level. This will also involve prioritising certain control actions over others. An example of such an overarching rule could be minimising of energy use by controlling air scour of submerged membranes in relation to the nitrifying performance of the biological nutrient removal processes and the affect this has on the removal of CECs, particularly the removal of precursors of NDMA.

8.3 KB-DSS as a tool to meet the EU's Regulation on minimum requirements for water reuse

According to the recently published Regulation of the European Parliament and of the Council on minimum requirements for water reuse (2018/0169):

> *Transparency and access to information is a critical aspect for promoting trust among users and also the general public as regards the safety of reclaimed water. Thus, emphasis has been made on providing information to the public instead of traditional reporting obligations.*
>
> (European Commission, 2018).

For this reason, the top-most level of the KB-DSS, the knowledge-based supervision and decision system (shown in Figure 8-1) is utilised as a link to various users of the information which is continuously generated and stored when monitoring the integrity and performance of the reclaimed water system. The use of such a KB-DSS for the timely transfer of information to stakeholders and users of the system whilst minimising the administrative burden of online reporting through the use of indicator-based reports to 'ensure transparency and accountability vis-à-vis citizens can help reach the objectives of the new European Regulation.

In practical terms this will be achieved by providing performance and integrity monitoring and prediction reports and alarms to the operator of the reclamation facility. To ensure transparency and accountability with external stakeholders such as the water utility distributing the reused water, the end user as well as the public health regulator, alarms or warnings can be provided directly by the system when the integrity of the system could be compromised through web-based reports or other 'modern ICT tools.

Other than ensuring transparency and accountability, the KB-DSS for IMS can also contribute to two other key components in the European Commission's minimum requirements for water reuse

- Water Reuse Risk Management Plan (Article 5)
- and reclamation process validation monitoring as a component of compliance with the minimum requirements and any additional conditions set by the competent authority. Validation monitoring has to be performed before the reclamation plant is put into operation, when equipment is upgraded, and when new equipment or processes are added (European Commission, 2018).

In a risk management plan an operator must 'ensure adequate quality control systems and procedures are in place'. This is typically carried out through the use of critical control points. The

use of a real-time KB-DSS can ensure that (1) prescribed critical-control points are observed, (2) verifiable actions were taken in the event of non-compliance and (3) timely communication with the competent authority and the end user(s) was carried out.

Validation monitoring aims to ensure that processes and procedures control hazards effectively and that the water reclamation system is capable of meeting its design requirements. Validation involves evaluating available scientific and technical information and, where necessary, undertaking investigations to validate system specific operational procedures, critical limits and target criteria. Utilising a KB-DSS will alert and record any deviations in process performance from those defined during the validation procedures.

Chapter 9 - Conclusion

The following chapter presents the main conclusions of the work together with ideas to build on the work presented in this thesis.

The following are the conclusions from each of the main chapters of the work:

Chapter 4 compared the removal of selected PhACs, metabolites and their TPs through MBR-RO and MBR-NF processes treating real wastewater to understand the extent of the difference in the rejection of such compounds when using low pressure NF membranes in the place of RO membranes. The results showed that the two consecutive membrane processes, when seen as a whole, become a highly efficient process to remove all the studied compounds, generating a highly concentrate stream which would require further treatment processes before being discharged into the natural environment. When comparing the removal efficiencies of the RO and NF membranes, as expected, the RO membrane showed near complete removals (>99%) of all the compounds over various process conditions, whereas the NF membrane resulted also in high removal efficiencies (> 90%).

Chapter 5 investigated the removal of NDMA FP and individual NDMA precursors by an MBR pilot plant that treats urban wastewater. In particular, changes in the percentage of removal due to the variation of nitrifying and non-nitrifying conditions of the MBR were studied. During normal aerobic operation, implying a fully nitrifying system, the MBR pilot plant was able to reduce NDMA formation potential above 94%, however this removal percentage was reduced to values as low as 72% when changing the conditions to avoid nitrification. These results suggest that a fully nitrifying MBR system will support better removal of NDMA precursors during wastewater reclamation. High removal for both NDMA FP (>90%) and individual NDMA precursors (>94%) was observed. Within the frame of the experiment duration (four months) this high removal was independent of the nitrifying conditions of the MBR and operating settings of NF system, showing that NF can be regarded as a reasonably independent barrier for NDMA precursors even when the nitrification in MBR could not be fully accomplished. However, the NDMA FP measured in the NF permeate was in many cases above 100 ng/L, which is above the regulation set for NDMA itself for potable water reclamation in countries such as U.S.A. and Australia.

Chapter 6 showed that although there are limitations to the use of EC as a main parameter to deduce the individual ionic constituents in a wastewater, given the right assumptions, the work has shown that it is possible to obtain a useful profile for a particular EC value which could be used in an online / real-time optimisation system. The work also suggests how other online and offline water quality data could be incorporated to obtain a more accurate instantaneous water quality profile. Through the presentation of a case considering the cost of energy and pre-treatment chemicals, the work showed that there is scope for online optimisation tool in terms of associating a cost to the current operating process conditions and then questioning whether there is a more cost-effective way to ‘set’ the system. Industry standard RO simulation software which is available from all

membrane manufacturers was proposed as an offline method of developing a series of simulations whose results are used in creating rules for the online optimisation system. The offline RO simulation software was chosen as method which can be understood, and the results conceptualised by plant operators. A preliminary decision tree for online system optimisation was presented.

Chapter 7 showed that more can be done in terms of integrity monitoring utilising a sensor which operators of RO facilities are already familiar with, which if developed further would allow the creation of an 'open-source' standard method for improved integrity monitoring in smaller water reclamation facilities using RO/NF membranes. Which of the mentioned strategies would be best suited for implementation will very much depend on the system configuration, feedwater quality, membrane type, operating conditions and whether the integrity monitoring system is being retrofitted or is a being designed for a new installation.

Finally, Chapter 8 provides a framework together with an initial rule-base as part of a knowledge-based decision support system to be further developed with results from previous studies and validated on an operating IMS facility to satisfy the initial hypothesis of the thesis given in Chapter 3:

Integrated membrane systems for wastewater reclamation can be operated with a high level of confidence with regards to membrane integrity, process reliability and performance optimisation by utilising real time detection of water quality fluctuations and treatment process condition deviations which can be processed to make real-time critical process decisions to ensure the safety of reclaimed water delivered to customers while optimising process performance.

Chapter 10 - References

The following is a list of references utilised throughout this thesis.

(NWRI), J.C., 2010. Regulatory Aspects of Direct Potable Reuse in California. Natl. Water Res. Inst. White Pap.

Abbas, A., 2005. Simulation and analysis of an industrial water desalination plant 44, 999–1004. https://doi.org/10.1016/j.cep.2004.12.001

Alahmad, M., 2010. Prediction of performance of seawater reverse osmosis units. Desalination 261, 131–137.

Alatiqi, I.M., Ghabris, A.H., Ebrahim, S., 1989. System identification and control of reverse osmosis desalination. Desalination 75, 119–140.

AlGhusain, I., 2013. The Sulaibiya Wastewater Treatment and Reclamation Plant, in: 6th Zayed Seminar, Green Economy, Manama, May 2013.

Alturki, A.A., Tadkaew, N., McDonald, J. a., Khan, S.J., Price, W.E., Nghiem, L.D., 2010. Combining MBR and NF/RO membrane filtration for the removal of trace organics in indirect potable water reuse applications. J. Memb. Sci. 365, 206–215. https://doi.org/10.1016/j.memsci.2010.09.008

ASTM, n.d. ASTM D3739-88 Calculation and Adjustment of the Langelier Saturation Index for Reverse Osmosis.

Bartels, C., Franks, R., Andes, K., n.d. Operational Performance and Optimization of RO Wastewater Treatment Plants. Hydranautics 1–12.

Bartels, C.R., Wilf, M., Andes, K., Iong, J., 2005. Design considerations for wastewater treatment by reverse osmosis. Water Sci. Technol. 51, 473–482.

Bartman, A.R., Zhu, A., Christofides, P.D., Cohen, Y., 2010. Minimizing energy consumption in reverse osmosis membrane desalination using optimization-based control. J. Process Control 20, 1261–1269. https://doi.org/10.1016/j.jprocont.2010.09.004

Batt, A.L., Kim, S., Aga, D.S., 2006. Enhanced Biodegradation of Iopromide and Trimethoprim in Nitrifying Activated Sludge. Environ. Sci. Technol. 40, 7367–7373. https://doi.org/10.1021/es060835v

Bellona, C., Drewes, J.E., 2007. Viability of a low-pressure nanofilter in treating recycled water for water reuse applications: A pilot-scale study. Water Res. 41, 3948–3958. https://doi.org/10.1016/j.watres.2007.05.027

Bellona, C., Drewes, J.E., Xu, P., Amy, G., 2004. Factors affecting the rejection of organic solutes during NF/RO treatment - A literature review. Water Res. 38, 2795–2809. https://doi.org/10.1016/j.watres.2004.03.034

Bellona, C., Heil, D., Yu, C., Fu, P., Drewes, J.E., 2012. The pros and cons of using nanofiltration in lieu of reverse osmosis for indirect potable reuse applications. Sep. Purif. Technol. 85, 69–76. https://doi.org/10.1016/j.seppur.2011.09.046

Bérubé, P., 2010. Membrane bioreactors: Theory and applications to wastewater reuse. Sustain. Sci. Eng. 2, 255–292. https://doi.org/10.1016/S1871-2711(09)00209-8

Bond, T., Huang, J., Templeton, M.R., Graham, N., 2011. Occurrence and control of nitrogenous disinfection by-products in drinking water – A review. Water Res. 45, 4341–4354. https://doi.org/https://doi.org/10.1016/j.watres.2011.05.034

Bonté, S. Le, Pons, M.-N., Potier, O., Rocklin, P., 2008. Relation Between Conductivity and Ion Content in Urban Wastewater. J. Watr Sci. 21, 429–438. https://doi.org/10.7202/019165ar

Brouwer, S., Maas, T., Smith, H., Frijns, J., 2015. D5.2 Trust in Water Reuse Review report on international experiences in public involvement and stakeholder collaboration.

Cartagena, P., Kaddouri, M. El, Cases, V., Trapote, A., Prats, D., 2013. Reduction of emerging micropollutants , organic matter , nutrients and salinity from real wastewater by combined MBR – NF / RO treatment. Sep. Purif. Technol. 110, 132–143. https://doi.org/10.1016/j.seppur.2013.03.024

Chen, W.-H., Young, T.M., 2008. NDMA Formation during Chlorination and Chloramination of Aqueous Diuron Solutions. Environ. Sci. Technol. 42, 1072–1077. https://doi.org/10.1021/es072044e

Cheng, L., Zhang, T., Vo, H., Diaz, D., Quanrud, D., Arnold, R., 2017. Effectiveness of engineered and natural wastewater treatment processes for the removal of trace organics in water reuse. J Env. Eng 143.

Chesters, S.P., del Vigo, F., Darton, E.G., 2007. Theoretical and practical experience of calcium phosphate inhibition in RO waters., in: IDA World Congress-Maspalomas,Gran Canaria –Spain October 21-26, 2007.

Choi, J., Valentine, R.L., 2002. Formation of N-nitrosodimethylamine (NDMA) from reaction of monochloramine: A new disinfection by-product. Water Res. 36, 817–824. https://doi.org/10.1016/S0043-1354(01)00303-7

Chon, K., Sarp, S., Lee, S., Lee, J.H., Lopez-Ramirez, J. a., Cho, J., 2011. Evaluation of a membrane bioreactor and nanofiltration for municipal wastewater reclamation: Trace contaminant control and fouling mitigation. Desalination 272, 128–134. https://doi.org/10.1016/j.desal.2011.01.002

Clara, M., Strenn, B., Gans, O., Martinez, E., Kreuzinger, N., Kroiss, H., 2005. Removal of selected pharmaceuticals, fragrances and endocrine disrupting compounds in a membrane bioreactor and conventional wastewater treatment plants. Water Res. 39, 4797–4807. https://doi.org/10.1016/j.watres.2005.09.015

Comas, J., Meabe, E., Sancho, L., Ferrero, G., Simpa, J., Monclus, H., Rodriguez-Roda, I., 2010. Knowledge-based system for automatic MBR control. Water Sci. Technol. 62, 2829–2836.

Côté, P., Masini, M., Mourato, D., 2004. Comparison of membrane options for water reuse and reclamation. Desalination 167, 1–11. https://doi.org/10.1016/j.desal.2004.06.105

Daigger, G.T., Hodgkinson, A., Skeels, P., Smith, J., Lozier, J., Fries, K., 2015. Full-scale experience with the membrane bioreactor-reverse osmosis water reclamation process. J. Water Reuse Desalin. jwrd2015178. https://doi.org/10.2166/wrd.2015.178

Dalmau Figueras, M., 2014. Integrated operation of membrane bioreactors: simulation and experimental studies.

Dalmau, M., Monclús, H., Gabarrón, S., Rodriguez-roda, I., Comas, J., 2014. Bioresource Technology Towards integrated operation of membrane bioreactors : Effects of aeration on biological and filtration performance. Bioresour. Technol. 171, 103–112. https://doi.org/10.1016/j.biortech.2014.08.031

Dalmau, M., Rodriguez-Roda, I., Ayesa, E., Odriozola, J., Sancho, L., Comas, J., 2013. Development of a decision tree for the integrated operation of nutrient removal MBRs based on simulation studies and expert knowledge. Chem. Eng. J. 217, 174–184. https://doi.org/10.1016/j.cej.2012.11.060

Dialynas, E., Diamadopoulos, E., 2009. Integration of a membrane bioreactor coupled with reverse osmosis for advanced treatment of municipal wastewater. Desalination 238, 302–311. https://doi.org/10.1016/j.desal.2008.01.046

Dolar, D., Gros, M., Rodriguez-Mozaz, S., Moreno, J., Comas, J., Rodriguez-Roda, I., Barceló, D., 2012. Removal of emerging contaminants from municipal wastewater with an integrated membrane

system, MBR-RO. J. Hazard. Mater. 239–240, 64–69. https://doi.org/10.1016/j.jhazmat.2012.03.029

Dotson, A., Westerhoff, P., Krasner, S.W., 2009. Nitrogen enriched dissolved organic matter (DOM) isolates and their affinity to form emerging disinfection by-products. Water Sci. Technol. 60, 135 LP-143.

Dow Water & Process Solutions, 1995. FILMTEC™ Reverse Osmosis Membranes Technical Manual.

Drewes, J.E., Anderson, P., Denslow, N., Olivieri, A., Schlenk, D., Snyder, S.A., Maruya, K.A., 2013. Designing monitoring programs for chemicals of emerging concern in potable reuse - what to include and what not to include? Water Sci. Technol. 67, 433–439.

Drewes, J.E., Hübner, U., Zhiteneva, V., Karakurt, S., 2017. Characterization of unplanned water reuse in the EU.

Dytczak, M.A., Londry, K.L., Oleszkiewicz, J.A., 2008. Biotransformation of estrogens in nitrifying activated sludge under aerobic and alternating anoxic/aerobic conditions. Water Environ. Res. 80, 47–52.

Eaton, A.D., Franson, M.A.H., Association, A.P.H., Association, A.W.W., Federation, W.E., 2005. Standard Methods for the Examination of Water & Wastewater, Standard Methods for the Examination of Water and Wastewater. American Public Health Association.

Eichhorn, P., Aga, D.S., 2004. Identification of a Photooxygenation Product of Chlortetracycline in Hog Lagoons Using LC/ESI-Ion Trap-MS and LC/ESI-Time-of-Flight-MS. Anal. Chem. 76, 6002–6011. https://doi.org/10.1021/ac0494127

EPA, 2017. Technical Fact Sheet – N-Nitroso-dimethylamine (NDMA) EPA 505-F-.

EPA, n.d. Integrated Risk Information System [WWW Document]. Environ. Prot. Agency, Off. Res. Dev. Natl. Cent. Environ. Assess. URL http://www.epa.gov/ngispgm3/iris/search.htm.

Epa, U.S., 2005. Note on the Membrane Filtration Guidance Manual. Environ. Prot.

European Commission, 2018. Regulation of the European Parlament and of the Council on minimum requirements for water reuse.

Farré, M.J., Insa, S., Mamo, J., Barceló, D., 2016. Determination of 15 N-nitrosodimethylamine precursors in different water matrices by automated on-line solid-phase extraction ultra-high-performance-liquid chromatography tandem mass spectrometry. J. Chromatogr. A. https://doi.org/10.1016/j.chroma.2016.06.064

Farré, M.J., Keller, J., Holling, N., Poussade, Y., Gernjak, W., 2011. Occurrence of N-nitrosodimethylamine precursors in wastewater treatment plant effluent and their fate during ultrafiltration-reverse osmosis membrane treatment. Water Sci. Technol. 63, 605–612. https://doi.org/10.2166/wst.2011.207

Farré, M.J., Reungoat, J., Argaud, F.X., Rattier, M., Keller, J., Gernjak, W., 2011. Fate of N-nitrosodimethylamine, trihalomethane and haloacetic acid precursors in tertiary treatment including biofiltration. Water Res. 45, 5695–5704. https://doi.org/10.1016/j.watres.2011.08.033

Fatta-Kassinos, D., Meric, S., Nikolaou, A., 2011. Pharmaceutical residues in environmental waters and wastewater: Current state of knowledge and future research. Anal. Bioanal. Chem. 399, 251–275. https://doi.org/10.1007/s00216-010-4300-9

Fernandez-Fontaina, E., Omil, F., Lema, J.M., Carballa, M., 2012. Influence of nitrifying conditions on the biodegradation and sorption of emerging micropollutants. Water Res. 46, 5434–5444. https://doi.org/10.1016/j.watres.2012.07.037

Ferrero, G., Monclus, H., Buttiglieri, G., Gabarron, S., Comas, J., Rodriguez-Roda, I., 2011. Development of an algorithm for air-scour optimization in membrane bioreactors. IFAC Proc. Vol. 44, 3795–3799. https://doi.org/https://doi.org/10.3182/20110828-6-IT-1002.02077

Fujioka, T., Kennedy, M., Amy, G., Dang, H.Q., Nghiem, L.D., Price, W.E., Sipma, J., Osuna, B., Collado, N., Monclús, H., Ferrero, G., Comas, J., Rodriguez-Roda, I., Water, H., Report, W., Steiner, J.S., Tarfusser, J.C., Yangali Quintanilla, V., Röhricht, M., Krisam, J., Weise, U., Kraus, U.R., Düring, R. a., Schäfer, a. I., Nghiem, L.D., Waite, T.D., Vergili, I., Xu, P., Bellona, C., Drewes, J.E., 2010. Removal of the natural hormone estrone from aqueous solutions using nanofiltration and reverse osmosis. J. Memb. Sci. 37, 177–187. https://doi.org/10.1021/es0102336

Fujioka, T., Khan, S.J., McDonald, J.A., Roux, A., Poussade, Y., Drewes, J.E., Nghiem, L.D., 2013a. N-nitrosamine rejection by reverse osmosis membranes: A full-scale study. Water Res. 47, 6141–6148. https://doi.org/https://doi.org/10.1016/j.watres.2013.07.035

Fujioka, T., Khan, S.J., McDonald, J.A., Roux, A., Poussade, Y., Drewes, J.E., Nghiem, L.D., 2013b. N-nitrosamine rejection by reverse osmosis membranes: A full-scale study. Water Res. 47, 6141–6148. https://doi.org/https://doi.org/10.1016/j.watres.2013.07.035

Fujioka, T., Khan, S.J., Poussade, Y., Drewes, J.E., Nghiem, L.D., 2012. N-nitrosamine removal by reverse osmosis for indirect potable water reuse - A critical review based on observations from laboratory-, pilot- and full-scale studies. Sep. Purif. Technol. 98, 503–515. https://doi.org/10.1016/j.seppur.2012.07.025

Gabarrón Fernández, S., 2014. Diagnosis, assessment and optimisation of the design and operation of municipal MBRs.

Gagne, D., 2005. The World's Largest Membrane Based Water Reuse Project. GE Water Process Technol.

García-Galán, M., Frömel, T., Müller, J., Peschka, M., Knepper, T., Díaz-Cruz, S., Barceló, D., 2012. Biodegradation studies of N 4-acetylsulfapyridine and N 4-acetylsulfamethazine in environmental water by applying mass spectrometry techniques. Anal. Bioanal. Chem. 402, 2885–2896. https://doi.org/10.1007/s00216-012-5751-y

Garcia-Galan, M.J., Anfruns, A., Gonzalez-Olmos, R., Rodriguez-Mozaz, S., Comas, J., 2016. Advanced oxidation of the antibiotic sulfapyridine by UV/H(2)O(2): Characterization of its transformation products and ecotoxicological implications. Chemosphere 147, 451–459. https://doi.org/10.1016/j.chemosphere.2015.12.108

García-Galán, M.J., Díaz-Cruz, M.S., Barceló, D., 2011. Occurrence of sulfonamide residues along the Ebro River basin: removal in wastewater treatment plants and environmental impact assessment. Environ. Int. 37, 462–73. https://doi.org/10.1016/j.envint.2010.11.011

García-Galán, M.J., Petrovic, M., Rodríguez-Mozaz, S., Barceló, D., 2016. Multiresidue trace analysis of pharmaceuticals, their human metabolites and transformation products by fully automated on-line solid-phase extraction-liquid chromatography-tandem mass spectrometry. Talanta 158, 330–341. https://doi.org/10.1016/j.talanta.2016.05.061

García Galán, M., Díaz-Cruz, M.S., Barceló, D., 2012. Removal of sulfonamide antibiotics upon conventional activated sludge and advanced membrane bioreactor treatment. Anal. Bioanal. Chem. 404, 1505–1515. https://doi.org/10.1007/s00216-012-6239-5

Garcia, N., Moreno, J., Cartmell, E., Rodriguez-Roda, I., Judd, S., 2013. The application of microfiltration-reverse osmosis/nanofiltration to trace organics removal for municipal wastewater reuse. Environ. Technol. 34, 3183–3189. https://doi.org/10.1080/09593330.2013.808244

Gasser, G., Pankratov, I., Elhanany, S., Werner, P., Gun, J., Gelman, F., Lev, O., 2012. Field and

laboratory studies of the fate and enantiomeric enrichment of venlafaxine and O-desmethylvenlafaxine under aerobic and anaerobic conditions. Chemosphere 88, 98–105. https://doi.org/10.1016/j.chemosphere.2012.02.074

Gerrity, D., Owens-Bennett, E., Venezia, T., Stanford, B.D., Plumlee, M.H., Debroux, J., Trussell, R.S., 2014. Applicability of Ozone and Biological Activated Carbon for Potable Reuse. Ozone Sci. Eng. 36, 123–137. https://doi.org/10.1080/01919512.2013.866886

Ghobeity, A., Mitsos, A., 2010. Optimal time-dependent operation of seawater reverse osmosis. Desalination 263, 76–88.

Göbel, A., McArdell, C.S., Joss, A., Siegrist, H., Giger, W., 2007. Fate of sulfonamides, macrolides, and trimethoprim in different wastewater treatment technologies. Sci. Total Environ. 372, 361–371. https://doi.org/10.1016/j.scitotenv.2006.07.039

Grebel, J.E., Young, C.C., Suffet, I.H. (Mel), 2006. Solid-phase microextraction of N-nitrosamines. J. Chromatogr. A 1117, 11–18. https://doi.org/https://doi.org/10.1016/j.chroma.2006.03.044

Greenberg, G., Hasson, D., Semiat, R., 2005. Limits of RO recovery imposed by calcium phosphate precipitation. Desalination 183, 273–288. https://doi.org/10.1016/j.desal.2005.04.026

Gros, M., Petrović, M., Ginebreda, A., Barceló, D., 2010. Removal of pharmaceuticals during wastewater treatment and environmental risk assessment using hazard indexes. Environ. Int. 36, 15–26. https://doi.org/10.1016/j.envint.2009.09.002

Gros, M., Rodriguez-Mozaz, S., Barcelo, D., 2012. Fast and comprehensive multi-residue analysis of a broad range of human and veterinary pharmaceuticals and some of their metabolites in surface and treated waters by ultra-high-performance liquid chromatography coupled to quadrupole-linear ion trap tandem. J. Chromatogr. A 1248, 104–121. https://doi.org/10.1016/j.chroma.2012.05.084

Gros, M., Rodríguez-Mozaz, S., Barceló, D., 2013a. Rapid analysis of multiclass antibiotic residues and some of their metabolites in hospital, urban wastewater and river water by ultra-high-performance liquid chromatography coupled to quadrupole-linear ion trap tandem mass spectrometry. J. Chromatogr. A 1292, 173–188. https://doi.org/https://doi.org/10.1016/j.chroma.2012.12.072

Gros, M., Rodríguez-Mozaz, S., Barceló, D., 2013b. Rapid analysis of multiclass antibiotic residues and some of their metabolites in hospital, urban wastewater and river water by ultra-high-performance liquid chromatography coupled to quadrupole-linear ion trap tandem mass spectrometry. J. Chromatogr. A 1292, 173–188. https://doi.org/https://doi.org/10.1016/j.chroma.2012.12.072

Guerra, P., Kim, M., Shah, A., Alaee, M., Smyth, S.A., 2014. Occurrence and fate of antibiotic, analgesic/anti-inflammatory, and antifungal compounds in five wastewater treatment processes. Sci. Total Environ. 473, 235–243. https://doi.org/10.1016/j.scitotenv.2013.12.008

Herman, J.G., Scruggs, C.E., Thomson, B.M., 2017. The costs of direct and indirect potable water reuse in a medium-sized arid inland community. J. Water Process Eng. 19, 239–247. https://doi.org/10.1016/j.jwpe.2017.08.003

Hydranautics, 2010. Optimizing Membrane Bioreactor/ Reverse Osmosis Performance For Treatment Of Municipal Wastewater.

Joss, A., Baenninger, C., Foa, P., Koepke, S., Krauss, M., McArdell, C.S., Rottermann, K., Wei, Y., Zapata, A., Siegrist, H., 2011. Water reuse: >90% water yield in MBR/RO through concentrate recycling and CO2 addition as scaling control. Water Res. 45, 6141–6151. https://doi.org/10.1016/j.watres.2011.09.011

JRC, 2017. Development of minimum quality requirements for water reuse in agricultural irrigation and aquifer recharge V.3.3.

Judd, S., Judd, C., 2008. The MBR book: Principles and Applications of Membrane Bioreactors in Water and Wastewater Treatment, Vasa. https://doi.org/10.1016/B978-185617481-7/50005-2

Justo, a., González, O., Aceña, J., Pérez, S., Barceló, D., Sans, C., Esplugas, S., 2013. Pharmaceuticals and organic pollution mitigation in reclamation osmosis brines by UV/H2O2 and ozone. J. Hazard. Mater. 263, 268–274. https://doi.org/10.1016/j.jhazmat.2013.05.030

Kemper, J.M., Walse, S.S., Mitch, W.A., 2010a. Quaternary Amines As Nitrosamine Precursors: A Role for Consumer Products? Environ. Sci. Technol. 44, 1224–1231. https://doi.org/10.1021/es902840h

Kemper, J.M., Walse, S.S., Mitch, W.A., 2010b. Quaternary Amines As Nitrosamine Precursors: A Role for Consumer Products? Environ. Sci. Technol. 44, 1224–1231. https://doi.org/10.1021/es902840h

Kern, S., Baumgartner, R., Helbling, D.E., Hollender, J., Singer, H., Loos, M.J., Schwarzenbach, R.P., Fenner, K., 2010. A tiered procedure for assessing the formation of biotransformation products of pharmaceuticals and biocides during activated sludge treatment. J. Environ. Monit. 12, 2100–2111. https://doi.org/10.1039/c0em00238k

Kimura, K., Hara, H., Watanabe, Y., 2005. Removal of pharmaceutical compounds by submerged membrane bioreactors (MBRs). Desalination 178, 135–140. https://doi.org/https://doi.org/10.1016/j.desal.2004.11.033

Kimura, K., Toshima, S., Amy, G., Watanabe, Y., 2004. Rejection of neutral endocrine disrupting compounds (EDCs) and pharmaceutical active compounds (PhACs) by RO membranes. J. Memb. Sci. 245, 71–78. https://doi.org/10.1016/j.memsci.2004.07.018

Kohut, K.D., Andrews, S.A., 2003. Polyelectrolyte age and N-nitrosodimethylamine formation in drinking water treatment. Water Qual. Res. J. Canada 38, 719–735.

Kostich, M.S., Batt, A.L., Lazorchak, J.M., 2014. Concentrations of prioritized pharmaceuticals in ef fl uents from 50 large wastewater treatment plants in the US and implications for risk estimation. Environ. Pollut. 184, 354–359. https://doi.org/10.1016/j.envpol.2013.09.013

Krasner, S.W., Mitch, W.A., McCurry, D.L., Hanigan, D., Westerhoff, P., 2013a. Formation, precursors, control, and occurrence of nitrosamines in drinking water: A review. Water Res. 47, 4433–4450. https://doi.org/https://doi.org/10.1016/j.watres.2013.04.050

Krasner, S.W., Mitch, W.A., McCurry, D.L., Hanigan, D., Westerhoff, P., 2013b. Formation, precursors, control, and occurrence of nitrosamines in drinking water: A review. Water Res. 47, 4433–4450. https://doi.org/https://doi.org/10.1016/j.watres.2013.04.050

Kraus, F., Remy, C., Seis, W., Miehe, U., 2016. D 3.3: Generic assessment of treatment trains concerning their environmental impact and risk reduction potential.

Krauss, M., Longrée, P., van Houtte, E., Cauwenberghs, J., Hollender, J., 2010a. Assessing the Fate of Nitrosamine Precursors in Wastewater Treatment by Physicochemical Fractionation. Environ. Sci. Technol. 44, 7871–7877. https://doi.org/10.1021/es101289z

Krauss, M., Longrée, P., Van Houtte, E., Cauwenberghs, J., Hollender, J., 2010b. Assessing the fate of nitrosamine precursors in wastewater treatment by physicochemical fractionation. Environ. Sci. Technol. 44, 7871–7877. https://doi.org/10.1021/es101289z

Kubo, S., Takahashi, T., Morinaga, H., Ueki, H., 1979. Inhibition of Calcium Phosphate Scale on Heat Exchanger: The Relation between Laboratory Test Results and Tests on Heat Transfer Surfaces. Corrosion’79 Paper No.2.

Kumar, M., Adham, S., DeCarolis, J., 2007. Reverse osmosis integrity monitoring. Desalination 214, 138–149. https://doi.org/10.1016/j.desal.2006.10.021

Lajeunesse, A., Smyth, S.A., Barclay, K., Sauvé, S., Gagnon, C., 2012. Distribution of antidepressant residues in wastewater and biosolids following different treatment processes by municipal wastewater treatment plants in Canada. Water Res. 46, 5600–5612. https://doi.org/https://doi.org/10.1016/j.watres.2012.07.042

Lee, H., Tan, T.P., 2016. Singapore's experience with reclaimed water: NEWater. Int. J. Water Resour. Dev. 32, 611–621. https://doi.org/10.1080/07900627.2015.1120188

Lew, C.H., Hu, J.Y., Song, L.F., Lee, L.Y., Ong, S.L., Ng, W.J., Seah, H., 2005. Development of an integrated membrane process for water reclamation. Water Sci. Technol. 51, 455–463.

Malki, M., Abbas, V., 2013. Relationship between phosphate scales and silica fouling in wastewater RO membrane systems. IDA J. Desalin. Water Reuse 5, 15–24.

Marti, E., Monclús, H., Jofre, J., Rodriguez-Roda, I., Comas, J., Balcázar, J.L., 2011. Removal of microbial indicators from municipal wastewater by a membrane bioreactor (MBR). Bioresour. Technol. 102, 5004–5009. https://doi.org/10.1016/j.biortech.2011.01.068

Melgarejo, J., Prats, D., Molina, A., Trapote, A., 2015. A case study of urban wastewater reclamation in Spain: comparison of water quality produced by using alternative processes and related costs. J. Water Reuse Desalin. jwrd2015147. https://doi.org/10.2166/wrd.2015.147

Melin, T., Jefferson, B., Bixio, D., Thoeye, C., De Wilde, W., De Koning, J., van der Graaf, J., Wintgens, T., 2006. Membrane bioreactor technology for wastewater treatment and reuse. Desalination 187, 271–282. https://doi.org/10.1016/j.desal.2005.04.086

Mitch, W. a., Gerecke, A.C., Sedlak, D.L., 2003. A N-Nitrosodimethylamine (NDMA) precursor analysis for chlorination of water and wastewater. Water Res. 37, 3733–3741. https://doi.org/10.1016/S0043-1354(03)00289-6

Mitch, W. a., Sedlak, D.L., 2004. Characterization and Fate of N -Nitrosodimethylamine Precursors in Municipal Wastewater Treatment Plants. Environ. Sci. Technol. 38, 1445–1454. https://doi.org/10.1021/es035025n

Mitch, W. a., Sedlak, D.L., 2002. Formation of N -Nitrosodimethylamine (NDMA) from Dimethylamine during Chlorination. Environ. Sci. Technol. 36, 588–595. https://doi.org/10.1021/es010684q

Mitch, W.A., Gerecke, A.C., Sedlak, D.L., 2003. A N-Nitrosodimethylamine (NDMA) precursor analysis for chlorination of water and wastewater. Water Res. 37, 3733–3741. https://doi.org/https://doi.org/10.1016/S0043-1354(03)00289-6

Monclús, H., Dalmau, M., Gabarrón, S., Ferrero, G., Rodríguez-Roda, I., Comas, J., 2015. Full-scale validation of an air scour control system for energy savings in membrane bioreactors. Water Res. 79, 1–9. https://doi.org/https://doi.org/10.1016/j.watres.2015.03.032

Monclús, H., Ferrero, G., Buttiglieri, G., Comas, J., Rodriguez-roda, I., 2011. Online monitoring of membrane fouling in submerged MBRs. DES 277, 414–419. https://doi.org/10.1016/j.desal.2011.04.055

Monclús, H., Sipma, J., Ferrero, G., Rodriguez-Roda, I., Comas, J., 2010. Biological nutrient removal in an MBR treating municipal wastewater with special focus on biological phosphorus removal. Bioresour. Technol. 101, 3984–91. https://doi.org/10.1016/j.biortech.2010.01.038

Monclús Sales, H., 2011. Development of a Decision Support System for the integrated control of membrane bioreactors.

NRMMC-EPHC-AHMC, 2006. Australian guidelines for water recycling: managing health and environmental risks: Phase 1. National Water Quality Management Strategy. Nat. Resour. Manag. Minist. Counc. Environ. Prot. Herit. Counc. Aust. Heal. Minist. Conf. Canberra, Aust.

OEHHA, 2006. Public Health Goal for N-nitrosodimethylamine in Drinking Water.

Ortiz de García, S., Pinto Pinto, G., García Encina, P., Irusta Mata, R., 2013. Consumption and occurrence of pharmaceutical and personal care products in the aquatic environment in Spain. Sci. Total Environ. 444, 451–465. https://doi.org/10.1016/j.scitotenv.2012.11.057

Pedrouzo, M., Borrull, F., Pocurull, E., Marcé, R.M., 2011. Presence of pharmaceuticals and hormones in waters from sewage treatment plants. Water. Air. Soil Pollut. 217, 267–281. https://doi.org/10.1007/s11270-010-0585-8

Pérez-González, a., Urtiaga, a. M., Ibáñez, R., Ortiz, I., 2012. State of the art and review on the treatment technologies of water reverse osmosis concentrates. Water Res. 46, 267–283. https://doi.org/10.1016/j.watres.2011.10.046

Petrie, B., Barden, R., Kasprzyk-hordern, B., 2015. A review on emerging contaminants in wastewaters and the environment : Current knowledge , understudied areas and recommendations for future monitoring. Water Res. 72.

Phan, H. V, Hai, F.I., Kang, J., Dam, H.K., Zhang, R., Price, W.E., Broeckmann, A., Nghiem, L.D., 2014. Simultaneous nitrification/denitrification and trace organic contaminant (TrOC) removal by an anoxic-aerobic membrane bioreactor (MBR). Bioresour. Technol. 165, 96–104. https://doi.org/10.1016/j.biortech.2014.03.094

Poch, M., Comas, J., Rodríguez-Roda, I., Sànchez-Marrè, M., Cortés, U., 2004. Designing and Building real Environmental Decision Support Systems. Environ. Model. Softw. 19, 857–873.

Puig, S., Coma, M., Monclús, H., van Loosdrecht, M.C.M., Colprim, J., Balaguer, M.D., 2008. Selection between alcohols and volatile fatty acids as external carbon sources for EBPR. Water Res. 42, 557–566. https://doi.org/10.1016/j.watres.2007.07.050

Qin, J.J., Kekre, K.A., Tao, G., Oo, M.H., Wai, M.N., Lee, T.C., Viswanath, B., Seah, H., 2006. New option of MBR-RO process for production of NEWater from domestic sewage. J. Memb. Sci. 272, 70–77. https://doi.org/10.1016/j.memsci.2005.07.023

QPC, 2005. Public Health Regulation 2005.

Radjenovic, J., Perez, S., Petrovic, M., Barcelo, D., 2008. Identification and structural characterization of biodegradation products of atenolol and glibenclamide by liquid chromatography coupled to hybrid quadrupole time-of-flight and quadrupole ion trap mass spectrometry. J. Chromatogr. A 1210, 142–153. https://doi.org/10.1016/j.chroma.2008.09.060

Radjenovic, J., Petrovic, M., Barceló, D., 2007. Analysis of pharmaceuticals in wastewater and removal using a membrane bioreactor. Anal. Bioanal. Chem. 387, 1365–1377. https://doi.org/10.1007/s00216-006-0883-6

Radjenović, J., Petrović, M., Barceló, D., 2009. Fate and distribution of pharmaceuticals in wastewater and sewage sludge of the conventional activated sludge (CAS) and advanced membrane bioreactor (MBR) treatment. Water Res. 43, 831–841. https://doi.org/10.1016/j.watres.2008.11.043

Radjenović, J., Petrović, M., Ventura, F., Barceló, D., 2008. Rejection of pharmaceuticals in nanofiltration and reverse osmosis membrane drinking water treatment. Water Res. 42, 3601–10. https://doi.org/10.1016/j.watres.2008.05.020

Raffin, M., Germain, E., Judd, S., 2012. Wastewater polishing using membrane technology: a review of existing installations. Environ. Technol. 1–11.

https://doi.org/10.1080/09593330.2012.710385

Raffin, M., Germain, E., Judd, S., 2012. Assessment of fouling of an RO process dedicated to indirect potable reuse. Desalin. Water Treat. 40, 302–308. https://doi.org/10.1080/19443994.2012.671171

Raffin, M., Germain, E., Judd, S., 2011. Optimising operation of an integrated membrane system (IMS) - A Box-Behnken approach. Desalination 273, 136–141. https://doi.org/10.1016/j.desal.2010.10.030

Reif, R., Suárez, S., Omil, F., Lema, J.M., 2008. Fate of pharmaceuticals and cosmetic ingredients during the operation of a MBR treating sewage. Desalination 221, 511–517. https://doi.org/https://doi.org/10.1016/j.desal.2007.01.111

Roback, S., 2015. NDMA Formation During Drinking Water Treatment: Veterinary Antibiotics as Precursors, the Effect of Natural Organic Matter and the Significance of Treatment Practices UCLA These.

Rodriguez-mozaz, S., Ricart, M., Köck-schulmeyer, M., Guasch, H., Bonnineau, C., Proia, L., Lopez, M., Alda, D., Sabater, S., Barceló, D., 2014. Pharmaceuticals and pesticides in reclaimed water: Efficiency assessment of a microfiltration–reverse osmosis (MF–RO) pilot plant. J. Hazard. Mater. https://doi.org/10.1016/j.jhazmat.2014.09.015

Rubirola, A., Llorca, M., Rodriguez-Mozaz, S., Casas, N., Rodriguez-Roda, I., Barcelo, D., Buttiglieri, G., 2014. Characterization of metoprolol biodegradation and its transformation products generated in activated sludge batch experiments and in full scale WWTPs. Water Res. 63, 21–32. https://doi.org/10.1016/j.watres.2014.05.031

Sacher, F., Schmidt, C., Carsten, K., Lee, C., von Gunten, U., 2008. Strategies for Minimizing Nitrosamine Formation During Disinfection Water Rese, 1–144.

Sato, N., Xie, R., Yoneda, T., Xing, Y., Noro, A., Robinson, K., Villalobos, R., 2014. Water Quality Improvement by Combined UF, RO, and Ozone/Hydrogen Peroxide System (HiPOx) in the Water Reclamation Process. Ozone Sci. Eng. 36, 153–165. https://doi.org/10.1080/01919512.2013.860003

Schlüsener, M.P., Hardenbicker, P., Nilson, E., Schulz, M., Viergutz, C., Ternes, T.A., 2015. Occurrence of venlafaxine, other antidepressants and selected metabolites in the Rhine catchment in the face of climate change. Environ. Pollut. 196, 247—256.

Schmidt, C., Sacheer, F., Brauch, H., 2006. Strategies for minimizing formation of NDMA and other nitrosamines during disinfection of drinking water, in: AWWA Water Quality Technology Conference, Denver, CO.

Schreiber, I.M., Mitch, W. a., 2006. Nitrosamine formation pathway revisited: The importance of chloramine speciation and dissolved oxygen. Environ. Sci. Technol. 40, 6007–6014. https://doi.org/10.1021/es060978h

Sedlak, D.L., Deeb, R. a, Hawley, E.L., Mitch, W. a, Durbin, T.D., Mowbray, S., Carr, S., 2005. Sources and fate of nitrosodimethylamine and its precursors in municipal wastewater treatment plants. Water Environ. Res. 77, 32–39. https://doi.org/10.2175/106143005X41591

Sgroi, M., Roccaro, P., Oelker, G., Snyder, S.A., 2016a. N-nitrosodimethylamine (NDMA) formation during ozonation of wastewater and water treatment polymers. Chemosphere 144, 1618–1623. https://doi.org/https://doi.org/10.1016/j.chemosphere.2015.10.023

Sgroi, M., Roccaro, P., Oelker, G., Snyder, S.A., 2016b. N-nitrosodimethylamine (NDMA) formation during ozonation of wastewater and water treatment polymers. Chemosphere 144, 1618–1623. https://doi.org/https://doi.org/10.1016/j.chemosphere.2015.10.023

Sgroi, M., Roccaro, P., Oelker, G.L., Snyder, S.A., 2015. N-nitrosodimethylamine (NDMA) formation at an indirect potable reuse facility. Water Res. 70, 174–183. https://doi.org/https://doi.org/10.1016/j.watres.2014.11.051

Shah, A.D., Krasner, S.W., Lee, C.F.T., von Gunten, U., Mitch, W.A., 2012a. Trade-Offs in Disinfection Byproduct Formation Associated with Precursor Preoxidation for Control of N-Nitrosodimethylamine Formation. Environ. Sci. Technol. 46, 4809–4818. https://doi.org/10.1021/es204717j

Shah, A.D., Krasner, S.W., Lee, C.F.T., von Gunten, U., Mitch, W.A., 2012b. Trade-Offs in Disinfection Byproduct Formation Associated with Precursor Preoxidation for Control of N-Nitrosodimethylamine Formation. Environ. Sci. Technol. 46, 4809–4818. https://doi.org/10.1021/es204717j

Shen, R., Andrews, S.A., 2011a. Demonstration of 20 pharmaceuticals and personal care products (PPCPs) as nitrosamine precursors during chloramine disinfection. Water Res. 45, 944–952. https://doi.org/https://doi.org/10.1016/j.watres.2010.09.036

Shen, R., Andrews, S.A., 2011b. Demonstration of 20 pharmaceuticals and personal care products (PPCPs) as nitrosamine precursors during chloramine disinfection. Water Res. 45, 944–952. https://doi.org/https://doi.org/10.1016/j.watres.2010.09.036

Solley, D., 2010. Managing the reverse osmosis concentrate from the Western Corridor Recycled Water Scheme. Water Pract. Technol. 5, 1–8. https://doi.org/10.2166/wpt.2010.018

Stierlin, H., Faigle, J.W., Sallmann, A., Kung, W., Richter, W.J., Kriemler, H.-P., Alt, K.O., Winkler, T., 1979. Biotransformation of diclofenac sodium (Voltaren®) in animals and in man. Xenobiotica 9, 601–610. https://doi.org/10.3109/00498257909042327

Suarez, S., Lema, J.M., Omil, F., 2010. Removal of Pharmaceutical and Personal Care Products (PPCPs) under nitrifying and denitrifying conditions. Water Res. 44, 3214–3224. https://doi.org/10.1016/j.watres.2010.02.040

Taheran, M., Brar, S.K., Verma, M., Surampalli, R.Y., Zhang, T.C., Valero, J.R., 2016. Membrane processes for removal of pharmaceutically active compounds (PhACs) from water and wastewaters. Sci. Total Environ. 547, 60–77. https://doi.org/10.1016/j.scitotenv.2015.12.139

Tchobanoglous, G., Franklin, L.B., Stensel, H.D., 2003. Wastewater Engineering, Treatment and Reuse / Metcalf & Eddy, Inc., 4th ed. re. ed.

Tran, N.H., Urase, T., Kusakabe, O., 2009. The characteristics of enriched nitrifier culture in the degradation of selected pharmaceutically active compounds. J. Hazard. Mater. 171, 1051–1057. https://doi.org/https://doi.org/10.1016/j.jhazmat.2009.06.114

Umar, M., Roddick, F., Fan, L., 2014. Effect of coagulation on treatment of municipal wastewater reverse osmosis concentrate by UVC/H2O2. J. Hazard. Mater. 266, 10–18. https://doi.org/10.1016/j.jhazmat.2013.12.005

USEPA, 2017. 2017 Potable Reuse Compendium.

USEPA, 2012. Guidelines for Water Reuse.

Van Houtte, E., Verbauwhede, J., 2008. Operational experience with indirect potable reuse at the Flemish Coast. Desalination 218, 198–207. https://doi.org/10.1016/j.desal.2006.08.028

Verlicchi, P., Al Aukidy, M., Zambello, E., 2012. Occurrence of pharmaceutical compounds in urban wastewater: Removal, mass load and environmental risk after a secondary treatment-A review. Sci. Total Environ. 429, 123–155. https://doi.org/10.1016/j.scitotenv.2012.04.028

Vrouwenvelder, J.S., Beyer, F., Dahmani, K., Hasan, N., Galjaard, G., Kruithof, J.C., Van Loosdrecht,

M.C.M., 2010. Phosphate limitation to control biofouling. Water Res. 44, 3454–3466. https://doi.org/10.1016/j.watres.2010.03.026

Wagner, J., Rosenwinkel, K.H., 2000. Sludge production in membrane bioreactors under different conditions. Water Sci. Technol. 41, 251–258.

WHO, 2006. Guidelines for the safe use of wastewater, excreta and greywater. Volume 2: Wastewater use in agriculture.

Wintgens, T., Melin, T., Schäfer, a., Khan, S., Muston, M., Bixio, D., Thoeye, C., 2005. The role of membrane processes in municipal wastewater reclamation and reuse. Desalination 178, 1–11. https://doi.org/10.1016/j.desal.2004.12.014

Xia, S., Jia, R., Feng, F., Xie, K., Li, H., Jing, D., Xu, X., 2012. Effect of solids retention time on antibiotics removal performance and microbial communities in an A/O-MBR process. Bioresour. Technol. 106, 36–43. https://doi.org/10.1016/j.biortech.2011.11.112

Xu, P., Bellona, C., Drewes, J.E., 2010. Fouling of nanofiltration and reverse osmosis membranes during municipal wastewater reclamation: Membrane autopsy results from pilot-scale investigations. J. Memb. Sci. 353, 111–121. https://doi.org/10.1016/j.memsci.2010.02.037

Yangali-Quintanilla, V., Maeng, S.K., Fujioka, T., Kennedy, M., Amy, G., 2010. Proposing nanofiltration as acceptable barrier for organic contaminants in water reuse. J. Memb. Sci. 362, 334–345. https://doi.org/10.1016/j.memsci.2010.06.058

Yoon, Y., Westerhoff, P., Snyder, S.A., Wert, E.C., 2006. Nanofiltration and ultrafiltration of endocrine disrupting compounds , pharmaceuticals and personal care products 270, 88–100. https://doi.org/10.1016/j.memsci.2005.06.045

Yu, J.T., Bouwer, E.J., Coelhan, M., 2006. Occurrence and biodegradability studies of selected pharmaceuticals and personal care products in sewage effluent. Agric. Water Manag. 86, 72–80. https://doi.org/10.1016/j.agwat.2006.06.015

Yuen, N.-T., 2008. Membranes Reclaim Wastewater at 86% Recovery in Singapore. WATER WASTES Dig. 30,46-47.

Zeng, T., Mitch, W.A., 2015. Contribution of N-Nitrosamines and Their Precursors to Domestic Sewage by Greywaters and Blackwaters. Environ. Sci. Technol. 49, 13158–13167. https://doi.org/10.1021/acs.est.5b04254

Zeng, T., Plewa, M.J., Mitch, W.A., 2016. N-Nitrosamines and halogenated disinfection byproducts in U.S. Full Advanced Treatment trains for potable reuse. Water Res. 101, 176–186. https://doi.org/https://doi.org/10.1016/j.watres.2016.03.062

Zhou, T., Lim, T.T., Chin, S.S., Fane, a. G., 2011. Treatment of organics in reverse osmosis concentrate from a municipal wastewater reclamation plant: Feasibility test of advanced oxidation processes with/without pretreatment. Chem. Eng. J. 166, 932–939. https://doi.org/10.1016/j.cej.2010.11.078

Zilouchian, A., Jafar, M., 2001. Automation and process control of reverse osmosis plants using soft computing methodologies. Desalination 135, 1–59.

Chapter 11 - Annexes

The following pages contain supplementary information pertaining to preceding chapters.

i. Supplementary information for Chapter 1 – Introduction.
ii. Supplementary information for Chapter 4 - The fate of PhACs and their transformation products through the MBR-RO/NF process.
iii. Supplementary information for Chapter 5 - Fate of NDMA precursors through an MBR-NF pilot plant for urban wastewater reclamation.
iv. Supplementary information for Chapter 6 - Towards online optimisation of RO systems in IMS.
v. Supplementary information for Chapter 7 - EC as an indicator for RO/NF membrane integrity monitoring.

11.1 Supplementary information for Chapter 1 – Introduction.

Table 11-1: Review of IMS facilities-

Integrated Membrane Systems	Output (MLD)	Application	MF/UF Pre-Treatment Details	MF/UF Details	Feed water details (mg/L)	NF/RO Pre-treatment details	NF/RO details	Energy Demand (kWh/m^3) Cost ($/$m^3$)	Other comments	Reference
Sulaibiya, Kuwait, 2004	WWTP: 425 MLD, UF: 375 MLD, RO: 319 MLD	Irrigation, Industrial reuse	Disk filter	Pentair/Norit, 304 640 $m^{2,}$ Pressurized CT (0.03 µm),	TDS: 1280 (max 3014, COD: 43, TSS: 20, Turb: 12 NTU		Toray, 42 skids each 72 PVs, 3-stage (4-2-1), Rec: 85%	MF: 1.1k Wh/m^3, RO: 1.2 kWh/m^3 Cost: 0.6 $/$m^3$ SWRO: 2$/$m^3$	Permeate degassing CO_2, pH adjusted with caustic, chlorine dosing, brine to sea	Raffin et al. (2012), Gagne, D (2005), Alghusain (2013)
Orange County, USA, 2008	328 MLD	Groundwater recharge	Rotating gravity screen/chloramination	Siemens/Memcor, 730 000 $m^{2,}$ Immersed HF (0.04 µm)	TDS: 950, COD: 54, TSS: 6, Turb: 1.8 NTU	H_2SO_4, Antiscalant: AWC A-102 Plus	Hydranautics, 580 000 m^2, 3-stage (78-48-24 PVs), 7 elem./PV, Rec: 85%, Avg. flux: 20.4 LMH	MF: 0.26 kWh/m^3, RO: 0.52 kWh/m^3		Raffin et al. (2012),
Changi, Singapore, 2010	232 MLD	Industrial reuse, IPR	Screen	Siemens/Memcor, Pressurized HF (0.04 µm)	TDS: 1100, COD: 45, TSS: 14, Turb: 6 NTU	H_2SO_4	Toray, 2-stage, Rec: 75%, Avg. flux 17 LMH			Raffin et al. (2012),
Ulu Pandan, Singapore, 2007	191 MLD	Industrial reuse, IPR	Screen	Asahi Kasei/Pall, 160 000m^2, Pressurized HF (0.1 µm),	TDS: 677, COD: 115, TSS: 10, Turb: 12 NTU	H_2SO_4	Hydranautics, 427 000 m^2, 2-stage (64-36 PVs), 7 elem./PV, Rec: 80%, Avg. flux: 18 LMH	MF: 0.4 kWh/m^3, RO: 0.29 kWh/m^3		Raffin et al. (2012), Yuen et al. (2008)
Luggage Point, 2008,	66 MLD		Coagulation/ Flocculation	Asahi Kasei/Pall,	TDS: 1020, COD: 60, TSS:		Toray, 4000 m^2, 3-stage	MF: 1.4 kWh/m^3, RO:		Raffin et al. (2012),

Integrated Membrane Systems	Output (MLD)	Application	MF/UF Pre-Treatment Details	MF/UF Details	Feed water details (mg/L)	NF/RO Pre-treatment details	NF/RO details	Energy Demand (kWh/m^3) Cost ($/$m^3$)	Other comments	Reference
Australia			/Clarification / Chloramination	Pressurized HF (0.2 μm), 85 400m^2,	8.8, Turb: 4.5 NTU		(120-60-30 PVs), 7 elem./PV, Rec: 85%, Avg. flux: 20 LMH	0.9 kWh/m^3		
Spain		Irrigation	Coagulation/ Flocculation/ media filtration	Zeeweed 1000 V3, Immersed HF (0.02 μm)	TDS: 900, COD: 43, TSS: 7.2, Turb: 1.5 NTU	$NaSO_4$	DOW BW30-400	Total 2.6 kWh/m^3		Garcia Lillo et al. (2014)
Torreele, Belgium,	6.9 MLD	Groundwater recharge	Longitudinal screen / Chloramination	GE/Zenon (ZW500C), Immersed HF (0.02μm), 15 600 m^2	TDS: 700, COD: 55, TSS: 3, Turb: 1.5 NTU	Monochloramine to UF filtrate + H_2SO_4 (40 mg/$L_{)+}$ antiscalant (2.4 mg/L) + $NaHSO_3$ (1 mg/L) to neutralize chlorine	DOW (30LE-440), 4002 m^2, 2-stage (21-11 PVs), 6 elem./PV, Rec: 75-80%, Avg. flux: 20 LMH	MF: 0.18 kWh/m^3, RO: 0.63 kWh/m^3	NaOH for pH adjustment (13 mg/L)	Van Houtte et al.(2008), Raffin et al. (2012),

CT – Capillary tube, HF – Hollow fibre

Table 11-2: RO process conditions, values were not confirmed with operators and are for illustration purposes only

Facility		Luggage Point	Ulu Pandan	Sulaibiya	Orange Country GWRS	Torreele	Rincon de Leon WWTP-WRP
Country		Australia	Singapore	Kuwait	USA	Belgium	Spain
Feed		Secondary + N removal	Secondary	Secondary + N&P removal	Secondary	Secondary + N&P removal	Secondary
MF/UF Type		Pressurized	Pressurized	Pressurized	Immersed	Submerged	Pressurized
Pore size	um	0.2	0.1	0.03	0.04	0.02	0.035
P-Removal		Yes - FeCl3	No	No	No	No	Yes- FeCl3
Chloramines		Yes	Yes	?	Yes	Yes	
RO type		Toray TML-10	Hydranautics ESPA2	Toray	Toray TML-20-400	BW-30-LE-440	BW30XFR-400-34i
Element Area (literature)	m2			37.2	37.2	40.9	37.2
Total Area	m2	137,500	371,280	806,496	580,000	15,706	69,955
Element/PV		7	7	7	7	6	6
Number of stages		3	2	3	3	2	2
Number of trains		4	13	42	15	2	5
PV/stage	1	120	64	41	48	21	
	2	60	36	21	24	11	
	3	30		10	20		
Average flux	LMH	20	18	18	20	20	15
Total permeate flow	m3/day	66,000	191,000	352,750	265,000	6,900	25,675
Recovery (Average)		85%	80%	83%	85%	75%	73%
Permeate flow/train	m3/day	16,500	14,692	8,398.81	17,667	3,450	5,135
PV/train		210	100	72	92	32	67
Total number of PVs		840	1300	3024	1380	64	336
Total number of elements		5880	9100	21680	9660	384	2,016
Element Area (from total area)	m2	23.38	40.80		60.04	40.90	
Element area (from flux)		23.38	40.80		60.04	40.90	
Total flow (calc)	L/h	2,750,000	6,683,040	14,697,917	11,600,000	314,112	1,049,325
Total flow (calc)	m3/d	66,000	160,393	352,750	278,400	7,539	25,184
Staging Ratio, R		1.9	2.2	1.8	1.9	2.0	1.9
Theoretical number of PVs/stage	1	116	69	39	51	21	44
	2	62	31	21	27	11	23
	3	33		12	14		
Reference		Raffin et al. (2012)	Raffin et al. (2012)	AlGhusain (2013), Gagne (2005)	Raffin et al. (2012)	Van Houtte & Verdauwhede (2008)	Melgarejo et al. (2016), Garcia Lillo (2014)

11.2 Supplementary information for Chapter 4 - The fate of PhACs and their transformation products through the MBR-RO/NF process.

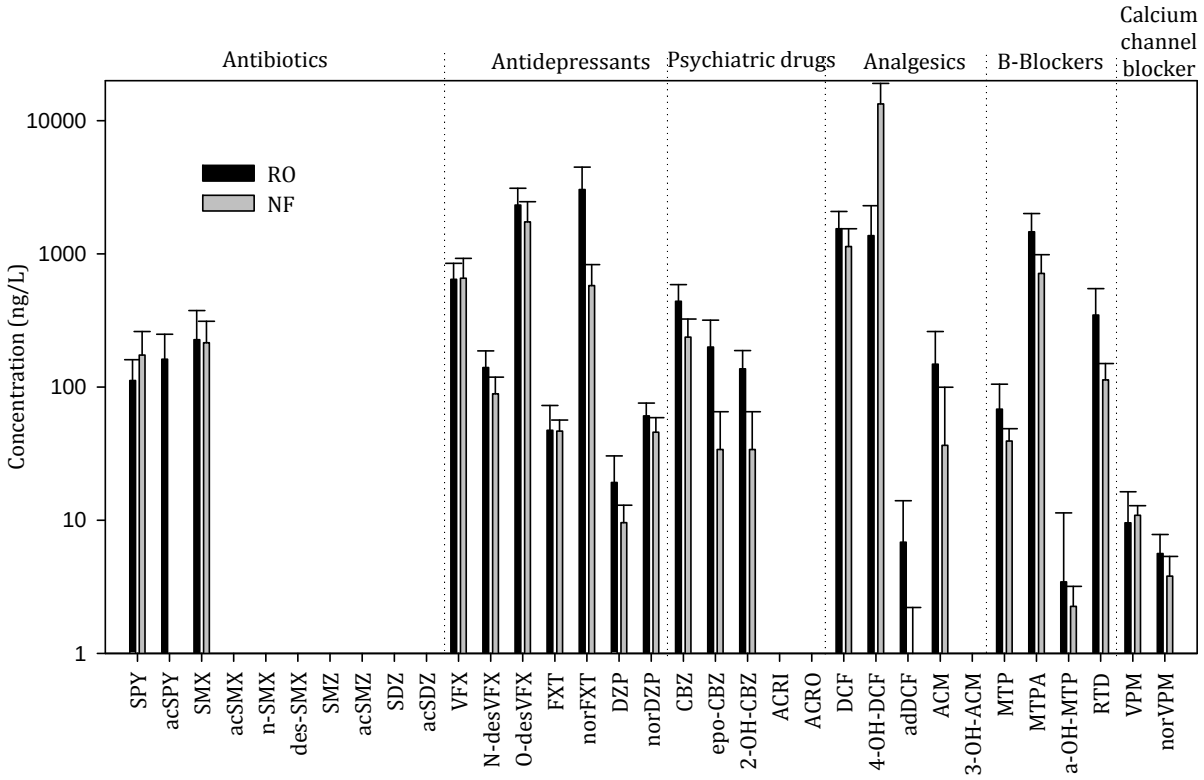

Figure 11-1: Concentration (ng L-1) of the studied compounds in the RO and NF concentrates. Gaps in the figure show that the analyte was not detected.

Table 11-3: Physico-chemical properties of the studied PhACs, metabolites and TPs (Source: National Centre for Biotechnology Information. PubChem Compound Database)

Therapeutic class	Compound		CAS number	Formula	MW (g/mol)	pK_a	Log K_{ow}	Charge at pH 7
Antibiotics	Sulfapyridine	SPY	144-83-2	$C_{11}H_{11}N_3O_2S$	249.3	Pk1= 8043, Pk2=2.3	0.35	Neut./Neg.
	N^4–acetylsulfapyridine	*acSPY*	19077-98-6	$C_{13}H_{13}N_3O_3S$	291.3		1.25	Neut./Neg.
	Sulfamethoxazole	SMX	723-46-6	$C_{10}H_{11}N_3O_3S$	253.3	5.7	0.89	Neut./Neg.
	N^4–acetylsulfamethoxazole	*acSMX*	21312-10-7	$C_{12}H_{13}N_3O_4S$	295.3		1.21	Neut./Neg.
	Nitrosulfamethoxazole	n-SMX	29699-89-6	$C_{10}H_9N_3O_5S$	283.3	5.62	1.22	
	Desaminosulfamethoxazole	*des-SMX*	-	-	238.3			
	Sulfamethazine	SMZ	57-68-1	$C_{12}H_{14}N_4O_2S$	278.3	2.65	0.89	Neut./Neg.
	N^4-Acetylsulfamethazine	*acSMZ*	100-90-3	$C_{14}H_{16}N_4O_3S$	320.4		1.48	Neut./Neg.
	Sulfadiazine	SDZ	68-35-9	$C_{10}H_{10}N_4O_2S$	250.3	pK1= 6.36 pK2= 2.1	-0.09	Neut./Neg.
	N^4-Acetylsulfadiazine	*acSDZ*	127-74-2	$C_{12}H_{12}N_4O_3S$	292.3		0.39	Neut./Neg.
Anti-depressants	Venlafaxine	VFX	93413-69-5	$C_{17}H_{27}NO_2$	277.4	14.42	3.28	positive
	N–Desmethylvenlafaxine	*N-desVFX*	149289-30-5	$C_{16}H_{25}NO_2$	263.4		3.07	positive
	O–Desmethylvenlafaxine	*O-desVFX*	93413-62-8	$C_{16}H_{25}NO_2$	263.4		2.72	positive
	Fluoxetine	FXT	54910-89-3	$C_{17}H_{18}F_3NO$	309.3	9.5	4.05	positive
	Norfluoxetine	*norFXT*	83891-03-6	$C_{16}H_{16}F_3NO$	295.3	9.05	4.07	
	Diazepam	DZP	439-14-5	$C_{16}H_{13}ClN_2O$	284.7	3.4	2.82	Neutral
	Desmethyldiazepam	*norDZP*	1088-11-5	$C_{15}H_{11}ClN_2O$	270.7		3.89	Neutral
Psychiatric drugs	Carbamazepine	CBZ	298-46-4	$C_{15}H_{12}N_2O$	236.3	13.9	2.45	Neutral
	10,11-Epoxy–Carbamazepine	*epo-CBZ*	36507-30-9	$C_{15}H_{12}N_2O_2$	252.3		0.95	Neutral
	2–Hydroxycarbamazepine	*2-OH-CBZ*	68011-66-5	$C_{15}H_{12}N_2O_2$	252.3		1.42	Neutral
	Acridine	ACRI	260-94-6	$C_{13}H_9N$	179.1	6.15	3.4	
	Acridone	ACRO	578-95-0	$C_{13}H_9NO$	195.2		1.69	Neutral
Analgesics/ anti-inflammatories	Diclofenac	DCF	15307-86-5	$C_{14}H_{11}Cl_2NO_2$	296.2		4.51	Negative
	4-OH-diclofenac	*4-OH-DCF*	64118-84-9	$C_{14}H_{11}Cl_2NO_3$	312.2			
	Diclofenac–amide	*adDCF*	15362-40-0	$C_{14}H_9Cl_2NO$	278.1	13.31	3.11	
	Acetaminophen	ACM	103-90-2	$C_8H_9NO_2$	151.2	9.38	0.46	Neutral
	3-OH-acetaminophen	*3-OH-ACM*	37519-14-5	$C_8H_9NO_3$				
B-Blockers	Metoprolol	MTP	37350-58-6	$C_{15}H_{25}NO_3$	267.4	9.6	1.88	Positive
	Metoprolol–acid	*MTPA*	56392-14-4	$C_{14}H_{21}NO_4$	267.3	3,54; 9,67	-2.34	Neutral
	Alfa–Metoprolol–OH	*α-OH-MTP*	56392-16-6	$C_{15}H_{25}NO_4$				
	Ranitidine	RTD	66357-35-5	$C_{13}H_{22}N_4O_3S$	314.4	2.4	0.27	Positive
Calcium channel blocker	Verapamil	VPM	52-53-9	$C_{27}H_{38}N_2O_4$	454.6	9.68	3.79	
	Norverapamil	norVPM	67018-85-3	$C_{26}H_{36}N_2O_4$	440.6	10.29	4.59	

Table 11-4: Concentration (ng L-1) of the studied PhACs, metabolites and TPs in the sewage entering the WWTP.

Therapeutic class	Compound	8:00 PM	10:00 PM	12:00 AM	2:00 AM	4:00 AM	6:00 AM	8:00 AM	10:00 AM	12:00 PM	2:00 PM	4:00 PM	6:00 PM
Antibiotics	**SPY**	123.20	195.42	195.92	390.69	251.77	112.51	134.93	201.44	214.02	266.10	245.28	320.35
	acSPY	128.52	357.07	235.11	472.44	284.58	92.79	109.31	253.03	170.70	202.81	287.67	223.67
	SMX	88.03	235.13	131.45	361.57	243.41	680.35	349.02	314.13	568.21	723.78	303.22	183.32
	acSMX	116.60	195.16	99.72	336.60	197.90	439.15	185.34	239.01	540.00	473.60	111.14	196.31
	n-SMX	31.5*	n.d.	n.d.	n.d.	n.d.	n.d.	n.d.	n.d.	n.d.	n.d.	n.d.	n.d.
	des-SMX	n.d.	n.d.	n.d.	n.d.	n.d.	n.d.	n.d.	<LOD	n.d.	n.d.	n.d.	n.d.
	SMZ	n.d.	n.d.	n.d.	n.d.	n.d.	n.d.	n.d.	n.d.	n.d.	n.d.	n.d.	n.d.
	acSMZ	n.d.	n.d.	n.d.	17.50	n.d.	n.d.	n.d.	n.d.	1.96*	4.51	n.d.	n.d.
	SDZ	n.d.	n.d.	<LOD	n.d.	n.d.	n.d.	n.d.	n.d.	175.47	n.d.	n.d.	n.d.
	acSDZ	8.66*	<LOQ	<LOD	n.d.	n.d.	n.d.	<LOD	<LOD	<LOQ	23.32*	n.d.	<LOD
Anti-depressants	**VFX**	268.67	344.62	318.34	390.90	347.93	278.86	210.06	400.02	246.44	288.57	347.78	281.41
	N-desVFX	38.09	46.83	33.88	50.81	44.67	40.79	26.18	83.72	37.03	41.40	38.44	36.46
	O-desVFX	607.46	638.12	640.97	602.04	711.32	640.85	413.59	854.10	592.17	629.73	631.64	554.48
	FXT	n.d.	<LOD	n.d.	33.98	<LOD	21.22	16.95*	24.85	25.25*	31.78	<LOD	n.d.
	norFXT	344.30	336.10	343.00	315.70	264.50	283.30	224.10	607.40	462.30	397.10	404.76	281.60
	DZP	1.55	2.10	4.79	28.59	2.02	1.24	0.50	2.18	3.20	5.94	3.62	<LOQ
	norDZP	13.58	14.00	13.96	19.46	13.51	19.61	9.23	23.15	16.84	26.97	20.51	15.96
Psychiatric drugs	**CBZ**	80.07	106.50	67.62	77.12	116.25	118.42	129.92	80.82	89.88	87.59	211.67	83.58
	epo-CBZ	n.d.	n.d.	n.d.	n.d.	n.d.	n.d.	n.d.	n.d.	n.d.	n.d.	n.d.	n.d.
	2-OH-CBZ	32.07	32.46	16.13	23.37	39.44	19.94	27.66	37.45	38.58	20.83	27.18	24.92
	ACRI	n.d.	n.d.	n.d.	n.d.	n.d.	n.d.	n.d.	n.d.	n.d.	n.d.	n.d.	n.d.
	ACRO	0.85	0.62	1.57	3.27	0.86	0.76	0.41	<LOD	<LOQ	<LOQ	<LOQ	0.66*
Analgesics/ anti-inflammatories	**DCF**	519	554	483	359	373	368	135	671	565	770	955	518
	4-OH-DCF	11789	13646	9254	4674	12104	10768	5759	22408	12345	15495	32590	18181
	adDCF	n.d.	n.d.	n.d.	n.d.	n.d.	n.d.	n.d.	n.d.	n.d.	n.d.	n.d.	n.d.
	ACM	23432	22950	25034	21876	25611	18041	20744	74160	43124	22460	42579	23746
	3-OH-ACM	n.d.	n.d.	n.d.	n.d.	n.d.	n.d.	n.d.	n.d.	n.d.	n.d.	n.d.	n.d.
B-Blockers	**MTP**	46.75	n.d.	26.96	37.97	35.63	45.30	39.38	72.79	59.96	64.54	41.15	38.66
	MTPA	1380.44	1404.29	1093.92	1434.19	1237.72	1022.95	835.30	2005.61	1947.00	1551.55	1345.17	1220.74
	α-OH-MTP	35.08	31.45	21.28	48.11	30.00	21.03	17.51	57.73	55.36	42.52	27.72	25.40
	RTD	191.02	306.51	208.71	177.26	175.77	264.12	143.47	1036.89	357.86	524.57	390.98	263.62
Calcium channel blocker	**VPM**	6.59	<LOQ	7.33	44.11	7.18	7.52	4.64	7.18	6.38	13.98	5.99	<LOQ
	norVPM	n.d.	n.d.	3.36	11.93	<LOQ	4.71	2.84	<LOQ	1.75	<LOQ	n.d.	<LOD

Table 11-5: A comparison of the concentration (ng L-1) of the studied PhACs, metabolites and TPs in the influent of the WWTP

			2013		2014	
Therapeutic class	Compound		Average	Standard Deviation	Average	Standard Deviation
Antibiotics	Sulfapyridine	SPY	96	36	123	42
	N^4–acetylsulfapyridine	*acSPY*	*132*	*47*	*202*	*67*
	Sulfamethoxazole	SMX	120	88	175	38
	N^4–acetylsulfamethoxazole	*acSMX*	*103*	*92*	*126*	*43*
	Nitrosulfamethoxazole	n-SMX	-	-	0	0
	Desaminosulfamethoxazole	*des-SMX*	-	-	*0*	*0*
	Sulfamethazine	SMZ	-	-	0	0
	N^4-Acetylsulfamethazine	*acSMZ*	-	-	*2*	*4*
	Sulfadiazine	SDZ	-	-	950	307
	N^4-Acetylsulfadiazine	*acSDZ*	-	-	*3*	*8*
Anti-depressants	Venlafaxine	VFX	159	50	272	61
	N–Desmethylvenlafaxine	*N-desVFX*	*25*	*8*	*33*	*10*
	O–Desmethylvenlafaxine	*O-desVFX*	*397*	*128*	*595*	*179*
	Fluoxetine	FXT	22	34	15	13
	Norfluoxetine	*norFXT*	*508*	*305*	*377*	*128*
	Diazepam	DZP	3	2	2	2
	Desmethyldiazepam	*norDZP*	*3*	*3*	*17*	*4*
Psychiatric drugs	Carbamazepine	CBZ	65	22	81	16
	10,11-Epoxy–Carbamazepine	*epo-CBZ*	*22*	*15*	*0*	*0*
	2–Hydroxycarbamazepine	*2-OH-CBZ*	*18*	*13*	*17*	*13*
	Acridine	ACRI	0	0	0	0
	Acridone	ACRO	-	-	1	1
Analgesics/ anti-inflammatories	Diclofenac	DCF	431	185	715	200
	4-OH-diclofenac	*4-OH-DCF*	*242*	*114*	*427*	*116*
	Diclofenac–amide	*adDCF*	*0*	*0*	*0*	*0*
	Acetaminophen	ACM	18733	7242	30766	8141
	3-OH-acetaminophen	*3-OH-ACM*	*0*	*0*	*0*	*0*
B-Blockers	Metoprolol	MTP	18	7	40	10
	Metoprolol–acid	*MTPA*	*623*	*195*	*1115*	*236*
	Alfa–Metoprolol–OH	*α-OH-MTP*	*15*	*6*	*24*	*5*
	Ranitidine	RTD	286	118	239	93
Calcium channel blocker	Verapamil	VPM	0	0	3	3
	Norverapamil	norVPM	3	2	0	0

Table 11-6: Method limits of detection (LOD) and quantification (LOQ) for the studied PhACs, metabolites and TPs

Therapeutic class	Compound		MBR INF (ng L^{-1})		MBR EFF (ng L^{-1})		RO-FEED (ng L^{-1})		RO-PERM (ng L^{-1})		RO-CONC (ng L^{-1})	
			LOD	LOQ	LOD	LOQ	LOD	LOQ	LOD	LOQ	LOD	LOQ
Antibiotics	Sulfapyridine	SPY	1.68	5.60	2.24	7.48	1.54	5.13	0.44	1.45	2.36	7.86
	N^4–acetylsulfapyridine	*acSPY*	1.33	4.44	0.80	2.66	0.52	1.72	0.08	0.25	2.12	7.07
	Sulfamethoxazole	SMX	2.63	8.77	2.24	7.46	1.47	4.89	0.23	0.76	3.76	12.54
	N^4–acetylsulfamethoxazole	*acSMX*	4.99	16.63	n.d.	n.d.	n.d.	n.d.	n.d.	n.d.	n.d.	n.d.
	Nitrosulfamethoxazole	n-SMX	-	-	-	-	-	-	-	-	-	-
	Desaminosulfamethoxazole	*des-SMX*	-	-	-	-	-	-	-	-	-	-
	Sulfamethazine	SMZ	-	-	-	-	-	-	-	-	-	-
	N^4-Acetylsulfamethazine	*acSMZ*	-	-	-	-	-	-	-	-	-	-
	Sulfadiazine	SDZ	-	-	-	-	-	-	-	-	-	-
	N^4-Acetylsulfadiazine	*acSDZ*	-	-	-	-	-	-	-	-	-	-
Anti-depressants	Venlafaxine	VFX	0.42	1.41	0.21	0.70	0.22	0.74	0.01	0.03	0.36	1.20
	N–Desmethylvenlafaxine	*N-desVFX*	0.94	3.14	0.28	0.92	0.28	0.94	n.d.	n.d.	0.64	2.13
	O–Desmethylvenlafaxine	*O-desVFX*	0.63	2.10	0.40	1.32	1.07	3.57	0.03	0.11	0.91	3.05
	Fluoxetine	FXT	0.42	1.39	0.10	0.33	0.09	0.29	n.d.	n.d.	0.53	1.77
	Norfluoxetine	*norFXT*	2.06	6.85	n.d.	n.d.	n.d.	n.d.	n.d.	n.d.	3.68	12.27
	Diazepam	DZP	0.09	0.30	0.02	0.07	0.01	0.05	n.d.	n.d.	0.19	0.62
	Desmethyldiazepam	*norDZP*	0.05	0.17	0.15	0.49	0.11	0.36	n.d.	n.d.	0.10	0.34
Psychiatric drugs	Carbamazepine	CBZ	0.10	0.34	0.10	0.33	0.07	0.23	0.00	0.01	0.19	0.64
	10,11-Epoxy–Carbamazepine	*epo-CBZ*	1.24	4.13	19.65	65.49	13.25	44.18	0.01	0.04	11.32	37.72
	2–Hydroxycarbamazepine	*2-OH-CBZ*	0.22	0.74	1.27	4.24	1.52	5.07	n.d.	n.d.	0.29	0.96
	Acridine	ACRI	n.d.	n.d.	0.30	0.99	0.30	0.99	0.18	0.60	n.d.	n.d.
	Acridone	ACRO	-	-	-	-	-	-	-	-	-	-
Analgesics/ anti-inflammatories	Diclofenac	DCF	7.91	26.36	19.41	64.72	10.18	33.94	n.d.	n.d.	2.29	7.63
	4-OH-diclofenac	*4-OH-DCF*	-	-	-	-	-	-	n.d.	n.d.	n.d.	n.d.
	Diclofenac–amide	*adDCF*	6.96	23.21	0.17	0.57	0.12	0.41	n.d.	n.d.	1.46	4.87
	Acetaminophen	ACM	52.69	175.65	43.71	145.68	23.68	78.94	7.36	24.54	65.76	219.19
	3-OH-acetaminophen	*3-OH-ACM*	0.00	0.00	0.00	0.00	0.00	0.00	0.00	0.00	0.00	0.00
B-Blockers	Metoprolol	MTP	0.41	1.36	0.26	0.87	0.19	0.63	n.d.	n.d.	0.49	1.63
	Metoprolol–acid	*MTPA*	5.15	17.18	4.18	13.92	3.72	12.40	0.52	1.73	2.94	9.80
	Alfa–Metoprolol–OH	*α-OH-MTP*	1.05	3.48	0.82	2.74	0.10	0.32	0.11	0.37	0.46	1.52
	Ranitidine	RTD	1.92	6.39	0.40	1.34	0.45	1.51	0.01	0.04	1.14	3.79
Calcium channel blocker	Verapamil	VPM	0.00	0.00	0.03	0.10	0.02	0.07	n.d.	n.d.	0.06	0.19
	Norverapamil	norVPM	0.27	0.91	0.01	0.05	n.d.	n.d.	n.d.	n.d.	0.14	0.48

Table 11-7: Concentration (ng L-1) of the studied compounds in the membranes feed, concentrate and permeate samples.

	Compound	NF Feed		NF Permeate		NF Concentrate		RO Feed		RO Permeate		RO Concentrate	
Antibiotics	Sulfapyridine	25,73	4,1	0,79	0,1	173,84	87,2	2,39	2,7	-	-	111,82	48,6
	N4–acetylsulfapyridine	21,98	1,8	-	-	-	-	28,07	14,5	0,25	0,6	161,78	87,8
	Sulfamethoxazole	82,94	12,7	0,52	0,4	215,29	96,5	41,03	21,5	0,91	2,2	226,78	148,2
	N4–acetylsulfamethoxazole	-	-	-	-	-	-	-	-	-	-	-	-
	Nitrosulfamethoxazole	-	-	-	-	-	-	-	-	-	-	-	-
	Sulfamethoxazole Amide	-	-	-	-	-	-	-	-	-	-	-	-
	Sulfamethazine	-	-	-	-	-	-	-	-	-	-	-	-
	N4-Acetylsulfamethazine	-	-	-	-	-	-	-	-	-	-	-	-
	Sulfadiazine	-	-	-	-	-	-	-	-	-	-	-	-
	N4-Acetylsulfadiazine	-	-	-	-	-	-	-	-	-	-	-	-
Antidepressants	Venlafaxine	261,31	42,3	8,37	2,0	657,31	268,4	174,21	38,8	-	-	642,84	206,1
	N–Desmethylvenlafaxine	30,51	7,9	2,23	0,3	88,95	29,5	30,60	7,2	-	-	140,08	46,9
	O–Desmethylvenlafaxine	665,05	126,2	36,21	15,8	1738,66	728,8	538,77	131,8	1,59	1,0	2322,19	793,6
	Fluoxetine	16,99	3,7	0,41	0,7	46,71	9,7	2,85	4,4	-	-	47,44	25,1
	Norfluoxetine	822,10	130,2	11,31	6,1	577,49	253,2	-	-	-	-	3046,71	1442,2
	Diazepam	1,36	0,6	-	-	9,58	3,4	0,15	0,3	-	-	19,18	11,2
	Desmethyldiazepam	17,27	3,7	0,92	0,0	45,73	13,3	14,00	4,9	-	-	60,83	14,9
Psychiatric drugs	Carbamazepine	96,90	19,1	15,47	8,8	237,14	87,5	95,49	30,5	-	-	440,91	146,9
	Epoxy– Carbamazepine	-	-	4,94	5,2	33,94	31,2	80,15	21,6	0,16	0,4	199,34	118,5
	2–Hydroxycarbamazepine	-	-	4,94	5,2	33,94	31,2	61,06	27,5	-	-	136,93	51,2
	Acridine	-	-	-	-	-	-	552,28	1219,3	0,34	0,7	0,00	0,0
Analgesics	Diclofenac	259,78	44,1	-	-	1137,46	404,1	343,36	127,6	-	-	1544,88	539,0
	Diclofenac–OH	884,40	137,0	17,60	20,2	1368,79	582,1	487,89	250,9	-	-	1368,64	929,4
	Diclofenac–amide	-	-	-	-	0,81	1,4	1,64	1,1	-	-	6,84	7,1
	Acetaminophen	39,47	0,0	12,27	0,0	36,53	63,3	24,96	35,3	-	-	148,52	112,3
	Acetaminophen–OH	-	-	-	-	-	-	-	-	-	-	-	-
B-Blockers	Metoprolol	46,87	4,2	9,73	0,7	39,33	9,3	22,21	12,4	-	-	68,31	36,7
	Metoprolol–acid	1582,52	259,2	-	-	712,96	274,7	933,37	467,6	5,39	8,8	1466,68	538,3
	Alfa–Metoprolol–OH	0,16	0,0	0,03	0,0	2,25	0,9	2,70	1,1	3,10	3,1	3,44	7,9
	O–Desmethyl–Metoprolol	10,98	0,0	-	-	61,30	27,8	-	-	-	-	19,91	32,1
Other drugs	Verapamil	4,00	0,9	0,06	0,1	10,88	2,0	3,76	1,2	-	-	9,56	6,8
	Norverapamil	1,19	1,0	0,14	0,0	3,80	1,5	-	-	-	-	5,61	2,2
	Ranitidine	35,79	9,4	2,83	0,5	113,20	37,2	194,66	139,5	0,01	0,0	346,86	200,3
	Acridone	0,22	0,4	2,50	0,3	-	-	-	-	-	-	-	

Table 11-8: Water quality parameters measured in the sewage entering the WWTP.

Parameter	Units	8:00 PM	10:00 PM	12:00 AM	2:00 AM	4:00 AM	6:00 AM	8:00 AM	10:00 AM	12:00 PM	2:00 PM	4:00 PM	6:00 PM
Elec. Conductivity	(µS/cm)	1440	1204	1143	1233	1276	1396	1408	1463	1376	1719	1697	1301
COD_T	(mg L^{-1})	542	660	706	889	282	170	157	433	535	606	586	448
COD_S	(mg L^{-1})	97	289	233	199	100	72	22	84	100	123	129	106
TKN_T	(mg N L^{-1})	54	59	58	77	49	50	38	84	77	55	51	49
TKN_S	(mg N L^{-1})	45	48	45	45	41	41	33	71	60	48	41	40
NH_4^+	(mg N L^{-1})	32	37	40	34	32	28	17	60	47	42	35	34
NO_3^-	(mg N L^{-1})	0	0	0	0	0	0	0	0	0	0	0	0
NO_2^-	(mg N L^{-1})	1.1	0	0	10	0	0	0	2.3	0	0.3	12.9	9.1
PO_4^{3-}	(mg L^{-1})	3.9	1.6	0.7	3.2	3.6	3.2	2.5	2.9	6.2	2.1	5.3	5.6

11.3 Supplementary information for Chapter 5 - Fate of NDMA precursors through an MBR-NF pilot plant for urban wastewater reclamation.

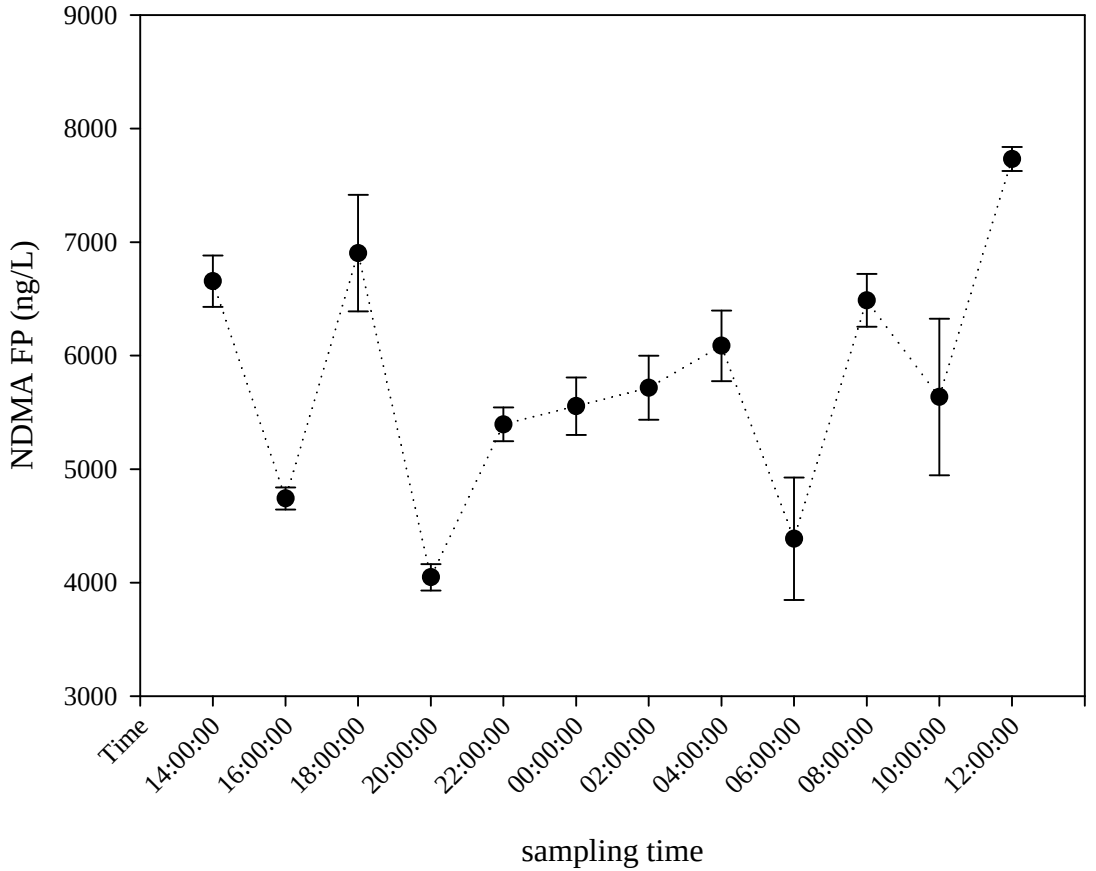

Figure 11-2: NDMA FP 24 hours profile of the primary effluent of Quart WWTP.

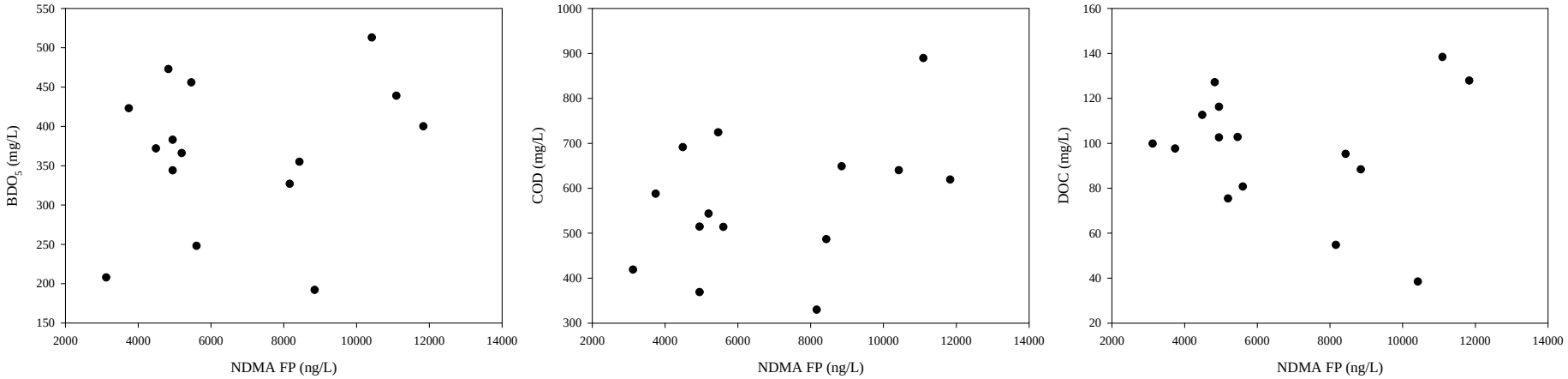

Figure 11-3: Scatter plots of NDMA FP and COD, BDO5 and DOC at the influent of the MBR.

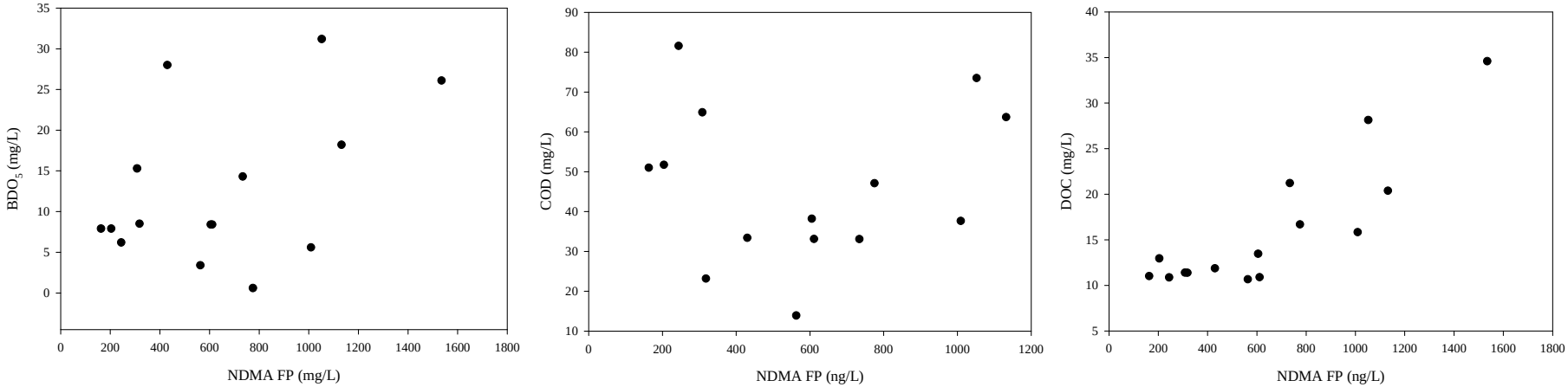

Figure 11-4: Scatter plots of NDMA FP and COD, BDO5 and DOC at the effluent of the MBR.

Table 11-9: Acquisition parameters for pharmaceutical analysis in SRM mode. CE: collision energy.

compound	Internal standard used	Precursor ion (m/z)	Product ion quantification (m/z)	CE (eV)	Product ion confirmation (m/z)	CE (eV)	SLens
Erythromycin	Erythromycin-N,$N^{13}C_2$	734.63	158.2	28	576.6	16	153
Clarithromycin	Erythromycin-N,$N^{13}C_2$	748.55	158.1	28	590.6	16	157
Azithromycin	Azithromycin-d_3	375.53	83.2	18	158.2	21	88
Citalopram	Citalopram-d_4	325.3	109.1	34	262.2	18	120
Ranitidine	Cimetidine-d_3	315.22	176.1	16	130.1	23	85
Venlafaxine	Venlafaxine-d_6	278.23	260.4	9	58.2	18	71
Oxytetracycline	Tetracyclined_6	461.33	426.3	18	443.4	11	119
Doxycycline	Tetracyclined_6	445.21	428.3	17	321.2	30	117
Chlorotetracycline	Tetracyclined_6	479.25	444.3	19	426.3	16	121
Spiramycin	Azithromycin-d_3	438.3	174.2	20	101.1	17	104
Tylosin	Erythromycin-N,$N^{13}C_2$	916.61	174.1	36	772.7	26	232
Roxithromycin	Erythromycin-N,$N^{13}C_2$	837.58	158.1	31	679.7	19	180
Tetracycline	Tetracycline-d_6	445.3	410.3	18	154.1	25	117
O-desmethylvenlafaxine	Venlafaxine-d_6	264.04	246.3	7	58.2	17	77
Erythromycin-N,$N^{13}C_2$		736.31	160.1	27	578.6	17	155
Azithromycin-d_3		376.58	83.1	19	158.1	21	109
Citalopram-d_4		328.87	113.1	19	266.2	17	96
Cimetidine-d_3		256	162.1	12	120.1	13	68
Tetracycline-d_6		451.2	416.2	18	160.1	25	107
Venlafaxine-d_6		283.86	64.1	20	121.1	25	71

Table 11-10: Operational parameters of the MBR during the experiment time.

Date	MBR MLSS (g/L)	MBR MLVSS (g/L)	SRT (days)	Perm flow	Flux LMH	DO in Aerated tank (mg/L)	Temperature (ºC)
28-Apr	3.8	3.1	-	200	25	1	19.6
4-May	-	-	-	200	25	1	22.1
7-May	5.3	4	37	200	25	1	23
15-May	11	8.8	30	200	25	0	24
20-May	10.9	9.2	30	200	25	0	20.8
27-May	9.2	7.5	30	200	25	1	24.1
19-Jun	10	7.8	30	200	25	1.21	27.0
26-Jun	-	-	-	200	25	0.82	27.2
1-Jul	9.9	7.8	19	200	25	0.55	29.5
9-Jul	9.5	7.3	18	200	25	0.59	32.6
15-Jul	9.5	7.5	18	200	25	0.6	30.7
22-Jul	9.5	7.6	17	200	25	0.58	32.09
29-Jul	8.1	6.6	19	200	25	0.58	29.4
5-Aug	7	5.7	20	200	25	0.5	30.4
12-Aug	7	6	19	200	25	0.01	28.6
13-Aug	7	6	19	200	25	0.02	30.9
19-Aug	7	6	19	200	25	0	-
21-Aug	7	6	19	180	22.5	0	27.8
26-Aug	5.9	5.3	20	180	22.5	0	26.3
28-Aug	5.9	5.3	20	180	22.5	0	28.5

Table 11-11: Analytical parameters measured in the MBR during the experimental time.

	carbon source							nitrogen source									phosphorous source	
Date	$COD_{T\ (in)}$	$COD_{S\ (in)}$	$COD_{(out)}$	$BOD_{5\ (in)}$	BOD_{5} (out)	$NPOC_{(in)}$	NPOC (out)	$TKN_{T\ (in)}$	$TKN_{S\ (in)}$	$TKN_{(out)}$	$NH_4^+{}_{(in)}$	NH_4^+ (out)	$NO_2^-{}_{(in)}$	$NO_2^-{}_{(out)}$	$NO_3^-{}_{(in)}$	$NO_3^-{}_{(out)}$	$PO_4^{3-}{}_{(in)}$	$PO_4^{3-}{}_{(out)}$
28-Apr	909.5	335.3	36.8	-	-	122.9	4.7	88.3	67.9	3.8	48.3	1.4	-	-	0.02	8.2	7.9	1.0
4-May	564.4	350.0	43.4	-	-	110.1	13.2	101.9	82.8	2.4	68.1	0.1	-	-	0.14	6.7	7.5	NR
7-May	854.4	465.6	28.8	-	-	156.6	12.0	89.3	73.7	1.9	47.0	0.7	-	-	0.17	2.5	9.6	0.1
15-May	889.4	400.0	37.7	439.0	5.6	138.4	15.8	93.3	88.6	46.6	63.1	46.6	-	-	0.11	0.4	9.0	8.8
20-May	330.0	162.4	38.2	327.0	8.4	54.8	13.5	60.7	43.7	33.9	37.6	31.4	-	-	0.14	0.2	5.1	0.2
27-May	640.0	205.4	33.4	513.0	28.0	38.5	11.9	93.0	75.1	10.2	116.6	0.6	-	-	0.03	0.0	7.5	0.1
19-Jun	619.4	237.5	33.1	400	8.4	127.9	10.89	95.1	74.09	5.85	64.17	2.09	-	-	0.07	4.7	8.4	4.7
26-Jun	649.1	261.4	13.9	-	3.4	88.38	10.67	100.09	74.05	6.15	66	2.05	-	-	0.10		8.8	1.3
1-Jul	486.8	176.2	23.18	355	8.5	95.27	11.39	76,15	60,01	2,47	49,93	<LOQ	-	-	0.05	16.9	8.0	1.9
9-Jul	-	-	64,9	473	15.3	127.2	11.4	80,19	62,39	1,87	48,3	<LOQ	-	-			9.2	3.8
15-Jul	514,6	310,6	51,0	383	7.9	116.2	11.02	82,3	64,64	2,57	52,44	<LOQ	-	-	0.00	18,39	6.1	2,07
22-Jul	691,2	268,8	81,6	372	6.2	112,6	10,87	72,41	56,06	1,61	44,1	<LOQ	-	-	0.00	21.4	0.1	4.9
29-Jul	724,4	357,5	51,74	456	7.9	102,8	12,96	88.52	60.63	3.34	53.6	<LOQ	-	-	0.06	28.3	7.9	7.6
5-Aug	487.15	234	33.43	293	5.7	94.56	11.82	70.9	NR	0	47.85	<LOQ	-	-	0.09	30.4	7.1	8.4

12-Aug	368.9	179.66	33.09	344	14.3	102.6	21.23	79.19	51.66	45.58	47.75	40.3	-	-	0.09	0.4	7.0	9.0
14-Aug	418.8	155.3	47.1	208	0.6	99.85	16.69	82.88	75.02	NR	49.47	40.25	-	-	0.07	0.1	7.5	5.9
19-Aug		219.7	23.8	772	12.6	120.6	12.5	106.1	59.49	45.97	53.85	41.74	-	-	<LOQ	<LOQ	9.4	10.6
21-Aug	543.7	264.5	63.7	366	18.2	75.41	20.39	77.14	60.51	63.52	56.61	57.53	-	0.18	0.02	0.1	7.9	8.9
26-Aug	587.8	249.8	73.5	423	31.2	97.65	28.14	80.65	63.52	62.25	56.18	56.84	-	0.08	0.09	0.1	9.2	9.6
28-Aug	513.91	188.78		248	26.1	80.72	34.59	79.21	59.74	64.99	48.42	55.15	-	-	0.03	0.0	7.3	

11.4 Supplementary information for Chapter 6 - Towards online optimisation of RO systems in IMS.

11.4.1 Determination of major foulants species

(This work was undertaken by Adiquimica, Barcelona)

One of the RO membranes utilized in the operational period of the study had the outer wrapping of the element removed and the membrane sheets were unrolled as shown in Fig 14-1 below. Deposits from the membrane surface were analysed utilizing a scanning electron microscopy (SEM, Stereoscan S-360, Cambridge Instruments) and Energy-dispersive X-ray spectroscopy (EDX, INCA Energy Series 200, Oxford Instruments). The SEM allows high image resolution of surface topographical and morphological features of the deposit and inorganic particles that have adhered to the surface of the membrane. The EDX analysis allows the identification of the composition of the deposit together with distribution of each of the elements making up the sample. Z-contrast images provided additional information on the composition of the deposit.

The analysis by energy dispersive X-ray (EDX) reveals the chemical elements present in the sample together with their distribution. The samples were dried by the critical point process and were coated with a thin layer of graphite to improve conductivity. The microphotographs corresponding to the images of "Z-contrast" provide additional information on the composition of the deposit.

Figure 11-5: Unrolling of the membrane element showing the presence of a brown deposit on the membrane surface

11.4.2 Membrane Autopsy Results

The membrane autopsy confirmed that the major foulants observed on the membrane being operated at the pilot plant are similar to those observed at full-scale plants utilizing RO membranes for wastewater recovery.

The results of the SEM and EDX analysis shown in Figures 2 and 3 indicate that the surface deposits on the membrane were mainly compose of organic matter that covered the entire surface of the membrane, silicates and aluminosilicates of colloidal clay origin together with calcium carbonate and calcium phosphate scaling.

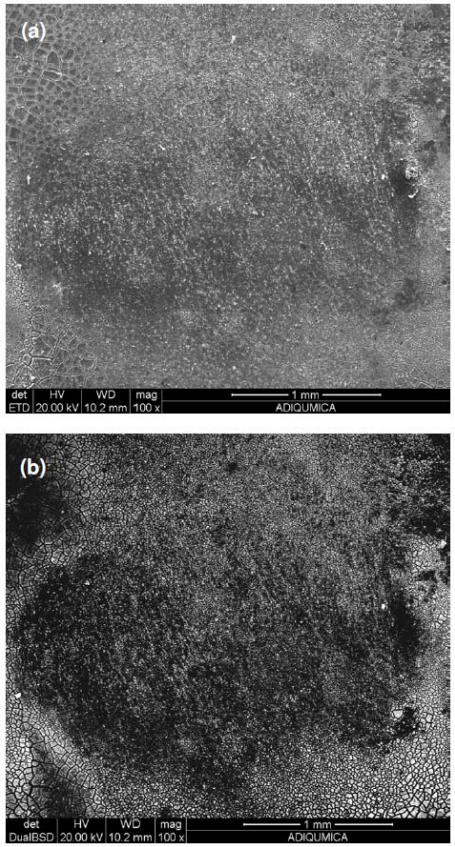

Figure 11-6: (a) Topographic low magnification micrograph (100x) obtained by SEM for the membrane entrance, (b) z-contrast image of the feed portion of the membrane

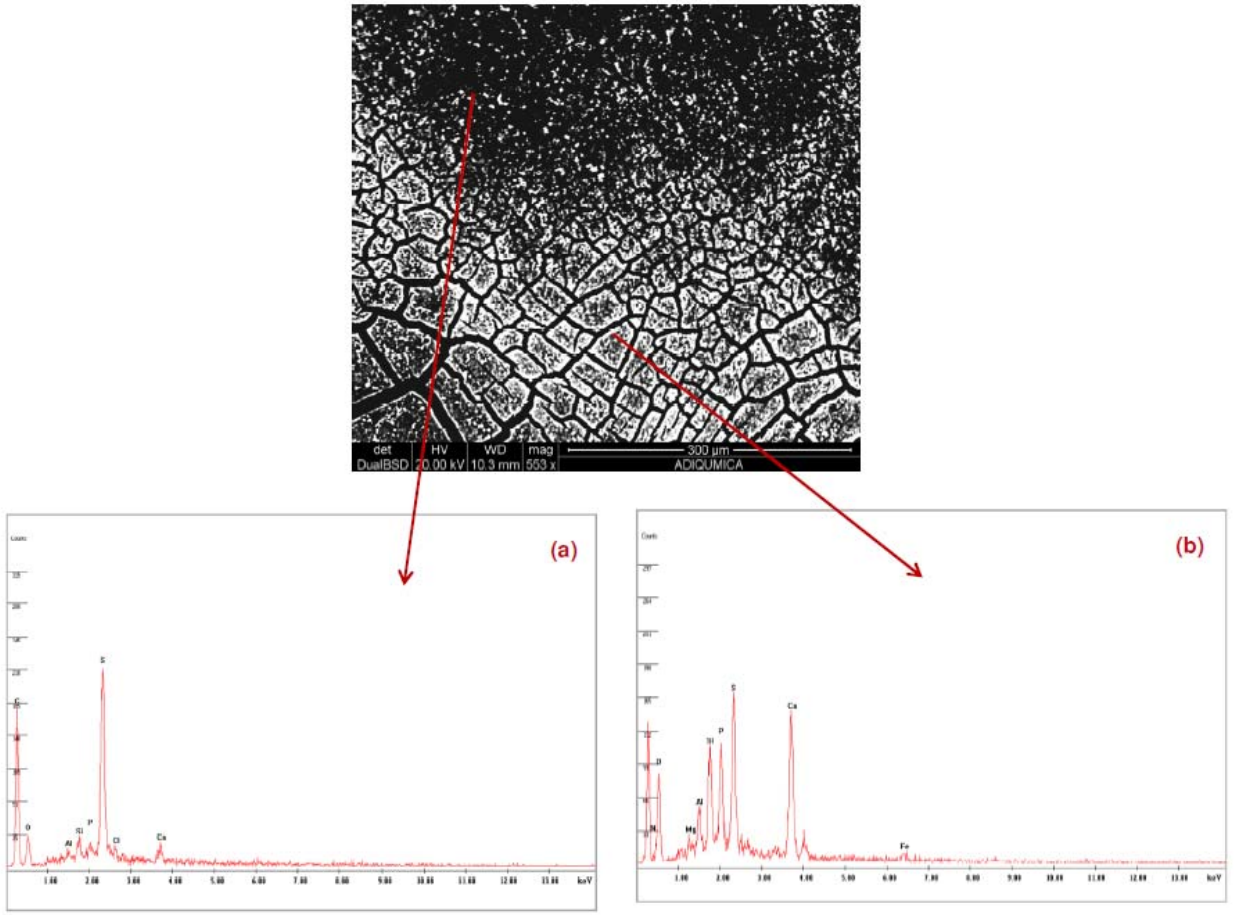

Figure 11-7: Z-contrast image obtained by the SEM (553x), (a) EDX analysis of the black area covering the entire surface area corresponding to organic matter, (b) white deposit corresponding to calcium phosphate, calcium carbonate and silicate

11.4.3 Wastewater Quality Datasets

Table 11-12: Dataset 1

Dataset 1 - Quart 24-hour WWTP influent profile	Laboratory Data												Calculations					
			Cations						Anions				Total Cations	Total Anions	Percent Difference	Approx EC	% Conservative	% Non-conservative
Date	EC	pH	Ca2+	Mg2+	Na+	K+	NH4+	ALC	Cl-	N-NO3-	SO42-	P-PO43-						
			mg/L	mg/L	mg/L	mg/L	mg/L	mg/L	mg/L	mg/L	mg/L	mg/L	meq/L	meq/L		uS/cm	% of TDS	% of TDS
mg/meq			20.04	12.15	22.98	39.10	18.04	61.02	35.45	62.01	48.03	31.66						
uS/cm/mg			1.99	4.36	2.23	1.93	4.09	0.78	2.20	1.20	1.71							
12/02/2015 18:00	1366	7.5	80.2	17.7	130.3	26.0	85.3	519	138.1		16.2	6.1	16.5	12.9	12%	1663	31%	69%
12/02/2015 21:00	1403	7.3	75.1	18.4	123.9	32.5	69.0	506	156.1		15.3	5.2	15.3	13.2	7%	1615	33%	67%
12/02/2015 16:00	1407	7.5	82.0	15.5	131.3	25.8	69.8	538	128.5		20.9	6.2	15.6	13.1	9%	1597	30%	70%
13/02/2015 04:00	1409	7.5	81.8	14.2	143.5	28.0	55.3	474	166.5		16.3	6.0	15.3	13.0	8%	1589	36%	64%
13/02/2015 00:00	1413	7.4	77.9	14.9	138.4	31.0	48.4	479	151.0		17.2	5.3	14.6	12.6	7%	1522	35%	65%
13/02/2015 01:00	1415	7.2	77.2	14.8	135.8	27.5	44.2	488	160.1		16.2	5.7	14.1	13.0	4%	1516	35%	65%
12/02/2015 17:00	1425	7.5	79.2	16.2	132.3	25.9	46.7	530	140.5		13.8	6.1	14.3	13.1	4%	1510	32%	68%
13/02/2015 09:00	1430	7.4	77.6	11.8	150.3	25.1	46.0	501	101.4		15.7	6.6	14.6	11.6	11%	1418	31%	69%
12/02/2015 23:00	1472	7.5	76.9	16.0	146.9	27.8	47.8	515	163.0		16.1	5.2	14.9	13.5	5%	1587	35%	65%
12/02/2015 22:00	1481	7.5	80.9	17.7	137.3	29.6	42.8	496	159.2		16.8	4.8	14.6	13.1	5%	1542	35%	65%
13/02/2015 03:00	1497	7.3	82.8	15.6	160.1	31.4	42.5	488	192.3		15.6	6.0	15.5	13.9	5%	1654	39%	61%
13/02/2015 06:00	1505	7.2	79.3	13.4	162.1	27.9	41.9	516	128.2		14.1	5.5	15.1	12.5	9%	1511	34%	66%
13/02/2015 12:00	1516	7.6	85.6	13.3	118.5	25.9	44.0	589			12.1	5.3	13.6	10.1	15%	1202	18%	82%
13/02/2015 11:00	1521	7.5	90.4	13.5	131.6	22.3	40.6	542	115.9		14.9	5.0	14.2	12.6	6%	1445	29%	71%
13/02/2015 02:00	1526	7.4	81.7	15.4	158.0	28.1	40.7	640	141.8		16.3	5.9	15.2	15.0	1%	1642	30%	70%
12/02/2015 15:00	1587	7.5	81.7	15.1	140.7	23.6	38.0	560	159.4		18.8	7.0	14.1	14.3	0%	1563	32%	68%
13/02/2015 10:00	1604	7.5	78.7	11.8	132.2	21.3	40.4	535.0	178.5		12.3	4.2	13.4	14.2	-3%	1540	34%	66%
12/02/2015 13:00	1637	7.6	81.3	14.6	133.2	23.0	42.3		155.0		20.5	8.0	14.0	5.1	47%	1116	68%	32%
12/02/2015 14:00	1677	7.5	86.3	15.4	158.7	22.4	40.0	570	202.8		20.5	7.7	15.3	15.7	-1%	1726	36%	64%
13/02/2015 05:00	1699	7.4	76.9	11.4	183.7	25.4	38.6	479	180.4		9.1	6.1	15.6	13.3	8%	1605	40%	60%
13/02/2015 08:00	1820	7.2	81.2	13.2	237.3	53.9	36.7	471	222.0		9.0	6.6	18.9	14.4	14%	1873	47%	53%
12/02/2015 19:00	1824	7.2	72.4	19.7	202.6	34.1	55.9	526	254.7		14.2	5.4	18.0	16.3	5%	1971	43%	57%
13/02/2015 07:00	1856	7.2	85.3	16.1	224.2	35.5	55.9	499	190.0		9.5	6.5	19.3	13.9	16%	1861	42%	58%
12/02/2015 20:00	2040	7.0	76.8	30.9	181.7	58.8	69.6	458	297.0		15.2	3.6	19.6	16.3	9%	2128	48%	52%
Min	1366	7	72	11	119	21	37	458	101		9						18%	32%
Max	2040	8	90	31	237	59	85	640	297		21	8.0					68%	82%
Avg	1564	7	80	16	154	30	49	518	169		15	6					36%	64%
Stdev	176	0	4	4	31	9	13	43	44		3	1					9%	9%
Avg - Stdev	1388.2	7.2	76.4	11.9	122.8	20.7	36.7	475.7	124.5		12.0	4.8						
Avg + Stdev	1739.3	7.5	84.3	19.5	185.1	38.7	61.8	560.7	213.0		18.5	6.8						
Correlation with EC			-0.04	0.46	0.77	0.65	-0.07	-0.18	0.83		-0.39	-0.07						
Notes: No result=blank, Result< LOQ= 0																		

Table 11-13: Dataset 2

Dataset 2 - Quart- NF Feed		Laboratory Data														Calculations					
						Cations						Anions				Total Cations	Total Anions	Percent Difference	Approx EC	% Conservative	% Non-conservative
Date	EC (Results)	EC (Bad)	pH	NPOC	TKN	Ca2+	Mg2+	Na+	K+	NH4+	ALC	Cl-	N-NO3-	SO42-	P-PO43-						
				mg/L	mg/L	mg/L	mg/L	mg/L	mg/L	mg/L	mg/L	mg/L	mg/L	mg/L	mg/L	meq/L	meq/L			% of TDS	% of TDS
mg/meq						20.04	12.15	22.98	39.10	18.04	61.02	35.45	62.01	48.03	31.66						
uS/cm/mg						1.99	4.36	2.23	1.93	4.09	0.78	2.20	1.20	1.71							
20-May	978	1198	7.4	10.4	33.9	59.1	7.8	115.8	13.5	32.2	240	192.4	0.7	18.0	1.0	10.8	9.8	5%	1210	48%	52%
26-Jun	1133	1141	7.2	10.1	6.3	68.9	11.9	123.2	22.9	1.9	193	202.0	23.3	18.8	1.0	10.5	9.7	4%	1171	54%	46%
01-Jul	1138	1221	7.2	10.2	1.7	70.2	13.1	137.6	26.4	1.8	270	229.5	19.0	21.2	1.6	11.3	11.7	-2%	1336	51%	49%
05-Aug	1152	1118	6.8	9.9	1.3	68.0	14.4	140.0	27.2		117	190.0	34.4	17.7	8.3	11.4	8.5	15%	1143	60%	40%
15-Jul	1227	1256	7.1	10.0	3.3	72.9	13.6	142.9		0.0	241	228.2	20.1	18.1	1.9	11.0	11.1	-1%	1268	52%	48%
09-Jul	1252	1296	7.3	10.0	1.4	68.9	13.4	153.3	25.0	0.0	273	267.6	2.8	19.7	5.9	11.9	12.7	-3%	1424	55%	45%
22-Jul	1276	1319	7.0	12.3	1.3	65.3	16.7	136.2		0.0	209	264.9	21.4	22.0	5.8	10.6	11.9	-6%	1315	56%	44%
19-Jun	1288	1301	7.4	11.0	5.4	71.1	15.6	147.1	31.6	2.1	266	260.8	4.7		4.6	12.2	11.9	1%	1394	57%	43%
27-May	1306	1295	7.5	11.0	4.1	23.4	14.6	112.8	27.8	0.6	377	204.4	1.1	23.3		8.0	12.4	-22%	1203	46%	54%
29-Jul	1343	1364	6.9	10.1	2.3	69.5	16.5	158.9	20.0	0.0	182	253.6	27.8	18.2	7.4	12.2	11.2	4%	1367	60%	40%
12-Aug	1558	1630	6.3	16.8	51.3	65.3	14.0	140.3	26.2	47.3	376	316.2	0.0	16.0	9.7	13.8	15.7	-6%	1764	49%	51%
26-Aug	1591	1574	7.5	48.1	66.7	84.8	15.4	152.9	34.9	59.9	593	197.7	0.0	1.4	10.2	16.4	15.6	2%	1789	35%	65%
25-Aug	1597	1592	6.4	21.9	63.4	82.3	15.9	136.2	28.3	57.1	417	277.5	0.0	2.1	9.1	15.2	15.0	1%	1764	45%	55%
12-Aug	1643	1735	4.4	11.3	44.3	82.2	14.6	145.5	28.0	38.4	250.0	423.7	0.1	8.2	6.7	14.5	16.4	-6%	1904	61%	39%
27-Aug	1674	1664	7.5	63.2	58.7	86.0	16.3	169.0	33.3	57.1	583	228.2	0.0	1.4	9.5	17.0	16.3	2%	1876	38%	62%
15-May	1675	1700	7.8	17.0	51.8	17.6	14.1	176.7	35.2	48.9	546	296.1	0.5	25.1	2.0	13.3	17.9	-15%	1879	45%	55%
21-Aug	1713	1716	6.3	12.2	42.7	78.5	15.8	165.6	30.2	41.7	295	371.7		15.0	10.6	15.5	16.0	-1%	1897	57%	43%
Min		1118	4.4	9.9	1.3	17.6	7.8	112.8	13.5	0.0	117.0	190.0	0.0	1.4	1.0					35%	39%
Max		1735	7.8	63.2	66.7	86.0	16.7	176.7	35.2	59.9	593.0	423.7	34.4	25.1	10.6					61%	65%
Avg		1419	6.9	17.4	25.9	66.7	14.3	144.3	27.4	24.3	319.3	259.1	9.7	15.4	5.9					51%	49%
Stdev		219	0.8	15.0	26.1	19.0	2.1	17.6	5.7	25.2	142.5	64.7	12.2	7.8	3.5					8%	8%
Avg - Stdev		1200.1	6.2			47.7	12.2	126.8	21.6	-0.9	176.8	194.4	-2.5	7.6	2.4						
Avg + Stdev		1637.6	7.7			85.7	16.5	161.9	33.1	49.5	461.8	323.7	21.9	23.2	9.5						
Correlation with EC						0.12	0.45	0.62	0.58	0.82	0.66	0.71	-0.66	-0.52	0.57						
Notes: No result=blank, Result< LOQ= 0																					

Table 11-14: Dataset 3

Dataset 3 - CPA - NF Fe	Laboratory Data													Calculations					
				Cations						Anions				Total Cations	Total Anions	Percent Difference	Approx EC	% Conservative	% Non-conservative
Date	EC	pH	NPOC	Ca2+	Mg2+	Na+	K+	NH4+	ALC	Cl-	N-NO3-	SO42-	P-PO43-						
			mg/L	mg/L	mg/L	mg/L	mg/L	mg/L	mg/L	mg/L	mg/L	mg/L	mg/L	meq/L	meq/L			% of TDS	% of TDS
mg/meq				20.04	12.15	22.98	39.10	18.04	61.02	35.45	62.01	48.03	31.66						
uS/cm/mg				1.99	4.36	2.23	1.93	4.09	0.78	2.20	1.20	1.71							
02-Apr	601	7.9	8.6	81.7	7.9	58.4	8.7	0.8	147	64.5	5.6	28.5	0.1	7.5	4.9	21%	659	35%	65%
03-Apr	762	7.2	8.8	97.3	10.3	78.5	9.5	0.0	204	91.0	3.2	26.9	0.1	9.4	6.5	18%	841	36%	64%
05-Apr	833	8.0	8.0	108.8	12.6	93.0	11.9	2.0	208		4.1	24.8		10.9	4.0	47%	720	25%	75%
08-Apr	858	8.2	8.2	107.0	15.8	133.4	22.6	0.0	185	149.2	6.9	42.2	0.0	13.0	8.2	23%	1176	48%	52%
10-Apr	874	8.4	10.3	114.2	11.4	102.0	13.3	0.0	205	111.3	7.5	43.6	0.1	11.4	7.5	21%	1018	39%	61%
07-May	906	7.5	6.1	125.5	13.1	116.5	17.3	0.0	169	121.2		29.6		12.9	6.8	31%	1049	45%	55%
03-May	911	7.7	8.1	106.7	11.1	108.5	15.5	0.0	138	121.3	2.5	21.7	0.6	11.4	6.2	30%	947	49%	51%
12-Apr	932	8.0	8.4	119.4	12.3	111.1	16.5	0.9	224		6.2	36.7	0.0	12.3	4.5	46%	820	27%	73%
10-May	947	7.6	6.5	130.7	13.4	126.0	18.4	0.0	175	130.7		22.3	0.1	13.6	7.0	32%	1097	47%	53%
14-May	949	7.6	6.8	99.6	15.1	100.3	15.0	0.0	541	119.6		21.5	0.1	11.0	12.7	-7%	1239	27%	73%
14-May	967	7.5		107.8	15.4	143.3	19.7	0.0	264.0	215.7	0.5	29.3		13.4	11.0	10%	1371	50%	50%
15-Apr	973	7.9	14.7	124.9	18.4	116.3	16.1	0.7	219	136.6	4.5	38.1	0.6	13.3	8.3	23%	1164	43%	57%
19-Apr	987	7.5	12.1	131.5	13.7	121.9	15.7	1.6	232	141.3	1.9	35.1	0.6	13.5	8.6	22%	1185	42%	58%
17-Apr	992	7.9	10.4	120.9	16.0	119.1	15.1	0.0	228	135.0	4.0	43.7	0.3	12.9	8.5	20%	1159	42%	58%
02-May	1002	7.7	6.9	103.1	16.2	136.5	14.8	4.1	138	153.7	3.5	32.7	0.3	13.0	7.3	28%	1131	53%	47%
20-Apr	1005	7.8	10.4	122.6	13.3	116.0	13.9	0.0	338	120.7	2.7	41.1	0.2	12.6	9.8	12%	1190	34%	66%
09-May	1096	7.5	8.1	124.1	16.0	121.7	21.7	0.0	175	126.3	0.5	32.2	0.1	13.4	7.1	31%	1100	46%	54%
Min	762	7.2	6.1	97.3	10.3	78.5	9.5	0.0	137.5	91.0	0.5	21.5	0.0					25%	47%
Max	1096	8.4	14.7	131.5	18.4	143.3	22.6	4.1	541.0	215.7	7.5	43.7	0.6					53%	75%
Avg	937	7.7	8.9	115.3	14.0	115.3	16.1	0.6	227.6	133.8	3.7	32.6	0.2					41%	59%
Stdev	80	0.3	2.3	11.1	2.2	16.5	3.4	1.1	96.7	28.4	2.2	7.8	0.2					9%	9%
Avg - Stdev	857.4	7.4		104.2	11.8	98.7	12.7	-0.6	130.9	105.4	1.5	24.8	0.0						
Avg + Stdev	1016.9	8.0		126.3	16.2	131.8	19.4	1.7	324.3	162.2	5.9	40.4	0.5						
Correlation with EC				0.72	0.76	0.79	0.64	0.05	0.22	0.61	-0.50	0.23	0.26						

Notes: No result=blank, Result< LOQ= 0

11.5 Supplementary information for Chapter 7 - EC as an indicator for RO/NF membrane integrity monitoring.

Table 11-15: RO system process conditions utilized in case study

Recovery	75%	Elements per vessel	6
Membrane type	BW30LE 4401	Temperature	15 °C
Stages	2	pH	7.6
Permeate flow	185 m^3/hour	Flux	23.6 LMH
1^{st} stage	21 PVs	Flow factor	0.85
2^{nd} stage	11 PVs		

Table 11-16: RO simulation results from case study

Feed water EC: 1000 µS/cm	Stage 1						Stage 2					
Element	1	2	3	4	5	6	1	2	3	4	5	6
Recovery	0.09	0.10	0.11	0.12	0.13	0.15	0.09	0.09	0.10	0.10	0.11	0.12
Perm Flow (m³/h)	1.09	1.06	1.04	1.01	0.99	0.97	0.92	0.89	0.86	0.82	0.79	0.76
Perm TDS (mg/l)	2.12	2.42	2.78	3.23	3.79	4.54	5.14	5.86	6.72	7.77	9.07	10.71
Perm mass flux (g/h)	2.31	2.57	2.89	3.26	3.75	4.40	4.73	5.22	5.78	6.37	7.17	8.14
Feed Flow (m³/h)	11.75	10.65	9.59	8.55	7.54	6.55	10.65	9.73	8.84	7.98	7.16	6.36
Feed TDS (mg/l)	500	551	612	686	778	895	1049	1148	1263	1398	1558	1751
Contaminant flow (m3/h)	0.00	0.00	0.00	0.00	0.00	0.00	0.00	0.00	0.00	0.00	0.00	0.00
Contaminant mass flux (g/h)	0.00	0.00	0.00	0.00	0.00	0.00	0.00	0.00	0.00	0.00	0.00	0.00
Feed Press (bar)	14.69	14.26	13.89	13.57	13.31	13.08	12.56	12.18	11.86	11.57	11.32	11.11
Feed water EC: 2000 µS/cm	Stage 1						Stage 2					
Element	1	2	3	4	5	6	1	2	3	4	5	6
Recovery	0.10	0.10	0.11	0.12	0.13	0.15	0.09	0.09	0.10	0.10	0.11	0.11
Perm Flow (m³/h)	1.12	1.09	1.06	1.03	1.00	0.97	0.91	0.87	0.83	0.79	0.75	0.71
Perm TDS (mg/l)	4.14	4.76	5.51	6.44	7.65	9.26	10.55	12.11	14.00	16.32	19.22	22.92
Perm mass flux (g/h)	4.64	5.19	5.84	6.63	7.65	8.98	9.60	10.54	11.62	12.89	14.42	16.27
Feed Flow (m³/h)	11.75	10.62	9.53	8.48	7.45	6.45	10.48	9.56	8.69	7.85	7.06	6.31
Feed TDS (mg/l)	1000	1105	1231	1384	1573	1815	2133	2336	2570	2842	3159	3532
Contaminant flow (m3/h)	0.00	0.00	0.00	0.00	0.00	0.00	0.00	0.00	0.00	0.00	0.00	0.00
Contaminant mass flux (g/h)	0.00	0.00	0.00	0.00	0.00	0.00	0.00	0.00	0.00	0.00	0.00	0.00
Feed Press (bar)	15.68	15.25	14.88	14.57	14.30	14.09	13.57	13.20	12.88	12.60	12.36	12.15
Feed water EC: 4000 µS/cm	Stage 1						Stage 2					
Element	1	2	3	4	5	6	1	2	3	4	5	6
Recovery	0.10	0.11	0.12	0.13	0.14	0.15	0.09	0.09	0.09	0.10	0.10	0.10
Perm Flow (m³/h)	1.19	1.14	1.10	1.06	1.01	0.96	0.89	0.84	0.78	0.73	0.67	0.60
Perm TDS (mg/l)	8.27	9.60	11.27	13.41	16.25	20.14	23.25	27.10	31.86	37.83	45.39	55.15
Perm mass flux (g/h)	9.84	10.94	12.40	14.21	16.41	19.33	20.69	22.76	24.85	27.62	30.41	33.09
Feed Flow (m³/h)	11.75	10.56	9.42	8.32	7.26	6.26	10.12	9.22	8.38	7.60	6.87	6.21
Feed TDS (mg/l)	2081	2314	2593	2934	3359	3897	4597	5040	5542	6110	6751	7469
Contaminant flow (m3/h)	0.00	0.00	0.00	0.00	0.00	0.00	0.00	0.00	0.00	0.00	0.00	0.00
Contaminant mass flux (g/h)	0.00	0.00	0.00	0.00	0.00	0.00	0.00	0.00	0.00	0.00	0.00	0.00
Feed Press (bar)	17.86	17.43	17.07	16.76	16.50	16.29	15.78	15.43	15.12	14.86	14.62	14.42
Feed water EC: 10000 µS/cm	Stage 1						Stage 2					
Element	1	2	3	4	5	6	1	2	3	4	5	6
Recovery	0.12	0.13	0.14	0.14	0.15	0.16	0.09	0.09	0.08	0.08	0.07	0.06
Perm Flow (m³/h)	1.38	1.31	1.23	1.13	1.03	0.90	0.81	0.72	0.62	0.53	0.45	0.37
Perm TDS (mg/l)	19.27	23.21	28.48	35.77	46.18	61.59	74.18	90.73	112.23	140.40	177.47	226.54
Perm mass flux (g/h)	26.59	30.41	35.03	40.42	47.57	55.43	60.09	65.33	69.58	74.41	79.86	83.82
Feed Flow (m³/h)	11.75	10.36	9.06	7.83	6.70	5.67	9.11	8.30	7.58	6.96	6.43	5.98
Feed TDS (mg/l)	5439	6161	7047	8146	9517	11230	13343	14633	16005	17429	18868	20274
Contaminant flow (m3/h)	0.00	0.00	0.00	0.00	0.00	0.00	0.00	0.00	0.00	0.00	0.00	0.00
Contaminant mass flux (g/h)	0.00	0.00	0.00	0.00	0.00	0.00	0.00	0.00	0.00	0.00	0.00	0.00
Feed Press (bar)	25.21	24.79	24.43	24.14	23.91	23.73	23.23	22.93	22.67	22.43	22.22	22.03

Feed water EC: 20000 µS/cm	Stage 1						Stage 2					
Element	1	2	3	4	5	6	1	2	3	4	5	6
Recovery	0.15	0.16	0.17	0.17	0.17	0.16	0.08	0.07	0.06	0.05	0.04	0.03
Perm Flow (m³/h)	1.71	1.57	1.40	1.20	0.99	0.76	0.62	0.50	0.40	0.31	0.24	0.18
Perm TDS (mg/l)	35.07	44.94	59.52	81.93	117.56	175.90	227.68	299.22	396.97	529.86	708.26	942.98
Perm mass flux (g/h)	59.97	70.56	83.33	98.32	116.38	133.68	141.16	149.61	158.79	164.26	169.98	169.74
Feed Flow (m³/h)	11.75	10.04	8.47	7.07	5.86	4.88	7.86	7.24	6.73	6.33	6.02	5.79
Feed TDS (mg/l)	11476	13425	15903	19043	22939	27552	32604	35400	38025	40387	42433	44148
Contaminant flow (m3/h)	0.00	0.00	0.00	0.00	0.00	0.00	0.00	0.00	0.00	0.00	0.00	0.00
Contaminant mass flux (g/h)	0.00	0.00	0.00	0.00	0.00	0.00	0.00	0.00	0.00	0.00	0.00	0.00
Feed Press (bar)	40.89	40.47	40.14	39.88	39.68	39.53	39.06	38.81	38.59	38.38	38.19	38.01

Table 11-17: Smallest detectable flow of feedwater through a breach with different ratios of EC sensors to PVs

Smallest detectable flow of water (mL/hr)

Feed water EC: 1000 µS/cm	Stage 1						Stage 2					
Element	1	2	3	4	5	6	7	8	9	10	11	12
1 in 1 PV	54	49	44	40	35	30	26	24	22	20	18	16
1 in 6 PVs	323	292	263	235	207	180	153	140	127	115	103	92
1 in 12 PVs	645	584	527	469	413	359	306	279	254	229	206	184
1 in 24 PVs	1289	1168	1051	937	826	717	611	558	507	458	411	366
1 in 48 PVs	2577	2335	2111	1873	1651	1434	1222	1116	1014	916	821	731

Smallest detectable flow of water (mL/hr)

Feed water EC: 2000 µS/cm	Stage 1						Stage 2					
Element	1	2	3	4	5	6	7	8	9	10	11	12
1 in 1 PV	27	25	22	20	17	15	13	12	11	10	9	8
1 in 6 PVs	161	145	130	116	102	88	75	69	62	56	51	45
1 in 12 PVs	321	290	260	231	203	176	150	137	124	112	101	90
1 in 24 PVs	641	579	520	462	406	352	299	273	248	224	202	180
1 in 48 PVs	1281	1158	1039	923	811	702	597	544	496	448	403	360

Smallest detectable flow of water (mL/hr)

Feed water EC: 4000 µS/cm	Stage 1						Stage 2					
Element	1	2	3	4	5	6	7	8	9	10	11	12
1 in 1 PV	13	12	11	9	8	7	6	6	5	5	4	4
1 in 6 PVs	76	69	61	54	47	41	35	32	29	26	24	21
1 in 12 PVs	152	137	122	108	94	81	69	63	57	52	47	42
1 in 24 PVs	303	273	243	215	188	162	137	125	114	103	93	84
1 in 48 PVs	607	546	486	429	375	323	274	249	227	206	186	168

Smallest detectable flow of water (mL/hr)

Feed water EC: 10000 µS/cm	Stage 1						Stage 2					
Element	1	2	3	4	5	6	7	8	9	10	11	12
1 in 1 PV	5	5	4	4	3	3	2	2	2	2	2	2
1 in 6 PVs	28	25	22	19	16	14	12	11	9	9	8	8
1 in 12 PVs	56	49	43	37	32	27	23	21	19	18	16	14
1 in 24 PVs	111	98	86	74	64	54	45	41	38	35	32	30
1 in 48 PVs	222	196	170	148	127	107	90	82	75	69	64	60

Smallest detectable flow of water (mL/hr)

Feed water EC: 20000 µS/cm	Stage 1						Stage 2					
Element	1	2	3	4	5	6	7	8	9	10	11	12
1 in 1 PV	3	2	2	2	2	1	1	1	1	1	1	1
1 in 6 PVs	14	12	9	8	7	6	5	5	4	4	4	4
1 in 12 PVs	27	23	20	16	14	11	10	9	8	8	8	7
1 in 24 PVs	54	46	39	32	27	22	19	18	16	15	15	14
1 in 48 PVs	107	91	77	64	53	44	37	36	32	30	29	28